CHRONIC INFLAMMATION AND NEURODEGENERATION IN RETINAL DISEASE

EDITED BY: Settimio Rossi, Michele D'Amico, Claudio Bucolo and Julie Sanderson
PUBLISHED IN: Frontiers in Pharmacology

frontiers Research Topics

ISSN 1664-8714
ISBN 978-2-88971-835-1
DOI 10.3389/978-2-88971-835-1

About Frontiers

Frontiers is more than just an open-access publisher of scholarly articles: it is a pioneering approach to the world of academia, radically improving the way scholarly research is managed. The grand vision of Frontiers is a world where all people have an equal opportunity to seek, share and generate knowledge. Frontiers provides immediate and permanent online open access to all its publications, but this alone is not enough to realize our grand goals.

Frontiers Journal Series

The Frontiers Journal Series is a multi-tier and interdisciplinary set of open-access, online journals, promising a paradigm shift from the current review, selection and dissemination processes in academic publishing. All Frontiers journals are driven by researchers for researchers; therefore, they constitute a service to the scholarly community. At the same time, the Frontiers Journal Series operates on a revolutionary invention, the tiered publishing system, initially addressing specific communities of scholars, and gradually climbing up to broader public understanding, thus serving the interests of the lay society, too.

Dedication to Quality

Each Frontiers article is a landmark of the highest quality, thanks to genuinely collaborative interactions between authors and review editors, who include some of the world's best academicians. Research must be certified by peers before entering a stream of knowledge that may eventually reach the public - and shape society; therefore, Frontiers only applies the most rigorous and unbiased reviews.
Frontiers revolutionizes research publishing by freely delivering the most outstanding research, evaluated with no bias from both the academic and social point of view. By applying the most advanced information technologies, Frontiers is catapulting scholarly publishing into a new generation.

What are Frontiers Research Topics?

Frontiers Research Topics are very popular trademarks of the Frontiers Journals Series: they are collections of at least ten articles, all centered on a particular subject. With their unique mix of varied contributions from Original Research to Review Articles, Frontiers Research Topics unify the most influential researchers, the latest key findings and historical advances in a hot research area! Find out more on how to host your own Frontiers Research Topic or contribute to one as an author by contacting the Frontiers Editorial Office: frontiersin.org/about/contact

CHRONIC INFLAMMATION AND NEURODEGENERATION IN RETINAL DISEASE

Topic Editors:
Settimio Rossi, Second University of Naples, Italy
Michele D'Amico, Università della Campania Luigi Vanvitelli, Italy
Claudio Bucolo, University of Catania, Italy
Julie Sanderson, University of East Anglia, United Kingdom

We would like to acknowledge and thank Francesco Petrillo, Carlo Gesualdo, Chiara Bianca Maria Platania and Maria Consiglia Trottafor their support on the collection's Editorial article.

Citation: Rossi, S., D'Amico, M., Bucolo, C., Sanderson, J., eds. (2021). Chronic Inflammation and Neurodegeneration in Retinal Disease.
Lausanne: Frontiers Media SA. doi: 10.3389/978-2-88971-835-1

Table of Contents

frontiers in Pharmacology

EDITORIAL
published: 18 October 2021
doi: 10.3389/fphar.2021.784770

Editorial: Chronic Inflammation and Neurodegeneration in Retinal Disease

Francesco Petrillo[1], *Carlo Gesualdo*[2], *Chiara Bianca Maria Platania*[3], *Michele D'Amico*[4]* *and Maria Consiglia Trotta*[4]

[1]Department of Ophthalmology, University of Catania, Catania, Italy, [2]Eye Clinic, Multidisciplinary Department of Medical, Surgical and Dental Sciences, University of Campania "Luigi Vanvitelli", Naples, Italy, [3]Department of Biomedical and Biotechnological Sciences, School of Medicine, University of Catania, Catania, Italy, [4]Department of Experimental Medicine, University of Campania "Luigi Vanvitelli", Naples, Italy

Keywords: chronic inflammation, neurodegeneration, retinitis pigmenstosa, age-related macular degeneration, diabetic retinopathy, glaucoma

Editorial on the Research Topic

Chronic Inflammation and Neurodegeneration in Retinal Disease

Retinal diseases represent one of the main causes of blindness all around the world, with tremendous social and economic impact. A deeper description of their pathophysiology is essential for improving their diagnostic and therapeutic management. Chronic inflammation and neurodegeneration have been recently recognized as important players in retinal damage. However, the exact mechanisms through which the function of retinal pigment epithelium (RPE) and neurons is impaired, leading to photoreceptors cell death, have still to be clarified. Therefore, the aim of the present Research Topic is to highlight the most recent discoveries in the field of retinal chronic inflammation and neurodegeneration, in order to collect the best evidence and the novel pharmacological approaches in the management of retinal diseases. Several articles published in this Research Topic are devoted to the main retinal pathologies, such as retinitis pigmentosa (RP), age-related macular degeneration (AMD), diabetic retinopathy (DR) and glaucoma.

It is well known that RP is the most common inherited retinal dystrophy, with no specific therapy against its progression. It is characterized by a progressive dysfunction of the photoreceptors, due retinal oxidative stress, glial and vascular changes which affects first the rods and then the cones. A great attention has been recently focused on the role of microglial activation in RP. Indeed, glial alterations were evident in a mouse model of RP (rd1 mouse) (Gimeno-Hernández et al.). These were reversed by the administration of thioredoxin (TRX), which also decreased the photoreceptors death, by activating glutathione (GSH) pathway (Gimeno-Hernández et al.). Accordingly, in human RP, microglia activation was present in retinal nuclear layer of regions populated by death committed rods (Micera et al.).

Concerning AMD, it is a complex multifactorial degenerative disease and the leading cause of blindness in individuals over the age of 55 in developed countries. During AMD pathogenesis, RPE cells lose their integrity, also by interacting with lymphocytes and macrophages trough integrins. To this regard, specific integrin antagonists were used as a strategy to interfere in the RPE-lymphocyte crosstalk (Baiula et al.). Integrin antagonists reduced ARPE-19 cell death and expression of IL-1β, then representing a novel opportunity to fight dry AMD (Baiula et al.). Another molecule considered as a novel therapeutic option in AMD is the antioxidant agent paraoxonase-1 (PON1), whose activity has been reported to be negatively correlated with malondialdehyde (MDA) levels in patients with AMD, by inhibiting lipid peroxidation (Micera et al.).

Among the constitutional risk factors favoring AMD, age is certainly the main one. However, gender has emerged as an important additional risk factor. To this regard, biological sex was shown

OPEN ACCESS

Edited and reviewed by:
Dieter Steinhilber,
Goethe University Frankfurt, Germany

***Correspondence:**
Michele D'Amico
michele.damico@unicampania.it

Specialty section:
This article was submitted to Inflammation Pharmacology, a section of the journal Frontiers in Pharmacology

Received: *28 September 2021*
Accepted: *06 October 2021*
Published: *18 October 2021*

Citation:
Petrillo F, Gesualdo C, Platania CBM, D'Amico M and Trotta MC (2021) Editorial: Chronic Inflammation and Neurodegeneration in Retinal Disease. Front. Pharmacol. 12:784770. doi: 10.3389/fphar.2021.784770

to influence the expression of different age-related miRNAs (Hermenean et al.). Interestingly, miR-27a-3p, miR-27b-3p, miR-20a-5p and miR-20b-5p levels correlated with the thickness of specific retinal layers (Hermenean et al.). Concerning the genetic AMD risk factors, new insights on the polymorphisms of complement factor H (*CFH*) gene, the greatest genetic variations associated to AMD, have been reported (Stravalaci et al.). Specifically, the overexpression of long pentraxin 3 (PTX3) protein in RPE cells, cultured in inflammatory AMD-like conditions, along with the formation of a stable ternary complex between PTX3, factor H and its target C3b, was evidenced. This reduced *CFH* dysregulation in AMD (Stravalaci et al.).

Noteworthy, DR is the leading cause of blindness in working-age individuals in industrialized countries and is favored by a combination of microvascular damage, neuroinflammation and neurodegeneration processes. DR microvascular damage is triggered by hyperglycemia and retinal hypoxia. Interesting insights in epigenetic regulation of vascular endothelial growth factor A (VEGFA) and placental growth factor (PlGF), both increased during retinal hypoxic conditions, have been reported by Lazzara et al. Particularly, in human retinal endothelial cells (HRECs) challenged with chemical hypoxic stimuli (CoCl2), the authors showed that a focused set of HypoxamiRs, which are regulated by HIF-1α dependent or independent mechanisms, correlated not only with VEGFA levels but also with expression of TGFβ signaling pathway genes. These findings suggest the use of novel pharmacological/molecular approach, such as antagomiRs and agomir, to counteract microvascular damage induced by hypoxia (Lazzara et al.).

Retinal neurodegeneration is another key event in the progression of DR. Indeed, the death of retinal ganglion cells (RGCs) provoked by retinal insult could lead to irreversible blindness, since retina is characterized by limited repair capacity. Recently, plasma rich in growth factors (PRGF) was evaluated in ocular models for its capacity to promote neural survival (Ruzafa et al.). Particularly, the effect of the PRGF obtained from human, as well as from pig blood, was tested in organotypic cultures from adult pig retinas. PRGF induced microglial migration to the outer nuclear layers as a sign of inflammation. Due to the presence of several pro-inflammatory cytokines (Ruzafa et al.). Moreover, gliosis, proliferation and RGC survival were not affected by PGRF in organotypic cultures of adult porcine retinas. This effect was further investigated on primary cell cultures of RGCs and Müller cells alone or in co-cultures (Ruzafa et al.). Interestingly, the authors showed a selective protective effect of PGRF on Müller cells, since RGC survival was reduced in presence or absence of Müller cells (Ruzafa et al.).

Finally, glaucoma is the second leading cause of irreversible blindness in the world. It is a multifactorial neurodegenerative disease, characterized by the progressive death of RGCs and optic nerve head cupping. Particularly, the progressive damage to the optic nerve fibers is favored by an imbalance between the neuroinflammatory and neuroprotective mediators. Furthermore, glaucoma can be caused by the neurotoxic effects of glutamate, nitric oxide and oxidative stress. In this context, it has been demonstrated that the pro-inflammatory status induced in chronic rat model of glaucoma, can be reduced through stimulation of δ-opioid receptor activation by a selective ligand, SNC-121 (Husain et al.). Specifically, SNC-121 completely inhibited the increase in pro-inflammatory cytokines (Husain et al.). Further pre-clinical and clinical studies are necessary to fully understand the mechanisms underlying the onset of glaucoma. In this line, interesting anatomical changes have been highlighted in different mouse strains affected by glaucoma (Fiedorowicz et al.). Particularly, C57Bl/6J and DBA/2J mice showed different ocular dimensions, correlated to intraocular pressure (IOP) values (Fiedorowicz et al.).

Overall, the topic in retinal neurodegeneration and chronic inflammation highlights new preclinical findings in rodent models of ocular pathologies and pave the way to new biomarkers, pharmacological targets and therapeutic tools in retinal disease diagnosis and management.

AUTHOR CONTRIBUTIONS

All authors listed have made a substantial, direct, and intellectual contribution to the work and approved it for publication.

Conflict of Interest: The authors declare that the research was conducted in the absence of any commercial or financial relationships that could be construed as a potential conflict of interest.

Publisher's Note: All claims expressed in this article are solely those of the authors and do not necessarily represent those of their affiliated organizations, or those of the publisher, the editors and the reviewers. Any product that may be evaluated in this article, or claim that may be made by its manufacturer, is not guaranteed or endorsed by the publisher.

frontiers in Pharmacology

ORIGINAL RESEARCH
published: 17 July 2020
doi: 10.3389/fphar.2020.01063

Stabilization of HIF-1α in Human Retinal Endothelial Cells Modulates Expression of miRNAs and Proangiogenic Growth Factors

Francesca Lazzara[1†], Maria Consiglia Trotta[2†], Chiara Bianca Maria Platania[1†], Michele D'Amico[2], Francesco Petrillo[2], Marilena Galdiero[2], Carlo Gesualdo[3], Settimio Rossi[3], Filippo Drago[1,4] and Claudio Bucolo[1,4]*

[1] Department of Biomedical and Biotechnological Sciences, School of Medicine, University of Catania, Catania, Italy, [2] Department of Experimental Medicine, Division of Pharmacology, University of Campania "Luigi Vanvitelli", Naples, Italy, [3] Eye Clinic, Multidisciplinary Department of Medical, Surgical and Dental Sciences, University of Campania "Luigi Vanvitelli", Naples, Italy, [4] Center for Research in Ocular Pharmacology-CERFO, University of Catania, Catania, Italy

OPEN ACCESS

Edited by:
Annalisa Bruno, University of Studies G. d'Annunzio Chieti and Pescara, Italy

Reviewed by:
Neeru M. Sharma, University of Nebraska Medical Center, United States
Massimo Dal Monte, University of Pisa, Italy

***Correspondence:**
Claudio Bucolo
claudio.bucolo@unict.it

[†]These authors have contributed equally to this work

Specialty section:
This article was submitted to Inflammation Pharmacology, a section of the journal Frontiers in Pharmacology

Received: *16 March 2020*
Accepted: *30 June 2020*
Published: *17 July 2020*

Citation:
Lazzara F, Trotta MC, Platania CBM, D'Amico M, Petrillo F, Galdiero M, Gesualdo C, Rossi S, Drago F and Bucolo C (2020) Stabilization of HIF-1α in Human Retinal Endothelial Cells Modulates Expression of miRNAs and Proangiogenic Growth Factors. Front. Pharmacol. 11:1063. doi: 10.3389/fphar.2020.01063

Retinal hypoxia is one of the causative factors of diabetic retinopathy and is also one of the triggers of VEGF release. We hypothesized that specific dysregulated miRNAs in diabetic retinopathy could be linked to hypoxia-induced damage in human retinal endothelial cells (HRECs). We investigated in HRECs the effects of chemical ($CoCl_2$) hypoxia on the expression of HIF-1α, VEGF, PlGF, and of a focused set of miRNAs. We found that miR-20a-5p, miR-20b-5p, miR-27a-3p, miR-27b-3p, miR-206-3p, miR-381-3p correlated also with expression of TGFβ signaling pathway genes in HRECs, challenged with chemical hypoxic stimuli. In conclusion, our data suggest that retinal angiogenesis would be promoted, at least under HIF-1α activation, by upregulation of PlGF and other factors such as miRNAs, VEGFA, and TGFβ1.

Keywords: hypoxia-inducible-factor-1α, vascular endothelial growth factor, transforming growth factor beta, retina, diabetic retinopathy, inflammation

INTRODUCTION

Diabetic retinopathy (DR), a complication of diabetes, is a microvascular disease with a strong inflammatory imprinting. Vascular endothelial growth factor (VEGF) is a key player in retinal neovascularization, and intraocular injections of anti-VEGF agents are currently the established therapies for diabetic macular edema, along with steroids (Bandello et al., 2012). Although not fully elucidated, alterations in retinal hemodynamics and reduced blood flow may be detrimental for DR, along with uncontrolled hyperglycemia (Schmetterer and Wolzt, 1999; Schmidl et al., 2015). Furthermore, during DR progression, local or global changes in retinal oxygenation may cause the development of hypoxic areas (Arden and Sivaprasad, 2012) and oxidative stress (Bucolo et al., 2006). Similar to the etiopathogenesis of retinopathy of prematurity (ROP), induction of hypoxia-inducible factor-1 α (HIF-1α) may be responsible for the production of vascular endothelial growth factor (VEGFA), which is the main cause of retinal neovascularization (Aiello et al., 1994; Arjamaa and Nikinmaa, 2006; Abu El-Asrar et al., 2012). Furthermore, HIF-1α and VEGFA crosstalk in ocular neovascularization has been widely investigated (Ozaki et al., 1999; Rodrigues et al., 2016). In

particular, the HIF-1α inhibition strategy has also been explored for treatment of retinal neovascularization (Iwase et al., 2013; D'Amico et al., 2015; D'Amico et al., 2017; Zeng et al., 2017).

Besides VEGFA, HIF-1α can also induce the placental growth factor (PlGF) (Zimna and Kurpisz, 2015; Charnock-Jones, 2016; Mitsui et al., 2018), an emerging target in retinal neovascular diseases (Kwon and Jee, 2018; Lee et al., 2018; Saddala et al., 2018; Lazzara et al., 2019; Van Bergen et al., 2019). Furthermore, HIF-1α is involved in expression of several microRNAs (miRNAs), that are named HypoxamiRs if they bear in their promoter region the hypoxia responsive elements (HREs) (Nallamshetty et al., 2013; Bertero et al., 2017). Indeed, HypoxamiRs, regulated by HIF-1α dependent or independent mechanisms, are tightly involved in molecular and cellular changes triggered by hypoxia (Cottrill et al., 2014; Gee et al., 2014; Greco et al., 2014; Bertero et al., 2017). Moreover, several genes, that are target of HypoxamiRs, belong to the VEGFR2 signaling pathway (Gupta et al., 2018). This pathway regulates angiogenic response of endothelial cells (Abhinand et al., 2016), and represents the target of current approved treatments for neovascular retinal degenerations (Bandello et al., 2012). We recently evidenced the dysregulation of expression pattern of 8 miRNAs (miR-20a-5p, miR-20a3p, miR-20b-5p, miR-106a-5p, miR-27a-5p, miR-27b-3p, miR-206-3p, and miR-381-3p) in retina and serum of diabetic mice, representing intriguing and potent mediators in the DR pathological mechanisms (Platania et al., 2019). HREs were found in promoter region of miR-20a, miR-20b, miR-106, miR-27a, that indeed, have been enlisted as Hypoxamirs (Nallamshetty et al., 2013). Although HREs are not present in miR-206-3p, miR-381 and miR-27b promoter regions, these miRNAs were found to be modulated in several hypoxic experimental setting (Yue et al., 2013; Choudhry and Mole, 2016; Gupta et al., 2018; Lu et al., 2018).

Therefore, we hereby hypothesized that these eight miRNAs could also be involved in activation of HIF-1/angiogenic axis in retinal endothelial cells. With this aim, we stabilized, by cobalt chloride treatment, HIF-1α protein in human retinal endothelial cells (HRECs), in order to analyze the activation of HIF-1/VEGFA-PlGF axis, along with expression of a focused set of miRNAs, previously found to be dysregulated in an *in vivo* model of DR (Platania et al., 2019). A bioinformatic approach guided the identification and *in vitro* validation of alternative target genes of miRNAs, dysregulated after inhibition of HIF-1α degradation. We analyzed the expression of genes of the TGFβ (Transforming growth factor beta) signaling pathway, which is an emerging target in DR (Li et al., 2018; Stafiej et al., 2018) and was found to be one of top pathways modulated by HypoxamiRs target genes (Gupta et al., 2018).

MATERIAL AND METHODS

Reagents

Mouse monoclonal anti-HIF-1α (catalog n. sc-13515), mouse anti-GAPDH (catalog n. 2118) antibodies were purchased from Santa Cruz Biotechnology, Inc. (CA, USA), and Cell-Signaling Technology (Leiden, Netherlands), respectively. Secondary goat anti-mouse IRDye 680LT, (catalog n. 926-68020) were purchased from LI-COR (Lincoln, NE, USA). Cobalt chloride (0.1 M solution, catalog n. 15862) from Sigma-Aldrich (Saint Louis, MO, USA).

Cell Culture

Human retinal endothelial cells were purchased from Innoprot® (Derio – Bizkaia, Spain). Cells were cultured at 37°C, in humidified atmosphere (5% CO_2), in Endothelial cell medium (ECM) supplemented with 5% fetal bovine serum (FBS), 1% ECGS (Endothelial Cell Growth Supplement) and 100 U/ml penicillin 100 μg/ml streptomycin. HRECs (cell passage number 4) for each experiment were seeded setting 4×10^5 as final cell density.

Induction of Chemical Hypoxia In Vitro

Cobalt chloride ($CoCl_2$) is commonly used to stabilize HIF-1α, because it inhibits the HIF-1α degradation, as shown in several *in vitro* settings, including primary human retinal endothelial cells cultures as previously described (Gao et al., 2008; Hu et al., 2012; Li et al., 2017; He et al., 2019). Preliminary studies were carried out and HRECs cultures were treated with various concentrations of $CoCl_2$ (100–200 μM), in order to assess cell tolerability for 24 h with MTT test (**Supplementary Data**). The concentration used for all experiments was 200 μM, accordingly to previous $CoCl_2$ concentrations tested on retinal ganglion cells (Balaiya et al., 2012; Li et al., 2017). Cells were seeded in Petri dishes (passage number 4, cell density 4×10^5); after reaching confluence (approximately 80%), cells were treated with $CoCl_2$ for 30 min, 2 and 8 h to induce HIF-1α accumulation/nuclear translocation.

Western Blot

HRECs were cultured in 60 mm Petri dishes (cell density 4×10^5). Proteins from cell lysates were extracted with RIPA Buffer, including protease and phosphatase inhibitors cocktail (Sigma-Aldrich, St. Louis, MO, USA). Total protein content, in each cell lysate sample, was determined by the BCA Assay Kit (Pierce™ BCA Protein Assay Kit, Invitrogen, Life Technologies, Carlsbad, CA, USA). Extracted proteins (40 μg) were loaded on 4%–12% tris-glycine gel. After electrophoresis proteins were transferred into a nitrocellulose membrane (Invitrogen, Life Technologies, Carlsbad, CA, USA). Immunoblot was preceded by addition of Odyssey Blocking Buffer (LI-COR Lincoln, NE, USA) to membranes. Therefore, membranes were incubated overnight (4°C) with appropriate primary HIF-1α (1:200 dilution) and anti-GAPDH (1:500 dilution) antibodies. GAPDH was selected as control for protein expression, accordingly to previous reports (Botlagunta et al., 2011; Ao et al., 2015; Evrard et al., 2016; Gao et al., 2019). After overnight incubation, the membranes were then incubated with secondary fluorescent antibodies (1: 10,000 dilution) for 1 h at room temperature. Immunoblot was detected through Odyssey imaging system (LI-COR, Lincoln, NE, USA). Densitometry analyses of blots were performed at nonsaturating exposures and analyzed using the ImageJ software (NIH,

Bethesda, MD, USA; available at http://rsb.info.nih.gov/ij/index.html). Values were normalized to GAPDH, which was also used as loading control (see **supplemental information** for whole gel membranes immunoblots).

Extraction of Total RNA and cDNA Synthesis

Extraction of the total RNA was performed with TRIzol Reagent (Invitrogen, Life Technologies, Carlsbad, CA, USA). The A260/A280 ratio of the optical density of RNA samples (measured with Multimode Reader Flash di Varioskan™) was 1.95–2.01. This RNA purity was confirmed with the electrophoresis in nondenaturing 1% agarose gel (in TAE), that showed an adequate RNA purity, concentration, and integrity. cDNA was synthesized from 2 μg RNA with a reverse transcription kit (SuperScript™ II Reverse Transcriptase, Invitrogen, ThermoFisher Scientific, Carlsbad, CA, USA).

Real-Time Reverse Transcriptase-Polymerase Chain Reaction (qRT-PCR) for PlGF and VEGFA

Real-time RT-PCR was carried out with LightCycler ® 2.0 (Real-Time PCR System Roche Life Science). The amplification reaction mix included iTaq™ Universal SYBR® Green Supermix (Bio-Rad, Hercules, CA, USA) and 1 μl (100 ng) of cDNA. Forty-five amplification cycles were carried out for each sample. Results were analyzed with the $2^{-\Delta\Delta}$Ct method. VEGF and PlGF mRNAs expression were normalized to human 18S mRNA levels. Primers used in qPCR for 18S, VEGF-A, PlGF expression are: 18S (human) Forward (5'-AGTCCC TGCCCTTTGTACACA-3'), Reverse (5'-GATCCGAG GGCCTCACTAAAC-3'); PlGF (human) Forward (5′-ATGTTCAGCCCATCCTGTGT-3′) Reverse (5′-CTTCATC TTCTCCCGCAGAG-3′); VEGF-A (human) Forward (5'-GAGGTTTGATCCGCATAATCTG-3') Reverse (5'-ATCTTCAAGCCATCCTGTGTGC- 3').

Analysis of miRNAs

HRECs total RNA, including small RNAs, was obtained following the miRNeasy Mini Kit (21700400, Qiagen), according to the manufacturer's protocol "Purification of Total RNA, Including Small RNAs, from Animal Cells". Particularly, for miRNAs isolation, Syn-cel-miR-39-3p miScript miRNA Mimic 5 nM (MSY0000010, Qiagen) was added to each sample before RNA purification in order to monitor miRNAs isolation efficacy. RNA quality and concentration were determined by using NanoDrop 2000c spectrophotometer (Thermo Fisher Scientific, Carlsbad, CA, USA). Gene Amp PCR System 9700 (Applied Biosystems Thermo Fisher Scientific, Carlsbad, CA, USA) was used for reverse-transcription phase. Mature miRNAs were converted in cDNA according the MiScript II Reverse Transcription Kit (218161, Qiagen, Germantown, MD, USA), starting from 615 ng of total RNA.CFX96 Real-Time System C1000 Touch Thermal Cycler (Bio-Rad, Hercules, CA, USA) was used to evaluate the expression levels of hsa-miR-20a-5p (Accession number MIMAT0000075), hsa-miR-20b-5p (Accession number MIMAT0001413); hsa-miR-27a-3p (Accession number MIMAT0000084), hsa-miR-27b-3p (Accession number MIMAT0000419), hsa-miR-206-3p (Accession number MIMAT0000462) and hsa-miR-381-3p (Accession number MIMAT0000736). Real time PCR was carried out with miScript SYBR Green PCR kit (218073, Qiagen, Germantown, MD, USA) and specific miScript primer Assays (MS00003199, MS00003206, MS00003241, MS00031668, MS00003787 and MS00004116, Qiagen, Germantown, MD, USA). The expression of the 6 miRNAs analyzed was normalized by using Ce_miR-39-3p (MIMAT0000010) as control (MS00019789, Qiagen, Germantown, MD, USA).

TGFβ Pathway qRT-PCR

Total RNA (615 ng) was subjected to reverse-transcription reaction with the Gene Amp PCR System 9700 (Applied Biosystems Life Technologies, Carlsbad, CA, USA) and Quantitect Reverse Transcription kit (205311, Qiagen, Germantown, MD, USA), following the manufacturer's protocol "Reverse Transcription with Elimination of Genomic DNA for Quantitative, Real-Time PCR". The expression levels of human TGFB1 (Transforming Growth Factor Beta 1-Gene ID 7040), TGFBR1 (Transforming growth factor beta receptor 1-Gene ID 7046), TGFBR2 (Transforming growth factor beta receptor 2-Gene ID 7048) and SMAD2 (Small mother against decapentaplegic 2-Gene ID 4087) genes were evaluated by real time PCR measurement, by using a CFX96 Real-Time System C1000 Touch Thermal Cycler (BioRad Laboratories, Inc), Quantitect SYBR Green PCR Kit (204143, Qiagen, Germantown, MD, USA) and specific Quantitect Primer Assays (QT00000728, QT00083412, QT00014350 and QT00004207, Qiagen, Germantown, MD, USA) following the manufacturer's protocol "Two-Step RT-PCR (Standard Protocol)". Human GAPDH (Gene ID 2597) (QT00079247, Qiagen, Germantown, MD, USA) was used as control to normalize the expression of the 4 genes analyzed; accordingly to previous reports (Botlagunta et al., 2011; Ao et al., 2015; Lin et al., 2015; Rosen et al., 2015; Evrard et al., 2016; Shao and Yao, 2016; Gao et al., 2019; Jiang and Xu, 2019).

MicroRNA or TGFβ Signaling Pathway Genes Expression Determination Analysis

CFX Manager™ Software (Bio-Rad, Hercules, CA, USA) was used to calculate Cycle threshold (Ct) values. Data analysis was carried out with the $2^{-\Delta\Delta}$Ct method. Particularly, ΔCt value for each miRNA or gene profiled was calculated as $\Delta Ct = Ct_{miRNA} - Ct_{Ce\_miR\text{-}39\text{-}5p}$ or as $\Delta Ct = Ct_{gene} - Ct_{GAPDH}$. Then, ΔΔCt was calculated as $\Delta Ct_{time\ x} - \Delta Ct_{time\ 0}$, where time x is the analyzed time point and time 0 is the expression of the target miRNA normalized to Ce-miR-39-5p or of the target gene normalized to GAPDH (Livak and Schmittgen, 2001). Where data are reported as fold-regulation, this was the inverse negative of fold change ($2^{\wedge -\Delta\Delta}$Ct) for fold change values lower than one (downregulation). In case of upregulation, the fold-regulation was equal to fold change ($2^{\wedge -\Delta\Delta}$Ct) for fold change values greater than 1.

Bioinformatics

In order to explore alternative factors and pathways regulated by miRNAs, dysregulated with induction of chemical hypoxia in human retinal endothelial cells, we predicted the combinatorial effect of hsa-miR-20a-5p, hsa-miR-20b-5p, hsa-miR-27a-3p, has-miR-27b-3p, has-miR-260b-3p, and has-miR-381-3p on biological pathways by means of the DIANA miRPath webserver (Vlachos et al., 2015). The miRNA:target interactions were analyzed with application of Tarbase algorithm (Riffo-Campos et al., 2016), which is based on experimental validated miRNA:target interaction.

Statistical Analysis

All results were reported as mean ± SD from four independent in-vitro experiments, where each group was triplicated in plates as technical replicate. The results were analyzed using one-way ANOVA, followed by Tukey-Kramer post-hoc multiple comparisons test. Differences between groups were considered significant for p-value < 0.05. Graphs design and statistical analysis were carried out with GraphPad Prism 5 software (GraphPad Inc., San Diego, CA, USA).

RESULTS

Chemical Hypoxia in HRECs and Angiogenic Factors

$CoCl_2$ treatment, by inhibition of HIF-1α degradation, significantly increased stabilization of HIF-1α protein in HRECs (**Figure 1A** and **Supplementary Data**). HIF-1α is a well-known inducer of VEGFA and PlGF (Aiello et al., 1994; Ozaki et al., 1999; Arjamaa and Nikinmaa, 2006; Abu El-Asrar et al., 2012; Zimna and Kurpisz, 2015; Charnock-Jones, 2016; Rodrigues et al., 2016; Mitsui et al., 2018), but the HIF-1α protein levels did not correlate with expression pattern of VEGFA, within the analyzed time-points (**Figure 1B**). Two hours after $CoCl_2$ treatment, VEGFA expression increased, compared to control HRECs. While, after 8 h, VEGFA levels significantly ($p<0.05$) decreased, compared to levels detected 2 h after, $CoCl_2$ treatment. On the other hand, the expression pattern of PlGF correlated with HIF-1α protein levels, within the analyzed time-points (**Figure 1C**).

Expression Analysis of miRNAs Induced by $CoCl_2$ Treatmet of HRECs

Six miRNAs (miR-20a-5p, miR-20b-5p, miR-27a-3p, miR-27b-3p, miR-260b-3p, miR-381-3p), out of eight analyzed, were found to be significantly ($p<0.05$) dysregulated in HRECs, treated with 200 μM $CoCl_2$, compared to control cells (**Figure 2**). All dysregulated miRNAs were found to be significantly ($p<0.05$) upregulated, 2 h after $CoCl_2$ treatment, compared to control cells (**Figure 3A**). On the contrary, four miRNAs were significantly ($p<0.05$) dysregulated (upregulated) 8 h after $CoCl_2$ treatment, compared to control cells (**Figure 3B**). Furthermore, after 8 h of exposure to $CoCl_2$, five miRNAs (miR-20a, miR-20b, miR-27a, miR-27b, miR-206-3p) were significantly downregulated ($p<0.05$), compared to levels detected in cells treated for 2 h with 200 μM $CoCl_2$, with exception of miR-381-3p (**Figure 3C**).

TGFβ Signaling Pathway in HRECs Challenged With $CoCl_2$

A bioinformatic approach was used to predict the combinatorial effect of miR-20a-5p, miR-20b-5p, miR-27a-3p, miR-27b-3p, miR-206-3p, and miR-381-3p on biological pathways. The pathways dysregulated by these miRNAs were predicted by means of DIANA miRPath, applying the Tarbase algorithm, which generates, as output, pathways related to experimental validated miRNA:mRNA interactions (Vlachos et al., 2015). Based on this bioinformatic approach, we found that the TGFβ signaling pathway was the top-scored among the pathways significantly ($p<0.05$) dysregulated by hypoxia-induced miRNA in HRECs (**Figure 4**). The HIF-1α pathway was predicted to be regulated by miR-20a-5p, miR-20b-5p, miR-27a-3p, miR-27b-3p, miR-260-3p, miR-381-3p, according to the *in vitro* model of retinal chemical hypoxia. Moreover, PI3K-AKT, MAP kinases and Jak-STAT signaling pathways were predicted to be modulated by the six miRNAs, that were dysregulated in HRECs treated with $CoCl_2$.

Therefore, we focused our study on analysis of transcription of TGFβ signaling pathway genes (*TGFB1* encoding for TGFβ1, *TGFBR1* encoding for the TGFβR1 receptor, *TGFBR2* encoding for the TGFβR2 receptor and *SMAD2* encoding for SMAD2), in HRECs treated with 200μM $CoCl_2$ (**Table 1**). These genes were significantly ($p<0.05$) dysregulated in HRECs, 2 and 8 h after $CoCl_2$ treatment (**Figure 5**). Furthermore, we correlated gene expression with dysregulated miRNAs in the analyzed time-points (**Figure 6**, **Table 1**). After 2 h of $CoCl_2$ treatment, *TGFBR2* and *TGFB1* gene expression increased significantly, TGFBR1 decreased ($p<0.05$) (**Figure 6A**), and all analyzed miRNA were significantly upregulated, particularly miR-27a. The mRNA of *TGFBR1* is an experimental validated target of miR-20a, miR-20b, miR-27a, miR-27b, and miR-381, therefore the upregulation of this miRNAs significantly decreased the *TGFBR1* mRNA levels (**Table 1**). Moreover *TGFB1*, and *TGFBR2* are experimental validated targets of miR-27a and miR-20a, respectively, which even if overexpressed did not reduce the expression of these two genes, 2 h after $CoCl_2$ treatment (**Figure 6A**). Eight hours after $CoCl_2$ treatment, miR-20a, miR-27a, miR-27b, and miR-381-3p were significantly ($p<0.05$) upregulated in HRECs, compared to control cells (**Figure 6B**). This pattern of miRNA expression positively correlated with *TGFB1*, *TGFBR2*, and *SMAD2* expression (**Figure 6B**). Although not significantly, 8h after $CoCl_2$ treatment, mRNA levels of TGFβ1, TGFβR2 and SMAD2 were higher, compared to HRECs treated for 2 h with $CoCl_2$ (**Table 1**). On the other hand, TGFβR1 mRNA expression levels were significantly upregulated 8 h after $CoCl_2$ treatment, compared to cells treated for 2 h with $CoCl_2$ (**Figure 6C**). This expression pattern negatively correlated with downregulation of

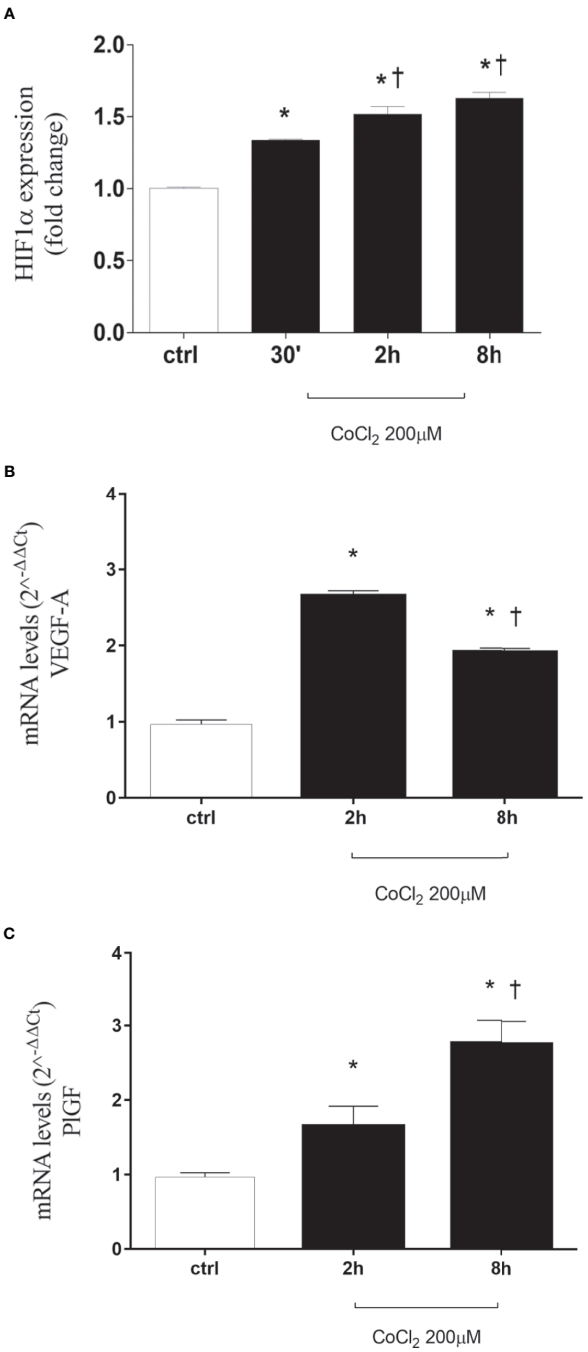

FIGURE 1 | $CoCl_2$ treatment induces HIF-1α stabilization, vascular endothelial growth factor (VEGFA), and placental growth factor (PlGF) expression in human retinal endothelial cells. **(A)** Densitometric analysis of western blot of HIF-1α and GAPDH in human retinal endothelial cells (HRECs) exposed to $CoCl_2$ for 30 min, 2 h and 8 h; each bar represents the mean value ± SD (n=4). *p< 0.05 vs. control; †p < 0.05 vs. 30 min $CoCl_2$ treatments. **(B)** $CoCl_2$ treatment increased VEGF-A mRNA expression. Each bar represents the mean value ± SD. *p < 0.05 $CoCl_2$ vs. control; †p < 0.05 8 h vs. 2 h $CoCl_2$ treatment; (n=4). **(C)** $CoCl_2$ treatment increased PlGF mRNA expression. Each bar represents the mean value ± SD. *p < 0.05 $CoCl_2$ vs. control; †p < 0.05 8 h vs. 2 h $CoCl_2$ treatment; (n=4). The mRNA levels were evaluated by qRT-PCR.

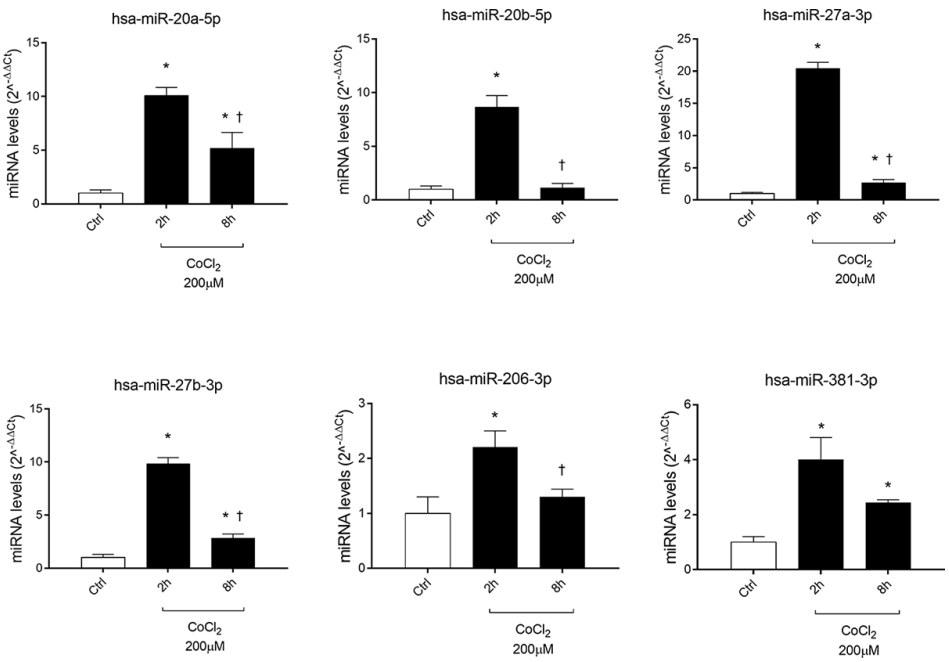

FIGURE 2 | Pattern expression of microRNAs (miRNAs) in human retinal endothelial cells (HRECs) treated with $CoCl_2$, for 2 and 8 h treatment. Expression of miRNAs was analyzed with qRT-PCR. Each bar represents the mean value ± SD. *p < 0.05 200 μM $CoCl_2$ vs. control (ctrl); †p<0.05 8h vs. 2h $CoCl_2$ treatment; (n=4).

miR-20a, miR-20b, miR-27a, miR-27b, and miR-206, according to the opposite trend observed 2 h after chemical hypoxia.

DISCUSSION

Previous data report that eight miRNAs (miR-20a-5p, miR-20a3p, miR-20b-5p, miR-106a-5p, miR-27a-5p, miR-27b-3p, miR-206-3p, and miR-381-3p) were significantly dysregulated both in serum and retina of 5–10 months diabetic mice (Platania et al., 2019). Because retinal hypoxia is detrimental in DR, exacerbating retinal damage and angiogenesis (Aiello et al., 1994; Arjamaa and Nikinmaa, 2006; Abu El-Asrar et al., 2012), we aimed at testing the hypothesis that these miRNAs would be modulated in human retinal endothelial cells, treated with $CoCl_2$ in order to stabilize HIF-1α.

In DR, the role of angiogenesis linked to hypoxic events (i.e. increased VEGFA production stimulated by HIF-1α) has been largely proven (Arjamaa and Nikinmaa, 2006; B. Arden and Sivaprasad, 2012; Kurihara et al., 2014; Li et al., 2017). Furthermore, HIF-1α can induce expression of another proangiogenic factor, the PlGF (Tudisco et al., 2014; Lazzara et al., 2019). In this study we found a correlation, in terms of time-dependent expression, between HIF-1α and PlGF, after $CoCl_2$ treatment (**Figure 1**). Instead, VEGF mRNA levels did not correlate with HIF-1α protein (**Figure 1**). For this reason, we hypothesized that other factors could regulate VEGFA expression in an *in vitro* model of chemical hypoxia, such as miRNAs. Involvement of miRNAs in retinal neovascular diseases has been widely studied (Romano et al., 2017; Natoli and Fernando, 2018; Martinez and Peplow, 2019; Platania et al., 2019). We found that six miRNAs (miR-20a-5p, miR-20b-5p, miR-27a-3p, miR-27b-3p, miR-206-3p, miR-381-3p), out of eight tested, were dysregulated in human retinal endothelial cells after $CoCl_2$ treatment (**Figure 2**). These miRNAs have been previously found to be either HypoxamiRs (bearing HREs in their promoting region) or linked to hypoxic microenvironment (Nallamshetty et al., 2013; Yue et al., 2013; Choudhry and Mole, 2016; Gupta et al., 2018; Lu et al., 2018).

After 8 h, similarly to VEGFA expression, we found a shift in expression pattern of miRNAs, compared levels detected 2 h after $CoCl_2$ treatment (**Figure 3**). Experimental validated miRNA : VEGFA mRNA interactions were found for miR-20a-5p and miR-20b-5p (Platania et al., 2019), and in hepatocellular carcinoma for miR-381-3p (Tsai et al., 2017; Wang et al., 2018). Therefore, VEGFA expression levels could be related to the expression pattern of miRNAs, 2 to 8 h after stabilization of HIF-1α, because VEGFA is a target of miR-20a, miR-20b, miR-381, and indirectly of miR-27b (Veliceasa et al., 2015). On the contrary, PlGF is not a validated or predicted target of any miRNAs dysregulated in HRECs treated with $CoCl_2$. Particularly, the role of PlGF in regulation retinal angiogenesis, under hypoxic stimuli, is still unknown. On the other hand, several reports support the detrimental role of PlGF in the pathogenesis and progression of DR (Carmeliet et al., 2001; Huang et al., 2015), likely through HIF-1α, or indirectly by

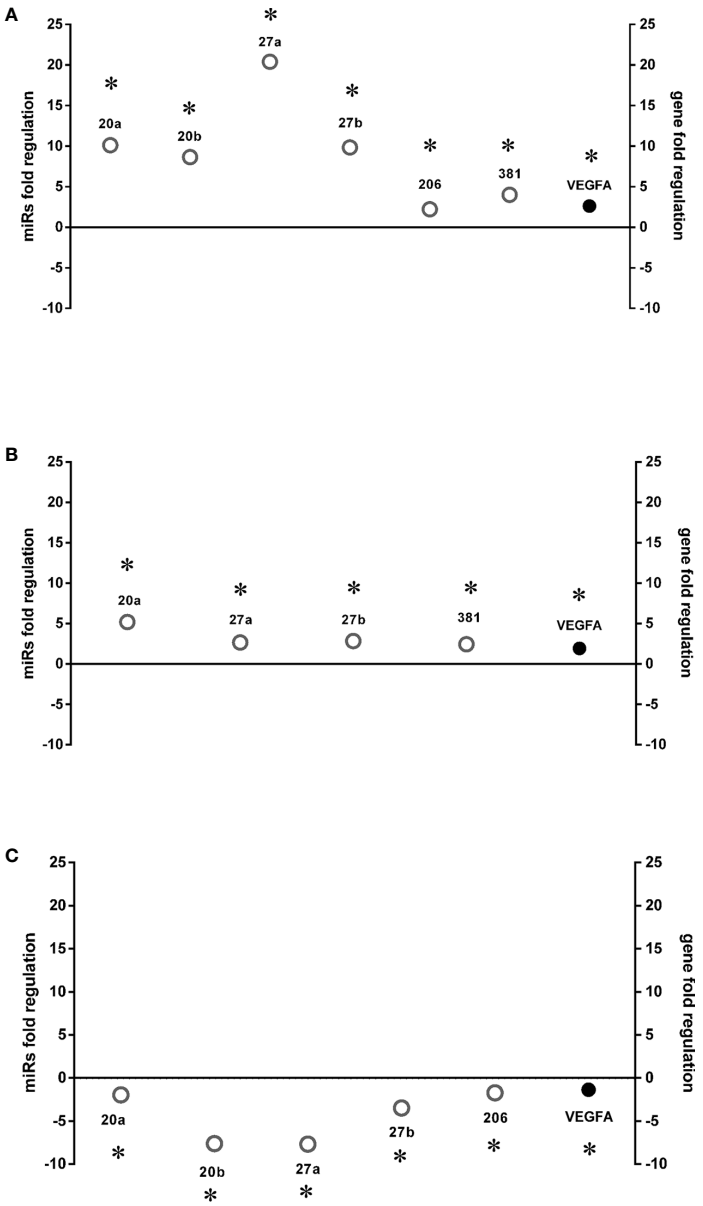

FIGURE 3 | HIF-1α stabilization induced microRNAs (miRNAs) and correlation with vascular endothelial growth factor (VEGFA) expression. Correlation of microRNAs and VEGFA expression (Fold regulation). **(A)** *p < 0.05 2 h $CoCl_2$ treatment vs. control; **(B)** *p < 0.05 8 h $CoCl_2$ vs. control (ctrl); **(C)** *p < 0.05 8h vs. 2h $CoCl_2$ treatment; (n=4).

miRNAs and the PI3K/AKT signaling pathways (**Figure 4**) (Zhou et al., 2016; Jin et al., 2018).

Therefore, our hypothesis is based on retinal angiogenesis regulated by miRNAs under hypoxic stimuli, and miRNAs can be considered alternative and/or ancillary components to VEGFA and PlGF pathways. Indeed, we analyzed other putative miRNAs targets (gene and pathways) and identified, through a bioinformatic approach, the TGFβ signaling pathway as the top-scored pathway dysregulated by identified miRNAs (**Figure 4**). Then, we found that miRNAs, dysregulated after $CoCl_2$ treatment, (miR-20a-5p, miR-20b-5p, miR-27a-3p, miR-27b-3p, miR-206-3p, miR-381-3p) influenced mRNA levels of TGFβ1, TGFβR1, TGFβR2 and SMAD2, according to experimental validated miRNA:mRNA interactions (**Figures 5** and **6**, **Table 1**). TGFβ1, TGFβR2 and SMAD2, were upregulated 2 and 8 h after HIF-1α stabilization. Interestingly, the expression of TGFβR1 receptor, which is target of most of analyzed miRNAs (**Table 1**), correlated with expression pattern shift of miRNAs at 2 h and 8 h after $CoCl_2$ treatment. Several reports support a detrimental role of TGFβR1 in DR, particularly, TGFβR1 immunoreactivity was found to be increased

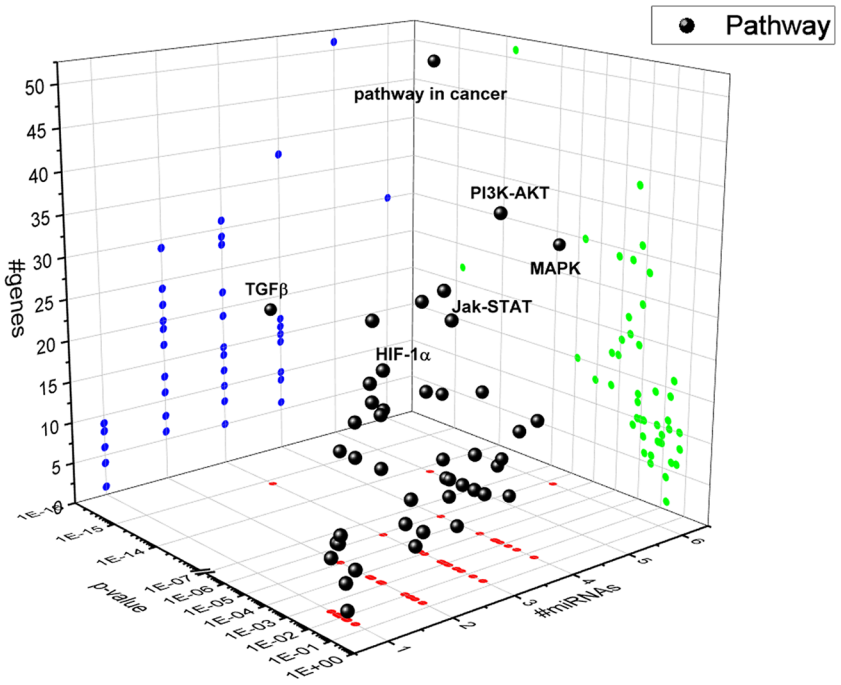

FIGURE 4 | 3D scatter plot of pathways regulated by HypoxamiRs in human retinal endothelial cells (HRECs), challenged with $CoCl_2$. Blue dots represent #gene projection of #miRNAs dimension. Green dots represent p-value projection of #genes dimension. Red dots represent #miRNA projection of p-value dimension.

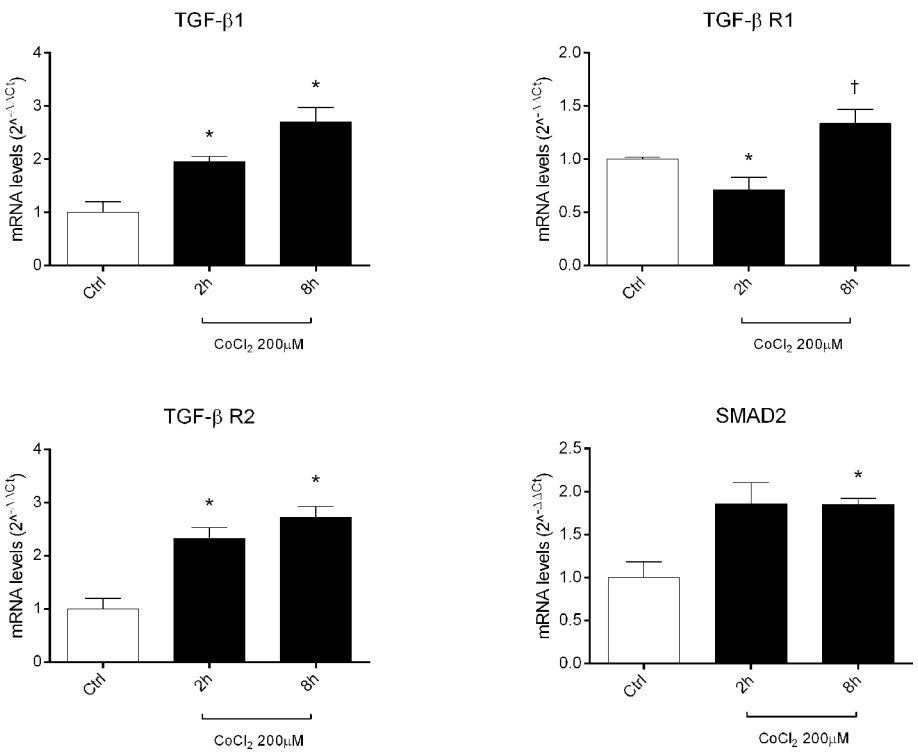

FIGURE 5 | Expression of genes of TGFβ signaling pathway in human retinal endothelial cells (HRECs) treated with $CoCl_2$, for 2 and 8 h. The mRNA levels were evaluated by qRT-PCR. Each bar represents the mean value ± SD. *$p < 0.05$ $CoCl_2$ vs. control (ctrl); †$p < 0.05$ 8h vs. 2h $CoCl_2$ treatment. (n=4).

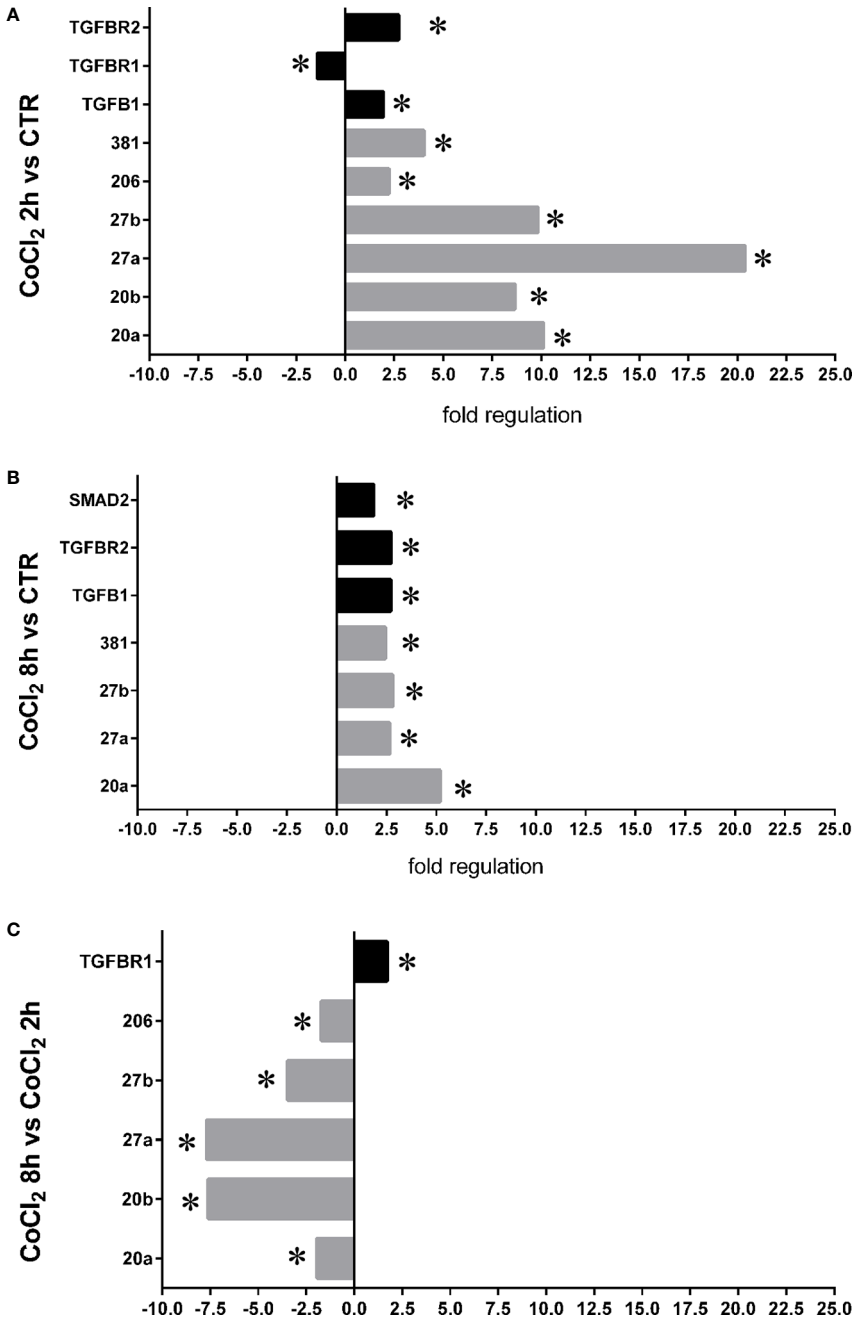

FIGURE 6 | Correlation of microRNAs (miRNAs) and TGFβ signaling pathway genes expression in human retinal endothelial cells (HRECs), under chemical hypoxic stimuli. Fold regulation of miRNAs and TGFβ signaling genes: **(A)** *p < 0.05 2 h CoCl2 treatment vs. control (ctr); **(B)** *p < 0.05 8 h CoCl2 treatment vs. control (ctr); **(C)** *p < 0.05 8 h vs. 2 h $CoCl_2$ treatment; (n=4).

in retinal capillaries of diabetic rats (Gerhardinger et al., 2009; van Geest et al., 2010).

The HIF-1/TGF-β1 axis, and related stimulation of angiogenesis, has been investigated in different experimental settings (Han et al., 2013; Mingyuan et al., 2018), including endothelial cells (Iruela-Arispe and Sage, 1993; Peshavariya et al., 2014). On the contrary, few reports demonstrated a putative link between HIF-1α/miRNAs/TGFβ signaling pathway and angiogenesis (Xing et al., 2014). Furthermore, only one study analyzed the role miRNAs in regulation of hypoxia-TGFβ-angiogenesis pathway in a model of corneal neovascularization (Zhang Y. et al., 2019). According to our findings, miR-27 was reported to be involved in regulation of HIF-1/TGFβ axis, at least in an *in vitro* model of cardiac ischemia (Zhang X. L. et al., 2019). However, there are still no evidences about

TABLE 1 | Differential expression of genes of the TGFβ signaling pathway.

Gene	Fold regulation$CoCl_2$ 2h vs CTR(p value)	Fold regulation$CoCl_2$ 8h vs CTR(p value)	Fold regulation$CoCl_2$8h vs 2h (p value)	Regulating miRNAs (tarbase)
TGFB1	1.9466 (p<0.01)	2.7128 (p<0.05)	1.3936	miR-27a
TGFBR1	−1.419 (p<0.05)	1.3352	1.7166 (p<0.05)	miR-20a, miR-27a, miR-27b, miR-20b, (microT-CDS), miR-381 (microT-CDS)
TGFBR2	2.327 (p<0.05)	2.7213 (p<0.05)	1.1694	miR-20a, miR-20b
SMAD2	1.5014	1.8547 (p<0.05)	1.2354	miR-20b, miR-206 (microT-CDS), miR-381 (microT-CDS)

The microRNAs (miRNAs), targeting each gene, were predicted with application of Tarbase, or whenever written with microT-CDS algorithm.

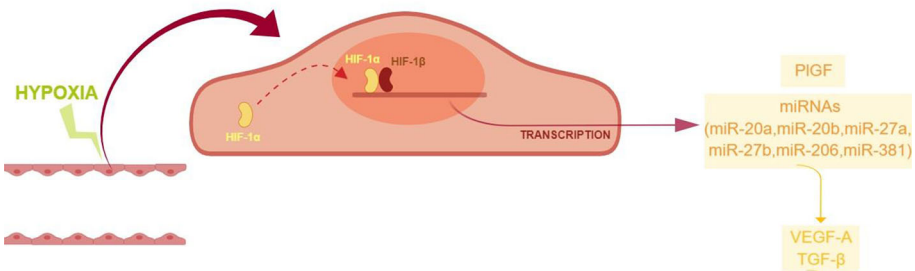

FIGURE 7 | Proposed model of angiogenic shift in retinal endothelial cells exposed to chemical hypoxia. $CoCl_2$-induced hypoxia leads to the stabilization of HIF-1α, with the subsequent translocation into the nucleus and transcription of hypoxia-related genes.

a putative link in retinal disease between hypoxia, miRNAs, VEGFA, and TGFβ pathway.

High throughput miRNA expression analysis on retinal endothelial cells, challenged with chemical hypoxic stimuli, could reveal the involvement of other miRNAs, along with the focused set analyzed in this study. However, those high throughput analyses are expensive and need quantitative qPCR validation (de Ronde et al., 2018). Despite the small set of analyzed miRNAs, our study suggested that ocular neovascularization, during hypoxia, would be promoted by the upregulation of PlGF and other factors induced by HIF-1α/miRNAs, i.e. VEGFA, and genes of the TGFβ1 signaling pathway (**Figure 7**). Therefore, these data warranting further *in vivo* studies to explore the use of pharmacological/molecular approach such as antagomiRs and agomir.

Indeed, the present findings highlighted that proangiogenic factors are worthy to be further explored as potential targets for pharmacological modulation of local retinal hypoxic events, which are generally transient but detrimental in retinal degenerations.

DATA AVAILABILITY STATEMENT

The datasets generated for this study are available on request to the corresponding author.

AUTHOR CONTRIBUTIONS

CB, MD'M, and SR made substantial contributions to conception, design, and interpretation of data. FL, MT, and CP carried out experiments. FL, MT, CP, FP, and CG carried out formal analysis of data. FL, MT, CP, and CB wrote initial draft of the manuscript. CB, MD'M, SR, FD, and MG reviewed the manuscript critically for important intellectual content and gave final approval of the version to be submitted.

FUNDING

This work was supported by National Grant PRIN 2015JXE7E8 from the Italian Ministry of Education, University and Research (MIUR) and the Italian Ministry of Economic Development (MISE) PON-Innovative PhD Program. Grant from University of Catania, Piano Triennale Ricerca Linea Intervento 2. Fondi di Ateneo 2020-2022, Università di Catania, linea intervento 4 Open Access.

SUPPLEMENTARY MATERIAL

The Supplementary Material for this article can be found online at: https://www.frontiersin.org/articles/10.3389/fphar.2020.01063/full#supplementary-material

REFERENCES

Abhinand, C. S., Raju, R., Soumya, S. J., Arya, P. S., and Sudhakaran, P. R. (2016). VEGF-A/VEGFR2 signaling network in endothelial cells relevant to angiogenesis. *J. Cell Commun. Signal.* 10, 347–354. doi: 10.1007/s12079-016-0352-8

Abu El-Asrar, A. M., Nawaz, M.II, Kangave, D., Abouammoh, M., and Mohammad, G. (2012). High-mobility group box-1 and endothelial cell angiogenic markers in the vitreous from patients with proliferative diabetic retinopathy. *Mediators Inflamm.* 2012, 697489. doi: 10.1155/2012/697489

Aiello, L. P., Arrigg, P. G., Shah, S. T., Keyt, B. A., Avery, R. L., Jampel, H. D., et al. (1994). Vascular Endothelial Growth Factor in Ocular Fluid of Patients with Diabetic Retinopathy and Other Retinal Disorders. *New Engl. J. Med.* 331, 1480–1487. doi: 10.1056/NEJM199412013312203

Ao, Q., Su, W., Guo, S., Cai, L., and Huang, L. (2015). SENP1 desensitizes hypoxic ovarian cancer cells to cisplatin by up-regulating HIF-1α. *Sci. Rep.* 5, 16396. doi: 10.1038/srep16396

Arden, G. B., and Sivaprasad, S. (2012). Hypoxia and Oxidative Stress in the Causation of Diabetic Retinopathy. *Curr. Diabetes Rev.* 7, 291–304. doi: 10.2174/157339911797415620

Arjamaa, O., and Nikinmaa, M. (2006). Oxygen-dependent diseases in the retina: Role of hypoxia-inducible factors. *Exp. Eye Res.* 83, 473–483. doi: 10.1016/j.exer.2006.01.016

Balaiya, S., Ferguson, L. R., and Chalam, K. V. (2012). Evaluation of sirtuin role in neuroprotection of retinal ganglion cells in hypoxia. *Invest. Ophthalmol. Visual Sci.* 53 (7), 4315–4322. doi: 10.1167/iovs.11-9259

Bandello, F., Berchicci, L., La Spina, C., Battaglia Parodi, M., and Iacono, P. (2012). Evidence for anti-VEGF treatment of diabetic macular edema. *Ophthal. Res.* 48, 16–20. doi: 10.1159/000339843

Bertero, T., Rezzonico, R., Pottier, N., and Mari, B. (2017). Impact of MicroRNAs in the Cellular Response to Hypoxia. *Int. Rev. Cell Mol. Biol.* 333, 91–158. doi: 10.1016/bs.ircmb.2017.03.006

Botlagunta, M., Krishnamachary, B., Vesuna, F., Winnard, P. T., Bol, G. M., Patel, A. H., et al. (2011). Expression of DDX3 is directly modulated by hypoxia inducible factor-1 alpha in breast epithelial cells. *PLoS One* 6 (3), e17563. doi: 10.1371/journal.pone.0017563

Bucolo, C., Drago, F., Lin, L. R., and Reddy, V. N. (2006). Sigma receptor ligands protect human retinal cells against oxidative stress. *NeuroReport* 17 (3), 287–291. doi: 10.1097/01.wnr.0000199469.21734.e1

Carmeliet, P., Moons, L., Luttun, A., Vincenti, V., Compernolle, V., De Mol, M., et al. (2001). Synergism between vascular endothelial growth factor and placental growth factor contributes to angiogenesis and plasma extravasation in pathological conditions. *Nat. Med.* 7, 575–583. doi: 10.1038/87904

Charnock-Jones, D. S. (2016). Placental hypoxia, endoplasmic reticulum stress and maternal endothelial sensitisation by sFLT1 in pre-eclampsia. *J. Reprod. Immunol.* 114, 81–85. doi: 10.1016/j.jri.2015.07.004

Choudhry, H., and Mole, D. R. (2016). Hypoxic regulation of the noncoding genome and NEAT1. *Briefings Funct. Genomics* 15, 174–185. doi: 10.1093/bfgp/elv050

Cottrill, K. A., Chan, S. Y., and Loscalzo, J. (2014). Hypoxamirs and mitochondrial metabolism. *Antioxid. Redox Signal.* 21, 1189–1201. doi: 10.1089/ars.2013.5641

D'Amico, A. G., Maugeri, G., Reitano, R., Bucolo, C., Saccone, S., Drago, F., et al. (2015). PACAP Modulates Expression of Hypoxia-Inducible Factors in Streptozotocin-Induced Diabetic Rat Retina. *J. Mol. Neurosci.* 57 (4), 501–509. doi: 10.1007/s12031-015-0621-7

D'Amico, A. G., Maugeri, G., Bucolo, C., Saccone, S., Federico, C., Cavallaro, S., et al. (2017). Nap Interferes with Hypoxia-Inducible Factors and VEGF Expression in Retina of Diabetic Rats. *J. Mol. Neurosci.* 61 (2), 256–266. doi: 10.1007/s12031-016-0869-6

de Ronde, M. W. J., Ruijter, J. M., Moerland, P. D., Creemers, E. E., and Pinto-Sietsma, S.-J. (2018). Study Design and qPCR Data Analysis Guidelines for Reliable Circulating miRNA Biomarker Experiments: A Review. *Clin. Chem.* 64 (9), 1308–1318. doi: 10.1373/clinchem.2017.285288

Evrard, S. M., Lecce, L., Michelis, K. C., Nomura-Kitabayashi, A., Pandey, G., Purushothaman, K. R., et al. (2016). Endothelial to mesenchymal transition is common in atherosclerotic lesions and is associated with plaque instability. *Nat. Commun.* 7, 11853. doi: 10.1038/ncomms11853

Gao, R., Zhu, B. H., Tang, S. B., Wang, J. F., and Ren, J. (2008). Scutellarein inhibits hypoxia- and moderately-high glucose-induced proliferation and VEGF expression in human retinal endothelial cells. *Acta Pharmacol. Sin.* 29 (6), 707–712. doi: 10.1111/j.1745-7254.2008.00797.x

Gao, L., Dou, Z. C., Ren, W. H., Li, S. M., Liang, X., and Zhi, K. Q. (2019). CircCDR1as upregulates autophagy under hypoxia to promote tumor cell survival via AKT/ERK½/mTOR signaling pathways in oral squamous cell carcinomas. *Cell Death Dis.* 10 (10), 745. doi: 10.1038/s41419-019-1971-9

Gee, H. E., Ivan, C., Calin, G. A., and Ivan, M. (2014). HypoxamiRs and cancer: From biology to targeted therapy. *Antioxid. Redox Signal.* 21, 1220–1238. doi: 10.1089/ars.2013.5639

Gerhardinger, C., Dagher, Z., Sebastiani, P., Yong, S. P., and Lorenzi, M. (2009). The transforming growth factor-β pathway is a common target of drugs that prevent experimental diabetic retinopathy. *Diabetes.* doi: 10.2337/db08-1008

Greco, S., Gaetano, C., and Martelli, F. (2014). HypoxamiR regulation and function in ischemic cardiovascular diseases. *Antioxid. Redox Signal.* 21, 1202–1219. doi: 10.1089/ars.2013.5403

Gupta, A., Sugadev, R., Sharma, Y. K., Ahmad, Y., and Khurana, P. (2018). Role of miRNAs in hypoxia-related disorders. *J. Biosci.* 43, 739–749. doi: 10.1007/s12038-018-9789-7

Han, W. Q., Zhu, Q., Hu, J., Li, P. L., Zhang, F., and Li, N. (2013). Hypoxia-inducible factor prolyl-hydroxylase-2 mediates transforming growth factor beta 1-induced epithelial-mesenchymal transition in renal tubular cells. *Biochim. Biophys. Acta - Mol. Cell Res.* 1833, 1454–1462. doi: 10.1016/j.bbamcr.2013.02.029

He, C., Shan, N., Xu, P., Ge, H., Yuan, Y., Liu, Y., et al. (2019). Hypoxia-induced Downregulation of SRC-3 Suppresses Trophoblastic Invasion and Migration Through Inhibition of the AKT/mTOR Pathway: Implications for the Pathogenesis of Preeclampsia. *Sci. Rep.* 9, 10349. doi: 10.1038/s41598-019-46699-3

Hu, J., Song, X., He, Y. Q., Freeman, C., Parish, C. R., Yuan, L., et al. (2012). Heparanase and vascular endothelial growth factor expression is increased in hypoxia-induced retinal neovascularization. *Invest. Ophthalmol. Visual Sci.* 53, 6810–6817. doi: 10.1167/iovs.11-9144

Huang, H., He, J., Johnson, D., Wei, Y., Liu, Y., Wang, S., et al. (2015). Deletion of placental growth factor prevents diabetic retinopathy and is associated with akt activation and HIF1α-VEGF pathway inhibition. *Diabetes* 64, 200–212. doi: 10.2337/db14-0016

Iruela-Arispe, M. L., and Sage, E. H. (1993). Endothelial cells exhibiting angiogenesis in vitro proliferate in response to TGF-β1. *J. Cell. Biochem.* 52, 414–430. doi: 10.1002/jcb.240520406

Iwase, T., Fu, J., Yoshida, T., Muramatsu, D., Miki, A., Hashida, N., et al. (2013). Sustained delivery of a HIF-1 antagonist for ocular neovascularization. *J. Controlled Release* 172 (3), 625–633. doi: 10.1016/j.jconrel.2013.10.008

Jiang, S., and Xu, Y. (2019). Annexin A2 upregulation protects human retinal endothelial cells from oxygen–glucose deprivation injury by activating autophagy. *Exp. Ther. Med.* 18 (4), 2901–2908. doi: 10.3892/etm.2019.7909

Jin, Y.-P., Hu, Y.-P., Wu, X.-S., Wu, Y.-S., Ye, Y.-Y., Li, H.-F., et al. (2018). miR-143-3p targeting of ITGA6 suppresses tumour growth and angiogenesis by downregulating PLGF expression via the PI3K/AKT pathway in gallbladder carcinoma. *Cell Death Dis.* 9, 182. doi: 10.1038/s41419-017-0258-2

Kurihara, T., Westenskow, P. D., and Friedlander, M. (2014). Hypoxia-inducible factor (HIF)/vascular endothelial growth factor (VEGF) signaling in the retina. *Adv. Exp. Med. Biol.* 801, 275–281. doi: 10.1007/978-1-4614-3209-8_35

Kwon, J. W., and Jee, D. (2018). Aqueous humor cytokine levels in patients with diabetic macular edema refractory to anti-VEGF treatment. *PLoS One* 13 (9), e0203408. doi: 10.1371/journal.pone.0203408

Lazzara, F., Fidilio, A., Platania, C. B. M., Giurdanella, G., Salomone, S., Leggio, G. M., et al. (2019). Aflibercept regulates retinal inflammation elicited by high glucose via the PlGF/ERK pathway. *Biochem. Pharmacol.* 168, 341–351. doi: 10.1016/j.bcp.2019.07.021

Lee, Y. J., Ke, C. Y., Tien, N., and Lin, P. K. (2018). Hyperhomocysteinemia Causes Chorioretinal Angiogenesis with Placental Growth Factor Upregulation. *Sci. Rep.* 8, 15755. doi: 10.1038/s41598-018-34187-z

Li, T., Hu, J., Gao, F., Du, X., Chen, Y., and Wu, Q. (2017). Transcription factors regulate GPR91-mediated expression of VEGF in hypoxia-induced retinopathy. *Sci. Rep.* 7, 45807. doi: 10.1038/srep45807

Li, Q., Pang, L., Yang, W., Liu, X., Su, G., and Dong, Y. (2018). Long non-coding RNA of myocardial infarction associated transcript (LncRNA-MIAT) promotes diabetic retinopathy by upregulating transforming growth factor-β1 (TGF-β1) signaling. *Med. Sci. Monitor.* 24, 9497–9503. doi: 10.12659/MSM.911787

Lin, K., Ye, P., Liu, J., He, F., and Xu, W. (2015). Endostar inhibits hypoxia-induced cell proliferation and migration via the hypoxia-inducible factor-1alpha/vascular endothelial growth factor pathway in vitro. *Mol. Med. Rep.* 11, 3780–3785. doi: 10.3892/mmr.2014.3131

Livak, K. J., and Schmittgen, T. D. (2001). Analysis of relative gene expression data using real-time quantitative PCR and the 2-ΔΔCT method. *Methods* 25 (4), 402–428. doi: 10.1006/meth.2001.1262

Lu, L., Zhang, H., Dong, W., Peng, W., and Yang, J. (2018). MiR-381 negatively regulates cardiomyocyte survival by suppressing Notch signaling. *In Vitro Cell. Dev. Biol. - Anim.* 54 (8), 610–619. doi: 10.1007/s11626-018-0277-z

Martinez, B., and Peplow, P. (2019). MicroRNAs as biomarkers of diabetic retinopathy and disease progression. *Neural Regen. Res.* 14 (11), 1858–1869. doi: 10.4103/1673-5374.259602

Mingyuan, X., Qianqian, P., Shengquan, X., Chenyi, Y., Rui, L., Yichen, S., et al. (2018). Hypoxia-inducible factor-1α activates transforming growth factor-β1/Smad signaling and increases collagen deposition in dermal fibroblasts. *Oncotarget* 9, 3188–3197. doi: 10.18632/oncotarget.23225

Mitsui, T., Tani, K., Maki, J., Eguchi, T., Tamada, S., Eto, E., et al. (2018). Upregulation of angiogenic factors via protein kinase c and hypoxia-induced factor-1a pathways under high-glucose conditions in the placenta. *Acta Med. Okayama* 72, 359–367. doi: 10.18926/AMO/56171

Nallamshetty, S., Chan, S. Y., and Loscalzo, J. (2013). Hypoxia: A master regulator of microRNA biogenesis and activity. *Free Radical Biol. Med.* 64, 20–30. doi: 10.1016/j.freeradbiomed.2013.05.022

Natoli, R., and Fernando, N. (2018). MicroRNA as therapeutics for age-related macular degeneration. *Adv. Exp. Med. Biol.* 1074, 37–43. doi: 10.1007/978-3-319-75402-4_5

Ozaki, H., Yu, A. Y., Della, N., Ozaki, K., Luna, J. D., Yamada, H., et al. (1999). Hypoxia inducible factor-1alpha is increased in ischemic retina: temporal and spatial correlation with VEGF expression. *Invest. Ophthalmol. Visual Sci.* 40, 182–189.

Peshavariya, H. M., Chan, E. C., Liu, G. S., Jiang, F., and Dusting, G. J. (2014). Transforming growth factor-β1 requires NADPH oxidase 4 for angiogenesis in vitro and in vivo. *J. Cell. Mol. Med.* 18, 1172–1183. doi: 10.1111/jcmm.12263

Platania, C. B. M., Maisto, R., Trotta, M. C., D'Amico, M., Rossi, S., Gesualdo, C., et al. (2019). Retinal and circulating miRNA expression patterns in diabetic retinopathy: An in silico and in vivo approach. *Br. J. Pharmacol.* 176, 2179–2194. doi: 10.1111/bph.14665

Riffo-Campos, A. L., Riquelme, I., Brebi-Mieville, P., Riffo-Campos, Á. L., Riquelme, I., and Brebi-Mieville, P. (2016). Tools for Sequence-Based miRNA Target Prediction: What to Choose? *Int. J. Mol. Sci.* 17 (12), 1987. doi: 10.3390/ijms17121987

Rodrigues, M., Kashiwabuchi, F., Deshpande, M., Jee, K., Goldberg, M. F., Lutty, G., et al. (2016). Expression pattern of HIF-1α and VEGF supports circumferential application of scatter laser for proliferative sickle retinopathy. *Invest. Ophthalmol. Visual Sci.* 57 (15), 6739–6746. doi: 10.1167/iovs.16-19513

Romano, G. L. G. L., Platania, C. B. M. C. B., Drago, F., Salomone, S., Ragusa, M., Barbagallo, C., et al. (2017). Retinal and Circulating miRNAs in Age-Related Macular Degeneration: An In vivo Animal and Human Study. *Front. Pharmacol.* 8, 168. doi: 10.3389/fphar.2017.00168

Rosen, R., Vagaggini, T., Chen, Y., and Hu, D. N. (2015). Zeaxanthin 7inhibits hypoxia-induced VEGF secretion by RPE cells through decreased protein levels of hypoxia-inducible factors-1 α. *BioMed. Res. Int.* 2015, 687386. doi: 10.1155/2015/687386

Saddala, M. S., Lennikov, A., Grab, D. J., Liu, G. S., Tang, S., and Huang, H. (2018). Proteomics reveals ablation of PlGF increases antioxidant and neuroprotective proteins in the diabetic mouse retina. *Sci. Rep.* 8, 16728. doi: 10.1038/s41598-018-34955-x

Schmetterer, L., and Wolzt, M. (1999). Ocular blood flow and associated functional deviations in diabetic retinopathy. *Diabetologia* 42, 387–405. doi: 10.1007/s001250051171

Schmidl, D., Schmetterer, L., Garhöfer, G., and Popa-Cherecheanu, A. (2015). Gender differences in ocular blood flow. *Curr. Eye Res.* 40, 201–212. doi: 10.3109/02713683.2014.906625

Shao, J., and Yao, Y. (2016). Transthyretin represses neovascularization in diabetic retinopathy. *Mol. Vision* 22, 1188–1197.

Stafiej, J., Kazmierczak, K., Linkowska, K., Zuchowski, P., Grzybowski, T., and Malukiewicz, G. (2018). Evaluation of TGF-Beta 2 and VEGFalpha Gene Expression Levels in Epiretinal Membranes and Internal Limiting Membranes in the Course of Retinal Detachments, Proliferative Diabetic Retinopathy, Macular Holes, and Idiopathic Epiretinal Membranes. *J. Ophthalmol.* 2018, 8293452. doi: 10.1155/2018/8293452

Tsai, H. C., Tzeng, H. E., Huang, C. Y., Huang, Y. L., Tsai, C. H., Wang, S. W., et al. (2017). WISP-1 positively regulates angiogenesis by controlling VEGF-A expression in human osteosarcoma. *Cell Death Dis.* 13, e2750. doi: 10.1038/cddis.2016.421

Tudisco, L., Ragione, F. D., Tarallo, V., Apicella, I., D'Esposito, M., Matarazzo, M. R., et al. (2014). Epigenetic control of hypoxia inducible factor-1α-dependent expression of placental growth factor in hypoxic conditions. *Epigenetics* 9, 600–610. doi: 10.4161/epi.27835

Van Bergen, T., Etienne, I., Cunningham, F., Moons, L., Schlingemann, R. O., Feyen, J. H. M., et al. (2019). The role of placental growth factor (PlGF) and its receptor system in retinal vascular diseases. *Prog. Retin. Eye Res.* 69, 116–136. doi: 10.1016/j.preteyeres.2018.10.006

van Geest, R. J., Klaassen, I., Vogels, I. M. C., van Noorden, C. J. F., and Schlingemann, R. O. (2010). Differential TGF-β signaling in retinal vascular cells: A role in diabetic retinopathy? *Invest. Ophthalmol. Visual Sci.* 51 (4), 1857–1865. doi: 10.1167/iovs.09-4181

Veliceasa, D., Biyashev, D., Qin, G., Misener, S., Mackie, A. R., Kishore, R., et al. (2015). Therapeutic manipulation of angiogenesis with miR-27b. *Vasc. Cell.* 7, 6. doi: 10.1186/s13221-015-0031-1

Vlachos, I. S., Zagganas, K., Paraskevopoulou, M. D., Georgakilas, G., Karagkouni, D., Vergoulis, T., et al. (2015). DIANA-miRPath v3.0: deciphering microRNA function with experimental support. *Nucleic Acids Res.* 43, W460–W466. doi: 10.1093/nar/gkv403

Wang, J., Wu, S., and Huang, T. (2018). Expression and role of VEGFA and miR-381 in portal vein tumor thrombi in patients with hepatocellular carcinoma. *Exp. Ther. Med.* 15, 5450–5456. doi: 10.3892/etm.2018.6129

Xing, Y., Hou, J., Guo, T., Zheng, S., Zhou, C., Huang, H., et al. (2014). MicroRNA-378 promotes mesenchymal stem cell survival and vascularization under hypoxic-Ischemic conditions in vitro. *Stem Cell Res. Ther.* 5 (6), 130. doi: 10.1186/scrt520

Yue, J., Guan, J., Wang, X., Zhang, L., Yang, Z., Ao, Q., et al. (2013). MicroRNA-206 is involved in hypoxia-induced pulmonary hypertension through targeting of the HIF-1α/Fhl-1 pathway. *Lab. Investig.* 93 (7), 748–759. doi: 10.1038/labinvest.2013.63

Zeng, M., Shen, J., Liu, Y., Lu, L. Y., Ding, K., Fortmann, S. D., et al. (2017). The HIF-1 antagonist acriflavine: visualization in retina and suppression of ocular neovascularization. *J. Mol. Med.* 95 (4), 417–429. doi: 10.1007/s00109-016-1498-9

Zhang, X. L., An, B. F., and Zhang, G. C. (2019). MiR-27 alleviates myocardial cell damage induced by hypoxia/reoxygenation via targeting TGFBR1 and inhibiting NF-κB pathway. *Kaohsiung J. Med. Sci.* 35 (10), 607–614. doi: 10.1002/kjm2.12092

Zhang, Y., Yuan, F., Liu, L., Chen, Z., Ma, X., Lin, Z., et al. (2019). The Role of the miR-21/SPRY2 Axis in Modulating Proangiogenic Factors, Epithelial Phenotypes, and Wound Healing in Corneal Epithelial Cells. *Invest. Ophthalmol. Visual Sci.* 60, 3854–3862. doi: 10.1167/iovs.19-27013

Zhou, Y., Tu, C., Zhao, Y., Liu, H., and Zhang, S. (2016). Placental growth factor enhances angiogenesis in human intestinal microvascular endothelial cells via PI3K/Akt pathway: Potential implications of inflammation bowel disease. *Biochem. Biophys. Res. Commun.* 470, 967–974. doi: 10.1016/j.bbrc.2016.01.073

Zimna, A., and Kurpisz, M. (2015). Hypoxia-Inducible factor-1 in physiological and pathophysiological angiogenesis: Applications and therapies. *BioMed. Res. Int.* 2015, 549412. doi: 10.1155/2015/549412

Conflict of Interest: The authors declare that the research was conducted in the absence of any commercial or financial relationships that could be construed as a potential conflict of interest.

frontiers in Pharmacology

ORIGINAL RESEARCH
published: 04 September 2020
doi: 10.3389/fphar.2020.573238

Changes of Ocular Dimensions as a Marker of Disease Progression in a Murine Model of Pigmentary Glaucoma

Michał Fiedorowicz[1,2†], Marlena Wełniak-Kamińska[1,2†], Maciej Świątkiewicz[1,2], Jarosław Orzeł[2,3], Tomasz Chorągiewicz[4], Mario Damiano Toro[4,5], Robert Rejdak[4], Piotr Bogorodzki[2,3] and Paweł Grieb[1]*

[1] Department of Experimental Pharmacology, Mossakowski Medical Research Centre, Polish Academy of Sciences, Warsaw, Poland, [2] Small Animal Magnetic Resonance Imaging Laboratory, Mossakowski Medical Research Centre, Polish Academy of Sciences, Warsaw, Poland, [3] Faculty of Electronics and Information Technology, Warsaw University of Technology, Warsaw, Poland, [4] Department of General Ophthalmology, Medical University of Lublin, Lublin, Poland, [5] Faculty of Medical Sciences, Collegium Medicum, Cardinal Stefan Wyszyński University, Warsaw, Poland

OPEN ACCESS

Edited by:
Claudio Bucolo,
University of Catania, Italy

Reviewed by:
Simona Gabriela Bungau,
University of Oradea, Romania
Javier Sancho-Pelluz,
Catholic University of Valencia San Vicente Mártir, Spain

***Correspondence:**
Michał Fiedorowicz
mfiedorowicz@imdik.pan.pl

[†]These authors have contributed equally to this work

Specialty section:
This article was submitted to Inflammation Pharmacology, a section of the journal Frontiers in Pharmacology

Received: 16 June 2020
Accepted: 17 August 2020
Published: 04 September 2020

Citation:
Fiedorowicz M, Wełniak-Kamińska M, Świątkiewicz M, Orzeł J, Chorągiewicz T, Toro MD, Rejdak R, Bogorodzki P and Grieb P (2020) Changes of Ocular Dimensions as a Marker of Disease Progression in a Murine Model of Pigmentary Glaucoma. Front. Pharmacol. 11:573238. doi: 10.3389/fphar.2020.573238

Purpose: The elevation of intraocular pressure (IOP), a major risk factor in glaucoma, is an important parameter tracked in experimental models of this disease. However, IOP measurement in laboratory rodents is challenging and may not correlate with some key pathological events that occur in the development of glaucoma. The aims of this study were to quantify changes in ocular morphology in DBA/2J mice that develop spontaneous, age-dependent, pigmentary glaucoma and to check the possible correlation of these parameters with IOP.

Method: Eye morphology was evaluated with MRI in DBA/2J, DBA/2J-Gpnmb^{+}/SjJ, and C57BL/6J female mice ages 3, 6, 9, 12, and 15 months. The animals were anesthetized with isoflurane. A planar receive-only surface coil (inner diameter = 10 mm) was placed over each animal's left eye and the image was acquired with a 7T small animal-dedicated magnetic resonance tomograph and T2-weighted TurboRARE sequence. Ocular dimensions were manually quantitated using OsiriX software. IOP was measured with rebound tonometry.

Results: In the control animals, no age-related changes in the ocular morphology were noted. Since 6 months of age, the anterior chamber deepening and elongation of the eyeballs of DBA/2J mice was detectable. We found a significant, positive correlation between IOP and axial length, anterior chamber area, or anterior chamber width in C57BL/6J mice but not in DBA/2J mice. However, after excluding the measurements performed in the oldest DBA/2J mice (i.e. analyzing only the animals ages 3 to 12 months), we demonstrated a significant positive correlation between IOP and anterior chamber width.

Conclusion: High-resolution magnetic resonance imaging of the eye area in mice enables reproducible and consistent measures of key dimensions of the eyeball. We observed

age-dependent alterations in the eye morphology of DBA/2J mice that mostly affected the anterior chamber. We also demonstrated a correlation between some of the ocular dimensions and the IOP of C57Bl/6J mice and DBA/2J mice with moderately advanced glaucomatous pathology.

Keywords: glaucoma, ocular dimensions, ocular biomechanics, intraocular pressure, DBA/2J, MRI

INTRODUCTION

Glaucoma is a heterogeneous group of chronic disorders characterized by a relatively selective, progressive loss of retinal ganglion cells and their axons which form the optic nerve. It is the most common cause of irreversible blindness worldwide, currently affecting almost 80 million people (Tham et al., 2014), or more than 1% of the global population. Ocular hypertension (OH) is a major and modifiable risk factor for the onset and progression of glaucoma. Lowering intraocular pressure (IOP), currently the only accepted method of glaucoma treatment, may be achieved pharmacologically, and in some cases surgically (Crawley et al., 2012; Lusthaus and Goldberg, 2019).

Treatments aimed at decreasing IOP are ineffective in many cases. Surgical intervention, considered the most effective procedure for lowering IOP in uncontrolled glaucoma with OH, is not available to the vast majority of patients in need; similarly, surgery is unavailable to more than three-quarters of patients suffering from vision impairment due to cataract or uncorrected refractive error, conditions that are fully treatable surgically (Flaxman et al., 2017). Moreover, glaucoma surgery is risky, because of various potentially dangerous complications (Giovingo, 2014). Pharmacological treatment, on the other hand, requires lifelong daily instillation of IOP-lowering eye drops, and this type of drug formulation suffers from particularly low long-time adherence and persistence (Yeaw et al., 2009). Considering the above, there is an urgent need to develop more efficacious methods for chronic IOP control.

The assessment of safety and efficacy of a new treatment with the use of animal models is usually a prerequisite for initiating the clinical development phase. The preclinical assessment of drugs aimed at lowering IOP has been traditionally performed on monkeys with artificially increased IOP (Wang et al., 2000), but such experiments are prohibitively expensive and currently rarely conducted due to ethical reasons. Instead, following the development of non-invasive technologies of IOP measurement applicable to small animals, IOP-dependent rodent models have become popular, in which OH is artificially induced (Millar and Pang, 2015; Biswas and Wan, 2019). Although these models reproduce certain aspects of human glaucoma, since retinal ganglion cell (RGC) loss does not develop naturally, an increase in IOP is usually abrupt and may not be long-lasting, and inflammatory components due to physical injury may be a confounding factor.

Few rodent models of IOP-dependent glaucoma have been described in which no surgical intervention is required and the disease develops spontaneously with age (Chen and Zhang, 2015). Among them, the most popular involves the DBA/2J strain of mice. Its predecessor, the original DBA strain initiated in 1909 at Harvard University, is the oldest of all inbred murine strains (Harada et al., 2019; Jackson Laboratory, 2020). DBA/2J mice develop progressive eye abnormalities that mimic human pigmentary glaucoma. The onset of disease symptoms begins between three and four months of age. Mutations in glycoprotein nonmetastatic melanoma protein B (*Gpnmb*) and tyrosinase-related protein 1 (*Tyrp1*) genes causing iris atrophy and iris pigment dispersion leading to elevated IOP, although OH is not the only causative factor (Anderson et al., 2006; Scholz et al., 2008).

In spite of the popularity of this model among investigators, the development of glaucoma in the DBA/2J mouse is highly variable, presenting significant challenges for preclinical studies of anti-glaucoma therapies. In particular, IOP measurements may be confounded by factors such as corneal calcification, etc. (Turner et al., 2017). On the other hand, imaging techniques such as whole-eye optical coherence tomography (Chou et al., 2011) and dynamic, contrast-enhanced magnetic resonance imaging (MRI) (Crosbie et al., 2019) revealed characteristic, age-dependent changes of eyeball morphology in DBA/2J mice, including an increased anterior chamber depth. Such structural changes did not occur in the control C57Bl/2J mice; therefore they seem to stem from chronic OH. However, contributions from other genetic factors differentiating these two strains of mice cannot be excluded. Despite some available data on changes in ocular morphology in DBA/2J mice (Chou et al., 2011; Crosbie et al., 2019), the age-related changes in ocular morphology in the course of spontaneous glaucoma were not extensively characterized to date. In particular, the correlation between the ocular dimensions and IOP needs further investigation with imaging methods that allow *in vivo* evaluation of the whole eye globe. Such data would be crucial for future application of selected ocular dimensions as imaging markers of the glaucoma progression and effectiveness of IOP-lowering therapies in this model of glaucoma.

The primary aim of this study was to evaluate age-dependent changes in the ocular morphology in the course of glaucoma in DBA/2J mice. We also aimed to verify the hypothesis that parameters describing ocular morphology correlate with IOP. Age-matched DBA/2J-Gpnmb^{+}/SjJ and C57BL/6J mice were used as controls.

MATERIALS AND METHODS

Animals

All experimental procedures were performed in compliance with the ARVO Statement for the Use of Animals in Ophthalmic and

Vision Research and in accordance with the provisions for animal care and use described in the European Communities council directive of September 22, 2010 (2010/63/EU) and respective local regulations for animal experiments; the experiments were approved by the respective local ethics committee (Warsaw IV Local Ethics Committee, approval nos. 88/2012, 94/2012, 11/2015). The experiment was performed on three groups: (1) DBA/2J model of glaucoma (n = 10); (2) C57BL/6J (n = 10; RRID : IMSR_JAX:000664) which were obtained from the murine breeding colony at the Mossakowski Medical Research Centre; and (3) the DBA/2J-Gpnmb^{+}/SjJ mice (n = 8, RRID : IMSR_JAX:000664) which were obtained from Jackson Laboratory. Due to the fact that DBA/2J females develop iris atrophy and glaucoma earlier than males (John et al., 1998; Anderson et al., 2001), all mice used in this study were female. The same mice were examined at 3, 6, 9, 12, and 15 months of age. Mice were maintained in the Mossakowski Medical Research Centre animal house at 12 h-12 h light-dark cycle and were provided a standardized diet and water *ad libitum*.

Administration of Manganese Chloride

To visualize the neural retina by the manganese-enhanced magnetic resonance imaging (MEMRI), a solution of manganese chloride (0.1 mol/L, Sigma Aldrich, Steinheim, Germany) was administered intraperitoneally (66 mg/kg body weight) 24 h prior to the imaging session (Calkins et al., 2008).

Magnetic Resonance Imaging

Animals were anesthetized with isoflurane (4% of isoflurane in oxygen for induction, 2% in oxygen for maintenance); this concentration was chosen to minimize eye movements during the acquisition (Woodward et al., 2007). Subsequently, the animals were positioned on a dedicated mice scan bed (Bruker, Ettlingen, Germany), and a planar receive-only surface coil (inner diameter = 10 mm; Bruker BioSpin, Ettlingen, Germany) was placed over the left eye of each animal. A rodent-dedicated 7T magnetic resonance (MR) tomograph (BioSpec 70/30USR Bruker, Ettlingen, Germany) was equipped with a transmit coil (inner diameter = 86 mm, Bruker). Physiological monitoring, including respiration rate and body temperature, was performed throughout the imaging sessions with an MR-compatible system (SA Instruments, Stony Brook, NY, USA). Details of the imaging protocol included:

1. Structural, high-resolution images were acquired with a T2-weighted TurboRARE sequence (TR/TEeff = 2700/30 ms, RARE factor = 8, NA = 12, spatial resolution = 0.62 mm x 0.62 mm x 0.3 mm, slices = 7, no gaps, scan time 16 min);
2. Visualization of accumulated manganese (MEMRI) with FLASH T1-weighted 3D sequence (TR/TE = 48/4 ms, NA = 5, FA = 25°, spatial resolution 68 µm x 68 µm x 68 µm, scan time 28 min).

Evaluation of Eye and Optic Nerve Dimensions

Ocular and optic nerve dimensions and areas were manually delineated and calculated with OsiriX software (version 5.8.2, 32 bit; Pixmeo, SARL, Bermex, Switzerland, RRID : SCR_013618) by a researcher unaware of the animal group or age. All measurements were performed on the middle image, i.e. the one with the visible optic nerve head and the largest pupil diameter (Chou et al., 2011). Areas of the anterior chamber (AC), lens (L), vitreous cavity (VC), and retina (R) were measured as shown in **Figure 1A**. The axial length (AL), horizontal length (HL), anterior chamber depth (ACD), anterior chamber width (ACW), lens thickness (LT), vitreous chamber depth (VCD), retinal thickness (RT [measured 0.5 mm from the optic disc center]), optic nerve head diameter (ONH), and iridocorneal angle were also measured (**Figure 1B**). The AL, ACD, LT, and VCD distances were appointed along the eye axial line passing through the center of the pupil and the center of optic nerve head. AL was established as the distance between the anterior cornea surface and the center sclera level of the

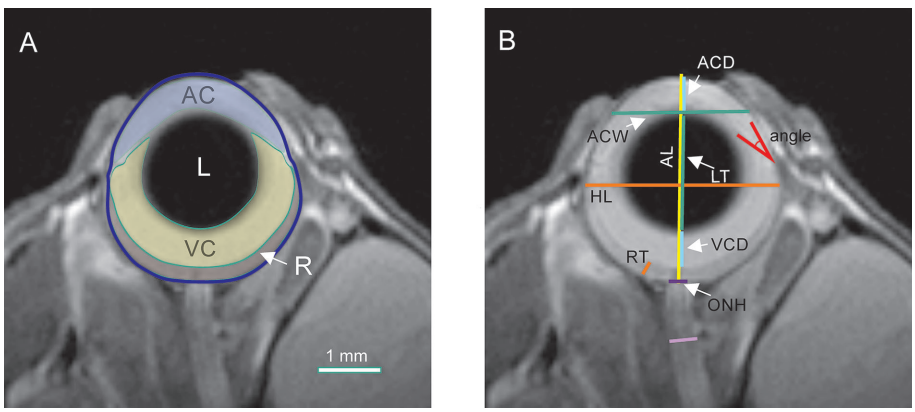

FIGURE 1 | Quantification of ocular morphology. **(A)** Areas of anterior chamber (AC), lens (L), vitreous chamber (VC), and retina (R). **(B)** Dimensions: axial length (AL), equatorial diameter (ED), anterior chamber depth (ACD), anterior chamber width (ACW), lens thickness (LT), vitreous chamber depth (VCD), retinal thickness (RT), optic nerve head diameter (ONH), and optic nerve diameter (ON).

intraocular optic nerve. The ED measurement was made at the widest place of the eye globe below the *ora serrata*. The RT was appointed as the distance between the nerve fiber layer and the retinal pigment epithelium (RPE).

The ACD was used to compute the corneal radius of curvature (CRC) according to the method described by Tkatchenko et al. (2010).

$$CRC = (ACD/2) + ACW^2/(8\ x\ ACD)$$

The first measurement of the optic nerve was performed on the ONH at the level of the sclera. The second was on the intraorbital segment of the optic nerve, below 0.8 mm behind the globe where myelinization of the nerve fibers starts (May and LüTjen-Drecoll, 2002).

IOP Measurements

A rodent-dedicated rebound tonometer (TonoLab; Icare, Finland) was used for IOP measurements as we described previously (Fiedorowicz et al., 2018; Świątkiewicz et al., 2020). In brief, the probe tip was situated in the long axis of the eye at 1 mm to 2 mm distance from the eye. Six valid measurements were acquired and the result was calculated as the mean of four readings (after excluding two outlier readings), which was displayed as a single reading. The measurement procedure was repeated three times for each eye. The measurements were performed on conscious animals to avoid the influence of anesthesia on IOP (Camras et al., 2010). To reduce the animals' stress during immobilization, habituation sessions took place on five consecutive days before the measurements. To exclude the influence of diurnal variations, all IOP measurements were performed at the same time each day (10 a.m. to 12 a.m.).

Statistical Analysis

Statistical analysis was performed with Statistica for Windows software (version 10, StatSoft, Inc. Tulsa, OK, USA, www.statsoft.com, RRID : SCR_014213) and GraphPad Prism (version 8.3.0, GraphPad Software, San Diego, CA, USA, www.GraphPad.com, RRID : SCR_002798). In cases of morphometric parameters or IOP, a two-way ANOVA followed by a Dunnett multiple comparisons test or a Sidak's test were used. MEMRI results were analyzed with Kruskal-Wallis non-parametric ANOVA followed by Dunn's multiple comparisons *post hoc* test. Data are presented as mean ± standard deviation. Differences were regarded as significant for $P < 0.05$. Spearman's rank correlation analysis was performed with GraphPad Prism. Correlations were regarded as significant for $P < 0.05$.

RESULTS

Anatomical images of the eye revealed no remarkable changes in the morphology of C57BL/6J (**Figures 2A–E**) or DBA/2J-Gpnmb$^+$/SjJ mice (**Figures 2F–J**). No differences were observed between the 3-month-old DBA/2J mice and the animals from the other groups. However, from 6 months of age, deepening of the anterior chamber was clearly visible in DBA/2J mice (**Figure 2K–O**) as well as optic disc cupping.

Quantitative analyses of these images confirmed these findings (**Figure 3**). No significant differences were noted in the ocular morphology between the control animals at any time. Parameters of the eye globe size in 3-month-old animals of different strains did not differ significantly: The eye globe area in DBA/2J was 8.592 ± 0.115 mm^2; in DBA/2J-Gpnmb$^+$/SjJ it was 8.490 ± 0.271 mm^2; and in C57BL/6J it was 8.302 ± 0.113 mm^2. However, from 6 months of age we noted anterior chamber deepening as well as enlargement and elongation of the eyeball in DBA/2J. Between the third and ninth months of age, the eye globe area increased by about 22% in DBA/2J, 12% in DBA/2J-Gpnmb$^+$/SjJ, and 3.0% in C57BL/6J. The eyeball lengthened in DBA/2J mice with age. AL was slightly longer in 3-month-old

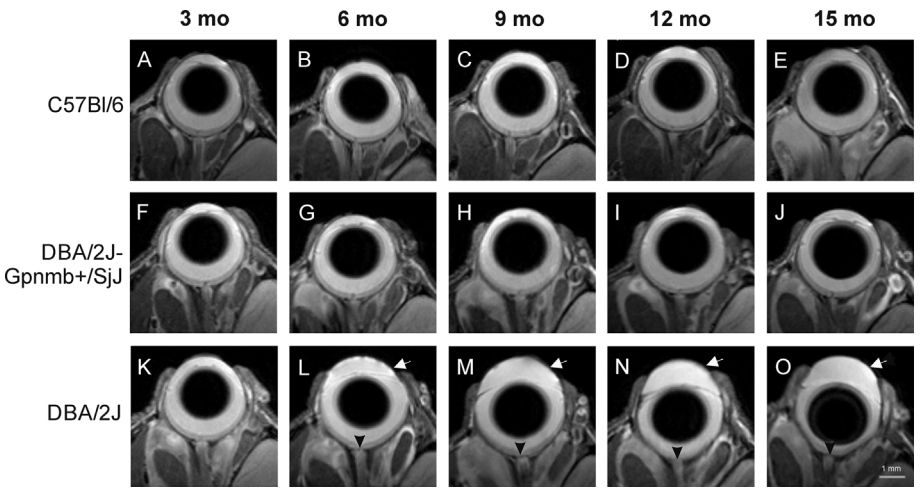

FIGURE 2 | Age-dependent changes in eye morphology in C57BL/6J (first row, **A–E**), DBA/2J-Gpnmb$^+$/SjJ (second row, **F–J**), and DBA/2J (third row, **K–O**) mice. DBA/2J mice display anterior chamber deepening (arrow) and optic disc cupping (arrowhead).

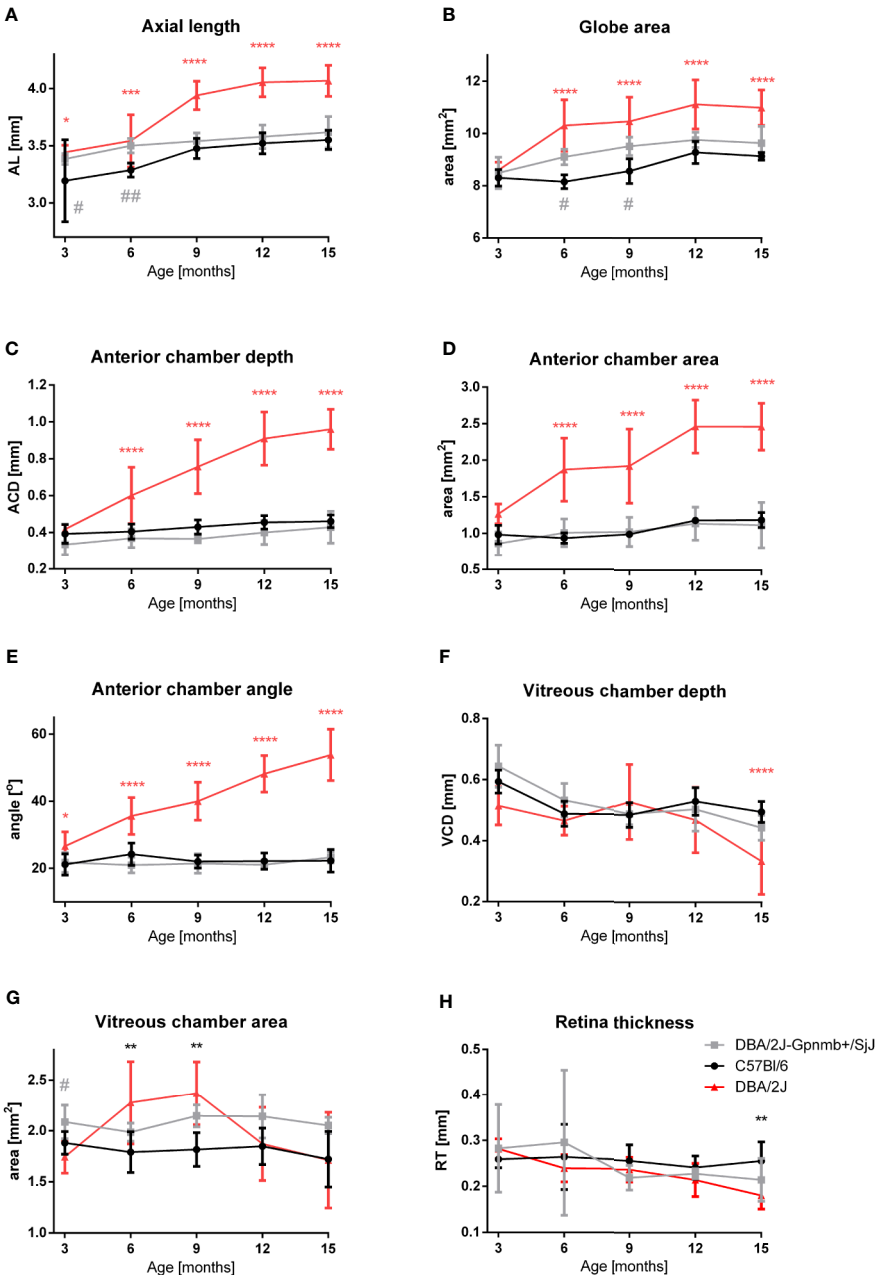

FIGURE 3 | Quantitative analysis of eye morphology in C57BL/6J, DBA/2J-Gpnmb+/SjJ, and DBA/2J mice. **(A)** axial length, **(B)** globe area, **(C)** anterior chamber depth, **(D)** anterior chamber area, **(E)** iridocorneal angle, **(F)** vitreous chamber depth, **(G)** vitreous chamber area, and **(H)** retinal thickness. Means ± SD. *P < 0.05, **P < 0.01, ***P < 0.001, ****P < 0.0001 DBA/2J vs. C57BL/6J; #P < 0.05, ##P < 0.01 DBA/2J-Gpnmb$^+$/SjJ vs. C57BL/6J. Two-way ANOVA followed by Dunnet's multiple comparisons test.

DBA (3.442 ± 0.024 vs. DBA/2J-Gpnmb$^+$/SjJ; P < 0.05; 3.383 ± 0.017 mm and C57BL/6J 3.193 ± 0.127 mm; P < 0.05) and from 6 months, AL significantly increased with age in DBA/2J mice. The most prominent elongation of AL in DBA/2J was from 6 months (3.542 ± 0.072 mm) to 9 months (3.939 ± 0.039 mm), compared with control mice (DBA/2J-Gpnmb$^+$/SjJ at 6 months AL = 3.499 ± 0.022 mm; P < 0.0001 and at 9 months 3.539 ± 0.027 mm; P < 0.0001; C57BL/6J in 6 months had 3.285 ± 0.20 mm; P < 0.0001 and in 9 months 3.476 ± 0.028 mm; P < 0.0001).

Anterior chamber enlargement seemed to contribute mainly to AL elongation. No significant differences were noted in 3-month-old mice between strains in ACD (DBA/2J 0.418 ± 0.010 mm; DBA/2J-Gpnmb$^+$/SjJ 0.334 ± 0.020; C57BL/6J 0.393 ± 0.018 mm)

and in ACA (1.265 ± 0.052; 0.859 ± 0.072;.982 ± 0.045mm^2; respectively). Thereafter, the ACD and ACA constantly increased in DBA/2J. The most pronounced ACD and ACA enlargement was in older DBA/2J mice. In 15-month-old DBA/2J mice, ACD was 0.961 ± 0.034 mm and ACA was 2.460 ± 0.134 mm^2 vs. DBA/2J-Gpnmb$^+$/SjJ ACD 0.429 ± 0.031 mm; P < 0.0001; ACA 1.113 ± 0.179 mm^2; P < 0.0001 and C57BL/6J ACD 0.461 ± 0.011 mm; P < 0.0001; ACA 1.185 ± 0.046 mm^2; P < 0.0001.

Similarly, we noted only a slight difference in the anterior chamber angle in 3-month-old animals (DBA/2J 26.620 ± 1.610^0 vs. DBA/2J-Gpnmb+/SjJ 21.757 ± 1.323^0; P < 0.05; P < 0.05; DBA/2J vs. C57BL/6J 21.163 ± 1.117^0; P < 0.05). However, in older DBA/2J mice the angle constantly widened and in 15-month-old animals it reached 53.794 ± 2.714^0. In the other strains, the angle remained stable (in DBA/2J-Gpnmb$^+$/SjJ: 23.258 ± 0.631^0; P < 0.0001 and in C57BL/6J: 22.256 ± 1.178^0; P < 0.0001). However, no significant changes in CRC between strains were noted at any time.

The area of the vitreous chamber was higher in 9-month-old mice (2.369 mm^2 ± 0.311, P < 0. 05) than in the 3-month-old DBA/2J mice (1.743 ± 0.159 mm^2). In older animals, VCA was similar as in the 3-month-old mice. Such an increase was not observed in either of the control strains. However, the depth of the vitreous body significantly dropped between the twelfth and fifteenth months in DBA/2J mice (0.470 ± 0.108 mm vs. 0.334 ± 0.109 mm, P < 0.01). In the control strains, VCD remained relatively stable. We did not notice significant differences in the lens area between the strains at any time.

A significant decrease in RT was observed in 15-month-old DBA/2J mice – it was 35.6% thinner than that of the 3-month-old animals (0.282 ± 0.022 mm vs. 0.182 ± 0.030 mm, respectively P < 0.0001). It was also significantly thinner than in the C57BL/6J mice (0.257 ± 0.042 mm, P < 0.001). However, we noted no significant differences in RT between C57BL/6J and DBA/2J-Gpnmb$^+$/SjJ mice at any time. In 18-month-old animals, manganese administration revealed a significantly higher signal enhancement in C57BL/6J mice than in DBA/2J mice (**Figure 4**). No significant changes in the optic nerve diameter were observed.

Age-dependent changes in the IOP were observed (**Figure 5**). When compared to 3-month-old mice, in 6-month-old DBA/2J mice, the IOP increased by 34.6% (13.3 ± 1.6 mm Hg vs. 18.8 ± 6.4 mm Hg); in 9-month-old mice it increased by 35.9% (19.1 ± 5.8 mm Hg); and it increased 47.5% in 12-month-old mice (19.9 ± 4.9 mm Hg). Between the twelfth and fifteenth months in DBA/2J mice, we observed a decrease in the IOP (15.7 ± 2.6 mm Hg). In C57BL/6J mice, the IOP increased in 12-month-old animals by 25.1% (11.7 ± 1.7 mm Hg in 3-month-old mice vs. 14.4 ± 1.6 mm Hg in 12-month-old mice) and by 23.6% in

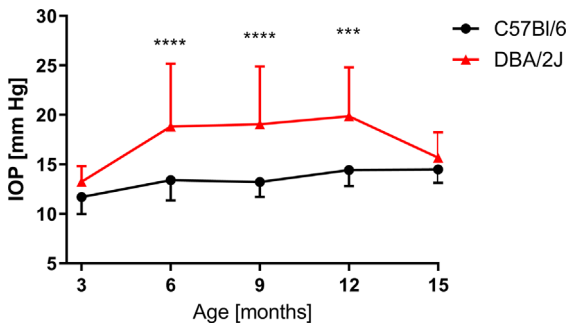

FIGURE 5 | Intraocular pressure (IOP) measured for DBA/2J (3 months, n = 12; 6 months, n = 40; 9 months, n = 34; 12 months, n = 38; 15 months, n = 42), for C57BL/6J (3 months, n = 17; 6 months, n = 27; 9 months, n = 14; 12 months, n = 14; 15 months, n = 19). Two-way ANOVA and *post hoc* Sidak's test: ***P < 0.001, ****P < 0.0001. Means and SD (for the sake of clarity, error bars are drawn only above, for DBA/2J, or below, for C57Bl/6, the point representing mean values).

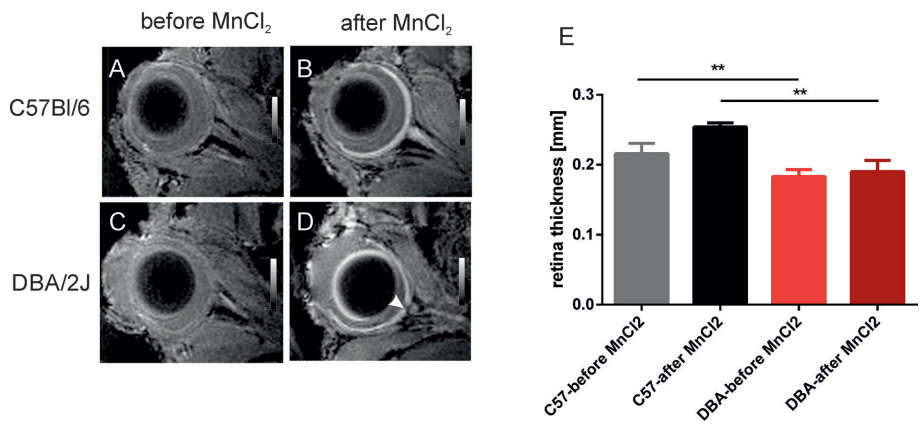

FIGURE 4 | Visualization and quantification of the retina after systemic administration of manganese. Left panel shows representative T1-weighted images of the eyes before **(A, C)** and 24 h after **(B, D)** intraperitoneal injection of manganese chloride in C57BL/6J **(A, B)** and DBA/2J mice **(C, D)**. The arrowhead indicates optic disc cupping in DBA/2J mice. **(E)** Results of quantification of retina thickness in these mice before and after $MnCl_2$ administration. **P < 0.01; Kruskal-Wallis non-parametric ANOVA followed by Dunn's multiple comparisons test.

15-month-old animals (14.5 ± 1.3 mm Hg) when compared to 3-month-old mice. We analyzed the IOP in 3- and 6-month-old DBA/2J-Gpnmb^{+}/SjJ mice and noted no significant differences between those and age-matched C57BL/6J.

The analysis of correlation between various parameters related to ocular morphology and the IOP revealed a significant positive correlation for AL (R^2 = 0.273, P = 0.0005), ACA (R^2 = 0.139, P = 0.016), and ACW (R^2 = 0.137, P = 0.026) in C57BL/6J mice (**Figures 6A, D, G**). On the contrary, such analysis in DBA/2J mice revealed no significant correlations (**Figures 6B, E, H**). However, after excluding the measurements performed in the oldest DBA/2J mice (i.e. analyzing only animals ages 3 to 12 months, **Figures 6C, F, I**), we demonstrated a significant positive correlation between IOP and ACW (R^2 = 0.17, P = 0.03).

DISCUSSION

Animal models provide valuable information about the diagnosis and course of disease. They also enable the development of new therapeutic approaches and allow for the monitoring of effects of the therapy (Harada et al., 2019). The DBA/2J mice strain is commonly used as an animal model that mimics many aspects of congenital human glaucoma, particularly pigmentary glaucoma (PG). High IOP in this murine strain is related to the RGC loss and morphological changes of the eyeball and the optic nerve (Schuettauf et al., 2004; Fiedorowicz et al., 2018; Crosbie et al., 2019). Despite the progress in the IOP evaluation methods, performing these measurements in animal models of glaucoma is challenging. In particular, in the DBA/2J mice model, the

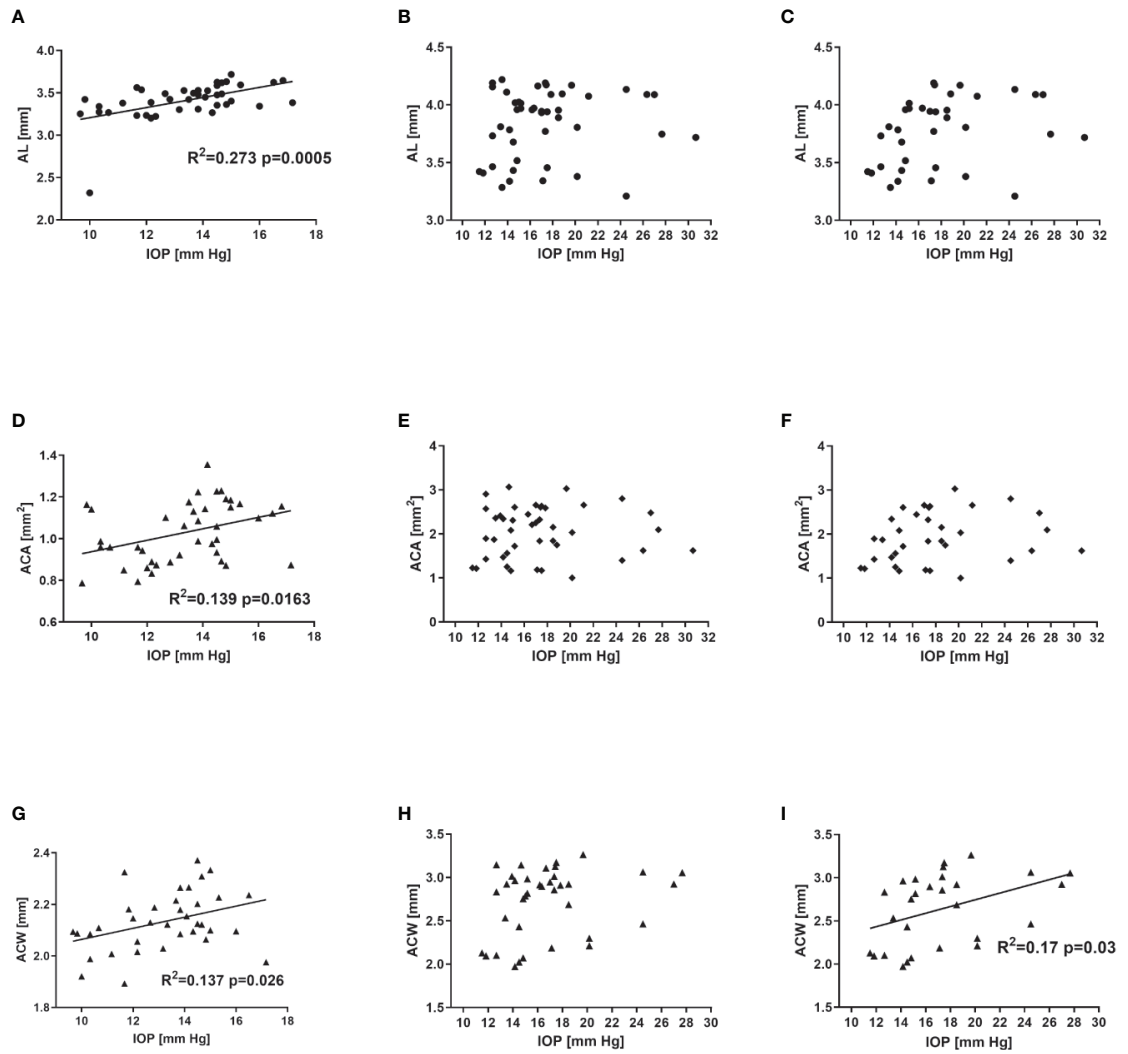

FIGURE 6 | Relationship between intraocular pressure and selected ocular dimensions in C57BL/6J ages 3 to 15 months (first column - **A**, **D**, **G**), DBA/2J mice ages 3 to 15 months (second column – **B**, **E**, **H**) or DBA/2J mice ages 3 to 12 months (third column **C**, **F**, **I**). Graphs illustrate axial length (AL, **A**–**C**), anterior chamber area (ACA, **D**–**F**), and anterior chamber width (ACW, **G**–**I**). Dots represent single values, lines represent linear correlations. Respective R^2 (if applicable) and P values are placed inside the panels.

profound anterior chamber, corneal calcification, and corneal neovascularization or hyphema can significantly impact the accuracy of IOP measurements and optical biometric methods (John et al., 1998; Turner et al., 2017; Harada et al., 2019). For this reason, additional, non-invasive, or low-invasive methods for monitoring the progression of glaucoma in animal models (and in particular in DBA/2J mice) are highly demanded. In this study we used MR techniques that proved to be useful, non-invasive tools for characterization of glaucoma-related changes in the visual pathway,for monitoring the progression of glaucoma, and assessing the efficacy of novel treatment strategies in animal models of glaucoma (Fiedorowicz et al., 2011). Although the spatial resolution of MRI is lower than optical techniques, it has no depth limitations and could be used to conduct a detailed anatomical study of the eyeball and optic nerve, as well as in cases of corneal, lens, or vitreous opacity (Cheng et al., 2006).

Two strains that are not affected by age-related glaucoma-like pathology were used as controls in this study. DBA/2J-Gpnmb^{+}/SjJ mice share the genetic background with DBA/2J mice but do not carry one of the mutations that are believed to be responsible for the ocular pathology in DBA/2J mice: *Gpnmb*^{R150X}. The presence of functional glycoprotein nonmelanosoma protein B (Gpnmb protein) in DBA/2J-Gpnmb^{+}/SjJ mice was shown to prevent the development of iris pigment dispersion (Anderson et al., 2002). However, they carry a mutation in a gene encoding TYRP1 (mutation *Tyrp1*^{b}), a major melanosomal glycoprotein and they develop iris stromal atrophy despite no elevation of IOP (Anderson et al., 2002; Howell et al., 2007; Anon, 2020). Another strain used as a control was C57BL/6J that only sporadically develops either easy-to-detect (microphthalmia/anophthalmia) or relatively mild ocular pathologies like corneal opacity. These conditions are believed to be mainly induced by exposure to environmental conditions (Smith et al., 1994). The C57BL/6J strain is also widely used as a control strain for DBA/2J mice (Wong and Brown, 2007; Yang et al., 2018). Not surprisingly, in neither of these strains did we observe a sudden increase in IOP between the third and sixth months of life. The C57BL/6J only displayed a mild, age-dependent IOP elevation that has been previously reported (Cone et al., 2012; Fiedorowicz et al., 2018). Ocular dimensions in both the control strains were also similar.

The progression of glaucoma-related changes in the ocular morphology and IOP in DBA/2J mice, on the other hand, seemed to be more complex. It appears that according to our data we can distinguish three stages of the ocular pathology in DBA/2J mice: (1) around the third month of life; (2) between 6 and 12 months; and (3) >12 months. In 3-month-old animals we noted no differences in the IOP nor in any of the measured ocular dimensions between DBA/2J mice and the control strains; similar results were reported by other groups (Chou et al., 2011). However, it was reported previously that despite no observable IOP elevation, there are some early degenerative processes that may begin around the third month of life in DBA/2J mice, e.g. diminution of anterograde axonal transport within the axons building the optic nerve (Fiedorowicz et al., 2018), reduced spectrin expression (Wilson et al., 2016), RGC apoptosis, degeneration of RGC axons, activation of Müller glial cells (Schuettauf et al., 2004), and microglia activation (Bosco et al., 2015). These neurodegenerative processes seemed, however, to not be advanced enough to be visible on a morphological level in our study.

In DBA/2J mice, between the 6 and 12 months of age, we observed an elevated IOP, which was significantly higher than in C57BL/6J mice. However, in both the control strains, the slope of the age-dependent IOP increase seemed to be similar. On the contrary, while most of the ocular dimensions increased only slightly in the control strains, in DBA/2J mice we observed a steep linear increase in ocular dimensions between the sixth and twelfth months of age. The eye was generally getting bigger as reflected by an increase in axial length and globe area, but it was an effect of alterations mainly of the anterior chamber morphology and, to a smaller extent, the growing of the vitreous chamber (however, the depth of the vitreous chamber remained unchanged). The anterior chamber depth, area, and angle reached significantly higher values in DBA/2J mice than in control strains and these parameters increased in DBA/2J mice between the sixth and twelfth months in a linear manner. Similar observations have been reported in children suffering from primary congenital glaucoma in severe cases, leading to a syndrome called buphthalmos (Hussein et al., 2014; Doozandeh et al., 2017). At this stage of pathology, retinal degeneration was already visible as optic disc cupping visible in T2w images and optic disc cupping was not visible in either of the control strains. Additionally, other groups reported various hallmarks of degeneration at this stage, including decrease of visuomotor function, alterations within the optic nerve, and the optic tract demonstrated by diffusion-weighted MRI (Yang et al., 2018).

Remarkably, we observed a decrease in the IOP between 12 and 15 months of age, similar to the values of those observed in C57BL/6J mice of the same age. Of course, these readings could have been affected by corneal calcification in DBA/2J mice, despite previously reported good agreement regarding the methods for determining IOP measurements involving the TonoLab rebound tonometer that we used in this study and invasive manometric methods (Pease et al., 2011). On the other hand, we noted some changes in the ocular morphology in those mice, which might explain the IOP decrease. Eyeball elongation seemed to stop after the twelfth month of life in DBA/2J mice – neither the axial length nor the globe area differed in animals ages 12 and 15 months. The anterior chamber area and depth also remained stable. However, at this advanced stage of pathology, the vitreous chamber started to be affected. The VCD decreased between the twelfth and fifteenth months of life and in the case of VCA, this effect was noticeable even earlier at the twelfth month of life in DBA/2J. This indicates that after around the twelfth month of life in DBA/2J mice, a disorganization of the eye structure occurs. This might be an effect of iris and ciliary muscular degeneration that fails to sustain the lens; a similar mechanism was postulated in humans (Cheon et al., 2010; Danielewska et al., 2014). In consequence, "pushing" the lens toward the vitreous chamber may, at least partially, compensate for the elevated IOP in the anterior chamber.

Despite the observed IOP decrease in DBA/2J older than 12 months, this stage of pathology seems to be characterized with high dynamics of neurodegenerative processes occurring in the retina and in the optic nerve. The results from our previous study showed a dramatic decrease in anterograde axonal transport within the optic nerve at this stage of pathology (Fiedorowicz et al., 2018) or a decrease in behavioral measures of visual acuity (Wong and Brown, 2007). In this study we demonstrated lower thickness of the retina in DBA/2J mice than in controls – both in T2w anatomical images without enhancement and in T1w images after manganese chloride administration that enhanced the neural retina. However, we did not observe any significant changes in the dimensions of the optic nerve. This could be due to the relatively low size of the optic nerve that results in large measurement errors and in consequent standard deviations.

Finally, we attempted to find ocular dimensions or other parameters that would correlate with the IOP. In mice that developed no glaucoma-like pathology, we found three such parameters: axial length, anterior chamber area, and anterior chamber width. The strongest positive correlation was observed between the AL and the IOP. Despite the results from some studies which have failed to demonstrate a correlation between axial length or other biometric measures of the eye and IOP in patients without glaucoma (Gye et al., 2015), axial length was shown in glaucoma patients to decrease after IOP normalization (Kim et al., 2016). No correlation between any of the biometric parameters in DBA/2J mice was observed – this could be explained by the fact that in the whole population, we included eyes that are affected in different ways – according to the different stages of the pathology that we described above. However, when we excluded 15-month-old mice, there was a significant correlation between ACW and IOP.

Some of the limitations of this study are a consequence of the eye imaging strategy. The use of a surface receive-only coil resulted in the gradual decrease of signal intensity with the distance from the coil. To reduce this effect, the coil size fitted the size of the murine eye and the positioning of the coil was adjusted to provide optimal visualization of all the eyeball structures. However, it is possible that deeper structures like the central retina or the optic nerve are characterized by poorer contrast. Another limitation is possibly imprecise planning of the slices in 2D imaging. In principle, the middle slice of each 2D image was planned to include the optic nerve head and pupil at its widest point. Some mistakes in planning of the middle slice at the image acquisition stage may potentially affect the measurements of the eyeball dimension. However, every image was thoroughly inspected immediately after the acquisition, and in case of any doubts, the measurement was repeated with corrected angles. Relatively low standard deviations in most of the finally calculated morphological parameters suggest that potential mistakes in the planning of slices did not affect these parameters remarkably.

CONCLUSION

Our data suggest that morphological changes within the anterior chamber and vitreous chamber could serve as markers of disease progression in animal models of hereditary glaucoma. They correlate with the IOP at the earlier stages of the pathology. However, in contrast to the IOP that could be difficult to measure in older animals, parameters like the anterior chamber area, the anterior chamber depth, or the iridocorneal angle were markedly elevated in animals with advanced pigmentary glaucoma. We propose that these parameters should be included in the evaluation of the efficacy of potential new IOP-lowering drugs in animal models of glaucoma as markers of disease progression and prolonged IOP elevation.

DATA AVAILABILITY STATEMENT

The raw data supporting the conclusions of this article will be made available by the authors, without undue reservation.

ETHICS STATEMENT

The animal study was reviewed and approved by Warsaw IV Local Ethics Committee.

AUTHOR CONTRIBUTIONS

MF designed the research and provided funding, MF, MW-K, JO, and MŚ carried out experiments. MF, MW-K, MŚ, JO, TC, MT, RR, and PB analyzed the experimental results. MF, MW-K, and MT wrote the manuscript, and RR, PB, and PG revised it.

FUNDING

This study was supported by Polish National Science Centre grant (DEC-2012/07/D/NZ4/04199) to MF.

ACKNOWLEDGMENTS

Project carried out with the use of CePT infrastructure financed by the European Union – the European Regional Development Found in the Operational Program "Innovative Economy" for 2007–2013. We would like to acknowledge Scribendi Inc. (Chatham, ON, Canada) for editing and proofreading of the manuscript.

REFERENCES

Anderson, M. G., Smith, R. S., Savinova, O. V., Hawes, N. L., Chang, B., Zabaleta, A., et al. (2001). Genetic modification of glaucoma associated phenotypes between AKXD-28/Ty and DBA/2J mice. *BMC Genet.* 2, 1–1. doi: 10.1186/1471-2156-2-1

Anderson, M. G., Smith, R. S., Hawes, N. L., Zabaleta, A., Chang, B., Wiggs, J. L., et al. (2002). Mutations in genes encoding melanosomal proteins cause

pigmentary glaucoma in DBA/2J mice. *Nat. Genet.* 30, 81–85. doi: 10.1038/ng794

Anderson, M. G., Libby, R. T., Mao, M., Cosma, I. M., Wilson, L. A., Smith, R. S., et al. (2006). Genetic context determines susceptibility to intraocular pressure elevation in a mouse pigmentary glaucoma. *BMC Biol.* 4, 20. doi: 10.1186/1741-7007-4-20

Anon (2020). *DBA/2J-Gpnmb+/SjJ Stock No: 007048* (Jackson Laboratory). Available at: https://www.jax.org/strain/007048 (Accessed 07-05-2020).

Biswas, S., and Wan, K. H. (2019). Review of rodent hypertensive glaucoma models. *Acta Ophthalmol.* 97, e331–e340. doi: 10.1111/aos.13983

Bosco, A., Romero, C. O., Breen, K. T., Chagovetz, A. A., Steele, M. R., Ambati, B. K., et al. (2015). Neurodegeneration severity can be predicted from early microglia alterations monitored in vivo in a mouse model of chronic glaucoma. *Dis. Model Mech.* 8, 443–455. doi: 10.1242/dmm.018788

Calkins, D. J., Horner, P. J., Roberts, R., Gradianu, M., and Berkowitz, B. A. (2008). Manganese-Enhanced MRI of the DBA/2J Mouse Model of Hereditary Glaucoma. *Invest. Ophthalmol. Visual Sci.* 49, 5083–5088. doi: 10.1167/iovs.08-2205

Camras, L. J., Sufficool, K. E., Camras, C. B., Fan, S., Liu, H., and Toris, C. B. (2010). Duration of anesthesia affects intraocular pressure, but not outflow facility in mice. *Curr. Eye Res.* 35, 819–827. doi: 10.3109/02713683.2010.494241

Chen, S., and Zhang, X. (2015). The Rodent Model of Glaucoma and Its Implications. *Asia Pac J. Ophthalmol. (Phila)* 4, 236–241. doi: 10.1097/apo.0000000000000122

Cheng, H., Nair, G., Walker, T. A., Kim, M. K., Pardue, M. T., Thulé, P. M., et al. (2006). Structural and functional MRI reveals multiple retinal layers. *Proc. Natl. Acad. Sci. U.S.A.* 103, 17525–17530. doi: 10.1073/pnas.0605790103

Cheon, M. H., Sung, K. R., Choi, E. H., Kang, S. Y., Cho, J. W., Lee, S., et al. (2010). Effect of age on anterior chamber angle configuration in Asians determined by anterior segment optical coherence tomography; clinic-based study. *Acta Ophthalmol.* 88, e205–e210. doi: 10.1111/j.1755-3768.2010.01960.x

Chou, T. H., Kocaoglu, O. P., Borja, D., Ruggeri, M., Uhlhorn, S. R., Manns, F., et al. (2011). Postnatal elongation of eye size in DBA/2J mice compared with C57BL/6J mice: in vivo analysis with whole-eye OCT. *Invest. Ophthalmol. Vis. Sci.* 52, 3604–3612. doi: 10.1167/iovs.10-6340

Cone, F. E., Steinhart, M. R., Oglesby, E. N., Kalesnykas, G., Pease, M. E., and Quigley, H. A. (2012). The effects of anesthesia, mouse strain and age on intraocular pressure and an improved murine model of experimental glaucoma. *Exp. Eye Res.* 99, 27–35. doi: 10.1016/j.exer.2012.04.006

Crawley, L., Zamir, S. M., Cordeiro, M. F., and Guo, L. (2012). Clinical options for the reduction of elevated intraocular pressure. *Ophthalmol. Eye Dis.* 4, 43–64. doi: 10.4137/oed.s4909

Crosbie, D. E., Keaney, J., Tam, L. C. S., Daniel Stamer, W., Campbell, M., and Humphries, P. (2019). Age-related changes in eye morphology and aqueous humor dynamics in DBA/2J mice using contrast-enhanced ocular MRI. *Magn Reson Imaging* 59, 10–16. doi: 10.1016/j.mri.2019.01.016

Danielewska, M. E., Krzyżanowska-Berkowska, P., and Iskander, D. R. (2014). Glaucomatous and age-related changes in corneal pulsation shape. The ocular dicrotism. *PloS One* 9, e102814. doi: 10.1371/journal.pone.0102814

Doozandeh, A., Yazdani, S., Ansari, S., Pakravan, M., Motevasseli, T., Hosseini, B., et al. (2017). Corneal profile in primary congenital glaucoma. *Acta Ophthalmologica* 95, e575–e581. doi: 10.1111/aos.13357

Fiedorowicz, M., Dyda, W., Rejdak, R., and Grieb, P. (2011). Magnetic resonance in studies of glaucoma. *Med. Sci. Monitor* 17, RA227–RA232. doi: 10.12659/MSM.881973

Fiedorowicz, M., Orzel, J., Kossowski, B., Welniak-Kaminska, M., Choragiewicz, T., Swiatkiewicz, M., et al. (2018). Anterograde Transport in Axons of the Retinal Ganglion Cells and its Relationship to the Intraocular Pressure during Aging in Mice with Hereditary Pigmentary Glaucoma. *Curr. Eye Res.* 43, 539–546. doi: 10.1080/02713683.2017.1416147

Flaxman, S. R., Bourne, R. R. A., Resnikoff, S., Ackland, P., Braithwaite, T., Cicinelli, M. V., et al. (2017). Global causes of blindness and distance vision impairment 1990–2020: a systematic review and meta-analysis. *Lancet Global Health* 5, e1221–e1234. doi: 10.1016/S2214-109X(17)30393-5

Giovingo, M. (2014). Complications of glaucoma drainage device surgery: a review. *Semin. Ophthalmol.* 29, 397–402. doi: 10.3109/08820538.2014.959199

Gye, H. J., Shim, S. H., Kim, J. M., Bae, J. H., Choi, C. Y., Kim, C. Y., et al. (2015). Effect of axial length on diurnal IOP in cataract patients without glaucoma. *Optom Vis. Sci.* 92, 350–356. doi: 10.1097/opx.0000000000000495

Harada, C., Kimura, A., Guo, X., Namekata, K., and Harada, T. (2019). Recent advances in genetically modified animal models of glaucoma and their roles in drug repositioning. *Br. J. Ophthalmol.* 103, 161–166. doi: 10.1136/bjophthalmol-2018-312724

Howell, G. R., Libby, R. T., Marchant, J. K., Wilson, L. A., Cosma, I. M., Smith, R. S., et al. (2007). Absence of glaucoma in DBA/2J mice homozygous for wild-type versions of Gpnmb and Tyrp1. *BMC Genet.* 8, 45. doi: 10.1186/1471-2156-8-45

Hussein, T. R., Shalaby, S. M., Elbakary, M. A., Elseht, R. M., and Gad, R. E. (2014). Ultrasound biomicroscopy as a diagnostic tool in infants with primary congenital glaucoma. *Clin. Ophthalmol. (Auckland N.Z.)* 8, 1725–1730. doi: 10.2147/OPTH.S66682

Jackson Laboratory (2020). https://www.jax.org/strain/000671.

John, S. W., Smith, R. S., Savinova, O. V., Hawes, N. L., Chang, B., Turnbull, D., et al. (1998). Essential iris atrophy, pigment dispersion, and glaucoma in DBA/2J mice. *Invest. Ophthalmol. Vis. Sci.* 39, 951–962.

Kim, C. S., Kim, K. N., Kang, T. S., Jo, Y. J., and Kim, J. Y. (2016). Changes in Axial Length and Refractive Error After Noninvasive Normalization of Intraocular Pressure From Elevated Levels. *Am. J. Ophthalmol.* 163, 132–139.e132. doi: 10.1016/j.ajo.2015.12.004

Lusthaus, J., and Goldberg, I. (2019). Current management of glaucoma. *Med. J. Aust.* 210, 180–187. doi: 10.5694/mja2.50020

May, C. A., and LüTjen-Drecoll, E. (2002). Morphology of the Murine Optic Nerve. *Invest. Ophthalmol. Visual Sci.* 43, 2206–2212.

Millar, J. C., and Pang, I. H. (2015). Non-continuous measurement of intraocular pressure in laboratory animals. *Exp. Eye Res.* 141, 74–90. doi: 10.1016/j.exer.2015.04.018

Pease, M. E., Cone, F. E., Gelman, S., Son, J. L., and Quigley, H. A. (2011). Calibration of the TonoLab tonometer in mice with spontaneous or experimental glaucoma. *Invest. Ophthalmol. Vis. Sci.* 52, 858–864. doi: 10.1167/iovs.10-5556

Scholz, M., Buder, T., Seeber, S., Adamek, E., Becker, C. M., and Lutjen-Drecoll, E. (2008). Dependency of intraocular pressure elevation and glaucomatous changes in DBA/2J and DBA/2J-Rj mice. *Invest. Ophthalmol. Vis. Sci.* 49, 613–621. doi: 10.1167/iovs.07-0745

Schuettauf, F., Rejdak, R., Walski, M., Frontczak-Baniewicz, M., Voelker, M., Blatsios, G., et al. (2004). Retinal neurodegeneration in the DBA/2J mouse-a model for ocular hypertension. *Acta Neuropathol.* 107, 352–358. doi: 10.1007/s00401-003-0816-9

Smith, R. S., Roderick, T. H., and Sundberg, J. P. (1994). Microphthalmia and associated abnormalities in inbred black mice. *Lab. Anim Sci.* 44, 551–560.

Świątkiewicz, M., Wełniak-Kamińska, M., Fiedorowicz, M., Kamińska, A., Rejdak, R., and Grieb, P. (2020). Peripheral Latanoprost Administration Lowers Intraocular Pressure in the Wistar Rat. *Ophthalmol. Ther.* 9, 1–8. doi: 10.1007/s40123-020-00256-8

Tham, Y. C., Li, X., Wong, T. Y., Quigley, H. A., Aung, T., and Cheng, C. Y. (2014). Global prevalence of glaucoma and projections of glaucoma burden through 2040: a systematic review and meta-analysis. *Ophthalmology* 121, 2081–2090. doi: 10.1016/j.ophtha.2014.05.013

Tkatchenko, T. V., Shen, Y., and Tkatchenko, A. V. (2010). Analysis of postnatal eye development in the mouse with high-resolution small animal magnetic resonance imaging. *Invest. Ophthalmol. Vis. Sci.* 51, 21–27. doi: 10.1167/iovs.08-2767

Turner, A. J., Vander Wall, R., Gupta, V., Klistorner, A., and Graham, S. L. (2017). DBA/2J mouse model for experimental glaucoma: pitfalls and problems. *Clin. Exp. Ophthalmol.* 45, 911–922. doi: 10.1111/ceo.12992

Wang, R. F., Serle, J. B., Gagliuso, D. J., and Podos, S. M. (2000). Comparison of the ocular hypotensive effect of brimonidine, dorzolamide, latanoprost, or artificial tears added to timolol in glaucomatous monkey eyes. *J. Glaucoma* 9, 458–462. doi: 10.1097/00061198-200012000-00007

Wilson, G. N., Smith, M. A., Inman, D. M., Dengler-Crish, C. M., and Crish, S. D. (2016). Early Cytoskeletal Protein Modifications Precede Overt Structural Degeneration in the DBA/2J Mouse Model of Glaucoma. *Front. Neurosci.* 10, 494. doi: 10.3389/fnins.2016.00494

Wong, A. A., and Brown, R. E. (2007). Age-related changes in visual acuity, learning and memory in C57BL/6J and DBA/2J mice. *Neurobiol. Aging* 28, 1577–1593. doi: 10.1016/j.neurobiolaging.2006.07.023

Woodward, W. R., Choi, D., Grose, J., Malmin, B., Hurst, S., Pang, J., et al. (2007). Isoflurane is an effective alternative to ketamine/xylazine/acepromazine as an anesthetic agent for the mouse electroretinogram. *Doc. Ophthalmol.* 115, 187–201. doi: 10.1007/s10633-007-9079-4

Yang, X.-L., Van Der Merwe, Y., Sims, J., Parra, C., C. Ho, L., Schuman, J., et al. (2018). Age-related Changes in Eye, Brain and Visuomotor Behavior in the DBA/2J Mouse Model of Chronic Glaucoma. *Sci. Rep.* 8, 4643. doi: 10.1038/s41598-018-22850-4

Yeaw, J., Benner, J. S., Walt, J. G., Sian, S., and Smith, D. B. (2009). Comparing adherence and persistence across 6 chronic medication classes. *J. Manag Care Pharm.* 15, 728–740. doi: 10.18553/jmcp.2009.15.9.728

Conflict of Interest: The authors declare that the research was conducted in the absence of any commercial or financial relationships that could be construed as a potential conflict of interest.

frontiers in Pharmacology

BRIEF RESEARCH REPORT
published: 26 November 2020
doi: 10.3389/fphar.2020.591908

Control of Complement Activation by the Long Pentraxin PTX3: Implications in Age-Related Macular Degeneration

*Matteo Stravalaci[1,2], Francesca Davi[2], Raffaella Parente[2], Marco Gobbi[3], Barbara Bottazzi[2], Alberto Mantovani[1,2,4], Anthony J. Day[5], Simon J. Clark[6,7], Mario R. Romano[1,8] and Antonio Inforzato[1,2]**

[1]Department of Biomedical Sciences, Humanitas University, Milan, Italy, [2]Humanitas Clinical and Research Center IRCCS, Milan, Italy, [3]Istituto di Ricerche Farmacologiche Mario Negri IRCCS, Milan, Italy, [4]The William Harvey Research Institute, Queen Mary University of London, London, United Kingdom, [5]Wellcome Trust Centre for Cell-Matrix Research and Lydia Becker Institute of Immunology and Inflammation, Division of Cell-Matrix Biology and Regenerative Medicine, School of Biological Sciences, Faculty of Biology, Medicine and Health, University of Manchester, Manchester Academic Health Science Centre, Manchester, United Kingdom, [6]Universitäts-Augenklinik Tübingen, Eberhard Karls University of Tübingen, Tübingen, Germany, [7]The Lydia Becker Institute of Immunology and Inflammation, Faculty of Biology Medicine and Health, The University of Manchester, Manchester, United Kingdom, [8]Eye Center, Humanitas Gavazzeni-Castelli, Bergamo, Italy

Dysregulation of the complement system is central to age-related macular degeneration (AMD), the leading cause of blindness in the developed world. Most of the genetic variation associated with AMD resides in complement genes, with the greatest risk associated with polymorphisms in the *complement factor H* (*CFH*) gene; factor H (FH) is the major inhibitor of the alternative pathway (AP) of complement that specifically targets C3b and the AP C3 convertase. Long pentraxin 3 (PTX3) is a soluble pattern recognition molecule that has been proposed to inhibit AP activation via recruitment of FH. Although present in the human retina, if and how PTX3 plays a role in AMD is still unclear. In this work we demonstrated the presence of PTX3 in the human vitreous and studied the PTX3-FH-C3b crosstalk and its effects on complement activation in a model of retinal pigment epithelium (RPE). RPE cells cultured in inflammatory AMD-like conditions overexpressed the PTX3 protein, and up-regulated AP activating genes. PTX3 bound RPE cells in a physiological setting, however this interaction was reduced in inflammatory conditions, whereby PTX3 had no complement-inhibiting activity on inflamed RPE. However, on non-cellular surfaces, PTX3 formed a stable ternary complex with FH and C3b that acted as a "hot spot" for complement inhibition. Our findings suggest a protective role for PTX3 in response to complement dysregulation in AMD and point to a novel mechanism of complement regulation by this pentraxin with potential implications in pathology and pharmacology of AMD.

Keywords: age-related macular degeneration, retinal pigmented epithelium, vitreous humor, complement system, alternative pathway, pentraxins, pentraxin 3

OPEN ACCESS

Edited by:
Claudio Bucolo,
University of Catania, Italy

Reviewed by:
Christina Lamers,
University of Basel, Switzerland
Annalisa Trenti,
University of Padua, Italy

****Correspondence:***
Antonio Inforzato
antonio.inforzato@humanitasresearch.it

Specialty section:
This article was submitted to Inflammation Pharmacology, a section of the journal Frontiers in Pharmacology

Received: *05 August 2020*
Accepted: *28 October 2020*
Published: *26 November 2020*

Citation:
Stravalaci M, Davi F, Parente R, Gobbi M, Bottazzi B, Mantovani A, Day AJ, Clark SJ, Romano MR and Inforzato A (2020) Control of Complement Activation by the Long Pentraxin PTX3: Implications in Age-Related Macular Degeneration. Front. Pharmacol. 11:591908. doi: 10.3389/fphar.2020.591908

INTRODUCTION

Age-related macular degeneration (AMD) is a neurodegenerative and multifactorial disease of the eye that distinctively manifests itself with ageing (Jager et al., 2008), and is recognized as the leading cause of irreversible visual impairment in the elderly (Wong et al., 2014). Early and intermediate AMD is characterized by the accumulation of extracellular deposits (called drusen) between the retinal pigment epithelium (RPE) and the Bruch's membrane (BrM). Eventually, the disease can progress either to dry AMD, with photoreceptor loss, or wet AMD, characterized by the formation of new blood vessels in the choroidal region that grow into the retina causing tissue disruption (Ambati et al., 2003).

Local dysregulation of the complement system and the associated chronic inflammation are major drivers of the disease (Ambati et al., 2013; Clark and Bishop, 2018). Complement proteins have been detected in the aqueous humor of AMD patients (Schick et al., 2017; Altay et al., 2019) and in drusen (Hageman et al., 2001; Crabb et al., 2002; Curcio, 2018). Moreover, most of the genetic variation underlying the risk of AMD resides in genes of the complement cascade (Fritsche et al., 2016; Cipriani et al., 2020). The rs1061170 single nucleotide polymorphism (SNP) in the *complement factor H* (*CFH*) gene (that leads to the Y402H amino acid substitution in the protein) has a strong association with the disease Edwards et al. (2005), Hageman et al. (2005), Haines et al. (2005). Factor H (FH) is the major soluble inhibitor of the alternative pathway (AP) of complement, and comprises 20 complement control protein (CCP) domains with distinct functions (Parente et al., 2017). CCPs1-4 mediate inhibition of assembly and stability of the AP C3 convertase (C3bBb), while CCPs6-8 and CCPs18-20 are involved in the recognition of "self" determinants (e.g., sulfated glycosaminoglycans, GAGs, and sialic acids) that are present on the surface of mammalian cells and extra-cellular matrices (ECMs), thus directing the inhibitory properties of FH towards host tissues (Clark et al., 2010; Clark et al., 2013; Blaum et al., 2015; Langford-Smith et al., 2015). The Y402H polymorphism (in CCP7) alters the binding of FH to heparan sulfate (in the BrM) (Parente et al., 2017; Clark and Bishop, 2018) and C reactive protein (CRP, which is present both in the BrM and choroid) (Sjoberg et al., 2007), thus leading to inappropriate complement activation and complement-driven inflammation, with pathological progression to AMD (Clark and Bishop, 2018).

One of the ligands of FH is the long pentraxin 3 (PTX3) (Deban et al., 2008), a multimeric glycoprotein with a distinctive quaternary structure (Bottazzi et al., 1997; Inforzato et al., 2008; Inforzato et al., 2010; Inforzato et al., 2012) that is produced by a number of somatic and immune cells, and plays key roles in innate immunity, tissue remodeling, and inflammation (Doni et al., 2019; Parente et al., 2019; Parente et al., 2020). Current evidence indicates that PTX3 is locally made by the RPE in the presence of pro-inflammatory cytokines (Woo et al., 2013), and in conditions of oxidative stress (Wang et al., 2016; Hwang et al., 2019). The protein has been detected in multiple layers of the human retina, including the BrM and the basement membrane of both RPE and choriocapillaris (Yamada et al., 2008). Furthermore, based on *in silico* analysis, *PTX3* transcription has been documented in the RPE/choroid region of the human eye, where it increases with age, although be it independently from the AMD status (Juel et al., 2015). Previously, we have reported that the PTX3 protein localizes underneath the BrM and in the choroid of both AMD and non-AMD donors (Swinkels et al., 2018), suggesting that PTX3 might act as a mediator of retinal homeostasis both in physiological and pathological conditions. Yet, the underlying mechanisms are still unclear. In this regard, in an animal model of AMD (induced by 4-hydroxynonenal, 4-HNE), genetic deficiency of *PTX3* led to enhanced complement activation, increased levels of C3a (a potent anaphylatoxin originating from proteolysis of C3) and the inflammatory cytokine IL-1β in the RPE, and accumulation of macrophages in the choroid (Wang et al., 2016), whereby PTX3 has been proposed to act as an anchoring molecule for FH in the BrM and RPE.

Here, we provided evidence that soluble PTX3 is present in the vitreous humor of both AMD and non-AMD human eyes. Using an established human RPE cell line (ARPE-19), we characterized the complement inhibiting-properties of PTX3 in physiological and inflammatory AMD-like (i.e., in the presence of TNF-α or IL-1β) conditions, and proposed a novel mechanism of complement regulation by this pentraxin with potential implications in the pathogenesis of AMD.

MATERIALS AND METHODS

Donor Eye Tissue

Vitrous humor specimens were obtained from human eyes collected from the Manchester Royal Eye Hospital Eye Bank after removal of the corneas for transplantation. Consent had been obtained for the eye tissue to be used for research and guidelines established in the Human Tissue Act of 2004 (UK) were adhered to. Ethical approval for the use of human donor eyes was given by North West – Greater Manchester Central Research Ethics Committee (REC reference 15/NW/0932).

Cell Cultures and Treatments

ARPE-19 cells (ATCC, CRL-2302) were cultured and stimulated as described in Supplementary Materials and Methods.

Enzyme-Linked Immunosorbent Assays

The concentration of IL-6, IL-8 and VEGF in the cell culture medium was measured using the Quantikine ELISA assay (R&D Systems). The concentration of PTX3 both in the conditioned medium of ARPE-19 cells and in the vitreous humor of AMD and non-AMD donors was assessed using an in-house developed ELISA assay (Canovi et al., 2014).

Binding Experiments

Binding of recombinant human PTX3 (rhPTX3) (Bottazzi et al., 1997) to ARPE-19 cells was assessed by flow cytometry. The interaction of C3b with rhPTX3 in the presence and absence of FH was assessed in solid phase and SPR binding experiments.

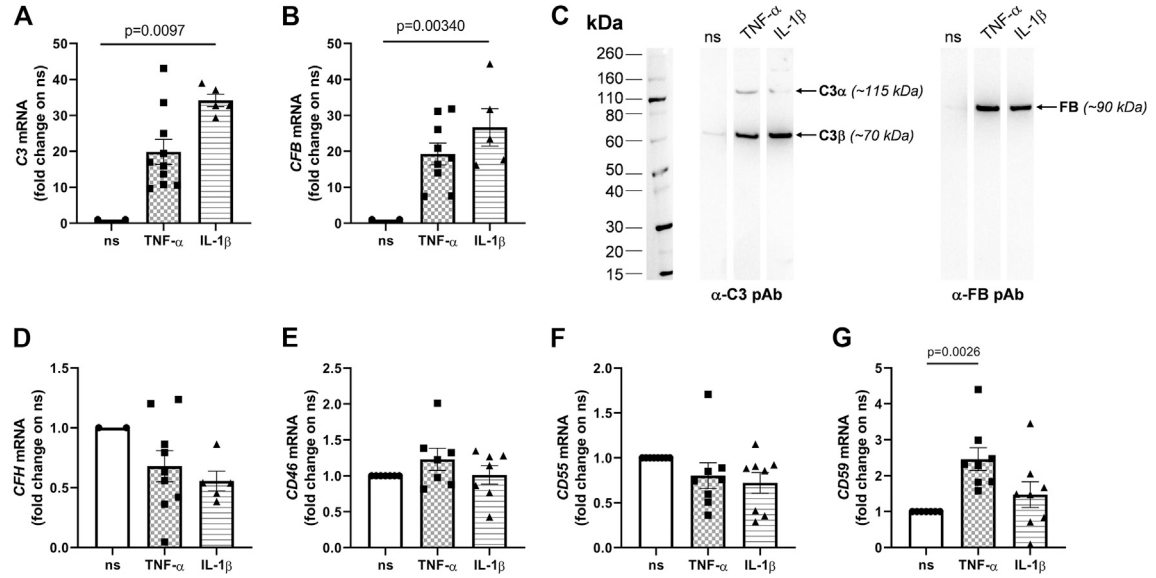

FIGURE 1 | Pro-inflammatory cytokines induce transcription of the *C3* and *CFB* genes and secretion of the C3 and FB proteins in ARPE-19 cells. ARPE-19 were treated with 10 ng/ml TNF-α, 10 ng/ml IL-1β, or vehicle alone for 24 h, and RNA levels of **(A)** *C3*, **(B)** *CFB*, **(D)** complement factor H (*CFH*), **(E)** *CD46*, **(F)** *CD55*, and **(G)** *CD59* were measured by qRT-PCR. Data were normalized based on the mRNA levels from non-stimulated cells (ns; $2^{-\Delta CT\ gene\ -\ GAPDH}$ values were in the range 0.00–0.04 for non-stimulated cells), and expressed as mean ± SEM (n = 5–10 from as many independent experiments). Statistical analysis was carried out using the Kruskall-Wallis test followed by Dunn's multiple comparison test. **(C)** Presence of the C3 and FB proteins in cell culture media was assessed by western blotting. Proteins were separated by SDS-PAGE in reducing conditions, transferred onto PVDF membranes, and C3 (i.e., both α and β chains) and FB were revealed by appropriate polyclonal antibodies. Gels are shown that are representative of two independent experiments. Positions and apparent molecular weights of the C3α, C3β and FB bands are indicated.

Quantitative Real-Time Polymerase Chain Reaction

Total RNA was extracted from ARPE-19 cells using the Direct-zol™ RNA MiniPrep (Zymo Research) system, reverse trascribed to cDNA with the High Capacity cDNA Reverse Transcription Kit (Applied Biosystems), and amplified using the Sybr Green PCR Master Mix (Applied Biosystems). See **Supplementary Table S1** for additional information.

Western Blotting Analyses

Synthesis and secretion of the C3 and FB proteins in the conditioned medium of cultured ARPE-19 cells was assessed by western blotting by adaptation of a previous protocol (Baranova et al., 2014).

Complement Activation Assays

Complement activation on plastic plate-immobilized and cell-bound proteins was evaluated by western blotting, ELISA and flow cytometry.

Statistical Analyses

All data were analyzed using the Prism 8.0 Software (GraphPad Software).

See Supplementary Information for more details.

RESULTS

Inflammatory Cytokines Induce Expression of Complement Activating Genes in ARPE-19 Cells

Dysregulation of the complement system, in particular of the AP, is a critical factor in AMD pathogenesis (Clark and Bishop, 2018). We evaluated whether inflammatory AMD-like conditions (i.e., stimulation with TNF-α and IL-1β) could induce changes in the expression of soluble components of the AP and membrane-associated complement inhibitors in ARPE-19 cells (see **Supplementary Table S1** for the sequence of the primers used in RT-PCR). The mRNA levels of both *C3* and *CFB* (components of the AP C3 convertase, C3bBb) significantly increased upon exposure to IL-1β, and showed an incremental trend following treatment with TNF-α (**Figure 1A,B**). Consistent with this, both cytokines induced synthesis and secretion of the C3 and FB proteins (**Figure 1C**). Furthermore, transcription of the *CFH* gene (**Figure 1D**) was somewhat (though not significantly) decreased, while *CD46* (also known as membrane cofactor protein, MCP, **Figure 1E**) and *CD55* (or decay-accelerating factor, DAF, **Figure 1F**) genes, encoding membrane associated AP inhibitors, did not change expression with the applied stimuli. Interestingly, *CD59* (or MAC-inhibitory protein, MAC-IP) mRNA (**Figure 1G**) was upregulated in ARPE-19 cells treated with TNF-α, but not IL-1β. These data indicate that

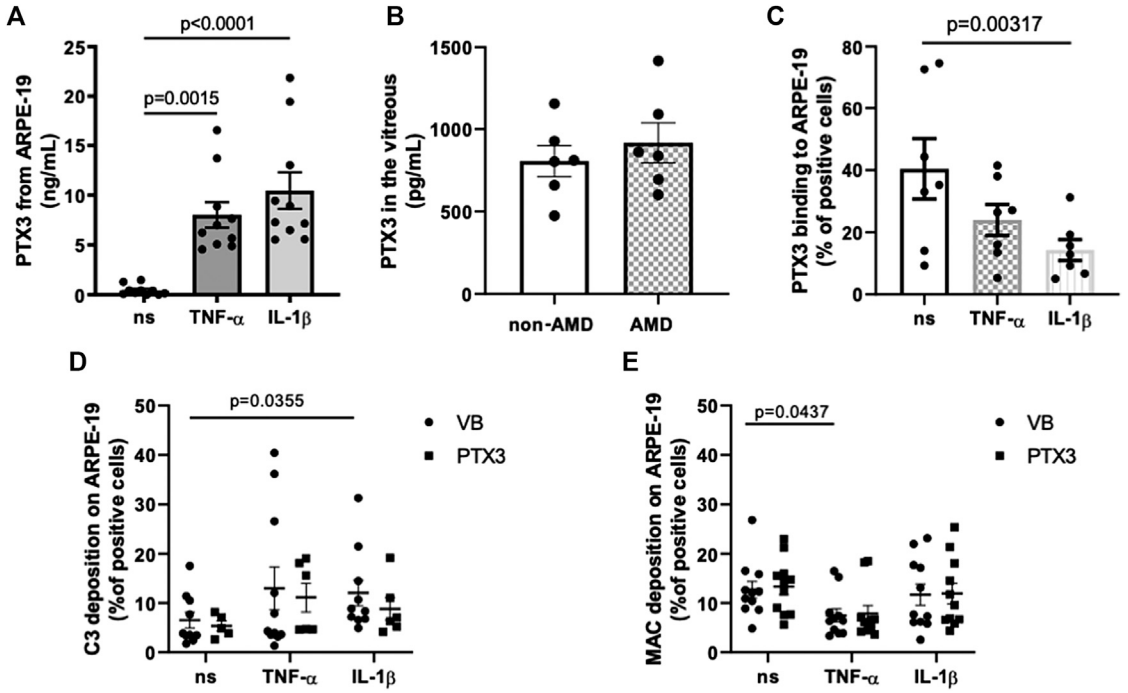

FIGURE 2 | PTX3 is present *in vivo* in the human vitreous, binds *in vitro* ARPE-19 cells in non-inflammatory conditions, and has no direct effect on complement activation on IL-1β- or TNF-α-stimulated ARPE-19 cells. **(A)** ARPE-19 cells were treated with 10 ng/ml TNF-α, 10 ng/ml IL-1β, or vehicle alone for 24 h. PTX3 levels were measured in the conditioned medium. Data are expressed as mean ± SEM, n = 10. Friedman test followed by Dunn's multiple comparison test. **(B)** Vitreous humor was collected from postmortem eyes of age-related macular degeneration (AMD) (*n* = 6) and non-AMD donors (*n* = 6) (see **Supplementary Table S1**), centrifuged for 15 min at 13,000 × g, and PTX3 levels were measured in the soluble fraction. Data are reported as mean ± SEM. **(C)** ARPE-19 cells were treated as described above and incubated with 10 μg/ml rhPTX3 for 30 min. Bound PTX3 was measured by flow cytometry (see **Supplementary Figure S2** for a representative plot of event counts *vs* fluorescence intensity). Data are expressed as percentage of positive cells (mean ± SEM, *n* = 7). Analyzed by Kruskall-Wallis test followed by Dunn's multiple comparison test. **(D,E)** ARPE-19 cells were stimulated with 10 ng/ml TNF-α or IL-1β for 24 h, followed by incubation with 10 μg/ml rhPTX3 (PTX3) or vehicle alone (Veronal Buffer, VB), and challenged with 10% normal human serum (NHS) for 30 min. Cell-bound C3 **(D)** and MAC **(E)** were measured by flow cytometry. Data are expressed as mean ± SEM, *n* = 9–11 from as many independent experiments. Analyzed by Kruskall-Wallis test, followed by Dunn's multiple comparison test.

inflammatory cytokines (particularly, IL-1β) induce an activation-prone profile in AP genes (i.e., increased levels of *C3* and *CFB* mRNAs and proteins) potentially leading to complement dysregulation in RPE cells. Moreover, when stimulated with IL-1β (and, to a lesser extent, TNF-α), these cells also synthesyzed and released pro-inflammatory (i.e., IL-6, IL-8) and pro-angiogenic (i.e., VEGF) factors (**Supplementary Figure S1**), which are involved in recruitment and activation of leukocytes (Tanaka et al., 2014; Harada et al., 1994; Shibuya, 2015), and might indirectly alter complement homeostasis in the RPE (Ambati et al., 2013; Luo et al., 2013).

PTX3 is Expressed by ARPE-19 Cells in Inflammatory Conditions and has No Direct Effect on Complement Activation on the Inflamed RPE

PTX3 is expressed by the RPE in the presence of pro-inflammatory cytokines (Woo et al., 2013). To model expression and function of PTX3 *in vitro* in inflammatory conditions, we treated ARPE-19 cells either with TNF-α or IL-1β, and measured the concentration of PTX3 in the culture medium (**Figure 2A**). Consistent with a previous report (Woo et al., 2013), both stimuli strongly induced synthesis and secretion of the protein (8.02 ± 1.27 ng/ml after TNF-α treatment, and 10.47 ± 1.83 ng/ml after IL-1β treatment, as compared to 0.43 ± 0.16 ng/ml in the absence of stimuli; mean ± SEM, n = 10). Moreover, we could detect endogenous PTX3 in the vitreous humor of a small cohort of 6 AMD and 6 non-AMD patients (**Supplementary Table S2**; **Figure 2B**). Similar protein levels were found in both groups with a trend towards increasing concentrations in AMD (805.2 ± 94.21 and 917.3 ± 121.1 pg/ml in non-AMD and AMD groups, respectively), indicating that soluble PTX3 (i.e., non-associated to the BrM) is present in the human eye both in physiological and pathological conditions.

PTX3 binds apoptotic cells and modulates complement deposition on these cells through engagement of FH (Deban et al., 2008) and C4b-binding protein (C4BP, Braunschweig and Jozsi, 2011). Furthermore, genetic deficiency of PTX3 is associated with increased deposition of C3 on sarcoma cells, and administration of the exogenous protein abrogates this effect via FH-dependent mechanisms (Bonavita et al., 2015). We therefore questioned if the secreted protein could bind the RPE cell line in basal and inflammatory (when complement activating genes are up-regulated) conditions. To this end, 10 μg/ml recombinant human PTX3 were added to ARPE-19

cells that had been previously treated with TNF-α or IL-1β, and the protein's binding was analyzed by flow cytometry (**Figure 2C**; **Supplementary Figure S2**). PTX3 bound these cells in all conditions, however with reduced strength following IL-1β stimulation. These findings extend the current view that inflammation up-regulates the synthesis of PTX3 in the RPE, and suggest that the recruitment of PTX3 onto the RPE is inhibited by the same inflammatory cytokines that promote its expression (particularly, IL-1β).

We then investigated the effect of RPE-bound PTX3 on complement activation. To this end, ARPE-19 cells stimulated either with TNF-α or IL-1β and pre-incubated with rhPTX3, were challenged with normal human serum (NHS), and complement activation was assessed by measuring cell-bound C3 and MAC by flow cytometry. Treatment with IL-1β led to increased deposition of C3 (**Figure 2D**), consistent with the effect of this cytokine on *C3* and *CFB* expression (**Figures 1A–C**), however it did not affect MAC formation (**Figure 2E**). Furthermore, TNF-α-stimulated ARPE-19 cells had reduced assembly of MAC (compared to non-stimulated cells, **Figure 2E**) and similar C3 deposition (**Figure 2D**), consistent with *CD59* (inhibitor of MAC) being up-regulated by TNF-α (**Figure 1G**). More importantly, pre-incubation of cells with PTX3 did not change the levels of C3 (and MAC) following IL-1β (and TNF-α) stimulation (**Figures 2D,E**), consistent with reduced protein's binding (**Figure 2C**). Furthermore, non-stimulated ARPE-19 cells had baseline levels of C3 and MAC deposition, which were not further reduced by PTX3. These findings suggest that inflammatory stimuli (mainly IL-1β) promote complement activation on the RPE, and PTX3 could not control this process due to an impairement of its interaction with the "inflamed" RPE.

Pentraxin 3 Modulates Alternative Pathway Activation and Membrane Attack Complex Formation on Non-Cellular Surfaces via Recruitment of C3b and Factor H

Following our observation that this pentraxin is not involved in the regulation of complement activation on ARPE-19 cells (stimulated with inflammatory cytokines), we investigated the mechanisms by which it modulates complement on non-cellular surfaces, using microtiter plastic plates as an *in vitro* model. To this end, we analyzed the binding of C3b to PTX3 in the presence or absence of FH (i.e., at a [C3b]:[FH] molar ratio of 2:1, which approximates that of [C3]:[FH] in the human plasma (Merle et al., 2015)), and observed that PTX3 recognized C3b, and the resulting complex was strenghtened by FH (**Figure 3A**). These interactions were further evaluated by SPR. C3b stably bound PTX3, due to slow dissociation. Conversely, FH rapidly associated to and dissociated from surface-captured PTX3, indicating a more dynamic interaction. However, when a mixture of C3b and FH was injected over PTX3-coated sensorchips, strong binding signals were observed with complex (non-Langmuir) kinetics (**Figure 3B**), indicating that surface-bound PTX3 recruits C3b with high affinity through formation of a stable ternary complex mediated by FH.

We then questioned whether the PTX3-bound C3b (either in the presence or in the absence of FH) retained the ability to activate complement. To this aim, microtiter plates were coated with PTX3 followed by either C3b or a mixture of C3b and FH, and incubated with FH-depleted human serum (FHDHS, to model complement dysregulation). The resulting protein complexes were retrieved from wells and analyzed by WB, where Bb bands are indicative of C3bBb convertase formation and AP activation (Hourcade, 2006) (see a representative gel in **Supplementary Figure S3**, and the combined data in **Figure 3C**). PTX3-bound C3b formed active C3bBb convertase, although to a lesser extent than C3b alone [possibly due to differences in the relative amounts of plastic-absorbed and PTX3-bound C3b, and to fluid phase C3b being unable to form covalently bound AP C3 convertase (Merle et al., 2015)] (lane 6 in **Supplementary Figure S3**, and **Figure 3C**). However, when FHDHS was added to PTX3-coated wells that had been incubated with a mixture of C3b and FH, no Bb band was observed, indicating that PTX3-and FH-bound C3b cannot form active C3bBb convertase (lane 7 in **Supplementary Figure S3**, and **Figure 3C**). No signal was recorded when PTX3-coated wells were incubated with FHDHS (lane 5 in **Supplementary Figure S3**). Formation of the MAC complex, terminal pathway of the complement cascade (Merle et al., 2015), was also investigated. Similar to C3bBb deposition, C3b supported MAC formation when in a binary complex with PTX3 but failed to do so when incubated both with PTX3 and FH (**Figure 3D**). In additional experiments, fluid phase PTX3 retained binding to C3b-coated plates, and this interaction was enhanced by FH, although to a minor extent compared to surface-bound PTX3 (**Supplementary Figures S4A** and, for comparison, **Figure 3A**). Furthermore, PTX3-bound C3b formed active C3bBb (similar to C3b alone), and lost this function when FH was added to the system (i.e. forming a C3b/PTX3/FH complex) (**Supplementary Figures S4B,C**).

DISCUSSION

An age-related decline in the physiological function of the RPE and subsequent alterations in immune homeostasis within and around the outer blood-retinal barrier contribute to the chronic inflammation that underlies AMD pathogenesis (Ambati et al., 2013). Complement dysregulation and the associated complement-driven inflammation are key events in the onset and progression of this disease (Clark and Bishop, 2018; Pauly et al., 2019). Complement effectors, such as C3a, C5a and the membrane attack complex (MAC), can induce the expression of pro-inflammatory cytokines (including TNF-α and IL-1β) and growth factors (e.g., VEGF) in the RPE (Lueck et al., 2011; Wang et al., 2016), a process that has been associated with AMD progression (Natoli et al., 2017b; Touhami et al., 2018). Moreover, up-regulation of C3 in microglia cells has been linked to retinal damage in AMD (Rutar et al., 2014; Natoli et al., 2017a). Here, we report that, when treated with IL-1β (and TNF-α), ARPE-19 cells (an *in vitro* model of the human RPE) up-regulated transcription of the *C3* and *CFB*, but not *CFH*, genes, and synthesis/secretion of the C3 and FB proteins, which is indicative of complement dysregulation in the inflamed RPE.

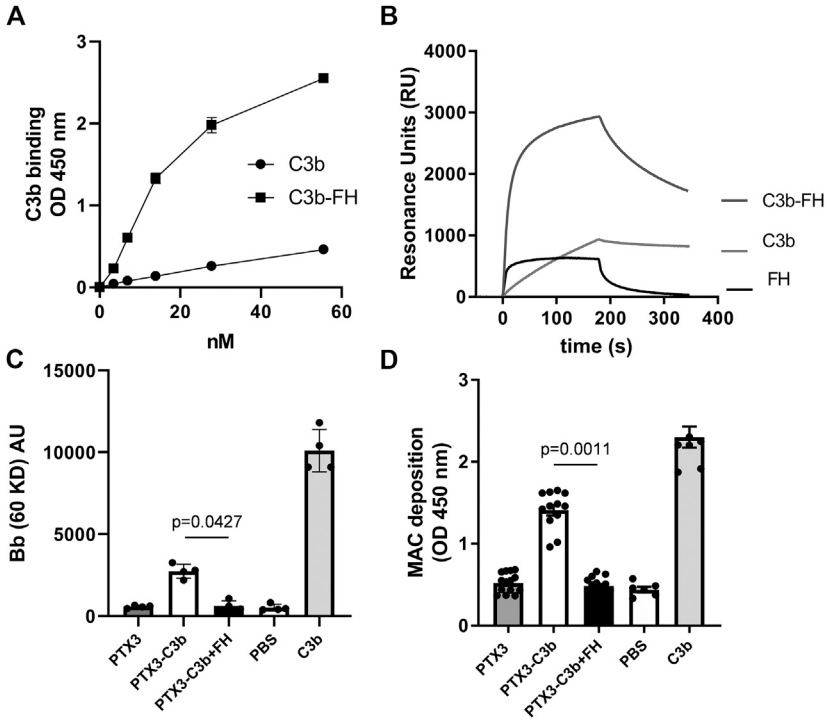

FIGURE 3 | PTX3 recruits C3b and FH on non-cellular surfaces and modulates C3bBb and MAC formation. **(A)** PTX3-coated wells were incubated with the indicated concentrations of C3b or mixtures of C3b and FH (at [C3b]:[FH] molar ratios of 2:1). Bound C3b was detected by ELISA, and data are presented as mean ± SEM from two independent experiments performed in triplicate ($n = 6$). **(B)** Representative SPR sensorgrams of the interaction of FH, C3b, and mixtures of C3b and FH with immobilized PTX3. **(C)** Microtiter plates were coated with C3b alone, PTX3 followed by C3b, or PTX3 followed by a mixture of C3b and FH, then incubated with FH-depleted human serum. Surface-bound proteins were analyzed by western blotting. Intact factor B and its proteolytic fragment Bb (indicative of C3bBb formation) were revealed as immune-reactive bands at apparent molecular weights of 93 kDa and 60 kDa. Band intensity for the Bb species was measured by densitometry. Results are expressed as mean ± SEM, $n = 4$. **(D)** Microtiter plates were coated and incubated as described in **(C)**, and MAC deposition was assessed by ELISA using an anti-sC5b-9 antibody. Data are expressed as mean ± SEM from four independent experiments performed in duplicate ($n = 8$). The p-values reported in **(C,D)** were from the Kruskall-Wallis test, followed by Dunn's multiple comparison test, for the PTX3/C3b and PTX3/C3b/FH complexes. Both in **(C,D)**, C3b-coated wells were used as a positive control for C3bBb formation, and not used for statistical comparison.

Similar profiles have been reported in ARPE-19 cells cultured in the presence of conditioned medium from activated microglia (Madeira et al., 2018) and *in vitro* polarized macrophages (Luo et al., 2013). In addition, treatment of ARPE-19 cells with TNF-α promoted expression of the MAC inhibitor CD59, potentially contributing to the control of complement-driven inflammation. In this regard, decreased levels of CD59 have been associated with AMD pathology (Lueck et al., 2011; Ebrahimi et al., 2013). Consistent with the observed gene expression profiles, IL-1β increased susceptibility of ARPE-19 cells to C3 deposition, whereas stimulation with TNF-α led to reduced MAC formation on the cell surface. These findings point to a complex relationship between inflammatory cytokines and complement activation/regulation in the RPE.

A close crosstalk between the long pentraxin PTX3 and the complement system has been described in diverse tissues and conditions, which regulates complement-dependent inflammatory responses. Current literature indicates that PTX3 is made locally by the RPE in conditions of inflammation (Woo et al., 2013) and oxidative stress (Wang et al., 2016; Hwang et al., 2019), and localizes in the BrM and the basement membrane of both RPE and choriocapillaris, concentrating in the intercapilary septa (Yamada et al., 2008; Swinkels et al., 2018). In agreement with previous evidence (Woo et al., 2013), here we report that ARPE-19 cells express high levels of this pentraxin, when exposed to TNF-α and IL-1β. Presence of the PTX3 protein in the RPE/BrM/choroid has been documented both in AMD (Yamada et al., 2008) and, more recently, in tissues from non-AMD donors (Swinkles et al., 2018). In the present study, we found soluble PTX3 protein in the humor vitreous of both AMD and non-AMD patients, consistent with the view that this pentraxin is constitutively expressed in the eye, and likely contributes to local tissue homeostasis. A trend of increasing concentrations of PTX3 in the AMD vitreous was observed (similar to that we have described in the choriocapillaris (Swinkels et al., 2018)), which however was not significant, likely due to the small sample size and the analyzed AMD specimens all being from donors in the early stage of the disease. At present, it is not clear if other cell types of the human eye, in addition to the RPE (and choroid), can

synthesize the protein. Given that PTX3 expression has been consistently documented in human leukocytes (Doni et al., 2019), it is plausible that this pentraxin is additionally made and released by vitreous body-resident phagocytes (and possibly, retinal microglia and Müller cells), contributing to complement homeostasis in the eye (Pauly et al., 2019).

PTX3 binds several complement proteins, including C1q, mannose binding lectin, ficolin-1 and -2, and activates the classical and lectin pathways (Bottazzi et al., 2010; Bally et al., 2019; Parente et al., 2020). In addition to activators, PTX3 interacts with complement inhibitors like FH and C4BP (Deban et al., 2008; Braunschweig and Jozsi, 2011). Based on an animal model of oxidative stress-induced AMD, PTX3 has been proposed to inhibit AP activation (and the subsequent complement-dependent inflammation) via recruitment of FH (Wang et al., 2016). Furthermore, PTX3 has been described to bind apoptotic and cancer cells and modulate complement activation on these cells through engagement of soluble complement inhibitors (Deban et al., 2008; Braunschweig and Jozsi, 2011; Bonavita et al., 2015). Based on this rationale, here we investigated the AP/PTX3 crosstalk in three different settings (i.e., cell-bound, surface-immobilized and fluid phase PTX3) that recapitulate biologically relevant ways of the presentation of this long pentraxin in the eye.

First, we observed that PTX3 bound ARPE-19 cells in physiological (non-inflammatory) conditions, and this interaction was significantly reduced when these cells were treated with IL-1β, but not TNF-α. Arguably, IL-1β induces modifications in structure/composition of the cell membrane that affect its binding to PTX3. In this regard, we observed that IL-1β prompted synthesis and secretion of IL-6, IL-8 and VEGF by ARPE-19 cells, thus establishing a "self-sustained" inflammatory status that likely modifies plasma membrane and membrane receptor dynamics (Kauppinen et al., 2016). Consistent with the observed binding properties of PTX3, this pentraxin could not protect IL-1β-treated ARPE-19 cells (that were more susceptible to C3 deposition) from complement activation. It is worth pointing out here that whole human serum was used in these experiments as a source of complement, which does not necessarily recapitulate composition and concentration of this system in the eye (Clark and Bishop, 2018; Pauly et al., 2019). Furthermore, the ARPE-19 cells were cultured in non-polarizing conditions, which raises the possibility that either the apical or basal surface (or both) of these cells might retain binding to PTX3 when exposed to inflammatory cytokines. These limitations notwithstanding, it is conceivable that the complement regulating functions of PTX3 mainly involve extracellular matrix (ECM) compartments of the eye, including the BrM, choroidal septa and, based on our evidence, vitreous body, where the protein has been localized.

We then investigated the mechanisms underlying the PTX3/complement crosstalk in a cell-free setting. Surface-absorbed and fluid phase PTX3 was able to bind C3b, key activator of the AP, and this association was strengthened by FH. To our knowledge, this is the first report of a direct interaction between PTX3 and C3b. Interestingly, in SPR experiments we found that immobilized PTX3 formed a ternary complex with FH and C3b with a distinctive association/dissociation profile as compared to that of individual FH and C3b. Detailed analysis of the underlying kinetics and binding mechanisms was beyond the scope of this study, however, it is worth noting here that this complex was long-lived in the applied conditions, with remarkably fast association and slow dissociation rates. To assess if C3b in the PTX3/C3b/FH complex retained complement-activating functions, we developed an *in vitro* assay where microtiter plates were coated with PTX3/C3b or PTX3/C3b/FH complexes, and incubated with human serum that lacked FH (to mimic AP dysregulation). These experiments demonstrated that C3b supports AP activation and MAC formation when bound to PTX3 (in a PTX3/C3b binary complex), and loses these functions when additionally associated with FH (in a PTX3/C3b/FH ternary complex), indicating that in the applied setting inhibition of complement activation is mediated by FH binding to C3b. Based on these findings, we propose that PTX3 cooperates with FH to form a "molecular trap" for C3b, which, when engaged by PTX3 and FH, is no longer accessible to FB and cannot activate the AP and amplify the complement cascade (see **Figure 4**). This mechanism is mostly apparent when PTX3 is bound to non-cellular surfaces (in a setting that mimics the ECM-attached protein) in the presence of soluble C3b. In these conditions, C3b likely has its activated thioester hydrolysed and cannot form covalently bound AP C3 convertase. However, it can still assemble the convertase in solution, and support generation of the anaphylatoxin C3a (Merle et al., 2015). It is therefore conceivable that the C3b-trapping properties of PTX3 (in concert with FH) reduce the intra-ocular levels of C3a (and, possibly, C3a-induced inflamatory mediators) as previously suggested by experimental modelling of AMD in *Ptx3*-deficient mice (Wang et al., 2016).

We found that, in response to inflammatory stimuli, ARPE-19 cells up-regulated synthesis and secretion of both PTX3 (AP inhibitor) and C3 and FB (AP C3 convertase components) proteins, pointing to a compensatory role for this pentraxin in inflammation. This mechanism could be relevant in the presence of the AMD-associated 402H variant of FH, which has been demonstrated to have a more restricted specificity for sulfated GAGs compared to 402Y (Clark et al., 2006; Prosser et al., 2007), and likely has decreased ability to control complement activation at ECM sites, such as the BrM (Clark et al., 2010; Clark and Bishop, 2018). In line with this hypothesis, PTX3 has been shown to co-localize with FH in the murine inner BrM and RPE (Wang et al., 2016). Also, we have described that the Y402H polymorphism alters the binding of FHL-1 (a truncated form of FH), but not FH, to PTX3 (Swinkles et al., 2018). FHL-1 predominates over FH in the BrM and choroid (Clark et al., 2014), and shares with PTX3 common sites within these regions (Swinkels et al., 2018). Thus, it is plausible that the interaction between PTX3 and FHL-1 (in addition to FH) control availability and function of this complement inhibitor (and FH).

In summary, our findings suggest a protective and compensatory role for PTX3 in response to complement dysregulation in AMD, and point to this pentraxin as a potential candidate for novel pharmacological treatments of the disease.

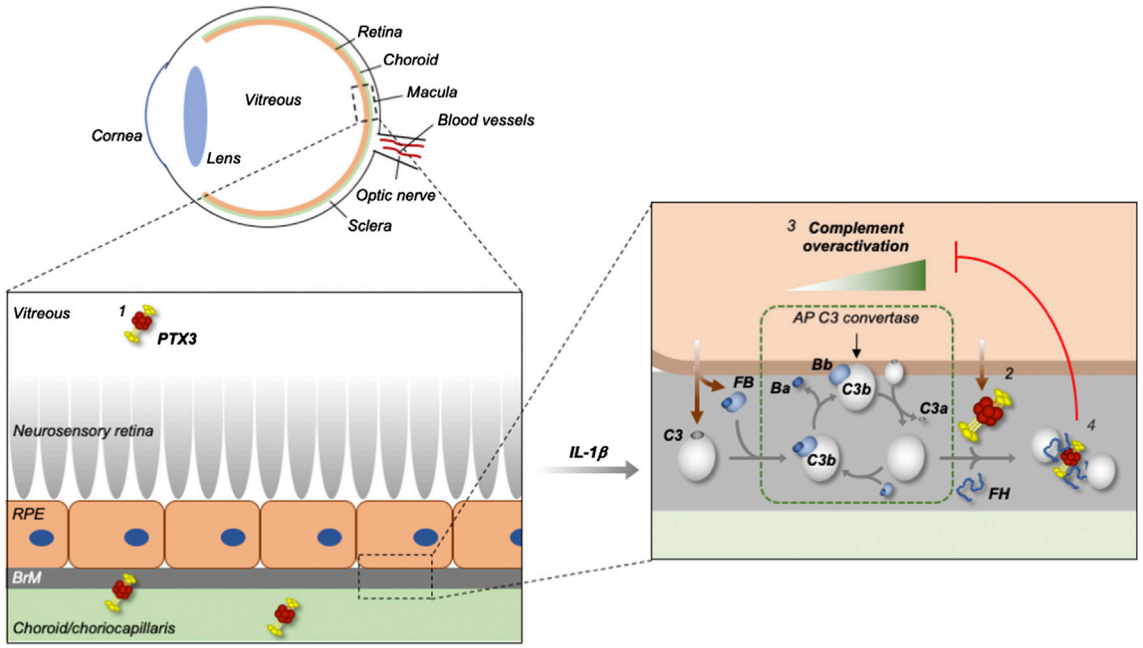

FIGURE 4 | Proposed mechanism for the control of complement dysregulation by PTX3 in the human eye. PTX3 is present in the human vitreous (in addition to the retinal pigment epithelium (RPE) and choroid) both in physiological and pathological (AMD) settings (1), and overexpressed by the RPE (modelled *in vitro* using ARPE-19 cells) in inflammatory conditions (2) that set the scene for complement (mainly AP) dysregulation (3). The secreted PTX3 protein has impaired binding to the inflamed RPE, and thus fails to protect it from complement activation, however it inhibits the AP on non-cellular surfaces (likely the extra-cellular matrix (ECM) of the Bruch's membrane (BrM) and choroid/choriocapillaris, as exemplified in the scheme), through formation of a stable PTX3/FH/C3b complex that acts as a "trap" for C3b and "hot spot" for complement inhibition (4).

DATA AVAILABILITY STATEMENT

The raw data supporting the conclusions of this article will be made available by the authors, without undue reservation.

ETHICS STATEMENT

The studies involving human participants were reviewed and approved by North West – Greater Manchester Central Research Ethics Committee (REC reference 15/NW/0932). The patients/participants provided their written informed consent to participate in this study.

AUTHOR CONTRIBUTIONS

MS designed and conducted all the experimental activities on this study and wrote the manuscript. FD, RP, and MG assisted on complement deposition, flow cytometry and SPR analyses, respectively. BB, AM, SJC, AJD, and MRR critically revised the manuscript. AI supervised the study and wrote the manuscript.

FUNDING

MRR is recipient of a Research Prize from the Italian Society of Ophtalmology (SOI) that funded FD. The financial support of Fondazione Beppe and Nuccy Angiolini to RP is greatly acknowledged.

ACKNOWLEDGMENTS

We gratefully appreciate Prof Paul Bishop (The University of Manchester) for assistance on transferring donor eye tissues from the Manchester Eye Tissue Repository (ETR).

SUPPLEMENTARY MATERIAL

The Supplementary Material for this article can be found online at: https://www.frontiersin.org/articles/10.3389/fphar.2020.591908/full#supplementary-material.

REFERENCES

Altay, L., Sitnilska, V., Schick, T., Widmer, G., Duchateau-Nguyen, G., Piraino, P., et al. (2019). Early local activation of complement in aqueous humour of patients with age-related macular degeneration. *Eye* 33, 1859–1864. doi:10.1038/s41433-019-0501-4

Ambati, J., Ambati, B. K., Yoo, S. H., Ianchulev, S., and Adamis, A. P. (2003). Age-related macular degeneration: etiology, pathogenesis, and therapeutic strategies. *Surv. Ophthalmol.* 48, 257–293. doi:10.1016/s0039-6257(03)00030-4

Ambati, J., Atkinson, J. P., and Gelfand, B. D. (2013). Immunology of age-related macular degeneration. *Nat. Rev. Immunol.* 13, 438–451. doi:10.1038/nri3459

Bally, I., Inforzato, A., Dalonneau, F., Stravalaci, M., Bottazzi, B., Gaboriaud, C., et al. (2019). Interaction of C1q with pentraxin 3 and IgM revisited: mutational studies with recombinant C1q variants. *Front. Immunol.* 10, 461. doi:10.3389/fimmu.2019.00461

Baranova, N. S., Inforzato, A., Briggs, D. C., Tilakaratna, V., Enghild, J. J., Thakar, D., et al. (2014). Incorporation of pentraxin 3 into hyaluronan matrices is tightly regulated and promotes matrix cross-linking. *J. Biol. Chem.* 289, 30481–30498. doi:10.1074/jbc.m114.568154

Blaum, B. S., Hannan, J. P., Herbert, A. P., Kavanagh, D., Uhrín, D., and Stehle, T. (2015). Structural basis for sialic acid-mediated self-recognition by complement factor H. *Nat. Chem. Biol.* 11, 77–82. doi:10.1038/nchembio.1696

Bonavita, E., Gentile, S., Rubino, M., Maina, V., Papait, R., Kunderfranco, P., et al. (2015). PTX3 is an extrinsic oncosuppressor regulating complement-dependent inflammation in cancer. *Cell* 160, 700–714. doi:10.1016/j.cell.2015.01.004

Bottazzi, B., Doni, A., Garlanda, C., and Mantovani, A. (2010). An integrated view of humoral innate immunity: pentraxins as a paradigm. *Annu. Rev. Immunol.* 28, 157–183. doi:10.1146/annurev-immunol-030409-101305

Bottazzi, B., Vouret-Craviari, V., Bastone, A., De Gioia, L., Matteucci, C., Peri, G., et al. (1997). Multimer formation and ligand recognition by the long pentraxin PTX3. *J. Biol. Chem.* 272, 32817–32823. doi:10.1074/jbc.272.52.32817

Braunschweig, A. and Jozsi, M. (2011). Human pentraxin 3 binds to the complement regulator c4b-binding protein. *PLoS One* 6, e23991. doi:10.1371/journal.pone.0023991

Canovi, M., Lucchetti, J., Stravalaci, M., Valentino, S., Bottazzi, B., Salmona, M., et al. (2014). A new surface plasmon resonance-based immunoassay for rapid, reproducible and sensitive quantification of pentraxin-3 in human plasma. *Sensors* 14, 10864–10875. doi:10.3390/s140610864

Cipriani, V., Lorés-Motta, L., He, F., Fathalla, D., Tilakaratna, V., McHarg, S., et al. (2020) Increased circulating levels of Factor H-Related Protein 4 are strongly associated with age-related macular degeneration. *Nat. Commun.* 11, 778. doi:10.1038/s41467-020-14499-3

Clark, S. J. and Bishop, P. N. (2018). The eye as a complement dysregulation hotspot. *Semin. Immunopathol.* 40, 65–74. doi:10.1007/s00281-017-0649-6

Clark, S. J., Higman, V. A., Mulloy, B., Perkins, S. J., Lea, S. M., Sim, R. B., et al. (2006). His-384 allotypic variant of factor H associated with age-related macular degeneration has different heparin binding properties from the non-disease-associated form. *J. Biol. Chem.* 281, 24713–24720. doi:10.1074/jbc.m605083200

Clark, S. J., Perveen, R., Hakobyan, S., Morgan, B. P., Sim, R. B., Bishop, P. N., et al. (2010). Impaired binding of the age-related macular degeneration-associated complement factor H 402H allotype to Bruch's membrane in human retina. *J. Biol. Chem.* 285, 30192–30202. doi:10.1074/jbc.m110.103986

Clark, S. J., Ridge, L. A., Herbert, A. P., Hakobyan, S., Mulloy, B., Lennon, R., et al. (2013). Tissue-specific host recognition by complement factor H is mediated by differential activities of its glycosaminoglycan-binding regions. *J. Immunol.* 190, 2049–2057. doi:10.4049/jimmunol.1201751

Clark, S. J., Schmidt, C. Q., White, A. M., Hakobyan, S., Morgan, B. P., and Bishop, P. N. (2014). Identification of factor H-like protein 1 as the predominant complement regulator in Bruch's membrane: implications for age-related macular degeneration. *J. Immunol.* 193, 4962–4970. doi:10.4049/jimmunol.1401613

Crabb, J. W., Miyagi, M., Gu, X., Shadrach, K., West, K. A., Sakaguchi, H., et al. (2002). Drusen proteome analysis: an approach to the etiology of age-related macular degeneration. *Proc. Natl. Acad. Sci. Unit. States Am.* 99, 14682–14687. doi:10.1073/pnas.222551899

Curcio, C. A. (2018). Antecedents of soft drusen, the specific deposits of age-related macular degeneration, in the biology of human macula. *Invest. Ophthalmol. Vis. Sci.* 59, AMD182–AMD181. doi:10.1167/iovs.18-24883

Deban, L., Jarva, H., Lehtinen, M. J., Bottazzi, B., Bastone, A., Doni, A., et al. (2008). Binding of the long pentraxin PTX3 to factor H: interacting domains and function in the regulation of complement activation. *J. Immunol.* 181, 8433–8440. doi:10.4049/jimmunol.181.12.8433

Doni, A., Stravalaci, M., Inforzato, A., Magrini, E., Mantovani, A., Garlanda, C., et al. (2019). The long pentraxin PTX3 as a Link between innate immunity, tissue remodeling, and cancer. *Front. Immunol.* 10, 712. doi:10.3389/fimmu.2019.00712

Ebrahimi, K. B., Fijalkowski, N., Cano, M., and Handa, J. T. (2013). Decreased membrane complement regulators in the retinal pigmented epithelium contributes to age-related macular degeneration. *J. Pathol.* 229, 729–742. doi:10.1002/path.4128

Edwards, A. O., Ritter, R., Abel, K. J., Manning, A., Panhuysen, C., and Farrer, L. A. (2005). Complement factor H polymorphism and age-related macular degeneration. *Science* 308, 421–424. doi:10.1126/science.1110189

Fritsche, L. G., Igl, W., Bailey, J. N. C., Grassmann, F., Sengupta, S., Bragg-Gresham, J. L., et al. (2016). A large genome-wide association study of age-related macular degeneration highlights contributions of rare and common variants. *Nat. Genet.* 48, 134–143. doi:10.1038/ng.3448

Hageman, G., Luthert, P. J., Victor Chong, N. H., Johnson, L. V., Anderson, D. H., and Mullins, R. F. (2001). An integrated hypothesis that considers drusen as biomarkers of immune-mediated processes at the RPE-Bruch's membrane interface in aging and age-related macular degeneration. *Prog. Retin. Eye Res.* 20, 705–732. doi:10.1016/s1350-9462(01)00010-6

Hageman, G. S., Anderson, D. H., Johnson, L. V., Hancox, L. S., Taiber, A. J., Hardisty, L. I., et al. (2005). From the Cover: a common haplotype in the complement regulatory gene factor H (HF1/CFH) predisposes individuals to age-related macular degeneration. *Proc. Natl. Acad. Sci. Unit. States Am.* 102, 7227–7232. doi:10.1073/pnas.0501536102

Haines, J. L., Hauser, M. A., Schmidt, S., Scott, W. K., Olson, L. M., Gallins, P., et al. (2005). Complement factor H variant increases the risk of age-related macular degeneration. *Science* 308, 419–421. doi:10.1126/science.1110359

Harada, A., Sekido, N., Akahoshi, T., Wada, T., Mukaida, N., and Matsushima, K. (1994). Essential involvement of interleukin-8 (IL-8) in acute inflammation. *J. Leukoc. Biol.* 56, 559–564. doi:10.1002/jlb.56.5.559

Hourcade, D. E. (2006). The role of properdin in the assembly of the alternative pathway C3 convertases of complement. *J. Biol. Chem.* 281, 2128–2132. doi:10.1074/jbc.m508928200

Hwang, N., Kwon, M. Y., Woo, J. M., and Chung, S. W. (2019). Oxidative stress-induced pentraxin 3 expression human retinal pigment epithelial cells is involved in the pathogenesis of age-related macular degeneration. *Int. J. Mol. Sci.* 20, 6028. doi:10.3390/ijms20236028

Inforzato, A., Baldock, C., Jowitt, T. A., Holmes, D. F., Lindstedt, R., Marcellini, M., et al. (2010). The angiogenic inhibitor long pentraxin PTX3 forms an asymmetric octamer with two binding sites for FGF2. *J. Biol. Chem.* 285, 17681–17692. doi:10.1074/jbc.m109.085639

Inforzato, A., Reading, P. C., Barbati, E., Bottazzi, B., Garlanda, C., and Mantovani, A. (2012). The "sweet" side of a long pentraxin: how glycosylation affects PTX3 functions in innate immunity and inflammation. *Front. Immunol.* 3, 407. doi:10.3389/fimmu.2012.00407

Inforzato, A., Rivieccio, V., Morreale, A. P., Bastone, A., Salustri, A., Scarchilli, L., et al. (2008). Structural characterization of PTX3 disulfide bond network and its multimeric status in cumulus matrix organization. *J. Biol. Chem.* 283, 10147–10161. doi:10.1074/jbc.m708535200

Jager, R. D., Mieler, W. F., and Miller, J. W. (2008). Age-related macular degeneration. *N. Engl. J. Med.* 358, 2606–2617. doi:10.1056/nejmra0801537

Juel, H. B., Faber, C., Munthe-Fog, L., Bastrup-Birk, S., Reese-Petersen, A. L., Falk, M. K., et al. (2015). Systemic and ocular long pentraxin 3 in patients with age-related macular degeneration. *PLoS One* 10, e0132800. doi:10.1371/journal.pone.0132800

Kauppinen, A., Paterno, J. J., Blasiak, J., Salminen, A., and Kaarniranta, K. (2016). Inflammation and its role in age-related macular degeneration. *Cell. Mol. Life Sci.* 73, 1765–1786. doi:10.1007/s00018-016-2147-8

Langford-Smith, A., Day, A. J., Bishop, P. N., and Clark, S. J. (2015). Complementing the sugar code: role of GAGs and sialic acid in complement regulation. *Front. Immunol.* 6, 25. doi:10.3389/fimmu.2015.00025

Lueck, K., Wasmuth, S., Williams, J., Hughes, T. R., Morgan, B. P., Lommatzsch, A., et al. (2011). Sub-lytic C5b-9 induces functional changes in retinal pigment epithelial cells consistent with age-related macular degeneration. *Eye* 25, 1074–1082. doi:10.1038/eye.2011.109

Luo, C., Zhao, J., Madden, A., Chen, M., and Xu, H. (2013). Complement expression in retinal pigment epithelial cells is modulated by activated macrophages. *Exp. Eye Res.* 112, 93–101. doi:10.1016/j.exer.2013.04.016

Madeira, M. H., Rashid, K., Ambrosio, A. F., Santiago, A. R., and Langmann, T. (2018). Blockade of microglial adenosine A2A receptor impacts inflammatory

mechanisms, reduces ARPE-19 cell dysfunction and prevents photoreceptor loss *in vitro*. *Sci. Rep.* 8, 2272. doi:10.1038/s41598-018-20733-2

Merle, N. S., Church, S. E., Fremeaux-Bacchi, V., and Roumenina, L. T. (2015). Complement system Part I - molecular mechanisms of activation and regulation. *Front. Immunol.* 6, 262. doi:10.3389/fimmu.2015.00262

Natoli, R., Fernando, N., Jiao, H., Racic, T., Madigan, M., Barnett, N. L., et al. (2017a). Retinal macrophages synthesize C3 and activate complement in AMD and in models of focal retinal degeneration. *Invest. Ophthalmol. Vis. Sci.* 58, 2977–2990. doi:10.1167/iovs.17-21672

Natoli, R., Fernando, N., Madigan, M., Chu-Tan, J. A., Valter, K., Provis, J., et al. (2017b). Microglia-derived IL-1beta promotes chemokine expression by Muller cells and RPE in focal retinal degeneration. *Mol. Neurodegener.* 12, 31. doi:10.1186/s13024-017-0175-y

Parente, R., Clark, S. J., Inforzato, A., and Day, A. J. (2017). Complement factor H in host defense and immune evasion. *Cell. Mol. Life Sci.* 74, 1605–1624. doi:10.1007/s00018-016-2418-4

Parente, R., Doni, A., Bottazzi, B., Garlanda, C., and Inforzato, A. (2020). The complement system in Aspergillus fumigatus infections and its crosstalk with pentraxins. *FEBS Lett.* 59, 2480–2501. doi:10.1002/1873-3468.13744

Parente, R., Sobacchi, C., Bottazzi, B., Mantovani, A., Grcevic, D., and Inforzato, A. (2019). The long pentraxin PTX3 in bone homeostasis and pathology. *Front. Immunol.* 10, 2628. doi:10.3389/fimmu.2019.02628

Pauly, D., Agarwal, D., Dana, N., Schäfer, N., Biber, J., Wunderlich, K. A., et al. (2019). Cell-type-Specific complement expression in the healthy and diseased retina. *Cell Rep.* 29, 2835–2848. doi:10.1016/j.celrep.2019.10.084

Prosser, B. E., Johnson, S., Roversi, P., Herbert, A. P., Blaum, B. S., Tyrrell, J., et al. (2007). Structural basis for complement factor H-linked age-related macular degeneration. *J. Exp. Med.* 204, 2277–2283. doi:10.1084/jem.20071069

Rutar, M., Valter, K., Natoli, R., and Provis, J. M. (2014). Synthesis and propagation of complement C3 by microglia/monocytes in the aging retina. *PLoS One* 9, e93343. doi:10.1371/journal.pone.0093343

Schick, T., Steinhauer, M., Aslanidis, A., Altay, L., Karlstetter, M., Langmann, T., et al. (2017). Local complement activation in aqueous humor in patients with age-related macular degeneration. *Eye* 31, 810–813. doi:10.1038/eye.2016.328

Shibuya, M. (2015). VEGF-VEGFR system as a target for suppressing inflammation and other diseases. *Endocr. Metab. Immune. Disord. Drug Targets* 15, 135–144. doi:10.2174/1871530315666150316121956

Sjöberg, A. P., Trouw, L. A., Clark, S. J., Sjölander, J., Heinegård, D., Sim, R. B., et al. (2007). The factor H variant associated with age-related macular degeneration (His-384) and the non-disease-associated form bind differentially to C-reactive protein, fibromodulin, DNA, and necrotic cells. *J. Biol. Chem.* 282, 10894–10900. doi:10.1074/jbc.m610256200

Swinkels, M., Zhang, J. H., Tilakaratna, V., Black, G., Perveen, R., Mcharg, S., et al. (2018). C-reactive protein and pentraxin-3 binding of factor H-like protein 1 differs from complement factor H: implications for retinal inflammation. *Sci. Rep.* 8, 1643. doi:10.1038/s41598-017-18395-7

Tanaka, T., Narazaki, M., and Kishimoto, T. (2014). IL-6 in inflammation, immunity, and disease. *Cold Spring Harb. Perspect. Biol.* 6, a016295. doi:10.1101/cshperspect.a016295

Touhami, S., Beguier, F., Augustin, S., Charles-Messance, H., Vignaud, L., Nandrot, E. F., et al. (2018). Chronic exposure to tumor necrosis factor alpha induces retinal pigment epithelium cell dedifferentiation. *J. Neuroinflammation* 15, 85. doi:10.1186/s12974-018-1106-8

Wang, L., Cano, M., Datta, S., Wei, H., Ebrahimi, K. B., Gorashi, Y., et al. (2016). Pentraxin 3 recruits complement factor H to protect against oxidative stress-induced complement and inflammasome overactivation. *J. Pathol.* 240, 495–506. doi:10.1002/path.4811

Wong, W. L., Su, X., Li, X., Cheung, C. M. G., Klein, R., Cheng, C.-Y., et al. (2014). Global prevalence of age-related macular degeneration and disease burden projection for 2020 and 2040: a systematic review and meta-analysis. *Lancet Glob. Health* 2, e106–e116. doi:10.1016/s2214-109x(13)70145-1

Woo, J. M., Kwon, M. Y., Shin, D. Y., Kang, Y. H., Hwang, N., and Chung, S. W. (2013). Human retinal pigment epithelial cells express the long pentraxin PTX3. *Mol. Vis.* 19, 303–310.

Yamada, Y., Tian, J., Yang, Y., Cutler, R. G., Wu, T., Telljohann, R. S., et al. (2008). Oxidized low density lipoproteins induce a pathologic response by retinal pigmented epithelial cells. *J. Neurochem.* 105, 1187–1197. doi:10.1111/j.1471-4159.2008.05211.x

Conflict of Interest: AJD is a co-Founder and Director of Link Biologics. SJC is a co-Founder and Director of Complement Therapeutics.

The remaining authors declare that the research was conducted in the absence of any commercial or financial relationships that could be construed as a potential conflict of interest.

The handling editor declared a past co-authorship with one of the authors MRR.

frontiers in Pharmacology

ORIGINAL RESEARCH
published: 23 December 2020
doi: 10.3389/fphar.2020.590572

Thioredoxin Delays Photoreceptor Degeneration, Oxidative and Inflammation Alterations in Retinitis Pigmentosa

*Roberto Gimeno-Hernández, Antolin Cantó, Angel Fernández-Carbonell, Teresa Olivar, Vicente Hernández-Rabaza, Inmaculada Almansa and María Miranda**

Departamento Ciencias Biomédicas, Universidad Cardenal Herrera-CEU, CEU Universities, Valencia, Spain

Retinitis pigmentosa (RP) is an inherited ocular disorder with no effective treatment. RP onset and progression trigger a cascade of retinal disorders that lead to the death of photoreceptors. After photoreceptors death, neuronal, glial and vascular remodeling can be observed in the retina. The purpose of this study was to study if thioredoxin (TRX) administration is able to decrease photoreceptor death in an animal model of RP (rd1 mouse), but also if it is able to modulate the retinal oxidative stress, glial and vascular changes that can be observed as the disease progresses. Wild type and rd1 mice received several doses of TRX. After treatment, animals were euthanized at postnatals days 11, 17, or 28. Glutathione (GSH) and other thiol compounds were determined by high performance liquid chromatography (HPLC). Glial fibrilary acidic protein (GFAP) and anti-ionized calcium binding adaptor molecule 1 (Iba1) were studied by immunohistochemistry. Vascular endothelial growth factor (VEGF) and hepatic growth factor (HGF) expression were determined by western blot. TRX administration significantly diminished cell death in rd1 mouse retinas and increased GSH retinal concentrations at postnatal day 11 (PN11). TRX was also able to reverse glial alterations at PN11 and PN17. No alterations were observed in retinal VEGF and HGF expression in rd1 mice. In conclusion, TRX treatment decreases photoreceptor death in the first stages of RP and this protective effect may be due in part to the GSH system activation and to a partially decrease in inflammation.

Keywords: retina, thioredoxin, glutathione, vascular endothelial growth factor, glia, hepatic growth factor

OPEN ACCESS

Edited by:
Julie Sanderson, University of East Anglia, United Kingdom

Reviewed by:
Zakiah Jubri, National University of Malaysia, Malaysia
Maria Muriach, University of Jaume I, Spain

****Correspondence:***
María Miranda
mmiranda@uchceu.es

Specialty section:
This article was submitted to Inflammation Pharmacology, a section of the journal Frontiers in Pharmacology

Received: *02 August 2020*
Accepted: *03 November 2020*
Published: *23 December 2020*

Citation:
Gimeno-Hernández R, Cantó A, Fernández-Carbonell A, Olivar T, Hernández-Rabaza V, Almansa I and Miranda M (2020) Thioredoxin Delays Photoreceptor Degeneration, Oxidative and Inflammation Alterations in Retinitis Pigmentosa. Front. Pharmacol. 11:590572. doi: 10.3389/fphar.2020.590572

INTRODUCTION

The name retinitis pigmentosa (RP) describes a heterogeneous group of degenerative and inherited ocular disorders that causes severe visual impairment (Wright et al., 2010; Daiger et al., 2013) and in many cases leads to total blindness. It is considered a rare disease with a worldwide prevalence of 1 in 4,000 individuals (Boughman et al., 1980). The most important RP clinical manifestations are nictalopia (also called night blindness), visual field loss, decrease in the ability to distinguish objects at low contrast (Lindberg et al., 1981) and photophobia.

RP onset and progression triggers a cascade of retinal disorders that lead to the death of photoreceptors. After photoreceptors death, a reorganization of the retinal circuits occurs, causing changes in morphology and in the establishment of new synapses between retinal cells. Although the

mechanisms of photoreceptors death are not completely clear, three phases can be distinguished in the RP degeneration process (Jones and Marc, 2005): i) phase I: photoreceptors suffer a period of stress, shortening of rods and a disorganization of their synaptic contacts is observed; ii) phase II: death of photoreceptors takes place, Müller cells form glial fibrotic walls throughout the retina and death of other retinal neurons can also occur; iii) phase III: neuronal, glial and vascular remodeling of the retina occurs (Jones et al., 2016). In this last stage of the disease, neural cells dye progressively, and Müller cells fill in the spaces left by them. This process is accompanied by a decrease in retinal blood flow in response to a reduced metabolic demand (Grunwald et al., 1996). The disappearance of retinal blood vessels has been related with a decrease in vascular endothelial growth factor (VEGF) in aqueous humor of patients with RP (Salom et al., 2008). VEGF was initially identified as a vascular permeability factor and recently it has been shown to influence the growth and survival of neurons (Sondell et al., 1999; Jin et al., 2000). Hepatic growth factor (HGF) plays also a role in ocular angiogenesis and neuroprotection of retinal neurons (Bussolino et al., 1992; Salom et al., 2010; Karamali et al., 2019; Lorenc et al., 2020), however it is still unknown whether alterations of this growth factor may be relevant in RP or not.

The retina is extremely rich in membranes with polyunsaturated lipids (Panfoli et al., 2012). This feature makes it especially sensitive to oxidative stress because they may suffer peroxidation. In addition, the rods are very active cells with high oxygen consumption. During the progression of the RP, when the rods die, oxygen consumption in the retina decreases and oxygen retinal concentration increases. Therefore, a situation of hyperoxia occurs that could induce oxidative damage. In this sense, antioxidant therapy has been suggested as a possible way to slow down the degenerative process in RP because they may decrease oxidative stress. On the other hand, antioxidants have some important advantages as their safety when being used in adult humans, being able to improve the vision, at least transiently. Regarding the use of important antioxidants: curcumin (Vasireddy et al., 2011), tauroursodeoxycholic acid (TUDCA) (Fernández-Sánchez et al., 2011), n-acetylcysteine (Lee et al., 2011; Yoshida et al., 2013), lutein (Berson et al., 2010), chlorogenic acid (Shin and Yu, 2014), or combinations of antioxidants such as lutein, zeaxanthin, alpha lipoic acid and glutathione (Sanz et al., 2007) have been studied in humans and animal models as possible therapies for RP.

Thioredoxin (TRX) family proteins contain the active center Cysteine-Glycine-Proline-Cysteine. They also present oxidized cysteine groups (Powis and Montfort, 2001). The TRX system participates in a wide range of functions within the cell, including protection against oxidative stress (Holmgren, 2000), DNA precursor synthesis, proliferation, regulation and cell differentiation, cell death control and immune system modulation (Gromer et al., 2004; Arnér and Holmgren, 2006). It also has anti-inflammatory functions (Nakamura et al., 2001). Thioredoxin is antioxidant because it facilitates the reduction of other proteins by cysteine thiol-disulfide exchange.

Levéillard et al. identified the rod-derived cone viability factor (RdCVF)) in 2004 (Léveillard et al., 2004). This factor, released by rods, is key in the conservation of cones viability and may protect them from death (Scholl et al., 2016). RdCVF is a truncated TRX type protein specifically expressed by photoreceptors (Léveillard and Sahel, 2010). The nucleoredoxin-like gene also known as NXNL1 encodes RdCVF. NXNL1 encodes for two proteins, one is RdCVF that does not have TRX (Chalmel et al., 2007). In addition, alternative processing of the gene results in a protein with TRX activity known as RdCVFL (thioredoxin-like protein rod-derived cone viability factor).

However, it has not been studied if TRX external administration may have a protective effect in RP. The main purpose of this study was to administrate TRX in an experimental RP animal model. It is well known that TRX is able to pass brain blood barrier and therefore it may pass the retinal blood barrier, and though we have not determined TRX retinal concentration we have determined its direct effect (such as the decrease in photoreceptor death and the increase in glutathione). We studied if TRX was able to decrease photoreceptor death and to modulate the retinal oxidative stress (determining TRX effect on the retinal concentration of one of the major intracellular antioxidants, glutathione), and glial and vascular changes that can be observed as the disease progress. Our study was performed at three different postnatal days: 11, 17, and 28.

The animal model used in this study was the rd1 mouse, which was first described by Keeler in 1924 (Keeler, 1924) and shows a rapid degeneration of photoreceptors. The disorder in this animal model is caused by a mutation in the gene that encodes the beta subunit of phosphodiesterase-6 (PDE6) of the rods (Lolley et al., 1980; Bowes et al., 1990). This enzymatic alteration causes the accumulation of cGMP. This accumulation makes the calcium channels generate an abnormal inflow (Gregory and Bird, 1995; Fox et al., 2003) that triggers a cascade of events that finally leads to the death of photoreceptor cells (Adler, 1996; Travis, 1998). The degeneration of photoreceptors, specifically of the rods, in rd1 mice is maximum between postnatal days 11 and 13 (PN11-13) (Paquet-Durand et al., 2006). At PN17, only a small percentage of the rods remain while 75% of the cones persist (Carter-Dawson et al., 1978). At PN28, the degeneration of the rods is complete, and the vascular system is affected (Blanks and Johnson, 1986).

MATERIALS AND METHODS

Control and rd1 mice were used in this study. Mice were housed in the facilities of the Research Unit of CEU Cardenal Herrera University. The animals were kept in cages under controlled conditions of temperature (20°C) and humidity (60%) and were housed under standard (12 h) cyclic lighting and had free access to water and to a standard diet (Harlan Ibérica S.L. (Barcelona, Spain)). Handling and care of the animals were approved by the CEU Cardenal Herrera Universities Committee for Animal Experiments (reference 11/013) and were also performed in accordance with ARVO (Association for Research in Vision and Ophthalmology) Statement for the use of animals in Ophthalmic and Vision Research.

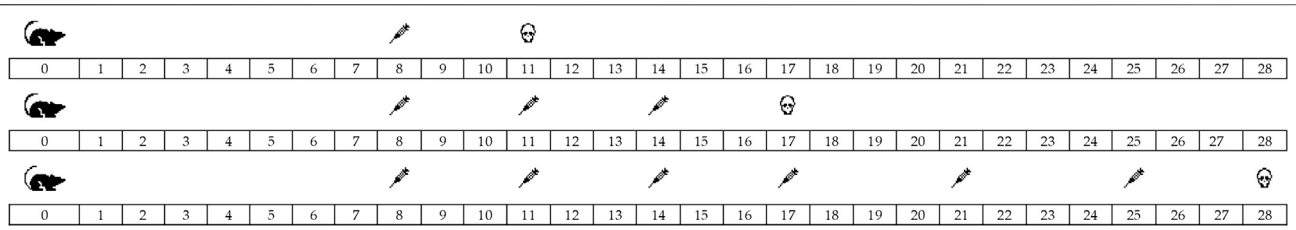

FIGURE 1 | Experimental design for thioredoxin treatment of control and rd1 mice (TRX dose: 5 mg/kg weight; via: i.p.). Numbers indicate postnatal day. Group 1: control mice that received vehicle treatment at P8 and were euthanized at PN11; Group 2: control mice that received TRX treatment at P8 and were euthanized at PN11; Group 3: rd1 mice that received vehicle treatment at P8 and were euthanized at PN11; Group 4: rd1 mice that received TRX treatment at P8 and were euthanized at PN11; Group 5: control mice treated with vehicle at PN8, PN11, and PN14 and euthanized at PN17; Group 6: control mice treated with TRX at PN8, PN11, and PN14 and euthanized at PN17; Group 7: rd1 mice treated with vehicle at PN8, PN11, and PN14 and euthanized at PN17; Group 8: rd1 mice treated with TRX at PN8, PN11, and PN14 and euthanized at PN17; Group 9: control mice that received vehicle treatment at PN8, PN11, PN14, PN17, PN21, PN25 and were euthanized at PN28; Group 10: control mice that received TRX treatment at PN8, PN11, PN14, PN17, PN21, PN25 and were euthanized at PN28; Group 11: rd1 mice that received vehicle treatment at PN8, PN11, PN14, PN17, PN21, PN25 and were euthanized at PN28; Group 12: rd1 mice that received TRX treatment at PN8, PN11, PN14, PN17, PN21, PN25 and were euthanized at PN28.

Day of birth was considered as post-natal day 0 (PN0). TRX treatment started at PN8 (5 mg/kg weight dissolved in 1 ml of saline). TRX (T0910) was purchased from Sigma-Aldrich (Madrid, Spain) and administered intraperitoneally. TRX dose and administration method were selected according to previous studies reporting its ability to cross blood brain barrier (BBB) (Tian et al., 2014; Wang et al., 2015). Moreover, TRX are expressed in various areas of the mouse, rat, and human brain as well as in the retina (Hanschmann et al., 2013).

Twelve experimental groups were used in this study (four groups for each postnatal day studied). Groups 1 to 4 were control and rd1 mice that received vehicle or TRX treatment at P8 and were euthanized at PN11. Groups 5 to 8 consisted on control and rd1 mice treated with vehicle or TRX at PN8, PN11 and PN14 and euthanized at PN17. Groups 9 to 12 control and rd1 mice that received vehicle or TRX treatment at PN8, PN11, PN14, PN17, PN21, PN25 and were euthanized at PN28 (**Figure 1**). The number of animals in each experimental group was at least 8.

Histological and Immunofluorescence Studies

Firstly, eyes were enucleated and fixed by immersion in 4% paraformaldehyde (PFA) for 2 h. Secondly, eyes were washed with 0.1 M phosphate buffered saline pH 7.2 (PBS). Finally, they were cryoprotected in increasing concentrations of PBS-sucrose (10–20–30%) at 4°C. After embedding in Tissue Tek (Sakura Europe, Spain), the eyes were sectioned in a Leica CM 1850 UV Ag protect cryostat, (Leica Microsistemas SLU, Barcelona, Spain) (8 µm sections) on superfrost slides (Thermo Fisher Scientific, Braunschweig, Germany) and kept at −20°C. Only one retina per mice was used in histological and immunofluorescence studies.

Terminal Deoxinucleotidyl Transferase Assay

Detection of dying cells with the TUNEL assay was performed with an *in situ* detection kit (Roche Diagnostics, Mannheim, Germany) as reported previously (Benlloch-Navarro et al., 2019). Retinal images were taken with the Nikon DS-Fi1 camera attached to a Leica DM 2000 microscope. The Leica application Suite version 2.7.0 R1 (Leica Microsystems SLU, Barcelona, Spain) program was used.

Retinal Immunohistochemistry

Retinal tissue cryosections were rehydrated in PBS and merged with blocking solution: 5% of normal goat serum in PBS-BSA 1% and Triton 0.3%. Sections were incubated at 4°C over night in primary antibodies: anti-glial fibrillary acidic protein (anti-GFAP) (1:500, Dako cytomation, Denmark) and anti-ionized calcium binding adaptor molecule 1 (anti-Iba1 (1:2,000, Abcam, Cambridge, United Kingdom). Primary antibodies were detected with the fluorescence-conjugated secondary antibody Alexa Fluor 488 (Invitrogen, Life Technologies, Madrid, Spain). Sections were mounted with Vectashield mounting medium with DAPI (Vector, Burlingame, United States). Retinal images were viewed with a Nikon DS-Fi1 camera attached to a Leica DM 2000 microscope. Representative images were taken of three areas of the retina (far periphery, medium and central retina). To evaluate changes in macrogliosis, the percentage of area occupied by GFAP antibody labeling was measured in total retina. To evaluate microglial activation, total Iba-1 positive cells were counted per ONL area. All these measurements were made with the help of the program image processing Image J 1.45s.

Biochemical Studies

Glutathione Assay

Both retinas per mice were homogenated together as described in Sanchez-Vallejo et al. (Sánchez-Vallejo et al., 2015). Reduced and oxidized glutathione (GSH, GSSG) as well as glutamate concentrations were quantified by means of the Reed method (Reed et al., 1980). Protein concentration was determined with the Lowry method (Lowry et al., 1951).

Western Blot

Two retinas of each animal were dissected and homogenized mechanically with 50 µL radioimmunoprecipitation (RIPA) buffer. Samples were then centrifuged at 13,000 rpm during 10 min at 4°C. Supernatant was removed and used for protein determination (Bradford, 1976). We used 75 µg of protein that

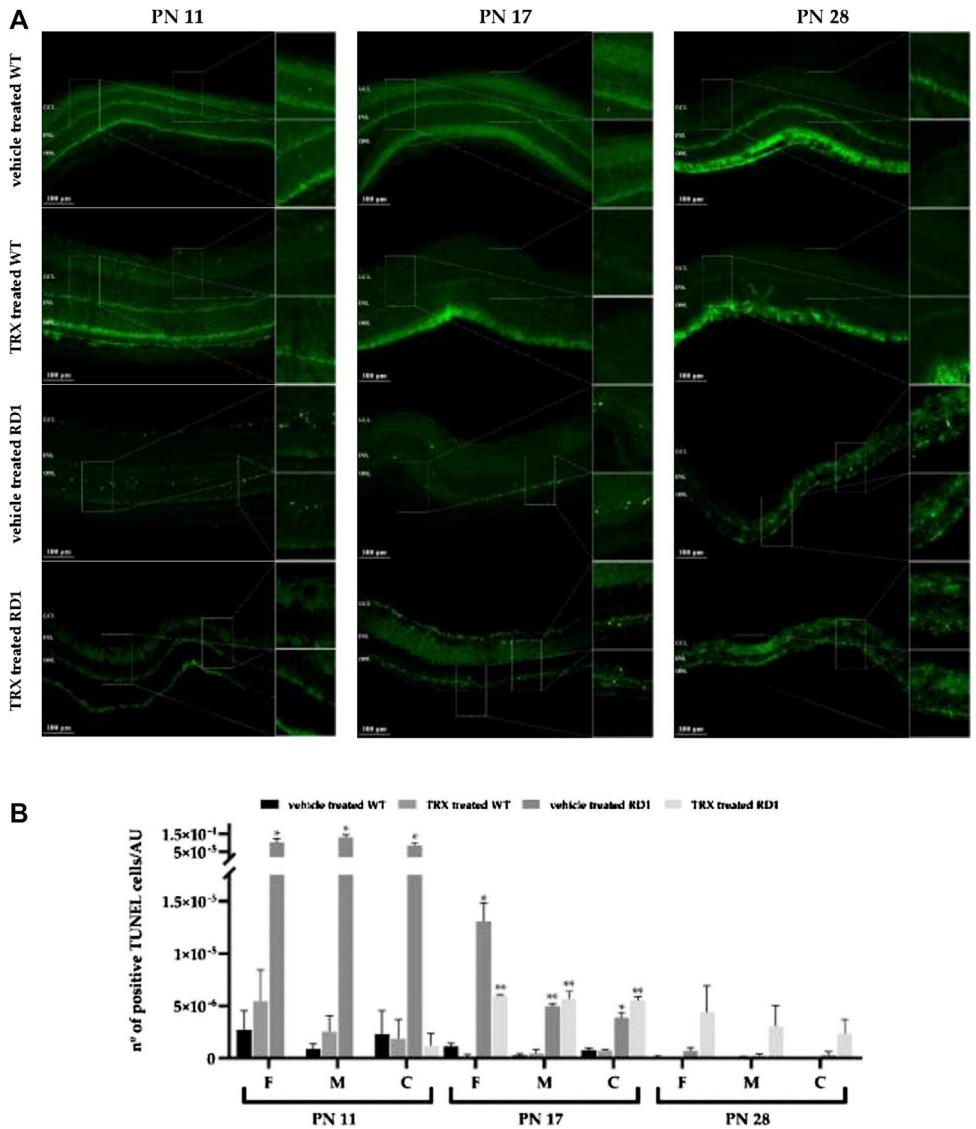

FIGURE 2 | Detection of dying cells with TUNEL staining. **(A)** Central retinal TUNEL images from non-treated and treated with TRX wild type (WT) and rd1 mice at PN11, PN17 and PN28. **(B)** Quantification of TUNEL positive cells/arbitrary units of area (AUA) at PN11, PN17 and PN28 in three retinal regions (far periphery, medium and central retina). Mean values and standard errors are shown in the graph. The images are representative for observations for at least three different animals for each group (*$p < 0.05$ vs. WT vehicle treated, WT TRX treated and rd1 TRX treated; **$p < 0.05$ vs. WT vehicle treated and WT TRX treated). N = at least six in each experimental group. The TUNEL positive cells were counted manually in the outer nuclear layer (ONL) of three different parts of the retina: far periphery, medium and central retina. TUNEL positive cells from referred to the area of the ONL which was used.

were resolved during 1 h on 10–15% acrylamide:bisacrylamide gels at 200 V. The proteins were moved to nitrocellulose membranes (AmershamTM Hybond ECL (GE Healthcare Life Sciences, Barcelona, España) and blocked for 1 h with 0.01 M PBS-Tween 20 0.1% with 5% w/v non-fat milk. Membranes were probed with vascular endothelial growth factor (VEGF) and hepatic growth factor (HGF) antibodies (Santa Cruz Biotechnology, Santa Cruz, United States). The membrane was incubated over night at RT, and bound antibody was detected with a horseradish peroxidase coupled secondary anti-rabbit antibody (F (ab′) 2–HRP, goat anti-rabbit) (Santa Cruz Biotechnology, Santa Cruz, United States). The signal was recognized with the enhanced chemiluminescence (ECL) developing kit (Amersham Biosciences, Buckinghamshire, United Kingdom) and quantified by densitometry (Image Quant™TL, GE Healthcare Life Sciences, Barcelona, Spain).

Statistical Analysis

The results are presented as mean values ± standard deviation. The analysis of variance (ANOVA) was used. When the ANOVA indicated a significant difference, the Bonferroni test was performed. Graphpad Prism 8 software package was used. The level of significance was stablished at $p < 0.05$.

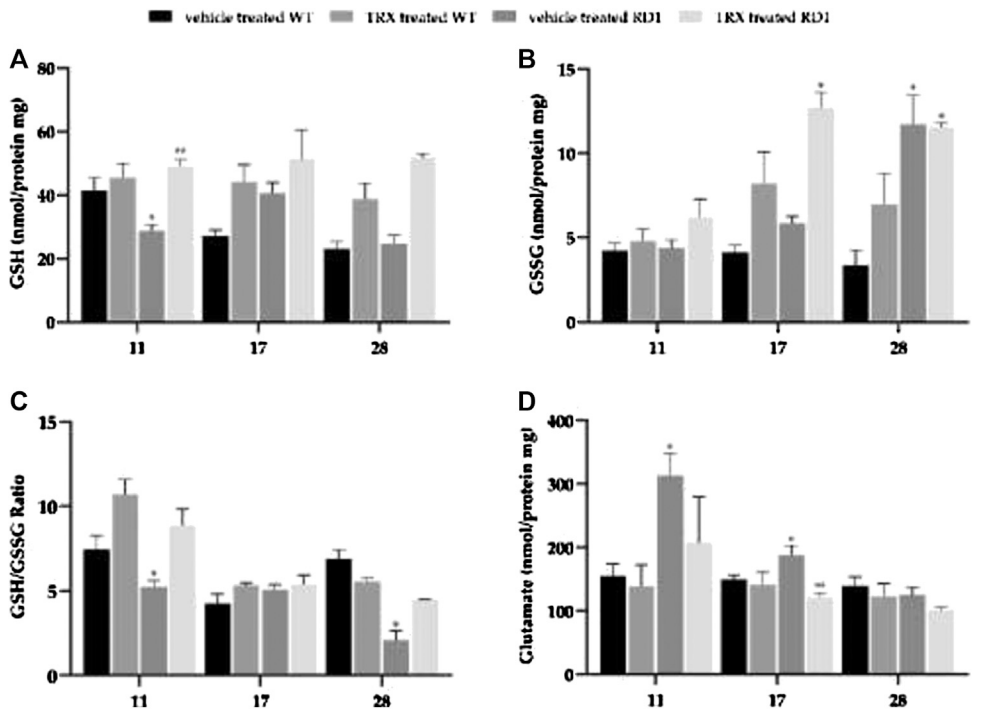

FIGURE 3 | Retinal concentration of GSH, GSSG, GSH/GSG ratio and glutamate concentrations at PN11, PN17 and PN28. (*$p < 0.05$ vs. all the other groups; **$p < 0.05$ vs. WT vehicle treated). N = at least six in each experimental group.

RESULTS

Thioredoxin Decreases Photoreceptor Death

Photoreceptor death and the possible neuroprotective effect of TRX was investigated with the TUNEL assay. At PN11 and PN17 a significant increase in the number of dead cells was found in the outer nuclear layer (ONL) of vehicle treated rd1 mice, when compared to both groups of wild type (WT) mice (vehicle and TRX treated) (**Figures 2A,B**). Moreover, TRX administration significantly diminish cell death in rd1 mouse retinas at PN11 in the three retinal areas studied (*$p < 0.05$). This result could show a neuroprotective effect of TRX treatment at this age (**Figure 2B**). However, at PN17 TRX was only able to decrease the number of TUNEL positive cells in the rd1 far periphery retina (*$p < 0.05$). In this sense, TRX treatment did not show any effect in photoreceptor death in the medium and central retina (**Figure 2B**). At PN28 no differences were observed between the number of TUNEL positive cells in wild type and rd1 mice. This result may be explained because at PN28 the degeneration in the rd1 retina is so advanced that there is almost no ONL left, and therefore, there are no more rods remaining and no death could be observed. No protective effect of TRX could be observed at PN28 (**Figure 2B**).

Glutathione Metabolism Alterations in rd1 Retina: Thioredoxin Effect

Figure 3 shows the representation of the retinal concentration of GSH, GSSG and GSH/GSG ratio as well as glutamate concentrations in the four studied groups per each of the four ages studied (vehicle treated WT, TRX treated WT, vehicle treated rd1, TRX treated rd1 mice).

At PN11 there were no significant changes in retinal GSH concentrations when WT mice were treated with TRX, as observed in **Figure 3A**. GSH concentration was significantly decreased in rd1 retinas when compared with all the other groups (*$p < 0.05$), with values 28.74 ± 2.05 8 nmol/mg protein (**Figure 3A**). There is also a statistically significant increase (approximately 40% of increase) in the concentration of GSH in the group of rd1 mice treated with TRX compared to the rd1 group treated with the vehicle. When the retinal degeneration has progressed and the decrease in the ONL layer is more evident (PN17 and PN28) no differences could be observed between retinal GSH concentrations in WT and rd1 mice. However, repeated doses of TRX induced a significant increase in GSH concentrations in both groups of animals.

Figure 3B shows GSSG concentrations in the retina of the different animal groups at the three ages studied. At PN11 and PN17 no differences were observed between GSSG concentrations in WT and rd1 treated with vehicle. Again, the administration of TRX increased significantly this retinal parameter in rd1 treated animals. At PN28, an increase in GSSG concentration was observed in rd1 treated with vehicle or TRX animals when compared to WT treated with vehicle or TRX mice.

Probably, a better marker of the retinal antioxidant defenses is the GSH/GSSG ratio. In our study, the results obtained regarding this marker are shown in **Figure 3C**. Our results suggest that

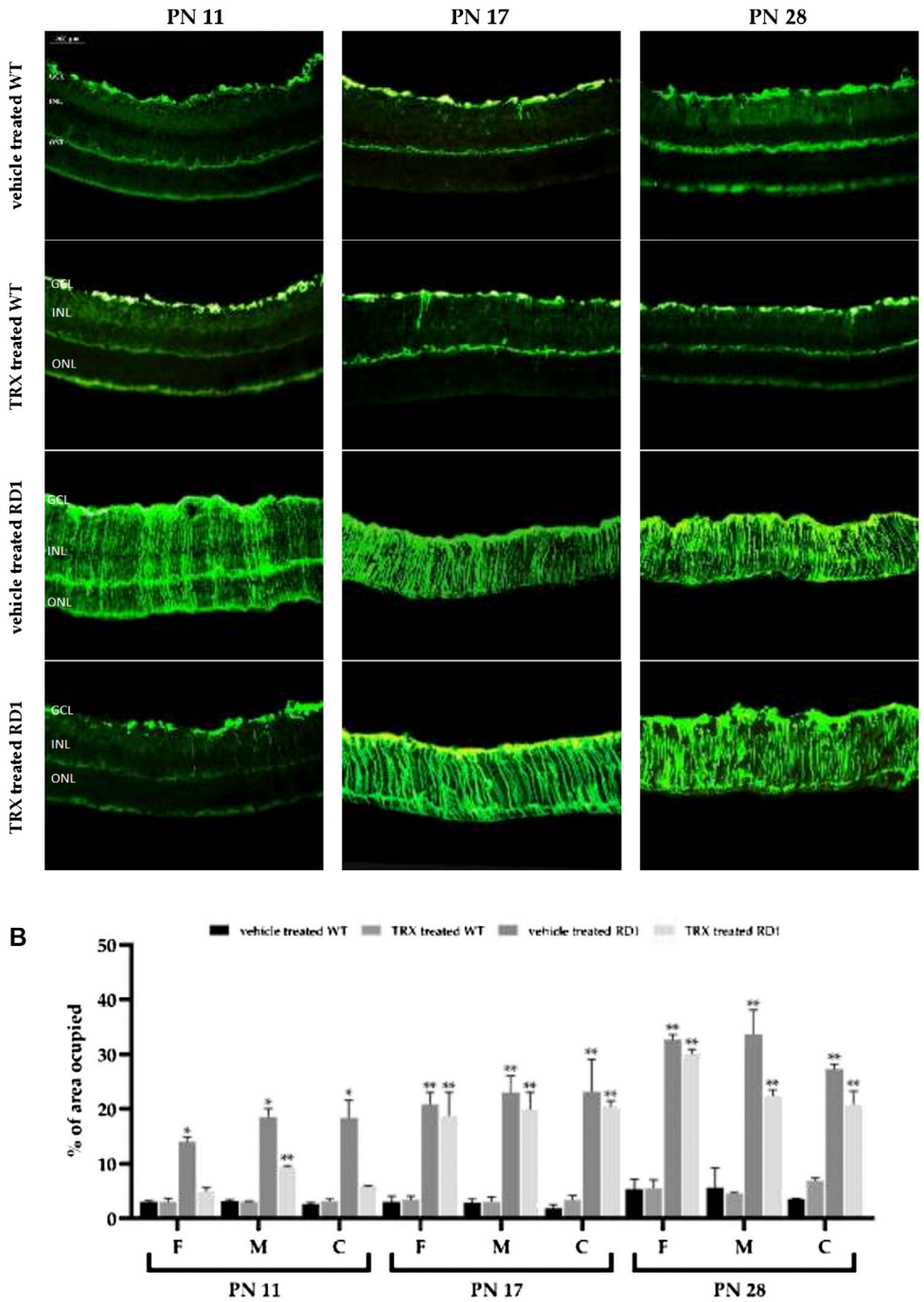

FIGURE 4 | Retinal GFAP immunoreactivity. GFAP is increased in rd1 retina and partially restored after TRX administration. **(A)** Images of GFAP fluorescent labeling. **(B)** Graphic representation of the quantification of the area occupied by retinal GFAP staining. The bars represent the percentage of are occupied by the positive GFAP cells (n = 4) and the error bars represent the standard error of the mean (*$p < 0.05$ vs. WT vehicle treated, WT TRX treated and rd1 TRX treated; **$p < 0.05$ vs. WT vehicle treated and WT TRX treated). N = at least six in each experimental group.

there is a significant alteration of GSH/GSSG ratio in rd1 mice at PN11 and PN28, and that this alteration is completely reverted with the administration of TRX.

Glutamate is the largest excitatory retinal neurotransmitter, but an excess of this transmitter may be toxic and may lead to degeneration. Our results show (**Figure 3D**) an increase in glutamate retinal concentrations in rd1 mice in comparison with WT animals but also in comparison with rd1 mice that where treated with TRX (*$p < 0.05$) at PN11 and PN17. No significant differences were observed at PN28, although the

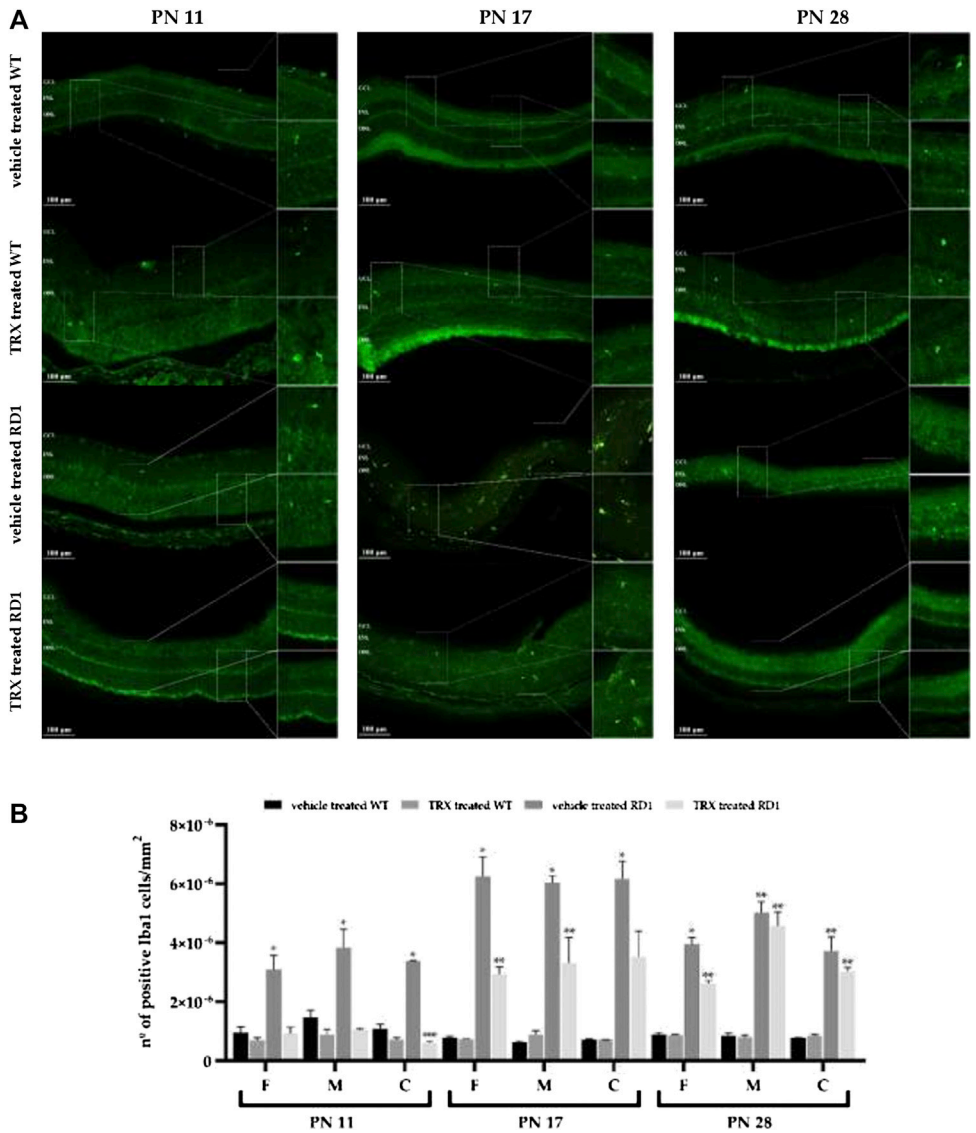

FIGURE 5 | TRX effect on Iba1 expression. **(A)** Images of Iba1 fluorescent labeling. **(B)** Graphic representation of the quantification of number of Iba1 positive cells. The bars represent the number of Iba1 positive cells per units of area (n = 4) and the error bars represent the standard error of the mean (*$p < 0.05$ vs. WT vehicle treated, WT TRX treated and rd1 TRX treated; **$p < 0.05$ vs. WT vehicle treated and WT TRX treated; ***$p < 0.05$ vs. rd1 vehicle treated). N = at least six in each experimental group. The number of Iba1 cells were counted manually in the outer nuclear layer (ONL) of three different parts of the retina: far periphery, medium and central retina. TUNEL positive cells from referred to the area of the ONL which was used.

minimum concentration corresponds to rd1 group treated with TRX (100.95 ± 4.97 nmol/mg protein).

Thioredoxin Treatment Partially Reduces Retinal Macro and Microgliosis in rd1 Mice

Similarly, to other retinal pathologies, inflammation plays an important role in RP. In this sense it is well known that the expression of glial fibrillary acidic protein (GFAP) is expressed at a low level in Müller glial cells in control animals. However, when the retina is damaged GFAP is strongly upregulated. Therefore, GFAP is a very sensitive marker for retinal inflammation (macrogliosis) and neurodegeneration.

In WT animals (treated with vehicle or TRX), retinal GFAP immunoreactivity was observed only next to the ganglion cell layer (GCL) (**Figure 4A**). In rd1 animals treated with vehicle, GFAP staining was found throughout the retina (**Figure 4A**). Quantification of the occupied area of the retina by the GFAP staining at PN11, PN17 and PN28 for the different experimental animal groups in each of the areas of the retina is shown in **Figure 4B**. We found statistically significant increases in these GFAP values in all areas of the retina at all the ages studied in rd1 treated with vehicle mice (*$p < 0.05$ vs. all other groups). Interestingly, we also observed that TRX treatment decreased GFAP reactivity in rd1 mice, but this effect was only observed at

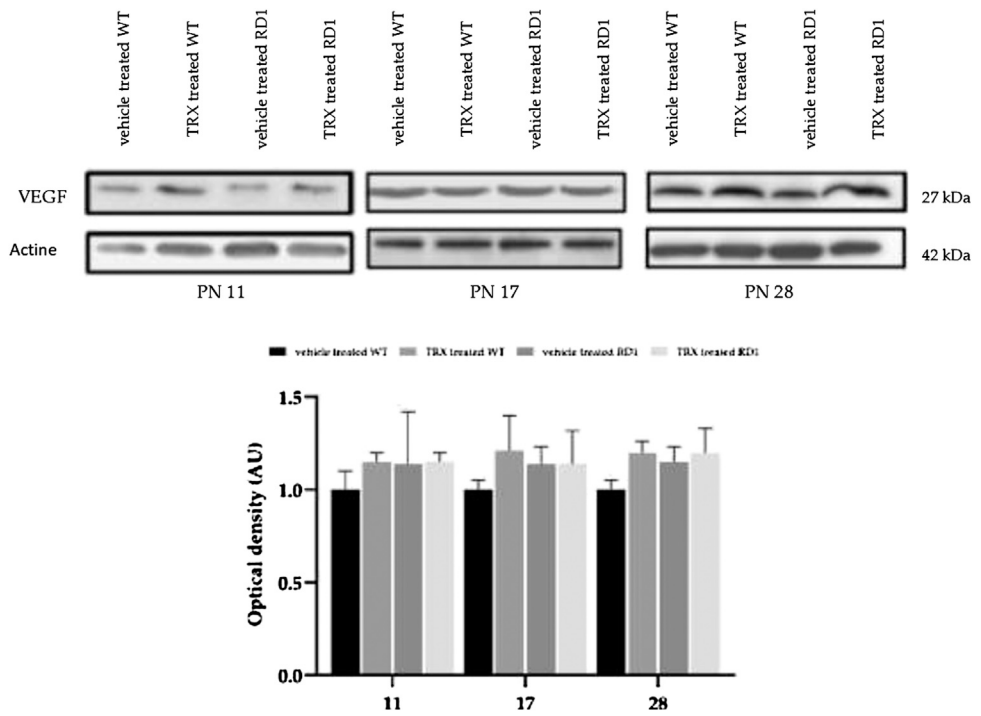

FIGURE 6 | Retinal VEGF determination by western-blot. **(A)** Western-blot bands images for control and rd1 mice (n = 3). **(B)** Histogram represents the bands optical density quantification (VEGF/Actin ratio) in each group. The error bars represent the standard error of the mean. N = at least four in each experimental group.

P11. No TRX effect was observed on the characteristic rd1 retinal macrogliosis at PN17 or PN28.

We have also studied whether TRX treatment was able to reduce microglial activation in rd1 retinas and, therefore, used the Iba1 antibody to identify microglial cells. Iba1 immunolabeling was upregulated in rd1 retinas compared to control retinas in all the areas and at all the ages studied (**Figures 5A,B**). These results are similar to those found for GFAP. TRX significantly reduced Iba1-positive immunolabelling in rd1 mice at PN11 and PN17, but not at PN28 (**Figure 5B**).

Vascular Endothelial and Hepatic Growth Factor Are Not Altered in the rd1 Model

VEGF is a trophic factor that increases endothelial cells survival, promotes proliferation and migration of endothelial cells and increases vascular permeability (Boehm et al., 1997). In addition, a decrease in VEGF has been reported in aqueous humor of RP patients (Salom et al., 2008). We have determined the retinal VEGF expression in WT and rd1 mice treated and non-treated with TRX, by western blot (**Figures 6A,B**). However, no differences were observed between VEGF expression in control and rd1 mice in none of the disease stages, moreover, no TRX effect was either observed.

HGF is another factor that has been related with ocular angiogenesis. To date it has not been studied its role in RP. Our western blot results show that though there is a significant increase in HGF expression at PN11 in WT treated mice when compared with WT animals, no differences were observed in HGF between WT and rd1 mice (**Figures 7A,B**). Likewise, GFAP results, TRX treatment did not change HGF retinal expression in WT and rd1 mice at PN17 or PN28.

DISCUSSION

TRX is a well known antioxidant that has been shown to be effective in a wide variety of animal models with oxidative and inflammatory disorders (Nakamura et al., 2009). However, TRX effect in animal models of RP has not been studied to date. In this work, we have investigated if TRX was able to increase photoreceptor survival in the rd1 model of RP. Moreover, we also studied its effect to restore other retinal alterations which may be induced by photoreceptor death, such as changes in inflammatory and vascular markers.

Thioredoxin Protects Photoreceptor Death in the rd1 Mice Retina

RP animal models, including the rd1 mouse model, present a rapid degeneration of photoreceptors that can be easily demonstrated with the help of the TUNEL assay. Several studies have described the way in which rods begin to degenerate in the rd1 mouse model and they all agree that rods degeneration peaks occurs around PN11-13 (Paquet-Durand et al., 2006) and that rods degeneration ends close to PN20 (Carter-Dawson et al., 1978).

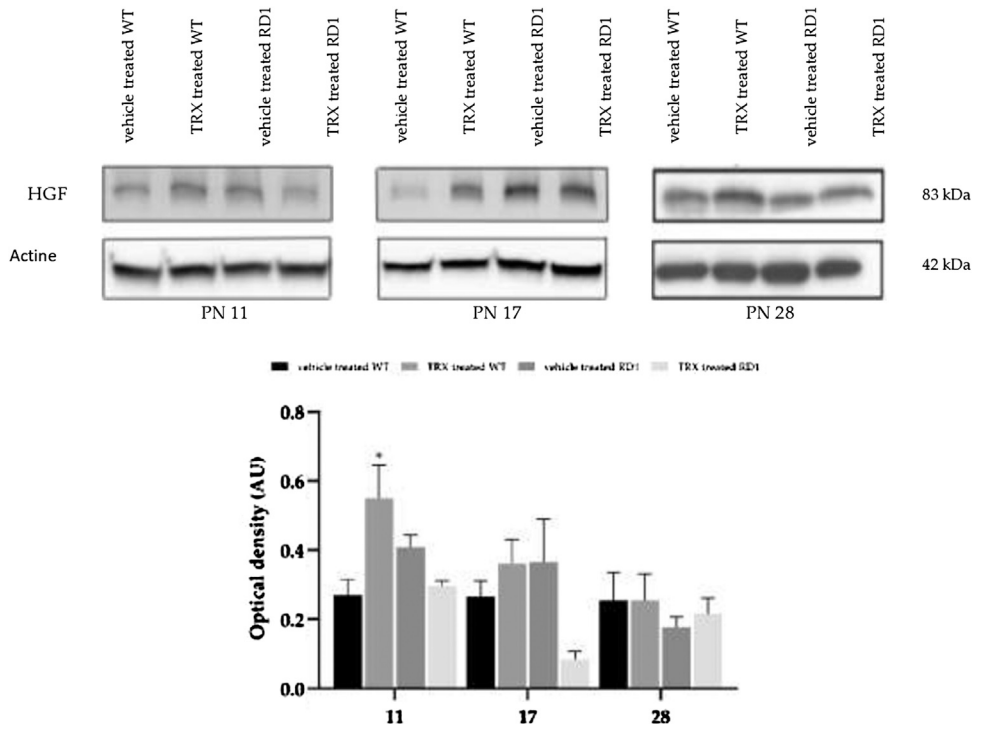

FIGURE 7 | Retinal HGF determination by western blot. **(A)** Western-blot bands images for control and rd1 mice (n = 3). **(B)** Histogram represents the bands optical density quantification (HGF/Actin ratio) in each group. The error bars represent the standard error of the mean. (*$p < 0.05$ vs. all the other groups). N = at least four in each experimental group.

The nuclei of photoreceptors are found in the ONL. The progressive deterioration of this layer of the retina, analyzed by measuring its thickness or by measuring the number photoreceptor rows in this layer, have been used in RP studies. However, though the maximum rate of cell death is produced around postnatal day 12 in this animal model, this cannot be demonstrated just determining the number of rows in the ONL. At PN11 and PN12 there is no difference in the ONL thickness in control and rd1 retina. In this sense, this parameter is not useful to determine the effect of different treatments at this post natal ages. For this reason we have decided to perform the TUNEL staining as it is a more precise technique to observe possible treatment effects.

Herein, we demonstrate that TRX treatment significantly decreases TUNEL positive photoreceptors in rd1 mouse retinas at PN11 in peripheral, medium and central retina (**Figure 2**). At PN17 TRX was only able to decrease the number of TUNEL positive cells in the rd1 far periphery retina (*$p < 0.05$) but could not decrease photoreceptor death in the medium and central retina (**Figure 2B**). This different response to TRX treatment of the different retinal areas studied may be related to the fact that there is a gradient in the rd1 degeneration, from the periphery to the central retina. Because of nearly no TUNEL staining could be observed in the retina of rd1 mice at PN28, probably due to the fact that at this stage rod degeneration is ended, we could not demonstrate any beneficial effect of TRX on cell survival at this age.

TRX protective effects have been recently reported in retinas exposed to perinatal hypoxia-ischemia (Holubiec et al., 2020) and in light-induced photoreceptor degeneration in diabetic mice (Kong et al., 2019). Some studies have also demonstrated the use of TRX and its effect to prevent cell death induced by cerebral ischemia (Hattori et al., 2004). Our results help us to conclude that TRX treatment may be helpful and slows down photoreceptor death in the first stages of the disease, while some rods are still present in the retina.

Thioredoxin Effect on Glutathione Metabolism Alterations in rd1 Retina

Oxidative stress is related to the pathogenesis of many retinal diseases and it has also been suggested to be involved in the pathogenesis of RP, both in animal models and in patients (Shen et al., 2005). In this sense, the normalization of the redox state through the manipulation of endogenous levels of thiol antioxidants, for example, with TRX, could be an effective therapeutic strategy for RP.

The glutathione system is one of the antioxidant defense systems. Moreover, it is present in most mammalian cells and therefore it plays a key role in the eye (Riley et al., 1980). Under normal conditions, retinal GSH is almost exclusively confined to Müller cells, astrocytes and horizontal cells (Pow and Crook, 1995). Retinal GSH concentrations are maintained thanks to *de novo* synthesis, to the glutathione disulfide regeneration (GSSG) and to extracellular GSH capture (Circu and Aw, 2012).

Our results may also indicate a prevalent role of GSH at the beginning of the disease in rd1 mice. At PN11, GSH concentration was significantly decreased in rd1 retinas when compared with all the other groups (**Figure 3A**). Nevertheless, when retinal degeneration has progressed no differences could be observed between retinal GSH concentrations in WT and rd1 mice. TRX treatment increased the amount of GSH concentrations in the retina of all of rd1 mice. Results regarding GSSG may be confusing because we have observed increases in GSSG concentrations after TRX treatment (**Figure 3B**). New studies determining the activity of different GSH metabolism enzymes should be performed to further clarify the role of this increase in GSSG concentration. In this sense, it should be interesting to analyze glutathione peroxidase (GPx) retinal activity. This enzyme uses GSH as a cofactor to reduce hydrogen peroxide, resulting in the formation of GSSG. Still, our results confirm that TRX administration is beneficial, considering its effect on GSH metabolism as we have observed an increase in GSG/GSSG ratio in rd1 treated mice. This ratio is commonly used to measure the redox status of the cell, so that it reflects the cellular antioxidant capacity (Schafer and Buettner, 2001).

These results may suggest that, at least, part of the protective effect in the initial phases of the photoreceptor degeneration exerted by TRX, may be due in part to the GSH system activation. Indeed, there is considerable evidence showing that the maintenance of GSH cell stores protects against cell death (Hall, 1999). As reported in the introduction section TRX is and antioxidant protein that regulates thiol modifications and redox signaling. GSH plays an important role in modulating redox homoeostasis and its depletion is involved in multiple diseases. The administration of TRX to RP mice ameliorates retinal damage because it decreases oxidative injury and inhibits cell death.

Thioredoxin Treatment Partially Reduces Retinal Macro and Microgliosis in rd1 Mice

Neuroinflammation is considered as a hallmark of numerous chronic degenerative disorders (Glass et al., 2010). The best-known aspect of the retinal glial response is that Müller cells upregulate GFAP, a protein that is considered as a marker for reactive gliosis, not only in the retina, but also in the CNS (Nakazawa et al., 2007). Müller cells are the predominant macroglial element of the retina, representing 90% of the glia. An increase in GFAP in glial cells has been demonstrated in both animal and human models of almost all retinal diseases, including glaucoma (Kim et al., 1998), retinal ischemia (Nishiyama et al., 2000) and in age-related macular degeneration (Guidry et al., 2002). Inflammation plays also a fundamental role in RP (Vecino et al., 2016). The glial reaction is thought to represent an attempt by the Müller cells to protect the retina from damage and to promote tissue repair. However, an acute activation of the macroglia has a neuroprotective effect, but continuous activation could be harmful.

As in the central nervous system (CNS), retinal microglial cells are sensors of possible disorders in the neuronal environment. Again, although microglial activation is commonly associated with neuroprotection, if activation is excessive or prolonged, it can lead to constant inflammation (Bignami and Dahl, 1979) and a chronic excessive activation, with serious pathological side effects. In RP, the interaction between neuronal damage and microglial activation generates a cycle that causes uncontrolled inflammation, contributing to the progression of disease (Gao and Hong, 2008).

To study the characteristics of Müller cells in the rd1 mouse retina we carried immunostainings of GFAP at different stages of retinal degeneration in RP. It has been shown that microglial cells express the ionized calcium binding adapter molecule 1 (Iba1). Therefore, Iba-1 staining was selected to study microglial activation.

Our results suggest that there is a reactive macro and microgliosis that is associated with degeneration in rd1 mice. We found statistically significant increases in GFAP and Iba1 in all areas of the retina, at all studied ages in vehicle treated rd1 mice (**Figures 4**,**5**). TRX treatment decreased GFAP reactivity in rd1 mice, but this effect was only observed at PN11. On the other hand, no TRX effect was observed on rd1 retinal macrogliosis at PN17 or PN28. Other authors have suggested that an increase in GSH may inhibit glial activation (Gouix et al., 2014), and this may explain the observed TRX effect on macroglia only at PN11.

Iba1 immunolabeling was upregulated in rd1 retinas compared to control retinas at all studied ages (**Figures 5A,B**). These results are similar to those found for GFAP. In the case of TRX, its effect was longer as it significantly reduced Iba1-positive immunolabelling in rd1 mice at PN11 and PN17.

Our results suggest that TRX may have protective effects at least in in the initial phases of the photoreceptor degeneration in this RP animal model. Oxidative stress is an important factor related to photoreceptor death in RP. Moreover, the manipulation of cellular redox status may be a therapeutic strategy to prevent also inflammation in RP. In this sense, TRX regulates oxidative stress because it increases the concentration of the antioxidant GSH and because of that it also combat inflammation. New studies should also be performed to be able to determine if increased doses of TRX may induce a longer beneficial effect.

Vascular Endothelial and Hepatic Growth Factor Are Not Altered in the rd1 Model

VEGF is a growth factor that is involved in numerous retinal pathologies, such as proliferative diabetic retinopathy (Gupta et al., 2013), diabetic macular edema (Penn et al., 2008), etc. HGF plays an important role in ocular angiogenesis and in neuroprotection of retinal tissue. It has been shown that retinal ischemia and diabetic retinopathy increases the expression of HGF (Nishimura et al., 1999; Simó et al., 2006). Anyhow, we have not demonstrated any changes in the expression of these two factors in rd1 mice retina compared to control mice (**Figures 6**,**7**). For this reason, we have not been able to demonstrate any effect of TRX on the vascular changes that are usually observed in last phases of this retinal degeneration. We

suggest that different vascular markers should be studied in order to demonstrate any therapeutically effects.

DATA AVAILABILITY STATEMENT

The raw data supporting the conclusions of this article will be made available by the authors, without undue reservation.

ETHICS STATEMENT

The animal study was reviewed and approved by CEU Cardenal Herrera Universities Committee for Animal Experiments (reference 11/013).

AUTHOR CONTRIBUTIONS

Conceptualization, MM and IA; methodology, VH-R.; investigation, RG-H; AC; AF-C; writing—original draft preparation, MM; writing—review and editing, MM and TR. All authors have read and agreed to the published version of the manuscript.

FUNDING

Cardenal Herrera CEU and University and San Pablo CEU Foundation University, grant numbers: INDI 19/35 and Consolidación 2018/19. Generalitat Valenciana (ACIF/2019/199) to A.C., Emergente (GV/2019/125) and Emergente (GV/2019/034) to VH-R.

REFERENCES

Adler, R. (1996). Mechanisms of photoreceptor death in retinal degenerations. From the cell biology of the 1990s to the ophthalmology of the 21st century? *Arch. Ophthalmol.* 114, 79–83. doi:10.1001/archopht.1996.01100130075012

Arnér, E. S., and Holmgren, A. (2006). The thioredoxin system in cancer. *Semin. Cancer Biol.* 16, 420–426. doi:10.1016/j.semcancer.2006.10.009

Benlloch-Navarro, S., Trachsel-Moncho, L., Fernández-Carbonell, Á., Olivar, T., Soria, J. M., Almansa, I., et al. (2019). Progesterone anti-inflammatory properties in hereditary retinal degeneration. *J. Steroid Biochem. Mol. Biol.* 189, 291–301. doi:10.1016/j.jsbmb.2019.01.007

Berson, E. L., Rosner, B., Sandberg, M. A., Weigel-DiFranco, C., Brockhurst, R. J., Hayes, K. C., et al. (2010). Clinical trial of lutein in patients with retinitis pigmentosa receiving vitamin A. *Arch. Ophthalmol.* 128, 403–411. doi:10.1001/archophthalmol.2010.32

Bignami, A., and Dahl, D. (1979). The radial glia of Müller in the rat retina and their response to injury. An immunofluorescence study with antibodies to the glial fibrillary acidic (GFA) protein. *Exp. Eye Res.* 28, 63–69. doi:10.1016/0014-4835(79)90106-4

Blanks, J. C., and Johnson, L. V. (1986). Vascular atrophy in the retinal degenerative rd mouse. *J. Comp. Neurol.* 254, 543–553. doi:10.1002/cne.902540407

Boehm, T., Folkman, J., Browder, T., and O'Reilly, M. S. (1997). Antiangiogenic therapy of experimental cancer does not induce acquired drug resistance. *Nature* 390, 404–407. doi:10.1038/37126

Boughman, J. A., Conneally, P. M., and Nance, W. E. (1980). Population genetic studies of retinitis pigmentosa. *Am. J. Hum. Genet.* 32, 223–235.

Bowes, C., Li, T., Danciger, M., Baxter, L. C., Applebury, M. L., and Farber, D. B. (1990). Retinal degeneration in the rd mouse is caused by a defect in the beta subunit of rod cGMP-phosphodiesterase. *Nature* 347, 677–680. doi:10.1038/347677a0

Bradford, M. M. (1976). A rapid and sensitive method for the quantitation of microgram quantities of protein utilizing the principle of protein-dye binding. *Anal. Biochem.* 72, 248–254. doi:10.1006/abio.1976.9999

Bussolino, F., Di Renzo, M. F., Ziche, M., Bocchietto, E., Olivero, M., Naldini, L., et al. (1992). Hepatocyte growth factor is a potent angiogenic factor which stimulates endothelial cell motility and growth. *J. Cell Biol.* 119, 629–641. doi:10.1083/jcb.119.3.629

Carter-Dawson, L. D., LaVail, M. M., and Sidman, R. L. (1978). Differential effect of the rd mutation on rods and cones in the mouse retina. *Invest. Ophthalmol. Vis. Sci.* 17, 489–498.

Chalmel, F., Léveillard, T., Jaillard, C., Lardenois, A., Berdugo, N., Morel, E., et al. (2007). Rod-derived Cone Viability Factor-2 is a novel bifunctional-thioredoxin-like protein with therapeutic potential. *BMC Mol. Biol.* 8, 74. doi:10.1186/1471-2199-8-74

Circu, M. L., and Aw, T. Y. (2012). Glutathione and modulation of cell apoptosis. *Biochim. Biophys. Acta.* 1823, 1767–1777. doi:10.1016/j.bbamcr.2012.06.019

Daiger, S. P., Sullivan, L. S., and Bowne, S. J. (2013). Genes and mutations causing retinitis pigmentosa. *Clin. Genet.* 84, 132–141. doi:10.1111/cge.12203

Fernández-Sánchez, L., Lax, P., Pinilla, I., Martín-Nieto, J., and Cuenca, N. (2011). Tauroursodeoxycholic acid prevents retinal degeneration in transgenic P23H rats. *Invest. Ophthalmol. Vis. Sci.* 52, 4998–5008. doi:10.1167/iovs.11-7496

Fox, D. A., Poblenz, A. T., He, L., Harris, J. B., and Medrano, C. J. (2003). Pharmacological strategies to block rod photoreceptor apoptosis caused by calcium overload: a mechanistic target-site approach to neuroprotection. *Eur. J. Ophthalmol.* 13 (Suppl. 3), S44–S56. doi:10.1177/112067210301303s08

Gao, H. M., and Hong, J. S. (2008). Why neurodegenerative diseases are progressive: uncontrolled inflammation drives disease progression. *Trends Immunol.* 29, 357–365. doi:10.1016/j.it.2008.05.002

Glass, C. K., Saijo, K., Winner, B., Marchetto, M. C., and Gage, F. H. (2010). Mechanisms underlying inflammation in neurodegeneration. *Cell* 140, 918–934. doi:10.1016/j.cell.2010.02.016

Gouix, E., Buisson, A., Nieoullon, A., Kerkerian-Le Goff, L., Tauskela, J. S., Blondeau, N., et al. (2014). Oxygen glucose deprivation-induced astrocyte dysfunction provokes neuronal death through oxidative stress. *Pharmacol. Res.* 87, 8–17. doi:10.1016/j.phrs.2014.06.002

Gregory, C. Y., and Bird, A. C. (1995). Cell loss in retinal dystrophies by apoptosis—death by informed consent! *Br. J. Ophthalmol.* 79, 186–190. doi:10.1136/bjo.79.2.186

Gromer, S., Urig, S., and Becker, K. (2004). The thioredoxin system–from science to clinic. *Med. Res. Rev.* 24, 40–89. doi:10.1002/med.10051

Grunwald, J. E., Maguire, A. M., and Dupont, J. (1996). Retinal hemodynamics in retinitis pigmentosa. *Am. J. Ophthalmol.* 122, 502–508. doi:10.1016/s0002-9394(14)72109-9

Guidry, C., Medeiros, N. E., and Curcio, C. A. (2002). Phenotypic variation of retinal pigment epithelium in age-related macular degeneration. *Invest. Ophthalmol. Vis. Sci.* 43, 267–273.

Gupta, N., Mansoor, S., Sharma, A., Sapkal, A., Sheth, J., Falatoonzadeh, P., et al. (2013). Diabetic retinopathy and VEGF. *Open Ophthalmol. J.* 7, 4–10. doi:10.2174/1874364101307010004

Hall, A. G. (1999). Review: the role of glutathione in the regulation of apoptosis. *Eur. J. Clin. Invest.* 29, 238–245. doi:10.1046/j.1365-2362.1999.00447.x

Hanschmann, E. M., Godoy, J. R., Berndt, C., Hudemann, C., and Lillig, C. H. (2013). Thioredoxins, glutaredoxins, and peroxiredoxins--molecular mechanisms and health significance: from cofactors to antioxidants to redox signaling. *Antioxid. Redox Signal* 19, 1539–1605. doi:10.1089/ars.2012.4599

Hattori, I., Takagi, Y., Nakamura, H., Nozaki, K., Bai, J., Kondo, N., et al. (2004). Intravenous administration of thioredoxin decreases brain damage following transient focal cerebral ischemia in mice. *Antioxid. Redox Signal* 6, 81–87. doi:10.1089/152308604771978372

Holmgren, A. (2000). Antioxidant function of thioredoxin and glutaredoxin systems. *Antioxid. Redox Signal* 2, 811–820. doi:10.1089/ars.2000.2.4-811

Holubiec, M. I., Galeano, P., Romero, J. I., Hanschmann, E. M., Lillig, C. H., et al. (2020). Thioredoxin 1 plays a protective role in retinas exposed to perinatal

hypoxia-ischemia. *Neuroscience* 425, 235–250. doi:10.1016/j.neuroscience.2019.11.011

Jin, K. L., Mao, X. O., and Greenberg, D. A. (2000). Vascular endothelial growth factor: direct neuroprotective effect in *in vitro* ischemia. *Proc. Natl. Acad. Sci. U.S.A.* 97, 10242–10247. doi:10.1073/pnas.97.18.10242

Jones, B. W., and Marc, R. E. (2005). Retinal remodeling during retinal degeneration. *Exp. Eye Res.* 81, 123–137. doi:10.1016/j.exer.2005.03.006

Jones, B. W., Pfeiffer, R. L., Ferrell, W. D., Watt, C. B., Marmor, M., and Marc, R. E. (2016). Retinal remodeling in human retinitis pigmentosa. *Exp. Eye Res.* 150, 149–165. doi:10.1016/j.exer.2016.03.018150

Karamali, F., Esfahani, M. N., Hajian, M., Ejeian, F., Satarian, L., and Baharvand, H. (2019). Hepatocyte growth factor promotes the proliferation of human embryonic stem cell derived retinal pigment epithelial cells. *J. Cell. Physiol.* 234, 4256–4266. doi:10.1002/jcp.27194

Keeler, C. E. (1924). The inheritance of a retinal abnormality in white mice. *Proc. Natl. Acad. Sci. U.S.A.* 10, 329–333. doi:10.1073/pnas.10.7.329

Kim, I. B., Kim, K. Y., Joo, C. K., Lee, M. Y., Oh, S. J., Chung, J. W., et al. (1998). Reaction of Müller cells after increased intraocular pressure in the rat retina. *Exp. Brain Res.* 121, 419–424. doi:10.1007/s002210050476

Kong, H., Ren, X., Zhang, H., Wang, N., Zhang, C., Li, L., et al. (2019). Thioredoxin is a potential therapy for light-induced photoreceptor degeneration in diabetic mice. *Neuroendocrinol. Lett.* 39, 561–566. doi:10.18632/oncotarget.18134

Léveillard, T., and Sahel, J. A. (2010). Rod-derived cone viability factor for treating blinding diseases: from clinic to redox signaling. *Sci. Transl. Med.* 2, 26ps16. doi:10.1126/scitranslmed.3000866

Lee, S. Y., Usui, S., Zafar, A. B., Oveson, B. C., Jo, Y. J., Lu, L., et al. (2011). N-acetylcysteine promotes long-term survival of cones in a model of retinitis pigmentosa. *J. Cell. Physiol.* 226, 1843–1849. doi:10.1002/jcp.22508

Léveillard, T., Mohand-Saïd, S., Lorentz, O., Hicks, D., Fintz, A. C., Clérin, E., et al. (2004). Identification and characterization of rod-derived cone viability factor. *Nat. Genet.* 36, 755–759. doi:10.1038/ng1386

Lindberg, C. R., Fishman, G. A., Anderson, R. J., and Vasquez, V. (1981). Contrast sensitivity in retinitis pigmentosa. *Br. J. Ophthalmol.* 65, 855–858. doi:10.1136/bjo.65.12.855

Lolley, R. N., Rayborn, M. E., Hollyfield, J. G., and Farber, D. B. (1980). Cyclic GMP and visual cell degeneration in the inherited disorder of rd mice: a progress report. *Vis. Res.* 20, 1157–1161. doi:10.1016/0042-6989(80)90054-1

Lorenc, V. E., Lima, E., Silva, R., Hackett, S. F., Fortmann, S. D., Liu, Y., et al. (2020). Hepatocyte growth factor is upregulated in ischemic retina and contributes to retinal vascular leakage and neovascularization. *FASEB Bioadv.* 18, 219–233. doi:10.1096/fba.2019-00074

Lowry, O. H., Rosebroughn, N. J., Farr, A. L., and Randall, R. J. (1951). Protein measurement with the folin phenol reagent. *J. Biol. Chem.* 193, 265–275.

Nakamura, H., Herzenberg, L. A., Bai, J., Araya, S., Kondo, N., Nishinaka, Y., et al. (2001). Circulating thioredoxin suppresses lipopolysaccharide-induced neutrophil chemotaxis. *Proc. Natl. Acad. Sci. U.S.A.* 98, 15143–15148. doi:10.1073/pnas.191498798

Nakamura, H., Hoshino, Y., Okuyama, H., Matsuo, Y., and Yodoi, J. (2009). Thioredoxin 1 delivery as new therapeutics. *Adv. Drug Deliv. Rev.* 61, 303–309. doi:10.1016/j.addr.2009.01.003

Nakazawa, T., Takeda, M., Lewis, G. P., Cho, K. S., Jiao, J., Wilhelmsson, U., et al. (2007). Attenuated glial reactions and photoreceptor degeneration after retinal detachment in mice deficient in glial fibrillary acidic protein and vimentin. *Invest. Ophthalmol. Vis. Sci.* 48, 2760–2768. doi:10.1167/iovs.06-1398

Nishimura, M., Ikeda, T., Ushiyama, M., Nanbu, A., Kinoshita, S., and Yoshimura, M. (1999). Increased vitreous concentrations of human hepatocyte growth factor in proliferative diabetic retinopathy. *J. Clin. Endocrinol. Metab.* 84, 659–662. doi:10.1210/jcem.84.2.5434

Nishiyama, T., Nishukawa, S., Hiroshi, Tomita., and Tamai, M. (2000). Müller cells in the preconditioned retinal ischemic injury rat. *Tohoku J. Exp. Med.* 191, 221–232. doi:10.1620/tjem.191.221

Panfoli, I., Calzia, D., Ravera, S., Morelli, A. M., and Traverso, C. E. (2012). Extra-mitochondrial aerobic metabolism in retinal rod outer segments: new perspectives in retinopathies. *Med. Hypotheses* 78, 423–427. doi:10.1016/j.mehy.2011.12.012

Paquet-Durand, F., Azadi, S., Hauck, S. M., Ueffing, M., van Veen, T., and Ekström, P. (2006). Calpain is activated in degenerating photoreceptors in the rd1 mouse. *J. Neurochem.* 96, 802–814. doi:10.1111/j.1471-4159.2005.03628.x

Penn, J. S., Madan, A., Caldwell, R. B., Bartoli, M., Caldwell, R. W., and Hartnett, M. E. (2008). Vascular endothelial growth factor in eye disease. *Prog. Retin. Eye Res.* 27, 331–371. doi:10.1016/j.preteyeres.2008.05.001

Pow, D. V., and Crook, D. K. (1995). Immunocytochemical evidence for the presence of high levels of reduced glutathione in radial glial cells and horizontal cells in the rabbit retina. *Neurosci. Lett.* 193, 25–28. doi:10.1016/0304-3940(95)11657-i

Powis, G., and Montfort, W. R. (2001). Properties and biological activities of thioredoxins. *Annu. Rev. Biophys. Biomol. Struct.* 30, 421–455. doi:10.1146/annurev.biophys.30.1.421

Reed, D. J., Babson, J. R., Beatty, P. W., Brodie, A. E., Ellis, W. W., and Potter, D. W. (1980). High-performance liquid chromatography analysis of nanomole levels of glutathione, glutathione disulfide, and related thiols and disulfides. *Anal. Biochem.* 106, 55–62. doi:10.1016/0003-2697(80)90118-9

Riley, M. V., Meyer, R. F., and Yates, E. M. (1980). Glutathione in the aqueous humor of human and other species. *Invest. Ophthalmol. Vis. Sci.* 19, 94–96.

Salom, D., Diaz-Llopis, M., García-Delpech, S., Udaondo, P., Sancho-Tello, M., and Romero, F. J. (2008). Aqueous humor levels of vascular endothelial growth factor in retinitis pigmentosa. *Invest. Ophthalmol. Vis. Sci.* 49, 3499–3502. doi:10.1167/iovs.07-1168

Salom, D., Diaz-Llopis, M., Quijada, A., García-Delpech, S., Udaondo, P., Romero, F. J., et al. (2010). Aqueous humor levels of hepatocyte growth factor in retinitis pigmentosa. *Invest. Ophthalmol. Vis. Sci.* 51, 3157–3161. doi:10.1167/iovs.09-4390

Sánchez-Vallejo, V., Benlloch-Navarro, S., López-Pedrajas, R., Romero, F. J., and Miranda, M. (2015). Neuroprotective actions of progesterone in an *in vivo* model of retinitis pigmentosa. *Pharmacol. Res.* 99, 276–288. doi:10.1016/j.phrs.2015.06.019

Sanz, M. M., Johnson, L. E., Ahuja, S., Ekström, P. A., Romero, J., and van Veen, T. (2007). Significant photoreceptor rescue by treatment with a combination of antioxidants in an animal model for retinal degeneration. *Neuroscience* 145, 1120–1129. doi:10.1016/j.neuroscience.2006.12.034

Schafer, F. Q., and Buettner, G. R. (2001). Redox environment of the cell as viewed through the redox state of the glutathione disulfide/glutathione couple. *Free Radic. Biol. Med.* 30, 1191–1212. doi:10.1016/s0891-5849(01)00480-4

Scholl, H. P., Strauss, R. W., Singh, M. S., Dalkara, D., Roska, B., Picaud, S., et al. (2016). Emerging therapies for inherited retinal degeneration. *Sci. Transl. Med.* 8 (368), 368rv6. doi:10.1126/scitranslmed.aaf2838

Shen, J., Yang, X., Dong, A., Petters, R. M., Peng, Y. W., Wong, F., et al. (2005). Oxidative damage is a potential cause of cone cell death in retinitis pigmentosa. *J. Cell. Physiol.* 203, 457–464. doi:10.1002/jcp.20346

Shin, J. Y., and Yu, H. G. (2014). Chlorogenic acid supplementation improves multifocal electroretinography in patients with retinitis pigmentosa. *J. Korean Med. Sci.* 29, 117–121. doi:10.3346/jkms.2014.29.1.117

Simó, R., Vidal, M. T., García-Arumí, J., Carrasco, E., García-Ramírez, M., Segura, R. M., et al. (2006). Intravitreous hepatocyte growth factor in patients with proliferative diabetic retinopathy: a case-control study. *Diabetes Res. Clin. Pract.* 71, 36–44. doi:10.1016/j.diabres.2005.05.017

Sondell, M., Lundborg, G., and Kanje, M. (1999). Vascular endothelial growth factor has neurotrophic activity and stimulates axonal outgrowth, enhancing cell survival and Schwann cell proliferation in the peripheral nervous system. *J. Neurosci.* 19, 5731–5740. doi:10.1523/JNEUROSCI.19-14-05731.1999

Tian, L., Nie, H., Zhang, Y., Chen, Y., Peng, Z., Cai, M., et al. (2014). Recombinant human thioredoxin-1 promotes neurogenesis and facilitates cognitive recovery following cerebral ischemia in mice. *Neuropharmacology* 77, 453–464. doi:10.1016/j.neuropharm.2013.10.027

Travis, G. H. (1998). Mechanisms of cell death in the inherited retinal degenerations. *Am. J. Hum. Genet.* 62, 503–508. doi:10.1086/301772

Vasireddy, V., Chavali, V. R., Joseph, V. T., Kadam, R., Lin, J. H., Jamison, J. A., et al. (2011). Rescue of photoreceptor degeneration by curcumin in transgenic rats with P23H rhodopsin mutation. *PLoS One* 6, e21193. doi:10.1371/journal.pone.0021193

Vecino, E., Rodriguez, F. D., Ruzafa, N., Pereiro, X., and Sharma, S. C. (2016). Glia-neuron interactions in the mammalian retina. *Prog. Retin. Eye Res.* 51, 1–40. doi:10.1016/j.preteyeres.2015.06.003

Wang, B., Tian, S., Wang, J., Han, F., Zhao, L., Wang, R., et al. (2015). Intraperitoneal administration of thioredoxin decreases brain damage from ischemic stroke. *Brain Res.* 1615, 89–97. doi:10.1016/j.brainres.2015.04.033

Wright, A. F., Chakarova, C. F., Abd El-Aziz, M. M., and Bhattacharya, S. S. (2010). Photoreceptor degeneration: genetic and mechanistic dissection of a complex trait. *Nat. Rev. Genet.* 11, 273–284. doi:10.1038/nrg2717

Yoshida, N., Ikeda, Y., Notomi, S., Ishikawa, K., Murakami, Y., Hisatomi, T., et al. (2013). Laboratory evidence of sustained chronic inflammatory reaction in retinitis pigmentosa. *Ophthalmology* 120, e5–e12. doi:10.1016/j.ophtha.2012.07.008

Conflict of Interest: The authors declare that the research was conducted in the absence of any commercial or financial relationships that could be construed as a potential conflict of interest.

frontiers in Pharmacology

REVIEW
published: 18 January 2021
doi: 10.3389/fphar.2020.601647

Biomarkers of Neurodegeneration and Precision Therapy in Retinal Disease

Alessandra Micera[1]*, *Bijorn Omar Balzamino*[1], *Antonio Di Zazzo*[2], *Lucia Dinice*[1], *Stefano Bonini*[2] and *Marco Coassin*[2]

[1]Research and Development Laboratory for Biochemical, Molecular and Cellular Applications in Ophthalmological Sciences, IRCCS - Fondazione Bietti, Rome, Italy, [2]Ophthalmology Operative Complex Unit, University Campus Bio-Medico, Rome, Italy

Vision-threatening retinal diseases affect millions of people worldwide, representing an important public health issue (high social cost) for both technologically advanced and new-industrialized countries. Overall RD group comprises the retinitis pigmentosa, the age-related macular degeneration (AMD), the diabetic retinopathy (DR), and idiopathic epiretinal membrane formation. Endocrine, metabolic, and even lifestyles risk factors have been reported for these age-linked conditions that represent a "public priority" also in this COVID-19 emergency. Chronic inflammation and neurodegeneration characterize the disease evolution, with a consistent vitreoretinal interface impairment. As the vitreous chamber is significantly involved, the latest diagnostic technologies of imaging (retina) and biomarker detection (vitreous) have provided a huge input at both medical and surgical levels. Complement activation and immune cell recruitment/infiltration as well as detrimental intra/extracellular deposits occur in association with a reactive gliosis. The cell/tissue aging route shows a specific signal path and biomolecular profile characterized by the increased expression of several glial-derived mediators, including angiogenic/angiostatic, neurogenic, and stress-related factors (oxidative stress metabolites, inflammation, and even amyloid formation). The possibility to access vitreous chamber by collecting vitreous reflux during intravitreal injection or obtaining vitreous biopsy during a vitrectomy represents a step forward for an individualized therapy. As drug response and protein signature appear unique in each single patient, therapies should be individualized. This review addresses the current knowledge about biomarkers and pharmacological targets in these vitreoretinal diseases. As vitreous fluids might reflect the early stages of retinal sufferance and/or late stages of neurodegeneration, the possibility to modulate intravitreal levels of growth factors, in combination to anti-VEGF therapy, would open to a personalized therapy of retinal diseases.

Keywords: retinal diseases, chronic inflammation, growth factors, angiogenesis, precision medicine, neurodegeneration, pharmacological targets

OPEN ACCESS

Edited by:
Settimio Rossi,
Second University of Naples, Italy

Reviewed by:
Anca Hermenean,
Vasile Goldiş Western University of Arad, Romania
Chiara Bianca Maria Platania,
University of Catania, Italy

***Correspondence:**
Alessandra Micera
alessandra.micera@fondazionebietti.it

Specialty section:
This article was submitted to Inflammation Pharmacology, a section of the journal Frontiers in Pharmacology

Received: *01 September 2020*
Accepted: *09 November 2020*
Published: *18 January 2021*

Citation:
Micera A, Balzamino BO, Di Zazzo A, Dinice L, Bonini S and Coassin M (2021) Biomarkers of Neurodegeneration and Precision Therapy in Retinal Disease. Front. Pharmacol. 11:601647. doi: 10.3389/fphar.2020.601647

INTRODUCTION

A recent evaluation of the current prevalence and pattern of retinal diseases (RD) in industrialized and nonindustrialized countries highlights that RD are increasing worldwide representing a serious problem even under COVID-19 emergency.

RD group includes the retinitis pigmentosa, the age-related macular degeneration, the diabetic retinopathy, and the idiopathic epiretinal membrane formations. Other than genetic background,

several risk factors (endocrine, metabolic, and even lifestyles influencers) have been reported for these age-linked conditions that represent a "public priority" as worldwide population is more long-lived and its life expectancy is increasing. The chronic inflammation and neurodegeneration affect the neuronal network, with different vitreoretinal interface impairment. As the vitreous chamber is significantly affected due to release of a plethora of soluble mediators, the latest diagnostic technologies of imaging (retina) and biomarker detection (vitreous) have provided a huge input at both medical and surgical levels. As per consecutive increase, the early complement activation, the immune cell recruitment/infiltration with local release of soluble mediators, and the formation of intra/extracellular deposits lead to impairment of the neuronal network, sustained by reactive gliosis. Tissue/cell aging shows a specific signal path and biomolecular profile characterized by the increased expression of several glial-derived mediators, including angiogenic/angiostatic, neurogenic, and stress-related factors (oxidative stress metabolites, inflammation, and even amyloid formation).

This review addresses the current knowledge about potential candidate biomarkers and pharmacological targets in these vitreoretinal diseases. As vitreous fluids might reflect the early stages of retinal sufferance and/or late stages of degeneration, the possibility to modulate intravitreal levels of growth factors will be also discussed as an additional way to improve treatment approaches, most of them in combination to anti-VEGF therapy.

PRECISION THERAPY FOR RETINAL DISEASES: STATE OF THE ART

Over the last years, numerous changes have been introduced to improve vitreoretinal surgery, such as the development of transconjunctival sutureless vitrectomy, ameliorated cutters, and new surgical approaches (Fujii et al., 2002). The possibility to collect vitreous biopsies represents a great opportunity of analysis for individualized medicine in retinal diseases (Oh and Oshima, 2014; Kasi et al., 2017; Coassin et al., 2020).

Globally, precision medicine approach represents a new way of thinking at prevention and treatment of multifactorial diseases, taking into consideration the individual variability in terms of genetic background, environment, and lifestyle. Although relatively new, the concept of precision medicine has represented for many years a fundamental aspect of healthcare outside ophthalmology. The possibility to predict and treat the disease depending on the specific local condition represents a crucial aspect of cancer therapy, and it is now extended to several other healthcare areas (Blix, 2014; Velez et al., 2018). In ophthalmology, precision medicine represents an effective approach for treating ocular tumors (Straatsma, 2018). In addition, this strategy is being applied successfully in the management of the inherited diseases (Ong et al., 2013). In the recent years, precision therapy has gained increasing interest for the management of retinal diseases. In particular, it has been recently proposed for intravitreal treatments in association with the biochemical analysis of vitreal reflux (Cacciamani et al., 2016). Collecting vitreous samples at the time of anti-VEGF intravitreal injection for wet AMD may be an effective method to elaborate further the precise clinical condition of the specific patient under treatment.

One aspect of precision medicine is the necessity of noninvasive indicators to drive the decision of the specialist. The contribution of computerized imaging, particularly the Optic Coherence Tomography (OCT) for examining the retinal layers in a noninvasive way, has improved drastically the posterior segment therapeutic approaches and reduced significantly healthcare costs, although a high percentage of senior population in industrialized countries is affected (Spaide et al., 2018). Diagnostic Imaging applied to retina and fundus has gained success worldwide, contributing to a better management of retinal diseases (Li et al., 2018). This computer-assisted technology has been recently associated with a considerable development of biomarkers coming from proteomic, metabolomic, and genetic basic and applied research investigation (Ristori et al., 2020).

RETINAL DISEASES: THE MECHANISMS BEHIND CLINICAL MANIFESTATIONS

Many RD have a multifactorial etiology, most probably driven by a combination of genetic and environmental factors, interacting to produce a wide range of phenotypes (Hull et al., 2014). Environmental stressors allow epigenetic modifications by influencing cellular activity and tissue response (Crick, 1970; Jafari et al., 2017). Some morphological and biostrumental biomarkers (subretinal fluid, intraretinal fluid, intraretinal cysts, hyperreflective foci, drusen/pseudodrusen, epiretinal/limiting membranes, geographic/outer retinal atrophy, and fibrovascular pigment epithelial detachment) are currently of great utility in addition to the biostrumental biomarkers provided by OCT scansion (Cacciamani et al., 2019). For sustainment, some health-recognized biomarkers are also used to discriminate between absence of, association of, or defined pathological states (Ahmed et al., 2014). The possibility to have inflammatory biomarkers, as quantified in vitreal or vitreal reflux samples or even biopsies whenever accessible, represents a step forward in grading pathological manifestation as well as in guiding the surgical decision (**Figure 1**). RD forms will be discussed stepwise with respect to biomarkers' association. RD group (RP, AMD, DR, and ERMs) will be discussed below with respect to clinical manifestations and biomarker association as quantified in vitreal fluids.

Retinitis Pigmentosa (RP)

RP is a neurodegenerative eye disease characterized by degeneration of rod/cone photoreceptors leading to night blindness, followed by a progressive mid-peripheral vision loss, and culminating in complete blindness (around mid-40s) (Hamel, 2006). RP is genetically and phenotypically heterogeneous: mutations occur between 0.025 and 0.04% of worldwide population (Van Soest et al., 1999; Dias et al., 2018). RP outcome, disease onset (age), progression rate, and

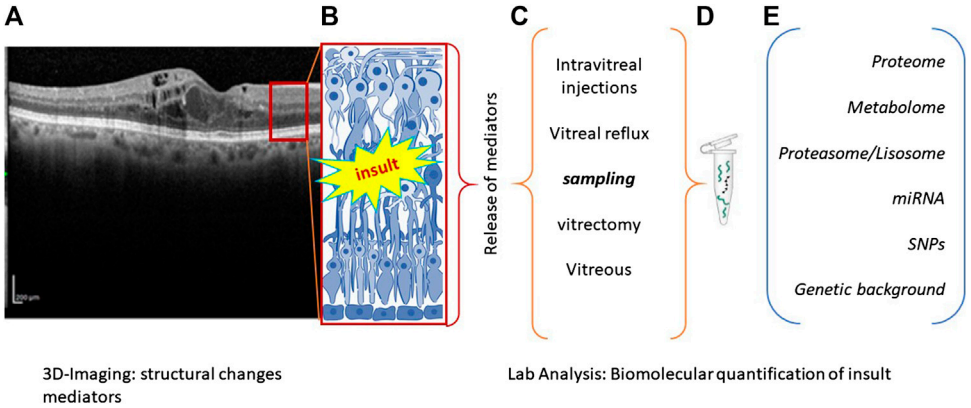

FIGURE 1 | Flowchart summarizing the main steps of precision medicine. **(A)**, **(B)** Biostrumental parameters' acquisition by computerized tomography. Representative image showing retinal layers **(A)** with a red square schematized in **(B)**. Retinal insult is followed by the release of a plethora of inflammatory mediators that can be quantified according to different sampling route **(C)**. Samples can be appropriately processed to release RNA, DNA, or proteins **(D)**, according to different new and old generation techniques **(E)**. The main biomarkers used as outcome indicator are listed in **(E)**.

secondary clinical signs are variable, even in parents and relatives (Guadagni et al., 2015). Mutant proteins implicated in some functional process of retina may trigger nonsyndromic RP, while mutations in genes working in cells/tissues result in systemic manifestations (syndromic RP) (Waters and Beales, 2011; Wheway et al., 2014; Dias et al., 2018). Mutations in proteins associated with the classical components of the phototransduction cascade (rhodopsin and phosphodiesterase), cell signaling factors (such as Crx, Nrl), disc membrane-associated glycoproteins (peripherin), ion channels (such as the light sensitive cationic ones), and the structural proteins of the cilium can contribute to disease heterogeneity (Roesch et al., 2012; Daiger et al., 2013). Genetic and environmental factors (light) are known to modulate the entire disease: faster disease progression occurring at the inferior retina may result from a modifying effect caused by light. It has been hypothesized that light sources privilege the superior visual field, implying that a greater exposure occurs at the inferior retina, accelerating whole retinal degeneration (Paskowitz et al., 2006). This aspect was particularly evident when rd10 mice were exposed to increasing light intensity: particularly, both retinal function and photoreceptors' number decreased as a function of light-dependent exposure, with morphological alterations and loss of synaptic connectivity inside the retinal network (Kutsyr et al., 2020).

Biomarkers in RP

Although genetic defects in photoreceptors or retinal pigment epithelium represent the primary causes of RP development, recent studies looked at the inflammatory response as a possible contributor for RP pathogenesis (Yoshida et al., 2013). In previous studies, Yoshida and coworkers showed that: i) inflammatory cells accumulate in the vitreous cavity of RP patients, mainly younger ones; ii) RP patients with increased inflammatory cells into vitreal cavity show decreased visual function; iii) increased proinflammatory cytokines and chemokines (IL-1α, IL-1β, IL-2, IL-4, IL-6, IL-8, IL-10, IFN-γ, GRO-α, I-309, IP-10, MCP-1, MCP-2, and TARC) typify both aqueous and vitreous from RP patients (Yoshida et al., 2013). All together, these aspects suggest the presence of a "strong" chronic inflammatory reaction depending on RP pathogenesis (Ohnaka et al., 2012). Similarly, proinflammatory cytokines and chemokines were quantified in retinas of rd10 experimental model (Ikeda et al., 2002; Ohnaka et al., 2012; Semba et al., 2013; Yoshida et al., 2013; Jové et al., 2014; Zhang et al., 2015; Kohler et al., 2016). Of those factors, MCP-1 levels were significantly increased in human RP aqueous and vitreous (Ikeda et al., 2002; Nakazawa et al., 2007; Ohnaka et al., 2012; Semba et al., 2013; Yoshida et al., 2013; Jové et al., 2014; Zhang et al., 2015; Kohler et al., 2016). As known from other diseases and experimental studies, the ability of MCP-1 is to recruit monocytes, activate dendritic cells, and stimulate memory T cells at injured sites (Ikeda et al., 2002; Nakazawa et al., 2007). More interestingly, MCP-1 activates microglia, which contributes to neuronal inflammation and subsequent neuronal apoptosis (Gupta et al., 2003; Minghetti et al., 2005). Nakazawa and coworkers demonstrated that MCP-1 contributes to photoreceptor apoptosis following retinal detachment, through a microglia/macrophage activation pathway (Nakazawa et al., 2007). In human RP retinas, another study demonstrated that an activated microglia phenotype was present in the outer nuclear layer of regions populated by death committed rods (Gupta et al., 2003). These data suggest that MCP-1, in concert with other soluble mediators, may play an important role in the inflammatory reactions and degenerative process of RP (Gupta et al., 2003; Nakazawa et al., 2007).

Age-Related Macular Degeneration (AMD)

AMD, a neurodegenerative late-onset retinal disease showing clinical and pathological aspects close to Alzheimer Diseases, is a retinal disease leading to central vision loss: it is characterized by neurodegeneration of the central region of retina and choroid (Haddad et al., 2006). Two major forms have been identified: atrophic (dry) and exudative (wet) AMD. While dry AMD (about

85% of cases) is characterized by yellow subretinal deposits (drusen) and/or retinal pigment epithelial (RPE) irregularities (hyperpigmentation/hypopigmentary changes), the wet form (around 15% of cases) is characterized by choroidal neovascularization and fibrovascular RPE detachments (Haddad et al., 2006). Both environment and genetic factors can contribute to developing and/or exacerbation of AMD (Haddad et al., 2006). The observation of 52 common and rare variants at 34 genetic loci, independently associated with late AMD, implies that genetic factors might represent a crucial aspect in the management of disease (Haddad et al., 2006). A strong genetic association in AMD pathogenesis was found for complement factor H (CFH) and complement factor I (CFI), as well as in the metalloproteinases tissue inhibitor 3 (TIMP3), due to the presence of rare coding variants (frequency < 0·1%) (Mitchell et al., 2018). Gene–environment interaction and factors such as age and race may lead to oxidative damage and inflammation (Sacca et al., 2009; Gemenetzi and Lotery, 2020). Strong association between several environmental factors and AMD has been reported and particularly the main demographic/environmental risk factors are aging, smoking, diet, fat intake, and obesity (Klein et al., 1992; Christen et al., 1996; Seddon et al., 1996; Cho et al., 2001; Seddon et al., 2003; Friedman et al., 2004). In the neovascular form of AMD, a higher risk of AMD development was associated with white populations, with respect to Hispanic and Black ones (Sommer et al., 1991; Cruickshanks et al., 1997). Protective effects came from diet (antioxidants, nuts, fish, and omega-3 fatty acids) (Age-Related Eye Disease Study Research Group, 2001). Other potential risk factors (hypertension, high cholesterol levels, and sunlight exposure) have been prospected although with no specific involvement (Seddon and Chen, 2004).

Biomarkers in AMD

Analytical procedures and related immunoassay for biomarker detection (screening and monitoring) would contribute significantly to the management of AMD, at both early and late disease (Nath et al., 2017). A strong biological correlation was observed between endothelial dysfunction and biomarkers of inflammation/oxidative stress. As anti-neovascular therapy is a popular strategy for AMD, the development of predictable biomarker would be of immense importance for strategizing therapeutic modalities based on the underlying pathology. Chau and coworkers determined matrix metalloproteinase-(MMP-) 2 and MMP-9 levels in the plasma collected from AMD suffering patients, highlighting that plasmatic MMP-9 levels were significantly higher in age-related maculopathy and choroidal neovascularization (CNV) groups, as compared to control groups (Chau et al., 2008). Machalinska and colleagues showed the presence of increased circulating endothelial cells (EndCs) and endothelial progenitor cells (EPCs) in AMD patients, as compared to healthy individuals. Authors highlighted that this specific increase would reflect a severe vascular disturbance (Machalińska et al., 2011). With respect to oxidative stress, Totan and coworkers showed the presence of increased Endothelin-1 (ET-1) and reduced Nitric Oxide (NO) plasmatic levels in AMD, suggesting an imbalance between vasoconstrictor and vasodilator agents, possibly reflecting either an endothelial dysfunction in AMD pathogenesis or a role of vasoconstriction in exudative AMD (Totan et al., 2015). Another study showed significant elevation of serum concentrations of IL-1α, IL-1β, IL-4, IL-5, IL-10, IL-13, and IL-17 in AMD patients compared to control subjects (Nassar et al., 2015). IL-1 is a macrophage-derived major proinflammatory cytokine acting mainly through the induction of a network of inflammatory cytokines, chemokines, and other small soluble mediators (Dinarello, 2009). IL-1 early release might elucidate, at least in part, the increased vascular exudation resulting in larger and persisting macular edema in these patients (Dinarello, 2009). Guymer et al. also demonstrated an association between elevated urinary cytokines, transforming growth factor- (TGF-) β1 and monocyte chemoattractant protein-1 (MCP-1), and AMD (Guymer et al., 2011). Therefore, the possibility to have a "urinary panel" (biomarkers) would facilitate the monitoring of disease progression or predicting vision-threatening complications or even measuring the response to treatments (Guymer et al., 2011). Some soluble receptors, taking actively part in the recognition of major proinflammatory cytokines, have gained increasing interest in the last years. For instance, the observation of increased plasma level of soluble Tumor Necrosis Factor Receptor-II (TNFR-II) in AMD supported the hypothesis of low-grade systemic inflammation in patients with AMD (Faber et al., 2015). Of crucial interest was the use of Paraoxonase-1 (PON1), an antioxidant agent used as an indicator of lipid peroxidation, to evaluate oxidative stress in patients with AMD. Authors reported a negative correlation between PON1 activity and Malondialdehyde (MDA) levels in patients with AMD. This may suggest some efficacy of antioxidant therapy to inhibit lipid peroxidation and that hypothetical agents able to increase PON1 activity could be a therapeutic option in AMD (Baskol et al., 2006).

Diabetic Retinopathy (DR)

DR, the result of diabetes causing damage to retinal blood vessels, is an ocular disease that may have different clinical characteristics but may lead to severe visual loss (Hayreh, 2014). Disease is associated with impaired glucose metabolism and after 20 years of type-1 diabetes, 80% of patients with insulin treated type-1 diabetes and 50% of patients with type-2 diabetes will have some degree of DR (Stitt et al., 2016). According to clinical manifestation, DR is currently categorized as mild, moderate, and severe nonproliferative diabetic retinopathy (NPDR) and proliferative diabetic retinopathy (PDR) in which retinal neovascularization is present (Cehofski et al., 2017). Diet and obesity have been reported to contribute massively to the development of type 2 diabetes. By the way, heritability can account for more than 52% of the advanced PDR, showing retinal neovascularization (Seddon, 2013).

Biomarkers in DR

DR is a common and often severe complication of diabetes. Nevertheless, despite the wide array of treatments available for

DR management, vision restoration in advanced stage of disease is difficult. Although it is well known that tight glycemic control may protect from end-organ damage, the risk of developing diabetic complications despite adequate blood sugar control may be demonstrated by validated biomarkers. Fasching et al. demonstrated that, irrespective of metabolic control, serum concentrations of intercellular adhesion molecule-1 (ICAM-1) and vascular cell adhesion molecule-1 (VCAM-1) were elevated in patients with insulin-dependent diabetes mellitus (IDDM), reflecting ongoing endothelial cell stimulation and leukocyte activation (Fasching et al., 1996). No difference in serum E-selectin concentration was detected between diabetic patients (with or without macroangiopathy) and normal subjects, suggesting the contribution of adhesion molecules in the development of atherosclerosis occurring in diabetes (Kado and Nagata, 1999). Sharma et al. reported that circulating markers of inflammation, endothelial injury, and TNF signaling were significantly associated with DR in patients with type-1 diabetes (T1Ds). TNF receptor-I (TNFR-I) and TNFR-II receptors were highly correlated, but DR are associated more strongly with TNFR-I (Sharma et al., 2015). Studies showed the importance of TNF-α system in diabetic retinal microvascular damage (Behl et al., 2008). TNF-α binding to two specific membrane receptors (TNFR-I and TNFR-II) starts a signal pathway leading to the activation of transcription factors (NF-κB and Bax) involved in the proinflammatory and apoptotic cascade (Aderka, 1996). The diabetes-related vascular complications have been correlated with C-reactive protein (CRP), TNF-α, and IL-6 in the EURODIAB Prospective Complication Study (Schram et al., 2005). Indeed, a positive correlation was reported for DR and cardiovascular inflammatory factors, highlighting that strategies focused to decrease inflammatory activity may prevent the development of vascular complications in type 1 diabetes (Schram et al., 2005). Of interest, increased plasma levels of Endothelin (ET-1), a potent endothelium-derived vasoconstrictive peptide, have been found in non-insulin-dependent diabetic (NIDDM) patients, prospecting ET-1 as new marker of vascular damage in diabetic subjects (Laurenti et al., 1997). Jacqueminet and coworkers proposed the peripheral blood MMP-9 levels as "a suitable substitute biomarker" of retinopathy in type-1 diabetes not associated with vascular complications (Jacqueminet et al., 2006). Transforming growth factor-β (TGF-β), the main inducer of extracellular matrix remodeling and associated with collagen production and fibrogenesis, was found overexpressed in NIDDM patients (Pfeiffer et al., 1996). Lee et al. showed elevated levels of circulating endothelial progenitor cells (EPCs) and serum Erythropoietin (Epo), VEGF, and Substance P (SP) which may be involved in the progression of DR, sustaining a systemic vasculogenesis rather than a local angiogenesis (Lee et al., 2006). Both level and type of serum oxidative stress products–Malondialdehyde (MDA), Conjugated Diene (CD), Advanced Oxidation Protein Products (AOPPs), protein carbonyl, and 8-hydroxydeoxyguanosine (8-OHdG)– have been reported to have a predictive role in the development and progression of DR (Pan et al., 2008).

Idiopathic Epiretinal Membrane Formations (ERMs)

ERMs are thin and avascular sheet of fibrous tissue developing over the retinal layer, at the vitreoretinal interphase, merely at the macular area of retina, causing changes in architectonics and functioning with consequent reduced vision. ERMs etiology is idiopathic in many cases (80%) or secondary to different situations, including retinal detachment or vascular or inflammatory retinal diseases (Bottós et al., 2012). Prognostic and therapeutic decisions occur principally by OCT evaluation (Unsal et al., 2019). Vitrectomy followed by ERM peel-off is the routine surgical approach. Nevertheless, ERMs and even the associated internal limiting membrane can reform due to genetic/epigenetic influences or particular conditions (Gemenetzi and Lotery, 2020).

Biomarkers in ERMs

A recent study investigated the possibility to use an interplay of OCT and biochemical markers to allow a grading of ERM formation, severity, and traction entity, an indirect marker of retinal status or detach (Stevenson et al., 2016). Other than cytokine release, some additional biomarkers have been recently identified and quantified in both vitreous and tissues (Ahmad et al., 2018). Some of those inflammatory mediators were recognized as tissue remodeling actors (IL6, IL33, and IL8), implying the possibility of a direct modulation of cell migration and collagen metabolism at the vitreoretinal interface (Dinice et al., 2020). A special note should be devoted to Osteopontin, a tissue remodeling biomarker of recent attention (Dinice et al., 2020). In addition to the cell phenotyping markers (GFAP, Iba1, and CD56), other molecular targets have been observed and some oxidative ones are highlighted at both molecular and biochemical level (Marrocco et al., 2017). None of these biomarkers can be tissue or disease specific, although their increased expression as well as just their presence can be of great diagnostic and prognostic value (Strimbu and Tavel, 2010). Last, it is important to mention that some OCT parameters could be used to predict postoperative visual outcomes in patients with iERM treated with PPV (Minami et al., 2019).

DR AND NOVEL POTENTIAL PLAYERS FOR PERSONALIZED MEDICINE

The possibility to select some biomarkers for predictive purposes will help to define patients suitable for therapy, according to the concept of precision medicine devoted to tailored individual needs. In the last decade, RNA and protein array approaches have been implemented by the metabolomic analysis, the proteasome/lysosome analysis, and the next generation sequencing coupled to the pharmacogenomics (PGx), as additional supports for individualized therapy (Laíns et al., 2019). Metabolome and associated pathways have been tested for improving our understanding of disease pathophysiology and associated mechanisms, as recently prospected for clarifying some aspects of a cicatricial disease of the ocular surface (Laíns et al., 2019; Di Zazzo et al., 2020). All the proteome and metabolome information should be verified with conventional approaches, bypassing some

limits of these multiparametric techniques (Miteva et al., 2013). As known, metabolomics is strictly dependent on the influence of external factors (external environment, nutrition habits, age, and microbiome, among others) (Patti et al., 2012). The study of metabolomic variations allows the possibility to: i) increase the understanding of disease pathophysiology at the molecular level, generating new hypotheses for disease mechanisms; ii) identify those predictive/diagnostic biomarkers; iii) assess disease progression/exacerbation; iv) elucidate the influence of environment/lifestyle exposures in disease; and finally, v) assess drug efficacy and/or toxicity as well as eventual adverse-drug reactions (Nicholson et al., 2012; Jové et al., 2014; Kohler et al., 2016).

Epigenetic Factors

In the recent years, the epigenetic mechanisms gained attention for their promising ability to reduce the gap between environmental factors and disease development/exacerbation, by means of gene modulation (Lanza et al., 2019). Although many efforts have been carried out to elucidate genetic and environmental risk factors for retinal diseases, little is still unknown about their molecular mechanisms. Recent studies highlighted the association between epigenetic changes and incidence/progression of retinal diseases associated with visual loss (Lanza et al., 2019). While several gene mutations have been reported for RP, the mechanisms underlying photoreceptor death remain to be elucidated (He et al., 2013). A recent study carried out in an experimental model of RP (rd1 mouse) showed an increased histone deacetylase (HDAC) activity just before photoreceptor degeneration, an effect significantly reduced in the presence of HDAC inhibitors (Sancho-Pelluz et al., 2010). A reduced electroretinography response was observed in degenerated retinal cells when the retinal endoribonuclease Dicer (a helicase with rnase motif enzyme) is specifically knocked down (Damiani et al., 2008). As well, epigenetic mechanisms, including chromatin modifications, have been implicated in AMD pathogenesis (Liu et al., 2012). Merely, Suuronen and coworkers demonstrated that the addition of HDAC inhibitors resulted in expression/secretion of clusterin (a major component of drusen) by human RPE cell line, suggesting that the management of HDAC activity is important to limit or even counteract drusen formation (Suuronen et al., 2007). By using the DNA methylation microarray and bisulfite pyrosequencing applied to frozen human RPE/choroid samples (donors), Hunter and coworkers observed the hypermethylation of glutathione S-transferase isoforms mu1 and mu5 (GSTM1 and GSTM5) in AMD compared with age-matched control tissues (Hunter et al., 2012). The ability of GSTM1 and GSTM5 to reduce oxidative stress appears of great interest, as oxidative stress was hypothesized to contribute to AMD pathophysiology (Hunter et al., 2012).

In diabetic complications, the epigenetic contribution has been proposed to explain the exacerbation of retinal damage in the presence of poor glycemic control (Villeneuve and Natarajan, 2010). As observed in streptozotocin- (STZ-) treated rats (an experimental model of diabetes) with poor glycemic control, retinas and related retinal endothelial cells showed an overexpression of the histone modifiers HADC1, HADC2, and HADC8 and a reduced activity of histone H3-specific acetyltransferase (Zhong and Kowluru, 2010). Since histone-associated impairments did not reverse upon glycemia stabilization, an epigenetic-driven metabolic memory was hypothesized as major reason for DR endurance even in the case of restoration of normal circulating glucose levels (Zhong and Kowluru, 2010). Other epigenetic modifications include the expression of histone H3K4me2 associated with the transcriptional activation and decrease of superoxide dismutase gene (SOD-2), as observed in human DR retinas (donors) (Zhong and Kowluru, 2013).

microRNAs and Pharmacogenetic Biomarkers

Several microRNAs (miRNAs) have been implicated in photoreceptor degeneration in RP, DR, and ERMs (Wang et al., 2012; Russo et al., 2017; Anasagasti et al., 2018). Briefly, miRNAs are small nucleotide non-coding RNA sequences (≈25mers) interfering negatively with gene expression, at the RNA-induced silencing complex (RIS) level, through a binding/degrading activity (nucleases associated pattern) of specific transcripts in the cytosol. Either degrading or reducing transcript activity/translation inside the ribosomal machinery, miRNAs represent key regulators for tissue development and more properly cell growth, development, and differentiation (Jeker and Marone, 2015). One miRNA can target more than one mRNA and its ability to buffer variations in gene expression due to environmental/microenvironmental changes, and not the basic cell functions, highlights their important contribution to maintaining cellular homeostasis and para-inflammation (Lee et al., 2019). Impaired or even a complete loss of miRNA activity can result in several defects and malfunctioning at both tissue and cell level (Gurtner et al., 2016). Pathological implications of miRNA dysregulation have been described for retinal tissues, under either normal or pathological states (diabetes, neovascularization) (Liu et al., 2020). The usefulness of miRNA, as diagnostic tool, has been prospected from experimental models of diabetic retinopathy. Merely, both serum and retina of diabetic mice were found to express dysregulated miRNAs implicated in the regulation of VEGF, BDNF, PPAR-α, and CREB1 expression before the retinal vasculopathy occurs (Platania et al., 2019). Recently, a strong association of specific miRNAs with the progression and severity of retinal as well as vitreoretinal impairments has been observed (Russo et al., 2017; Martins et al., 2020). Their quantification in ocular fluids has been correlated with disease staging and severity, with promising diagnostic and/or prognostic outcomes.

Neuroprotective Factors

A unique attention has been devoted for years to the role of growth factors, including neurotrophic and angiogenic/angiostatic mediators, whose positive role is undoubted in RD. Machalinska et al. reported a marked decrease in the Pigment Epithelium-Derived Factor (PEDF) plasma levels in patients with dry AMD, whereas a significant higher level of PEDF and Vascular Endothelial Growth Factor (VEGF) was observed in the wet form, suggesting that different manifestations of AMD may be the result of altered concentrations of counterbalancing stimulators/inhibitors of angiogenesis (Machalińska et al., 2012). In the last decades, NGF has displayed interesting abilities in the visual

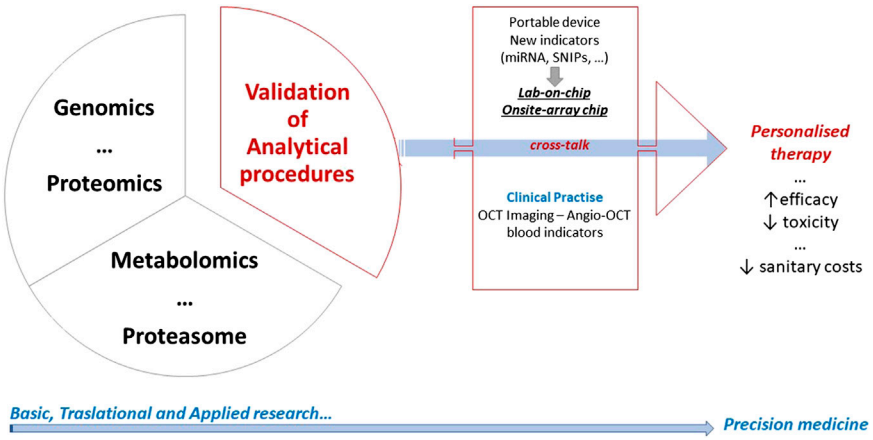

FIGURE 2 | A graphical abstract summarizing the long-lasting and difficult process leading to personalized therapy. Basic and translational research crosstalk to clinical practice, and all convey to precision medicine. Overall steps in research field inform each other with the goal of improving the efficiency and effectiveness of disease prevention, diagnosis, and treatment.

system, working at both ocular surface and retina/optic nerve levels. The pleiotropic NGF effects have been described either *in vitro* (cell culture models) or *in vivo* (experimental models and humans), leading to the development of clinical trials devoted to demonstrating the useful NGF administration in neurodegenerative eye diseases. Other than in neurotrophic ulcer application, this neurotrophic route was particularly evident in the treatment of impaired retinal signal in experimental retinitis pigmentosa and in retinal cell death/optic nerve degeneration in response to abnormal elevated intraocular pressure (Sposato et al., 2008; Sivilia et al., 2009). Our recent observation in experimental models supports the neuroprotective effect of NGF in insulted eye, chiefly for retina and optic nerve degeneration (Rocco et al., 2017). Based on our results, NGF protective effects might be related to an increased survival of retinal ganglion cells and nerves in the optic nerve. The cell survival and neuritis outgrowth in NGF exposed were confirmed by further results, by administration of NGF/αVEGF combination implying an additional effect of the single NGF treatment (Rocco et al., 2017). With respect to NGF alone, the NGF/αVEGF combination significantly delayed and/or protected photoreceptors as well as retinal cells from degeneration. The concept of angiogenic depletion coupled to drugs and/or growth factors has been tested recently (Heier et al., 2020).

All the above reported biomarkers represent a concrete support to complete the imaging information. Essentially, genomics, proteomics, metabolomics, proteasome, and pharmacogenomics can represent valid tools for precision therapy applied to retinal healthcare (**Figure 2**).

CONCLUSION AND FUTURE DIRECTIONS

As vitreous fluids might reflect the early stages of retinal sufferance and/or late stages of degeneration, the possibility to modulate intravitreal levels of growth factors, in combination to anti-VEGF therapy, would open to a new and more appropriate therapy to counteract retinal neurodegeneration. The pathways involved in this new way of thinking will be disclosed in the near future, opening to new alternative strategies of personalized therapies for a better management of retinal disorders through neuroprotection. The possibility to perform a grading of disease severity and finalize the surgical decisions is an adding value in personalized medicine.

Taken together, the above summarized findings sustain the great value of searching new research strategies for preserving the retina from neurodegeneration. The possibility to access vitreous chamber by collecting vitreous reflux during intravitreal injection or collecting vitreous biopsy at the time of vitrectomy represents a step forward for an individualized therapy. Drug response and protein signature appear to be unique in the single patient: therefore, therapies should be much as tailored as possible.

AUTHOR CONTRIBUTIONS

All authors have made a substantial, direct, and intellectual contribution to the work and approved it for publication.

FUNDING

The study was partially supported by the Italian Ministry of Health and 5x1000 (2016) project to IRCCS-Fondazione Bietti.

ACKNOWLEDGMENTS

Many thanks are due to Fondazione Roma (Italy) for continuous support. The study was partially supported by the Italian Ministry of Health and 5x1000 (2016) project to IRCCS-Fondazione Bietti. The authors apologize for undesired missing of information or papers related to this topic.

REFERENCES

Aderka, D. (1996). The potential biological and clinical significance of the soluble tumor necrosis factor receptors. *Cytokine Growth Factor Rev*. 7 (3), 231–240. doi:10.1016/s1359-6101(96)00026-3

Age-Related Eye Disease Study Research Group (2001). A randomized, placebo-controlled, clinical trial of high-dose supplementation with vitamins C and E, beta carotene, and zinc for age-related macular degeneration and vision loss: AREDS report no. 8. *Arch. Ophthalmol*. 119 (10), 1417–1436. doi:10.1001/archopht.119.10.1417

Ahmad, M. T., Zhang, P., Dufresne, C., Ferrucci, L., and Semba, R. D. (2018). The human eye proteome project: updates on an emerging proteome. *Proteomics* 18 (5-6), e1700394. doi:10.1002/pmic.201700394

Ahmed, R. M., Paterson, R. W., Warren, J. D., Zetterberg, H., O'Brien, J. T., Fox, N. C., et al. (2014). Biomarkers in dementia: clinical utility and new directions. *J. Neurol. Neurosurg. Psychiatry* 85 (12), 1426–1434. doi:10.1136/jnnp-2014-307662

Anasagasti, A., Ezquerra-Inchausti, M., Barandika, O., Muñoz-Culla, M., Caffarel, M. M., Otaegui, D., et al. (2018). Expression profiling analysis reveals key MicroRNA-mRNA interactions in early retinal degeneration in retinitis pigmentosa. *Invest. Ophthalmol. Vis. Sci*. 59 (6), 2381–2392. doi:10.1167/iovs.18-24091

Baskol, G., Karakucuk, S., Oner, A. O., Baskol, M., Kocer, D., Mirza, E., et al. (2006). Serum paraoxonase 1 activity and lipid peroxidation levels in patients with age-related macular degeneration. *Ophthalmologica* 220 (1), 12–16. doi:10.1159/000089269

Behl, Y., Krothapalli, P., Desta, T., DiPiazza, A., Roy, S., and Graves, D. T. (2008). Diabetes-enhanced tumor necrosis factor-alpha production promotes apoptosis and the loss of retinal microvascular cells in type 1 and type 2 models of diabetic retinopathy. *Am. J. Pathol*. 172 (5), 1411–1418. doi:10.2353/ajpath.2008.071070

Blix, A. (2014). Personalized medicine, genomics, and pharmacogenomics: a primer for nurses. *Clin. J. Oncol. Nurs*. 18 (4), 437–441. doi:10.1188/14.CJON.437-441

Bottós, J., Elizalde, J., Arevalo, J. F., Rodrigues, E. B., and Maia, M. (2012). Vitreomacular traction syndrome. *J. Ophthalmic Vis. Res*. 7 (2), 148–161.

Cacciamani, A., Esposito, G., Scarinci, F., Parravano, M., Dinice, L., Di Nicola, M., et al. (2019). Inflammatory mediators in the vitreal reflux of patients with diabetic macular edema. *Graefes Arch. Clin. Exp. Ophthalmol*. 257 (1), 187–197. doi:10.1007/s00417-018-4169-4

Cacciamani, A., Parravano, M., Scarinci, F., Esposito, G., Varano, M., and Micera, A. (2016). A simple spontaneous vitreal reflux collecting procedure during intravitreal injection: set-up and validation studies. *Curr. Eye Res*. 41 (7), 971–976. doi:10.3109/02713683.2015.1080282

Cehofski, L. J., Honoré, B., and Vorum, H. (2017). A review: proteomics in retinal artery occlusion, retinal vein occlusion, diabetic retinopathy and acquired macular disorders. *Int. J. Mol. Sci*. 18 (5), 907. doi:10.3390/ijms18050907

Chau, K. Y., Sivaprasad, S., Patel, N., Donaldson, T. A., Luthert, P. J., and Chong, N. V. (2008). Plasma levels of matrix metalloproteinase-2 and -9 (MMP-2 and MMP-9) in age-related macular degeneration. *Eye* 22 (6), 855–859.

Cho, E., Hung, S., Willett, W. C., Spiegelman, D., Rimm, E. B., Seddon, J. M., et al. (2001). Prospective study of dietary fat and the risk of age-related macular degeneration. *Am. J. Clin. Nutr*. 73, 209–218. doi:10.1093/ajcn/73.2.209

Christen, W. G., Glynn, R. J., Manson, J. E., Ajani, U. A., and Buring, J. E. (1996). A prospective study of cigarette smoking and risk of age-related macular degeneration in men. *J. Am. Med. Assoc*. 276 (14), 1147–1151. doi:10.1001/jama.1996.03540140035023

Coassin, M., Braconi, L., Sborgia, G., Mangano, G., Mastrofilippo, V., Di Zazzo, A., et al. (2020). One-port vs. three-port diagnostic vitrectomy for posterior segment diseases of unknown origin. *Int. Ophthalmol*. 40, 3217–3222. doi:10.1007/s10792-020-01504-3

Crick, F. (1970). Central dogma of molecular biology. *Nature* 227, 561–563. doi:10.1038/227561a0

Cruickshanks, K. J., Hamman, R. F., Klein, R., Nondahl, D. M., and Shetterly, S. M. (1997). The prevalence of age-related maculopathy by geographic region and ethnicity. The Colorado-Wisconsin Study of Age-Related Maculopathy. *Arch. Ophthalmol*. 115 (2), 242–250. doi:10.1001/archopht.1997.01100150244015

Daiger, S. P., Sullivan, L. S., and Bowne, S. J. (2013). Genes and mutations causing retinitis pigmentosa. *Clin. Genet*. 84, 132. doi:10.1111/cge.12203

Damiani, D., Alexander, J. J., O'Rourke, J. R., McManus, M., Jadhav, A. P., Cepko, C. L., et al. (2008). Dicer inactivation leads to progressive functional and structural degeneration of the mouse retina. *J. Neurosci*. 28 (19), 4878–4887. doi:10.1523/JNEUROSCI.0828-08.2008

Dinice, L., Cacciamani, A., Esposito, G., Taurone, S., Carletti, R., Ripandelli, G., et al. (2020). Osteopontin in vitreous and idiopathic epiretinal membranes. Graefes. *Arch. Clin. Exp. Ophthalmol*, 258 (7), 1503–1513. doi:10.1007/s00417-020-04685-w

Di Zazzo, A., Yang, W., Coassin, M., Micera, A., Antonini, M., Piccinni, F., et al. (2020). Signaling lipids as diagnostic biomarkers for ocular surface cicatrizing conjunctivitis. *J. Mol. Med*. 98 (5), 751–760. doi:10.1007/s00109-020-01907-w

Dias, M. F., Joo, K., Kemp, J. A., Ligório Fialho, S., da Silva Cunha, A., Jr., Woo, S. J., et al. (2018). Molecular genetics and emerging therapies for retinitis pigmentosa: basic research and clinical perspectives. *Prog. Retin. Eye Res*. 63, 107–131. doi:10.1016/j.preteyeres.2017.10.004

Dinarello, C. A. (2009). Immunological and inflammatory functions of the interleukin-1 family. *Annu. Rev. Immunol*. 27, 519–550. doi:10.1146/annurev.immunol.021908.132612

Faber, C., Jehs, T., Juel, H. B., Singh, A., Falk, M. K., Sørensen, T. L., et al. (2015). Early and exudative age-related macular degeneration is associated with increased plasma levels of soluble TNF receptor II. *Acta Ophthalmol*. 93 (3), 242–247. doi:10.1111/aos.12581

Fasching, P., Veitl, M., Rohac, M., Streli, C., Schneider, B., Waldhäusl, W., et al. (1996). Elevated concentrations of circulating adhesion molecules and their association with microvascular complications in insulin-dependent diabetes mellitus. *J. Clin. Endocrinol. Metab*. 81 (12), 4313–4317. doi:10.1210/jcem.81.12.8954033

Friedman, D. S., O'Colmain, B. J., Muñoz, B., Tomany, S. C., McCarty, C., de Jong, P. T., et al. (2004). Prevalence of age-related macular degeneration in the United States. *Arch. Ophthalmol*. 122, 564–572. doi:10.1001/archopht.122.4.564

Fujii, G. Y., De Juan, E., Jr., Humayun, M. S., Pieramici, D. J., Chang, T. S., Awh, C., et al. (2002). A new 25-gauge instrument system for transconjunctival sutureless vitrectomy surgery. *Ophthalmology* 109 (10), 1807–1813. doi:10.1016/s0161-6420(02)01179-x

Gemenetzi, M., and Lotery, A. J. (2020). Epigenetics in age-related macular degeneration: new discoveries and future perspectives. *Cell. Mol. Life Sci*. 77, 807–818. doi:10.1007/s00018-019-03421-w

Guadagni, V., Novelli, E., Piano, I., Gargini, C., and Strettoi, E. (2015). Pharmacological approaches to retinitis pigmentosa: a laboratory perspective. *Prog. Retin. Eye Res*. 48, 62–81. doi:10.1016/j.preteyeres.2015.06.005

Gupta, N., Brown, K. E., and Milam, A. H. (2003). Activated microglia in human retinitis pigmentosa, late-onset retinal degeneration, and age-related macular degeneration. *Exp. Eye Res*. 76 (4), 463–471. doi:10.1016/s0014-4835(02)00332-9

Gurtner, A., Falcone, E., Garibaldi, F., and Piaggio, G. (2016). Dysregulation of microRNA biogenesis in cancer: the impact of mutant p53 on Drosha complex activity. *J. Exp. Clin. Canc. Res*. 35, 45. doi:10.1186/s13046-016-0319-x

Guymer, R. H., Tao, L. W., Goh, J. K., Liew, D., Ischenko, O., Robman, L. D., et al. (2011). Identification of urinary biomarkers for age-related macular degeneration. *Invest. Ophthalmol. Vis. Sci*. 52, 4639–4644. doi:10.1167/iovs.10-7120

Haddad, S., Chen, C. A., Santangelo, S. L., and Seddon, J. M. (2006). The genetics of age-related macular degeneration: a review of progress to date. *Surv. Ophthalmol*. 51 (4), 316–363. doi:10.1016/j.survophthal.2006.05.001

Hamel, C. (2006). Retinitis pigmentosa. *Orphanet J. Rare Dis*. 1, 40. doi:10.1186/1750-1172-1-40

Hayreh, S. S. (2014). Ocular vascular occlusive disorders: natural history of visual outcome. *Prog. Retin. Eye Res*. 41, 1–25. doi:10.1016/j.preteyeres.2014.04.001

He, S., Li, X., Chan, N., and Hinton, D. R. (2013). Review: epigenetic mechanisms in ocular disease. *Mol. Vis*. 19, 665–674.

Heier, J. S., Wykoff, C. C., Waheed, N. K., Kitchens, J. W., Patel, S. S., Vitti, R., et al. (2020). Intravitreal combined aflibercept + anti-platelet-derived growth factor receptor β for neovascular age-related macular degeneration: results of the

phase 2 CAPELLA trial. *Ophthalmology* 127 (2), 211–220. doi:10.1016/j.ophtha.2019.09.021

Hull, S., Arno, G., Plagnol, V., Chamney, S., Russell-Eggitt, I., Thompson, D., et al. (2014). The phenotypic variability of retinal dystrophies associated with mutations in CRX, with report of a novel macular dystrophy phenotype. *Invest. Ophthalmol. Vis. Sci.* 55, 6934–6944. doi:10.1167/iovs.14-14715

Hunter, A., Spechler, P. A., Cwanger, A., Song, Y., Zhang, Z., Ying, G. S., et al. (2012). DNA methylation is associated with altered gene expression in AMD. *Invest. Ophthalmol. Vis. Sci.* 53 (4), 2089–2105. doi:10.1167/iovs.11-8449

Ikeda, Y., Yonemitsu, Y., Kataoka, C., Kitamoto, S., Yamaoka, T., Nishida, K., et al. (2002). Anti-monocyte chemoattractant protein-1 gene therapy attenuates pulmonary hypertension in rats. *Am. J. Physiol. Heart Circ. Physiol.* 283 (5), H2021–H2028. doi:10.1152/ajpheart.00919.2001

Jacqueminet, S., Ben Abdesselam, O., Chapman, M. J., Nicolay, N., Foglietti, M. J., Grimaldi, A., et al. (2006). Elevated circulating levels of matrix metalloproteinase-9 in type 1 diabetic patients with and without retinopathy. *Clin. Chim. Acta* 367 (1-2), 103–107. doi:10.1016/j.cca.2005.11.029

Jafari, M., Ansari-Pour, N., Azimzadeh, S., and Mirzaie, M. (2017). A logic-based dynamic modeling approach to explicate the evolution of the central dogma of molecular biology. *PloS One* 12, e0189922. doi:10.1371/journal.pone.0189922

Jeker, L. T., and Marone, R. (2015). Targeting microRNAs for immunomodulation. *Curr. Opin. Pharmacol.* 23, 25–31. doi:10.1016/j.coph.2015.05.004

Jové, M., Portero-Otín, M., Naudí, A., Ferrer, I., and Pamplona, R. (2014). Metabolomics of human brain aging and age-related neurodegenerative diseases. *J. Neuropathol. Exp. Neurol.* 73 (7), 640–657. doi:10.1097/NEN.0000000000000091

Kado, S., and Nagata, N. (1999). Circulating intercellular adhesion molecule-1, vascular cell adhesion molecule-1, and E-selectin in patients with type 2 diabetes mellitus. *Diabetes Res. Clin. Pract.* 46 (2), 143–148. doi:10.1016/s0168-8227(99)00083-2

Kasi, S. K., Hariprasad, S. M., and Hsu, J. (2017). Making the jump to 27-gauge vitrectomy: perspectives. *Ophthalmic Surg. Lasers Imaging Retina* 48 (6), 450–456. doi:10.3928/23258160-20170601-02

Klein, R., Klein, B. E., and Linton, K. L. (1992). Prevalence of age-related maculopathy. The beaver dam eye study. *Ophthalmology* 99, 933–943. doi:10.1016/s0161-6420(92)31871-8

Kohler, I., Verhoeven, A., Derks, R. J., and Giera, M. (2016). Analytical pitfalls and challenges in clinical metabolomics. *Bioanalysis* 8 (14), 1509–1532. doi:10.4155/bio-2016-0090

Kutsyr, O., Sánchez-Sáez, X., Martínez-Gil, N., de Juan, E., Lax, P., Maneu, V., et al. (2020). Gradual increase in environmental light intensity induces oxidative stress and inflammation and accelerates retinal neurodegeneration. *Invest. Ophthalmol. Vis. Sci.* 61 (10), 1. doi:10.1167/iovs.61.10.1

Laíns, I., Gantner, M., Murinello, S., Lasky-Su, J. A., Miller, J. W., Friedlander, M., et al. (2019). Metabolomics in the study of retinal health and disease. *Prog. Retin. Eye Res.* 69, 57–79. doi:10.1016/j.preteyeres.2018.11.002

Lanza, M., Benincasa, G., Costa, D., and Napoli, C. (2019). Clinical role of epigenetics and network analysis in eye diseases: a translational science review. *J. Ophthalmol.* 2019, 2424956. doi:10.1155/2019/2424956

Laurenti, O., Vingolo, E. M., Desideri, G. B., Ferri, C., Bellini, C., Cassone-Faldetta, M., et al. (1997). Increased levels of plasma endothelin-1 in non-insulin dependent diabetic patients with retinopathy but without other diabetes-related organ damage. *Exp. Clin. Endocrinol. Diabetes* 105 (Suppl. 2), 40–42. doi:10.1055/s-0029-1211795

Lee, I. G., Chae, S. L., and Kim, J. C. (2006). Involvement of circulating endothelial progenitor cells and vasculogenic factors in the pathogenesis of diabetic retinopathy. *Eye* 20 (59), 546–552. doi:10.1038/sj.eye.6701920

Lee, S. W. L., Paoletti, C., Campisi, M., Osaki, T., Adriani, G., Kamm, R. D., et al. (2019). MicroRNA delivery through nanoparticles. *J. Contr. Release* 313, 80–95. doi:10.1016/j.jconrel.2019.10.007

Li, Y., Xia, X., and Paulus, Y. M. (2018). Advances in retinal optical imaging. *Photonics* 5 (2), 9. doi:10.3390/photonics5020009

Liu, C. H., Huang, S., Britton, W. R., and Chen, J. (2020). MicroRNAs in vascular eye diseases. *Int. J. Mol. Sci.* 21 (2), 649. doi:10.3390/ijms21020649.

Liu, M. M., Chan, C. C., and Tuo, J. (2012). Genetic mechanisms and age-related macular degeneration: common variants, rare variants, copy number variations, epigenetics, and mitochondrial genetics. *Hum. Genom.* 6 (1), 13. doi:10.1186/1479-7364-6-13

Machalińska, A., Safranow, K., Dziedziejko, V., Mozolewska-Piotrowska, K., Paczkowska, E., Klos, P., et al. (2011). Different populations of circulating endothelial cells in patients with age-related macular degeneration: a novel insight into pathogenesis. *Invest. Ophthalmol. Vis. Sci.* 52 (1), 93–100. doi:10.1167/iovs.10-5756

Machalińska, A., Safranow, K., Mozolewska-Piotrowska, K., Dziedziejko, V., and Karczewicz, D. (2012). PEDF and VEGF plasma level alterations in patients with dry form of age-related degeneration--A possible link to the development of the disease. *Klin. Oczna.* 114 (2), 115–120.

Marrocco, I., Altieri, F., and Peluso, I. (2017). Measurement and clinical significance of biomarkers of oxidative stress in humans. *Oxid. Med. Cell Longev.* 2017, 6501046. doi:10.1155/2017/6501046

Martins, B., Amorim, M., Reis, F., Ambrósio, A. F., and Fernandes, R. (2020). Extracellular vesicles and MicroRNA: putative role in diagnosis and treatment of diabetic retinopathy. *Antioxidants* 9 (8), 705. doi:10.3390/antiox9080705

Minami, S., Shinoda, H., Shigeno, Y., Nagai, N., Kurihara, T., Watanabe, K., et al. (2019). Effect of axial length and age on the visual outcome of patients with idiopathic epiretinal membrane after pars plana vitrectomy. *Sci. Rep.* 9 (1), 19056. doi:10.1038/s41598-019-55544-6

Minghetti, L., Ajmone-Cat, M. A., De Berardinis, M. A., and De Simone, R. (2005). Microglial activation in chronic neurodegenerative diseases: roles of apoptotic neurons and chronic stimulation. *Brain Res. Brain Res. Rev.* 48 (2), 251–256. doi:10.1016/j.brainresrev.2004.12.015

Mitchell, P., Liew, G., Gopinath, B., and Wong, T. Y. (2018). Age-related macular degeneration. *Lancet* 392 (10153), 1147–1159. doi:10.1016/S0140-6736(18)31550-2

Miteva, Y. V., Budayeva, H. G., and Cristea, I. M. (2013). Proteomics-based methods for discovery, quantification, and validation of protein-protein interactions. *Anal. Chem.* 85 (2), 749–768. doi:10.1021/ac3033257

Nakazawa, T., Hisatomi, T., Nakazawa, C., Noda, K., Maruyama, K., She, H., et al. (2007). Monocyte chemoattractant protein 1 mediates retinal detachment-induced photoreceptor apoptosis. *Proc. Natl. Acad. Sci. U.S.A.* 104 (7), 2425–2430. doi:10.1073/pnas.0608167104

Nassar, K., Grisanti, S., Elfar, E., Lüke, J., Lüke, M., and Grisanti, S. (2015). Serum cytokines as biomarkers for age-related macular degeneration. *Graefes Arch. Clin. Exp. Ophthalmol.* 253 (5), 699–704. doi:10.1007/s00417-014-2738-8

Nath, M., Halder, N., and Velpandian, T. (2017). Circulating biomarkers in glaucoma, age-related macular degeneration, and diabetic retinopathy. *Indian J. Ophthalmol.* 65 (3), 191–197. doi:10.4103/ijo.IJO_866_16

Nicholson, J., Holmes, E., Kinross, J. M., Darzi, A. W., Takats, Z., and Lindon, J. C. (2012). Metabolic phenotyping in clinical and surgical environments. *Nature* 491 (7424), 384–392. doi:10.1038/nature11708

Oh, H., and Oshima, Y. (2014). Microincision vitrectomy surgery. Emerging techniques and technology. *Dev. Ophthalmol.* 54, 54–62. doi:10.1159/isbn.978-3-318-02661-0

Ohnaka, M., Miki, K., Gong, Y. Y., Stevens, R., Iwase, T., Hackett, S. F., et al. (2012). Long-term expression of glial cell line-derived neurotrophic factor slows, but does not stop retinal degeneration in a model of retinitis pigmentosa. *J. Neurochem.* 122 (5), 1047–1053. doi:10.1111/j.1471-4159.2012.07842.x

Ong, F. S., Kuo, J. Z., Wu, W. C., Cheng, C. Y., Blackwell, W. L., Taylor, B. L., et al. (2013). Personalized medicine in ophthalmology: from pharmacogenetic biomarkers to therapeutic and dosage optimization. *J. Personalized Med.* 3 (1), 40–69. doi:10.3390/jpm3010040

Pan, H. Z., Zhang, H., Chang, D., Li, H., and Sui, H. (2008). The change of oxidative stress products in diabetes mellitus and diabetic retinopathy. *Br. J. Ophthalmol.* 92 (4), 548–551. doi:10.1136/bjo.2007.130542

Paskowitz, D. M., LaVail, M. M., and Duncan, J. L. (2006). Light and inherited retinal degeneration. *Br. J. Ophthalmol.* 90, 1060. doi:10.1136/bjo.2006.097436

Patti, G. J., Yanes, O., and Siuzdak, G. (2012). Innovation: metabolomics: the apogee of the omics trilogy. *Nat. Rev. Mol. Cell Biol.* 13 (4), 263–269. doi:10.1038/nrm3314

Pfeiffer, A., Middelberg-Bisping, K., Drewes, C., and Schatz, H. (1996). Elevated plasma levels of transforming growth factor-beta 1 in NIDDM. *Diabetes Care* 19 (10), 1113–1117. doi:10.2337/diacare.19.10.1113

Platania, C. B. M., Maisto, R., Trotta, M., D'Amico, M., Rossi, S., Gesualdo, C., et al. (2019). Retinal and circulating miRNA expression patterns in diabetic retinopathy: an in silico and *in vivo* approach. *Br. J. Pharmacol.* 176 (13), 2179–2194. doi:10.1111/bph.14665

Ristori, M. V., Mortera, S. L., Marzano, V., Guerrera, S., Vernocchi, P., Ianiro, G., et al. (2020). Proteomics and metabolomics approaches towards a functional insight onto AUTISM spectrum disorders: phenotype stratification and biomarker discovery. *Int. J. Mol. Sci.* 21 (17), 6274. doi:10.3390/ijms21176274

Rocco, M. L., Balzamino, B. O., Esposito, G., Petrella, C., Aloe, L., and Micera, A. (2017). NGF/anti-VEGF combined exposure protects RCS retinal cells and photoreceptors that underwent a local worsening of inflammation. *Graefes Arch. Clin. Exp. Ophthalmol.* 255 (3), 567–574. doi:10.1007/s00417-016-3567-8

Roesch, K., Stadler, M. B., and Cepko, C. L. (2012). Gene expression changes within Müller glial cells in retinitis pigmentosa. *Mol. Vis.* 18, 1197.

Russo, A., Ragusa, M., Barbagallo, C., Longo, A., Avitabile, T., Uva, M. G., et al. (2017). miRNAs in the vitreous humor of patients affected by idiopathic epiretinal membrane and macular hole. *PloS One* 12 (3), e0174297. doi:10.1371/journal.pone.0174297

Sacca, S. C., Bolognesi, C., Battistella, A., Bagnis, A., and Izzotti, A. (2009). Gene-environment interactions in ocular diseases. *Mutat. Res.* 667 (1-2), 98–117. doi:10.1016/j.mrfmmm.2008.11.002

Sancho-Pelluz, J., Alavi, M. V., Sahaboglu, A., Kustermann, S., Farinelli, P., Azadi, S., et al. (2010). Excessive HDAC activation is critical for neurodegeneration in the rd1 mouse. *Cell Death Dis.* 1 (2), e24. doi:10.1038/cddis.2010.4

Schram, M. T., Chaturvedi, N., Schalkwijk, C. G., Fuller, J. H., and Stehouwer, C. D. (2005). EURODIAB prospective complications study groupmarkers of inflammation are cross-sectionally associated with microvascular complications and cardiovascular disease in type 1 diabetes–the EURODIAB prospective complications study. *Diabetologia* 48, 370–378. doi:10.1007/s00125-004-1628-8

Seddon, J. M., and Chen, C. (2004). The Epidemiology of age-related macular degeneration. *Int. Ophthalmol. Clin.* 44 (4), 17–39. doi:10.1097/00004397-200404440-00004

Seddon, J. M., Cote, J., Davis, N., and Rosner, B. (2003). Progression of age-related macular degeneration: association with body mass index, waist circumference, and waist-hip ratio. *Arch. Ophthalmol.* 121 (6), 785–792. doi:10.1001/archopht.121.6.785

Seddon, J. M., Willett, W. C., Speizer, F. E., and Hankinson, S. E. (1996). A prospective study of cigarette smoking and age-related macular degeneration in women. *J. Am. Med. Assoc.* 276 (14), 1141–1146.

Seddon, J. M. (2013). Genetic and environmental underpinnings to age-related ocular diseases. *Invest. Ophthalmol. Vis. Sci.* 54 (14), 28–30. doi:10.1167/iovs.13-13234

Semba, R. D., Enghild, J. J., Venkatraman, V., Dyrlund, T. F., and Van Eyk, J. E. (2013). The human eye proteome project: perspectives on an emerging proteome. *Proteomics* 13 (16), 2500–2511. doi:10.1002/pmic.201300075

Sharma, S., Purohit, S., Sharma, A., Hopkins, D., Steed, L., Bode, B., et al. (2015). Elevated serum levels of soluble TNF receptors and adhesion molecules are associated with diabetic retinopathy in patients with type-1 diabetes. *Mediat. Inflamm.* 2015, 279393. doi:10.1155/2015/279393

Sivilia, S., Giuliani, A., Fernández, M., Turba, M. E., Forni, M., Massella, A., et al. (2009). Intravitreal NGF administration counteracts retina degeneration after permanent carotid artery occlusion in rat. *BMC Neurosci.* 10, 52. doi:10.1186/1471-2202-10-52

Sommer, A., Tielsch, J. M., Katz, J., Quigley, H. A., Gottsch, J. D., Javitt, J. C., et al. (1991). Racial differences in the cause-specific prevalence of blindness in east Baltimore. *N. Engl. J. Med.* 325 (20), 1412–1417. doi:10.1056/NEJM199111143252004

Spaide, R. F., Fujimoto, J. G., Waheed, N. K., Sadda, S. R., and Staurenghi, G. (2018). Optical coherence tomography angiography. *Prog. Retin. Eye Res.* 64, 1–55. doi:10.1016/j.preteyeres.2017.11.003

Sposato, V., Bucci, M. G., Coassin, M., Russo, M. A., Lambiase, A., and Aloe, L. (2008). Reduced NGF level and TrkA protein and TrkA gene expression in the optic nerve of rats with experimentally induced glaucoma. *Neurosci. Lett.* 446 (1), 20–24. doi:10.1016/j.neulet.2008.09.024

Stevenson, W., Prospero Ponce, C. M., Agarwal, D. R., Gelman, R., and Christoforidis, J. B. (2016). Epiretinal membrane: optical coherence tomography-based diagnosis and classification. *Clin. Ophthalmol.* 10, 527–534. doi:10.2147/OPTH.S97722

Stitt, A. W., Curtis, T. M., Chen, M., Medina, R. J., McKay, G. J., Jenkins, A., et al. (2016). The progress in understanding and treatment of diabetic retinopathy. *Prog. Retin. Eye Res.* 51, 156–186. doi:10.1016/j.preteyeres.2015.08.001

Straatsma, B. R. (2018). Precision medicine and clinical ophthalmology. *Indian J. Ophthalmol.* 66 (10), 1389–1390. doi:10.4103/ijo.IJO_1459_18

Strimbu, K., and Tavel, J. A. (2010). What are biomarkers? *Curr. Opin. HIV AIDS.* 5 (6), 463–466. doi:10.1097/COH.0b013e32833ed177

Suuronen, T., Nuutinen, T., Ryhänen, T., Kaarniranta, K., and Salminen, A. (2007). Epigenetic regulation of clusterin/apolipoprotein J expression in retinal pigment epithelial cells. *Biochem. Biophys. Res. Commun.* 357 (2), 397–401. doi:10.1016/j.bbrc.2007.03.135

Totan, Y., Koca, C., Erdurmuş, M., Keskin, U., and Yiğitoğlu, R. (2015). Endothelin-1 and nitric Oxide levels in exudative age-related macular degeneration. *J. Ophthalmic Vis. Res.* 10 (2), 151–154. doi:10.4103/2008-322X.163765

Unsal, E., Cubuk, M. O., and Ciftci, F. (2019). Preoperative prognostic factors for macular hole surgery: which is better? *Oman J. Ophthalmol.* 12 (1), 20–24. doi:10.4103/ojo.OJO_247_2017

van Soest, S., Westerveld, A., de Jong, P. T., Bleeker-Wagemakers, E. M., and Bergen, A. A. (1999). Retinitis pigmentosa: defined from a molecular point of view. *Surv. Ophthalmol.* 43, 321–334. doi:10.1016/s0039-6257(98)00046-0

Velez, G., Tang, P. H., Cabral, T., Cho, G. Y., Machlab, D. A., Tsang, S. H., et al. (2018). Personalized proteomics for precision health: identifying biomarkers of vitreoretinal disease. *Transl. Vis. Sci. Tech.* 7, 12. doi:10.1167/tvst.7.5.12

Villeneuve, L. M., and Natarajan, R. (2010). The role of epigenetics in the pathology of diabetic complications. *Am. J. Physiol. Ren. Physiol.* 299 (1), F14–F25. doi:10.1152/ajprenal.00200.2010

Wang, S., Koster, K. M., He, Y., and Zhou, Q. (2012). miRNAs as potential therapeutic targets for age-related macular degeneration. *Future Med. Chem.* 4 (3), 277–287. doi:10.4155/fmc.11.176

Waters, A. M., and Beales, P. L. (2011). Ciliopathies: an expanding disease spectrum. *Pediatr. Nephrol.* 26, 1039–1056. doi:10.1007/s00467-010-1731-7

Wheway, G., Parry, D. A., and Johnson, C. A. (2014). The role of primary cilia in the development and disease of the retina. *Organogenesis* 10, 69–85. doi:10.4161/org.26710

Yoshida, N., Ikeda, Y., Notomi, S., Ishikawa, K., Murakami, Y., Hisatomi, T., et al. (2013). Laboratory evidence of sustained chronic inflammatory reaction in retinitis pigmentosa. *Ophthalmology* 120 (1), 5–12. doi:10.1016/j.ophtha.2012.07.008

Zhang, P., Dufresne, C., Turner, R., Ferri, S., Venkatraman, V., Karani, R., et al. (2015). The proteome of human retina. *Proteomics* 15 (4), 836–840. doi:10.1002/pmic.201400397

Zhong, Q., and Kowluru, R. A. (2013). Epigenetic modification of Sod2 in the development of diabetic retinopathy and in the metabolic memory: role of histone methylation. *Invest. Ophthalmol. Vis. Sci.* 54 (1), 244–250. doi:10.1167/iovs.12-10854

Zhong, Q., and Kowluru, R. A. (2010). Role of histone acetylation in the development of diabetic retinopathy and the metabolic memory phenomenon. *J. Cell. Biochem.* 110 (6), 1306–1313. doi:10.1002/jcb.22644

Conflict of Interest: The authors declare that the research was conducted in the absence of any commercial or financial relationships that could be construed as a potential conflict of interest.

frontiers in Pharmacology

ORIGINAL RESEARCH
published: 29 January 2021
doi: 10.3389/fphar.2020.617836

Leukocyte Integrin Antagonists as a Novel Option to Treat Dry Age-Related Macular Degeneration

*Monica Baiula[1], Alberto Caligiana[1], Andrea Bedini[1], Junwei Zhao[2], Federica Santino[2], Martina Cirillo[3], Luca Gentilucci[2], Daria Giacomini[3] and Santi Spampinato[1,4]**

[1]Laboratory of Cellular and Molecular Pharmacology, Department of Pharmacy and Biotechnology, University of Bologna, Bologna, Italy, [2]Department of Chemistry "G. Ciamician", University of Bologna, Bologna, Italy, [3]Laboratory of Design and Synthesis of Biologically Active Compounds, Department of Chemistry "G. Ciamician", University of Bologna, Bologna, Italy, [4]Specilization School of Hospital Pharmacy, Department of Pharmacy and Biotechnology, University of Bologna, Bologna, Italy

Age-related macular degeneration (AMD) is a complex multifactorial degenerative disease that leads to irreversible blindness. AMD affects the macula, the central part of the retina responsible for sharp central vision. Retinal pigment epithelium (RPE) is the main cellular type affected in dry AMD. RPE cells form a monolayer between the choroid and the neuroretina and are in close functional relationship with photoreceptors; moreover, RPE cells are part of the blood retina barrier that is disrupted in ocular diseases such as AMD. During ocular inflammation lymphocytes and macrophages are recruited, contact RPE and produce pro-inflammatory cytokines, which play an important role in AMD pathogenesis. The interaction between RPE and immune cells is mediated by leukocyte integrins, heterodimeric transmembrane receptors, and adhesion molecules, including VCAM-1 and ICAM-1. Within this frame, this study aimed to characterize RPE-leukocytes interaction and to investigate any potentially beneficial effects induced by integrin antagonists (DS-70, MN27 and SR714), developed in previous studies. ARPE-19 cells were co-cultured for different incubation times with Jurkat cells and apoptosis and necrosis levels were analyzed by flow cytometry. Moreover, we measured the mRNA levels of the pro-inflammatory cytokine IL-1β and the expression of adhesion molecules VCAM-1 and ICAM-1. We found that RPE-lymphocyte interaction increased apoptosis and necrosis levels in RPE cells and the expression of IL-1β. This interaction was mediated by the binding of $\alpha_4\beta_1$ and $\alpha_L\beta_2$ integrins to VCAM-1 and ICAM-1, respectively. The blockade of RPE-lymphocyte interaction with blocking antibodies highlighted the pivotal role played by integrins. Therefore, $\alpha_4\beta_1$ and $\alpha_L\beta_2$ integrin antagonists were employed to disrupt RPE-lymphocyte crosstalk. Small molecule integrin antagonists proved to be effective in reducing RPE cell death and expression of IL-1β, demonstrating that integrin antagonists could protect RPE cells from detrimental effects induced by the interaction with immune cells recruited to the retina. Overall, the leukocyte integrin antagonists employed in the present study may represent a novel opportunity to develop new drugs to fight dry AMD.

Keywords: age-related macular degeneration, retinal pigment epithelium cells, leukocyte integrins, inflammation, integrin antagonist, immune cells

OPEN ACCESS

Edited by:
Michele D'Amico, University of Campania Luigi Vanvitelli, Italy

Reviewed by:
Thomas Ach, University Hospital Bonn, Germany
Suet-Mien Tan, Nanyang Technological University, Singapore

****Correspondence:***
Santi Spampinato
santi.spampinato@unibo.it

Specialty section:
This article was submitted to Inflammation Pharmacology, a section of the journal Frontiers in Pharmacology

Received: *15 October 2020*
Accepted: *30 December 2020*
Published: *29 January 2021*

Citation:
Baiula M, Caligiana A, Bedini A, Zhao J, Santino F, Cirillo M, Gentilucci L, Giacomini D and Spampinato S (2021) Leukocyte Integrin Antagonists as a Novel Option to Treat Dry Age-Related Macular Degeneration. Front. Pharmacol. 11:617836. doi: 10.3389/fphar.2020.617836

INTRODUCTION

Age-related macular degeneration (AMD) is a progressive degenerative disease that leads to irreversible blindness in elderly people (Akyol and Lotery, 2020). AMD affects the macula, the ocular region responsible for sharp central vision. Two forms of AMD have been described: dry AMD is the most common type of the disease and causes atrophic degeneration of the macula leading to gradual vision loss (advanced AMD or geographic atrophy). On the contrary, wet AMD is characterized by choroidal neovascularization (CNV) that rapidly causes blindness (Ambati and Fowler, 2012). Since vascular endothelial growth factor (VEGF) is a predominant proangiogenic factor in CNV, wet AMD can be treated with intravitreous administration of anti-angiogenic agents such as aflibercept and ranibizumab (Supuran, 2019). Conversely, there is currently no effective pharmacological treatment for "dry" AMD although novel therapeutic strategies are under development (Akyol and Lotery, 2020). The pathogenesis of dry AMD is not completely understood and involves a complex interplay among several mechanisms. Oxidative stress, together with other factors, including aging, genetic factors, phototoxicity, complement system activation, can lead to retinal pigment epithelium (RPE) degeneration and photoreceptors death, and can raise in immune response and inflammation (Strauss, 2005; Hanus et al., 2015). RPE is a monolayer of cells embedded between the choroid and the neuroretina. Normal physiological functions of RPE cells are important for outer retina homeostasis and for normal vision. One of the late events in AMD pathogenesis is RPE cell death, associated with the degradation of the overlying photoreceptors and the underlying choriocapillaris (Van Lookeren Campagne et al., 2014). In addition, RPE is a component of the blood-retina barrier (BRB) limiting the penetration of blood components to the retina and is also implicated in the recruitment of immune cells during local inflammation. During ocular inflammatory process lymphocytes and macrophages are recruited to the posterior compartment of the eye and produce pro-inflammatory cytokines, including tumor necrosis factor α (TNFα), interleukin-1β (IL-1β) and IL-6 (Cousins et al., 2004), which play an important role in AMD pathogenesis. Adhesion molecules, such as intercellular adhesion molecules-1 (ICAM-1) and vascular cell adhesion molecule-1 (VCAM-1) mediate leukocyte adhesion and recruitment to RPE. Cultured RPE cells constitutively express ICAM-1 but not VCAM-1; both adhesion molecules are upregulated after treatment with pro-inflammatory cytokines (Platts et al., 1995). Adhesion molecules are physiological ligands of integrins, heterodimeric transmembrane proteins formed by non-covalent association of α and β subunit (Tolomelli et al., 2017; Baiula et al., 2019). Notably, leukocyte integrins, including $\alpha_4\beta_1$ and $\alpha_L\beta_2$, mediate immune cell recruitment to inflamed tissue. Some agents targeting integrins have already been approved for clinical practice (Raab-Westphal et al., 2017) and several new ligands are presently under development.

Within this frame, in previous studies, we investigated new ligands targeting different types of integrin (De Marco et al., 2015; Tolomelli et al., 2015; Baiula et al., 2016; Baiula et al., 2020; Dattoli et al., 2018; Martelli et al., 2019). In particular, we identified MN27, SR714, and DS-70 as potent and selective leukocyte integrin antagonists able to significantly reduce integrin-mediated cell adhesion and intracellular signaling activation in a concentration-dependent manner (Baiula et al., 2016; Dattoli et al., 2018). Therefore, considering integrins as a valuable drug target, the current study was designed to elucidate the crosstalk between RPE and leukocytes *in vitro* and to characterize any potentially beneficial effects induced by integrin antagonists within this frame. To this purpose ARPE-19 cells were co-cultured with immune cells for different time points and we analyzed apoptosis and necrosis levels, adhesion molecule expression, integrin-mediated cell adhesion, intracellular signaling activation and IL-1β expression. Moreover, we investigated the effects of integrin antagonists on RPE-leukocytes interaction. We found that integrin antagonists were able to disrupt RPE-immune cell interaction leading to reduced RPE cell death. Therefore, our results open up the possibility to exploit integrin antagonists as innovative therapeutics to fight dry AMD.

MATERIALS AND METHODS

Cell Culture and Treatments

ARPE-19 cells (American Type Culture Collection, ATCC, Rockville, MD; passages 4–7), a human spontaneously arising retinal pigment epithelia cell line, were grown in Dulbecco's modified Eagle's medium and Ham's F12 medium (DMEM/F12, Life Technologies, Monza, Italy) supplemented with 10% fetal bovine serum (FBS, Life Technologies) and antibiotic-antimycotic solution (Life Technologies). Jurkat E6.1 cells (ATCC; passages 5–10) were cultured in RPMI 1640 (Life Technologies) supplemented with 2 mM glutamine, 10% FBS and antibiotic-antimycotic solution. Cells were cultured at 37°C under 5% CO_2 humidified atmosphere.

To study ARPE-19-Jurkat cells interactions, ARPE-19 cells were seeded in 6-well plates and cultured until monolayers were formed. Then, Jurkat cells (10^6 cells/well) were added and co-cultured with ARPE-19 cells for different incubation periods (1, 16, 24 and 48 hours). ARPE-19-Jurkat co-culture were performed in the presence of 1 mM Mn^{2+} to ensure integrin activation and high affinity ligand binding. At the end of the co-culture, immune cells were removed by washing the wells three times with PBS (phosphate buffered saline, Life Technologies) and ARPE-19 cells were detached with Trypsin/EDTA 1% solution (Lonza). Finally, cells were centrifuged separately and pelleted to be stored at -80° for further analyses.

Neutralizing antibodies anti-VCAM-1 (clone 51-10C9, cat. n.555645) or anti-ICAM-1 (clone LB-2, cat. n.559047) (both from BD Pharmingen™) were added to ARPE-19 cells at saturation concentration (10 μg/mL) for one hour before the addition of Jurkat cells; alternatively, Jurkat cells were pre-incubated with anti-α_4 integrin (10 μg/mL, clone 44H6, cat. n. ab220, Abcam) or anti-α_L (clone HI111, cat. n.555381, BD Pharmingen) for 1 h before being overlaid on ARPE-19 cells. Thereafter, the co-culture

TABLE 1 | Solid-phase, SPA binding and inhibition of cell adhesion of integrin antagonists MN27, DS-70 and SR714 to VCAM-1 or ICAM-1 (2 μg/mL) (Baiula et al., 2016; Dattoli et al., 2018).

Integrin antagonists	Solid-phase binding/SPA[a] IC_{50} (nM)	Cell adhesion[b] Jurkat, $\alpha_4\beta_1$/VCAM-1 IC_{50} (nM)	Cell adhesion[b] Jurkat, $\alpha_L\beta_2$/ICAM-1 IC_{50} (nM)
MN27 ($\alpha_L\beta_2$)	6.7 ± 2.5 ($\alpha_L\beta_2$)	574.0 ± 1.7	0.39 ± 0.02
DS-70 ($\alpha_4\beta_1$)	8.3 ± 3.2 ($\alpha_4\beta_1$)	5.04 ± 0.51	>5000
SR714 ($\alpha_4\beta_1$)	1.1 ± 0.1 ($\alpha_4\beta_1$)	1.39 ± 0.04	>5000

[a]IC_{50} values of β-lactam compounds and DS-70 on leukocyte integrins determined by a competitive solid-phase binding assay to specific ligand (ICAM-1 for $\alpha_L\beta_2$) or by scintillation proximity assay (SPA, FN for $\alpha_4\beta_1$). Six independent experiments were run in quadruplicate. Data are expressed as means ± SD (Baiula et al., 2016; Dattoli et al., 2018).
[b]In a cell-based assay, the adhesion of a cell line preferentially expressing a specific integrin heterodimer to an immobilized adhesion molecule was measured. Six independent experiments were run in quadruplicate. Data are expressed as means ± SD (Baiula et al., 2016; Dattoli et al., 2018).

was extended for 24 hours. Cells were collected separately and stored as above described.

Integrin antagonists employed in this study have been previously investigated (Baiula et al., 2016; Dattoli et al., 2018). These compounds had displayed a strong antagonist activity against $\alpha_L\beta_2$ (MN27) or $\alpha_4\beta_1$ (DS-70 and SR714) integrins (**Table 1**). A stock solution (10^{-2} M) of integrin antagonists was prepared in dimethyl sulfoxide (DMSO, vehicle) and its final concentration did not exceed 0.1%; an equal volume of vehicle was added as control to vehicle cells. Cells were pre-incubated with different concentrations (1–100 nM) of integrin antagonists for 30 min at 37°C before adding Jurkat to ARPE-19 cells for 24 hours.

Adhesion Assay

ARPE-19 cells were plated in black 96-well plates (15000 well) and grown for 24–48 h. ARPE-19 cells were pretreated with or without anti-ICAM-1 or anti-VCAM-1 antibodies (10 μg/mL) for 1 h. Jurkat cells (50000 cells/well) were labelled with Cell Tracker green CMFDA (12.5 μM, 30 min at 37°C, Life Technologies) and, after three washes with PBS, were overlaid on ARPE-19 cells; the cells were incubated at 37°C for 3 h. Then, after three gently washes with PBS to remove nonadherent Jurkat cells, the remaining cells were lysed with 0.5% Triton X-100 in PBS (for 30 min at 4°C). The number of fluorescently labeled adherent Jurkat cells was determined measuring fluorescence (Ex485 nm/Em535 nm) in an EnSpire Multimode Plate Reader (PerkinElmer, Waltham, MA, USA). The number of adherent cells was determined by comparison with a standard curve built up in the same plate with known numbers of labelled Jurkat cells. To investigate the role of integrins in ARPE-19-Jurkat interactions, Jurkat cells were pre-incubated with 10 μg/mL of anti-$\alpha_4\beta_1$ integrin or anti-α_L antibody for 1 h. In another set of experiment, Jurkat cells were exposed to increasing concentrations (1–100 nM) of integrin antagonists (DS-70, MN27 or SR714) for specified times.

Apoptosis Detection

Apoptosis was analyzed by flow cytometry as previously described (Baiula et al., 2016; Dattoli et al., 2018). Phycoerythrin-conjugated annexin V (annexin V-PE) and 7-amino-actynomicin D (7-AAD; Guava Nexin Reagent, Millipore, Darmstadt, Germany) were employed to determine the percentage of viable, early apoptotic and late apoptotic/necrotic cells by flow cytometry. ARPE-19 and Jurkat cells were co-cultured for different time points and then cells were collected separately by centrifugation and resuspended in 100 μL of complete medium. For apoptosis/necrosis staining, 100 μL of Nexin reagent were added and ARPE-19 and Jurkat cells were incubated for 20 min at room temperature in the dark, following manufacturer's instructions. Thereafter, cells were analyzed on a Guava EasyCyte 5 flow cytometer (Millipore); at least 10000 cells/sample were acquired. Three populations of cells can be identified by this assay: viable cells (annexin V-PE and 7-AAD negative), early apoptotic cells (annexin V-PE positive and 7-AAD negative), and late stage apoptosis or necrotic cells (annexin V-PE and 7-AAD positive).

Flow Cytometry

To evaluate expression of integrins and adhesion molecules on ARPE-19 cells, anti-ICAM-1, anti-VCAM-1, anti-α_5 (clone VC5, cat. n.555651, BD Pharmingen), anti-α_M (clone M1/70, cat. n. MAB1387Z, Chemicon International), anti-α_L (clone HI111, cat. n.555381, BD Pharmingen), anti-β_1 (clone HUTS-21, cat. n. 556049, BD Pharmingen), anti-β_2 (clone 6.7, cat. n. 555923, BD Pharmingen), or anti-α_4 monoclonal antibody (cat. n. ab202969, Abcam), were used in 1% BSA/HBSS (Hanks' Balanced Salt Solution, Life Technologies) for 45 min at 4°C. After two washes in 1% BSA/HBSS cells were incubated with goat anti-rabbit IgG (H + L) secondary antibody, Alexa Fluor 488 in 1% BSA/HBSS (Life Technologies) for 45 min at 4°C. After two washes with 1% BSA/HBSS, cells were resuspended in PBS and analyzed at Guava® EasyCyte™ flow cytometer (Millipore) and at least 10000 cells/sample were analyzed. Evaluation of the relative fluorescence for nonspecific binding by exposing the cells to an isotype control monoclonal antibody FITC mouse IgG (BD Pharmingen) was done for data normalization (Dattoli et al., 2018).

Real Time RT-PCR

At the end of the co-culture, ARPE-19 and Jurkat cells were collected separately as described above and centrifuged (500 g for 5 min). PD 98059 (10 μM, 30 min; Sigma Aldrich), a non-competitive blocker of ERK1/2 activation (Di Toro et al., 2005; Baiula et al., 2012) was used to investigate the role of integrin-mediated ERK1/2 signaling. Total cellular RNA was extracted with Trireagent® (Sigma-Aldrich, Milan, Italy) and digested with Rnase-free Dnase (Thermo Fisher Scientific, Walthman, MA,

USA) for 15 min at 25°C. High Capacity cDNA reverse transcription kit (Life Technologies) was used to reverse transcribe a 2-μg sample, according to the manufacturer's instructions. Relative quantification of human IL-1β transcripts was performed by Real-Time PCR using the StepOne Instrument (Life Technologies). The GoTaq® qPCR master mix (Promega, Madison, Wisconsin, USA) was chosen to perform the reaction as follow: denaturation at 95°C for 10 min, followed by 40 cycles of 95°C for 30 sec, 68°C for 30 sec and 72°C for 30 sec. To amplify human IL-1β cDNA, a sense primer (5′-CAAGGGCTTCAG GCAGGCCG-3′) and an antisense primer (5′-TGAGTCCCG GAGCGTGCAGT-3′) were used at 0.25 μM concentration for producing a 213-bp fragment (261–474 bp; GenBank Accession no. NM_000576.2). As a control, a 169-bp fragment of the human L19 ribosomal protein gene (62–230 bp; GenBank Accession No. BC062709) was amplified with a sense primer (5′-CTAGTGTCC TCCGCTGTGG-3′) and an antisense primer (5′-AAGGTGTTT TTCCGGCATC-3′) at 0.25 μM concentration (Bedini et al., 2017). No-template controls and DNA melting curve analysis were employed as controls. Relative expression of RT-PCR products was determined using the $\Delta\Delta C_t$ method (Winer et al., 1999). Each sample was run in triplicate and L19 was chosen for normalization because of its consistent expression relative to other housekeeping genes among the experimental groups in our study.

Western Blot Analysis

Western blot analysis was performed as previously described (Dattoli et al., 2018) with the following modifications. Briefly, ARPE-19 cells were plated into 60 mm dishes until a confluence of 80–90% was reached; the cells were incubated with Jurkat cells (10^6 cells/well) as described in a previous section. Thereafter, the cells were homogenized in lysis buffer (50 mM Tris-HCl, 300 mM NaCl, 1 mM EDTA, 1 mM Na_3VO_4, 1 mM NaF, 10% glycerol, 1% Triton-X 100) supplemented with phosphatase inhibitor and protease inhibitor cocktail (both 1:100, Sigma-Aldrich SRL). The homogenates were sonicated for 10 sec and then centrifuged at 17000 g for 25 minutes at 4°C; protein concentration was determined by BCA assay (Pierce, Rockford, IL, USA). Protein extracts (15 μg) were denatured at 95°C for 3 min and separated by 12% SDS-PAGE. The membranes were blocked in 5% BSA in TBS-T (20 mM Tris-HCl, pH 7.5, 137 mM NaCl, 0.1 (v/v) % Tween 20) for 1 h and incubated with anti-phospho-ERK 1/2 (extracellular signal-regulated kinase 1/2, 1:1000; Cell Signaling Technology, Danvers, MA, USA) or anti-total ERK1/2 antibodies (1:1000; Cell Signaling Technology) overnight at 4°C. Subsequently, the membranes were incubated with peroxidase-conjugated anti-rabbit secondary antibodies at a 1:8000 dilution (Santa Cruz Biotechnology, Dallas, Texas, USA) at room temperature for 1.5 h. Digital images were acquired and analyzed according to a previously reported method (Bedini et al., 2008). Experiments were replicated independently at least four times.

Statistical Analysis

All data are presented as the mean ± SD for the number of experiments reported. Statistical comparisons were performed using one-way ANOVA followed by Newman-Keuls test (GraphPad Prism, version 5.0; GraphPad Software, Inc., La Jolla, CA, USA). Statistical significance is stated as $p < 0.05$.

RESULTS

Characterization of ARPE-19-Jurkat cells Interaction

Infiltration of mononuclear cells in the outer blood–retina barrier has been associated to several retinal diseases, including AMD (Gehrs et al., 2006). Moreover, RPE-to-immune cells contact and RPE apoptosis/necrosis were observed within AMD lesions (Ge-Zhi et al., 1996). Key mechanisms of RPE loss during AMD are both apoptosis and necrosis (Yang et al., 2011; Hanus et al., 2015). To evaluate the effects of RPE-immune cells interaction on apoptosis and necrosis, Jurkat cells were overlaid on ARPE-19 cells for different time points (1, 16, 24 and 48 h); thereafter, immune cells were removed by washing with PBS and collected by centrifugation, whereas ARPE-19 cells were detached by trypsinization and then centrifugated. Apoptosis/necrosis levels were evaluated by Annexin V assay as described in the methods section. Interactions between ARPE-19 and Jurkat cells led to a significant increase of apoptosis and necrosis in ARPE-19 cells (**Figure 1**). Increment in apoptosis and necrosis in ARPE-19 cells were observed after 16 h of co-culture and maintained up to 48 h. As regards immune cells, co-cultured with RPE for different incubation times, no significant changes of apoptosis or necrosis were found, as shown in **Figure 1** (panels C and D). Representative apoptosis/necrosis cytograms are shown in **Supplementary Figure S1**.

Adhesion molecules, such as ICAM-1 and VCAM-1, are endothelial- and leukocyte-associated membrane receptors playing a pivotal role in cell-cell interactions and in leukocyte transmigration across the endothelium. Both ICAM-1 and VCAM-1 are expressed on RPE cells (Holtkamp et al., 2001; Zhu et al., 2016) and can mediate RPE-leukocyte interaction. Thus, to determine the role of adhesion molecules in RPE-immune cells interaction in our *in vitro* model, expression levels of ICAM-1 and VCAM-1 were evaluated in both ARPE-19 and Jurkat cells at different co-culture intervals (1, 16, 24 and 48 h) by flow cytometry. In ARPE-19 cells VCAM-1 displayed low basal expression levels that were not altered at any of the considered time points following co-culture with Jurkat cells (**Figure 2A**). On Jurkat cells, expression of VCAM-1 expression was very low and was not significantly modified by interaction with ARPE-19 cells (**Figure 2C**). Similarly, we did not observe any changes in ICAM-1 levels on Jurkat cells after co-culturing them with ARPE-19 cells, although this adhesion molecule displayed higher basal expression levels on Jurkat cells as compared to VCAM-1 (**Figure 2D**). On the contrary, ARPE-19 cells displayed very high levels of ICAM-1 on their cell membrane; notably, ICAM-1 expression in ARPE-19 was significantly decreased by the interaction with Jurkat cells starting the effect after 1 h of co-culture and lasting up to 48 h of ARPE-

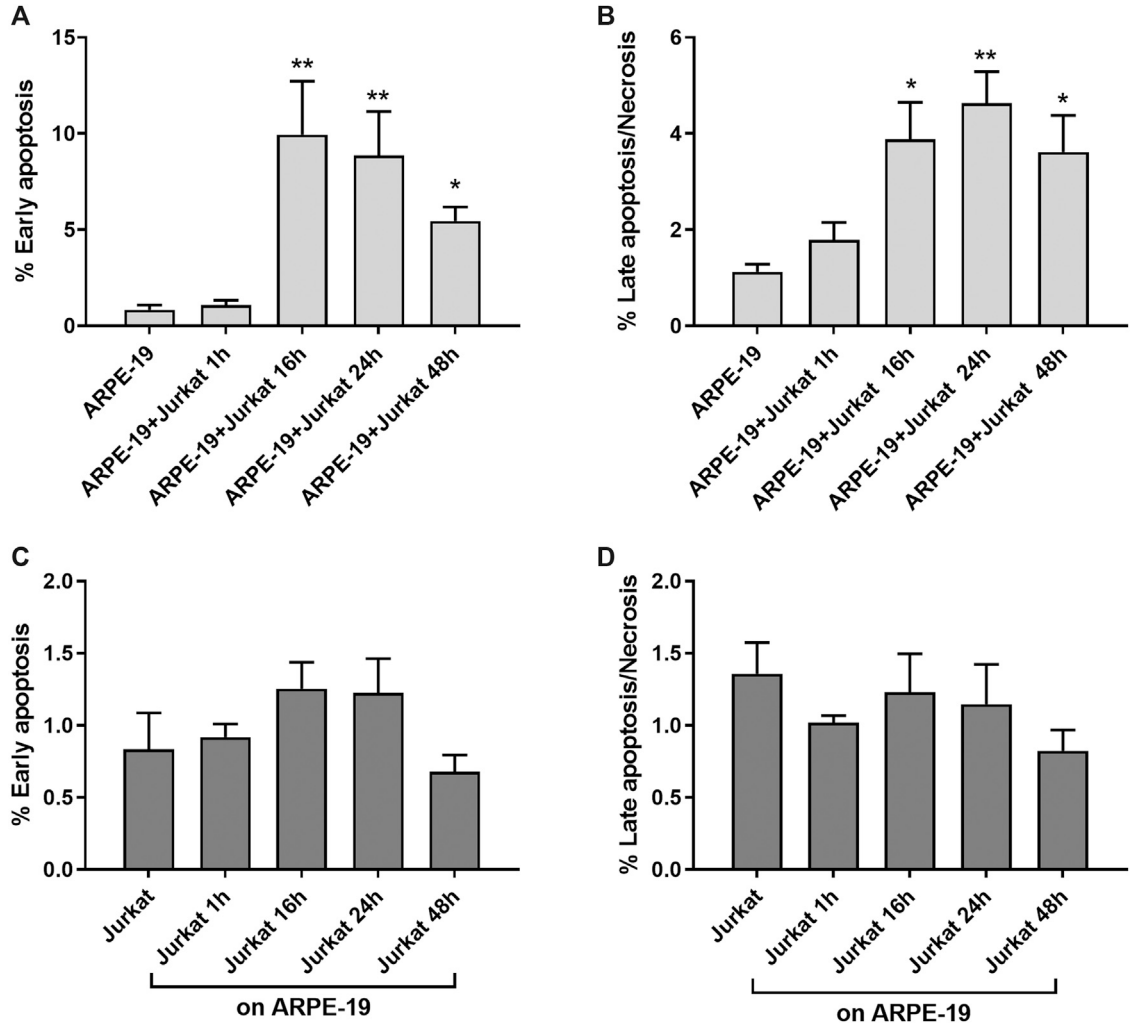

Figure 1 | ARPE-19-Jurkat cells co-culture resulted in increased apoptosis and necrosis. Interactions between ARPE-19 and Jurkat cells induced a significant increase of apoptosis **(A)** and necrosis **(B)** in ARPE-19 cells after 16 h of co-culture and up to 48 h. No significant changes in apoptosis **(C)** or necrosis **(D)** was observed in Jurkat cells incubated with ARPE-19 for different time points (0–48 h). Cells not co-cultured were considered as reference (shown as ARPE-19 or Jurkat in the figure). Apoptosis and necrosis were measured by flow cytometry and the results are presented as the percentage of early apoptotic and late apoptotic/necrotic cells. Values are mean ± SD from four experiments conducted in triplicate. *$p < 0.05$; **$p < 0.01$ vs ARPE-19/Jurkat (Newman-Keuls test after ANOVA).

19-Jurkat co-culture (**Figure 2B**). Representative histograms of VCAM-1 and ICAM-1 levels in both ARPE-19 and Jurkat cells are shown in **Supplementary Figure S2**.

MAPK ERK1/2 signaling is one of the most widely investigated intracellular pathway with regard to integrins and adhesion molecules (Hubbard and Rothlein, 2000; Cox et al., 2006; Meldolesi, 2016). Therefore, we analyzed ERK1/2 activation during ARPE-19-Jurkat co-culture. As shown in **Figure 3**, we observed a significant increase of ERK1/2 phosphorylation, evidence of ERK1/2 signaling activation, both in ARPE-19 and in Jurkat cells throughout co-culture duration. The interaction between RPE and immune cells led to a fast activation of ERK1/2 in ARPE-19 cells: accordingly, ERK1/2 phosphorylation increment was observed after 1 h of co-culture and was sustained up to 48 h (**Figure 3A,B**). In Jurkat cells, phosphorylation of ERK1/2 was significantly increased after 16 and 24 h of co-culture with ARPE-19 cells (**Figures 3C,D**).

Increased levels of inflammatory cytokines are detected in the eye of patients affected by AMD (Jonas et al., 2012). IL-1β is a pro-inflammatory cytokine that can be produced and released from different cells types. To evaluate changes in IL-1β expression during RPE-immune cells interaction, Jurkat cells were overlaid on ARPE-19 cells and co-cultured for different incubation times (1, 16, 24, 48 h). We observed a significant increment of IL-1β mRNA levels in ARPE-19 cells after 16 h and up to 48 h of co-culture with Jurkat cells (**Figure 4A**). In addition, ARPE-19-Jurkat interactions induced increased levels of IL-1β also in Jurkat cells after 24 and 48 h of co-culture (**Figure 4B**).

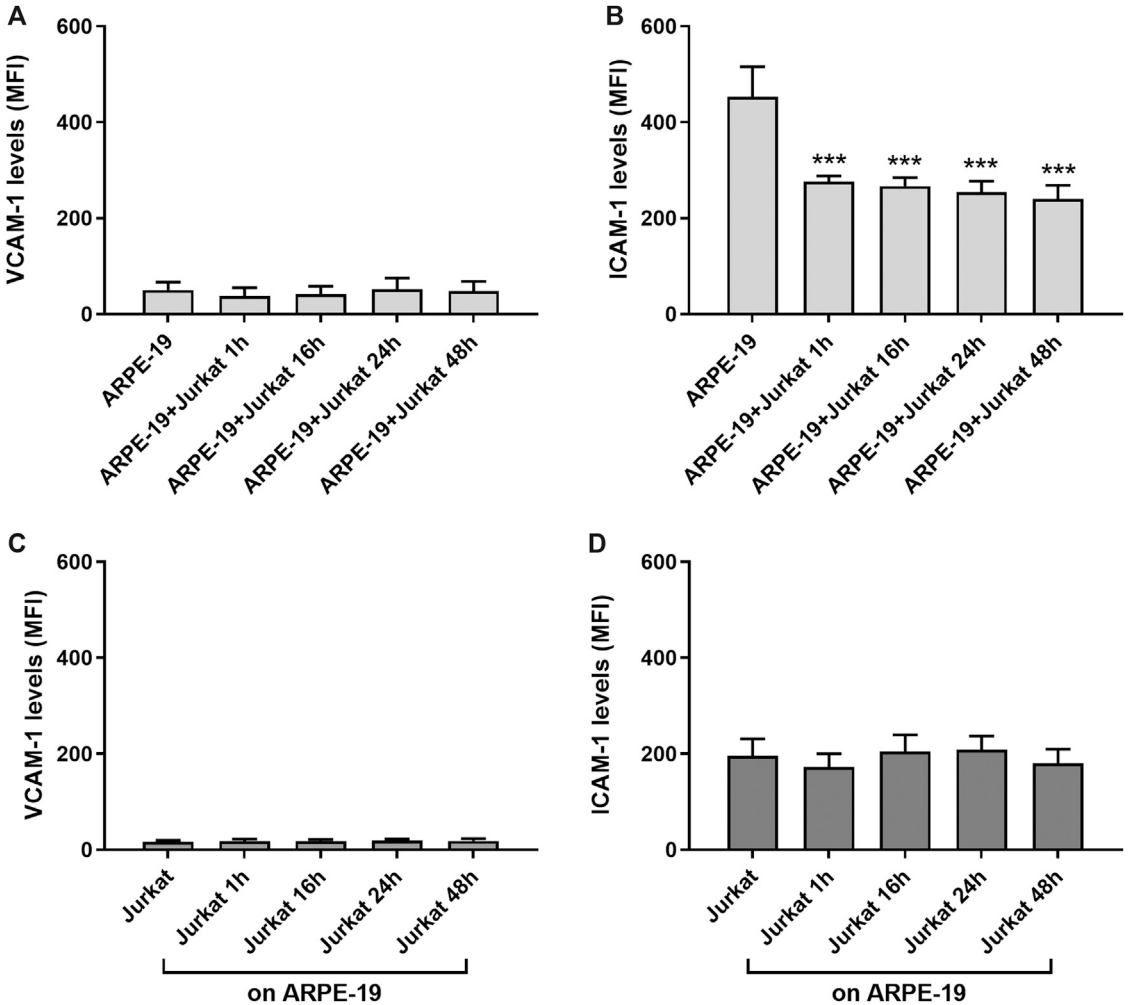

Figure 2 | Evaluation of ICAM-1 and VCAM-1 expression levels on ARPE-19 and Jurkat cells co-cultured for different time points (0–48 h). VCAM-1 expression was not influenced in both ARPE-19 **(A)** and Jurkat **(C)** cells. The interactions between ARPE-19 and Jurkat cells induced a significant reduction of ICAM-1 levels expressed on ARPE-19 cells at all time point considered **(B)**, whereas no changes were measured in ICAM-1 levels on Jurkat cells **(D)**. Data are expressed as mean fluorescence intensity (MFI) ± SD of four independent experiments carried out in triplicate. MFI values for respective isotype control mAb were set to 0. ***$p < 0.001$ versus ARPE-19 (Newman–Keuls test after ANOVA).

Integrins and Adhesion Molecules are Involved in ARPE-19-Jurkat Cell Interactions

In previous studies the expression of integrins and adhesion molecules on RPE has been described (Holtkamp et al., 2001; Elner et al., 2003; Bian et al., 2018); therefore, to confirm those results in our *in vitro* model, integrin expression on ARPE-19 cells was quantified by flow cytometry. High levels of α_5 integrin, VCAM-1 and ICAM-1 were observed for ARPE-19 cells (**Figures 2**, **5A**; see also **Supplementary Figure S3**). On the contrary, only low amounts of α_4, α_L, α_M, β_1, β_2 subunits were detectable on the surface of ARPE-19 cells (**Figure 5A**). Jurkat cells are considered a suitable cell model to study integrins and integrin-mediated cell adhesion and they express mainly $\alpha_4\beta_1$ and $\alpha_L\beta_2$ integrins (Tolomelli et al., 2015; Dattoli et al., 2018). To demonstrate the important role played by integrins and adhesion molecules into the cross-talk between RPE and leukocytes, Jurkat cells were pre-treated with a neutralizing anti-$\alpha_4\beta_1$ or anti-$\alpha_L\beta_2$ integrin antibodies, whereas ARPE-19 cells were pre-incubated with anti-ICAM-1 or anti-VCAM-1 blocking antibody for 1 h. All the antibodies were added at saturating concentration (10 μg/mL). After pre-treating cells with the above listed antibodies, ARPE-19 and immune cells were co-cultured for 24 h; afterwards, cells were collected for further analysis. Integrins and adhesion molecules expressed on ARPE-19 and Jurkat cells strongly mediated cell adhesion as shown **Figure 5B**. Neutralizing antibodies against adhesion molecules (VCAM-1 and ICAM-1) or α_4 and α_L integrin significantly reduced Jurkat cell adhesion to ARPE-19 cells (**Figure 5B**). Moreover, blocking adhesion molecules or integrins using mAbs led to the disruption of ARPE-19-

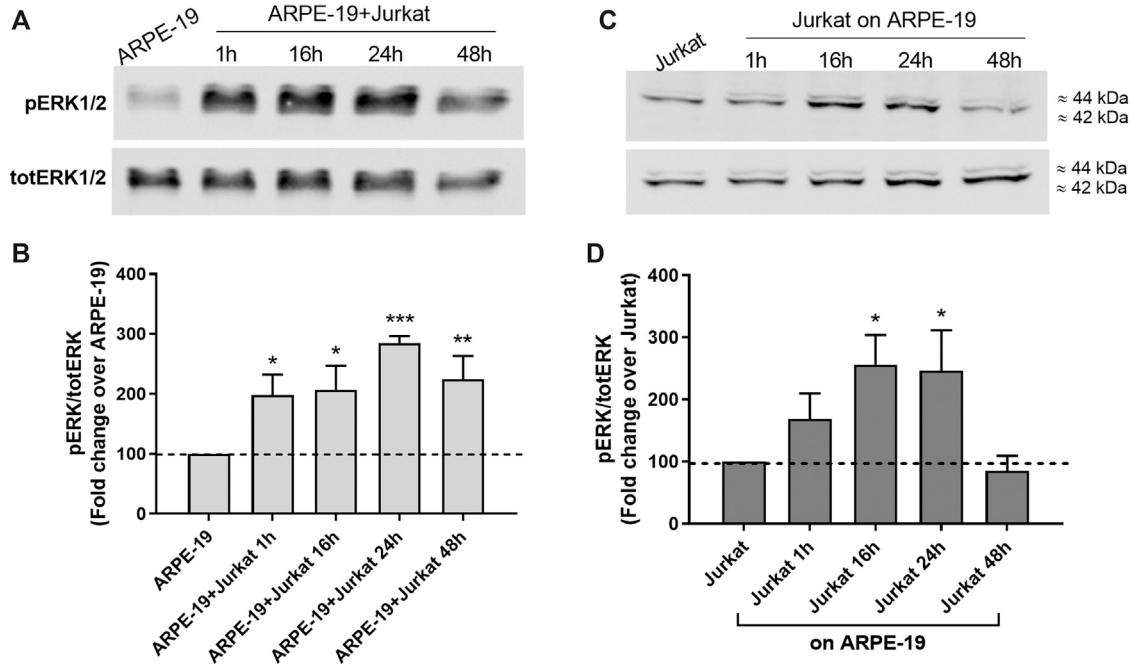

Figure 3 | Co-culture of RPE and immune cells induced activation of intracellular signaling leading to the phosphorylation of ERK1/2. ERK1/2 activation was observed soon after 1 h of co-culture in ARPE-19 cells and was maintained up to 48 h **(A-B)**; on the contrary, in Jurkat cells ERK1/2 phosphorylation was significantly increased after 16 h and 24 h of co-culture **(C-D)**. Representative Western blot images are shown **(A and C)** and the semiquantitative densitometric analysis of the bands **(B and D)** is represented in the graphs (mean ± SD of four independent experiments); the amount of pERK1/2 is normalized to that of totERK1/2. $^{*}p < 0.05$; $^{**}p < 0.01$; $^{***}p < 0.001$ versus ARPE-19/Jurkat (Newman–Keuls test after ANOVA).

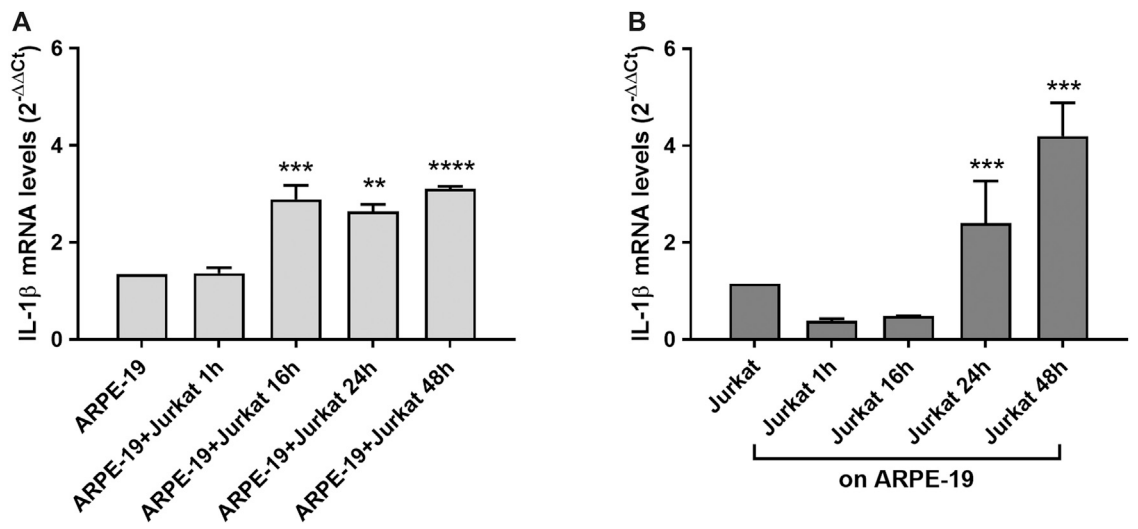

Figure 4 | Effects of ARPE-19-Jurkat cells co-culture on IL-1β evaluated as mRNA levels. IL-1β expression was significantly increased in both ARPE-19 **(A)** and Jurkat **(B)** cells after 16 h and 24 h of co-culture, respectively. The increment of IL-1β levels was maintained up to 48 h of co-culture. Data are expressed as mean ± SD of four independent experiments carried out in triplicate. $^{**}p < 0.01$; $^{***}p < 0.001$; $^{****}p < 0.0001$ versus ARPE-19/Jurkat (Newman–Keuls test after ANOVA).

Jurkat interactions and to the blockade of integrin-mediated signaling activation (**Figure 5**). Accordingly, neutralizing antibodies against VCAM-1, ICAM-1 or α_4 and α_L were able to prevent ERK1/2 phosphorylation induced by ARPE-19-Jurkat interaction within 24 h-long co-culture. Control experiments showed that mAbs were not able to activate ERK1/2 signaling pathway in ARPE-19 cells not cultured together with Jurkat cells (**Supplementary Figure S4**).

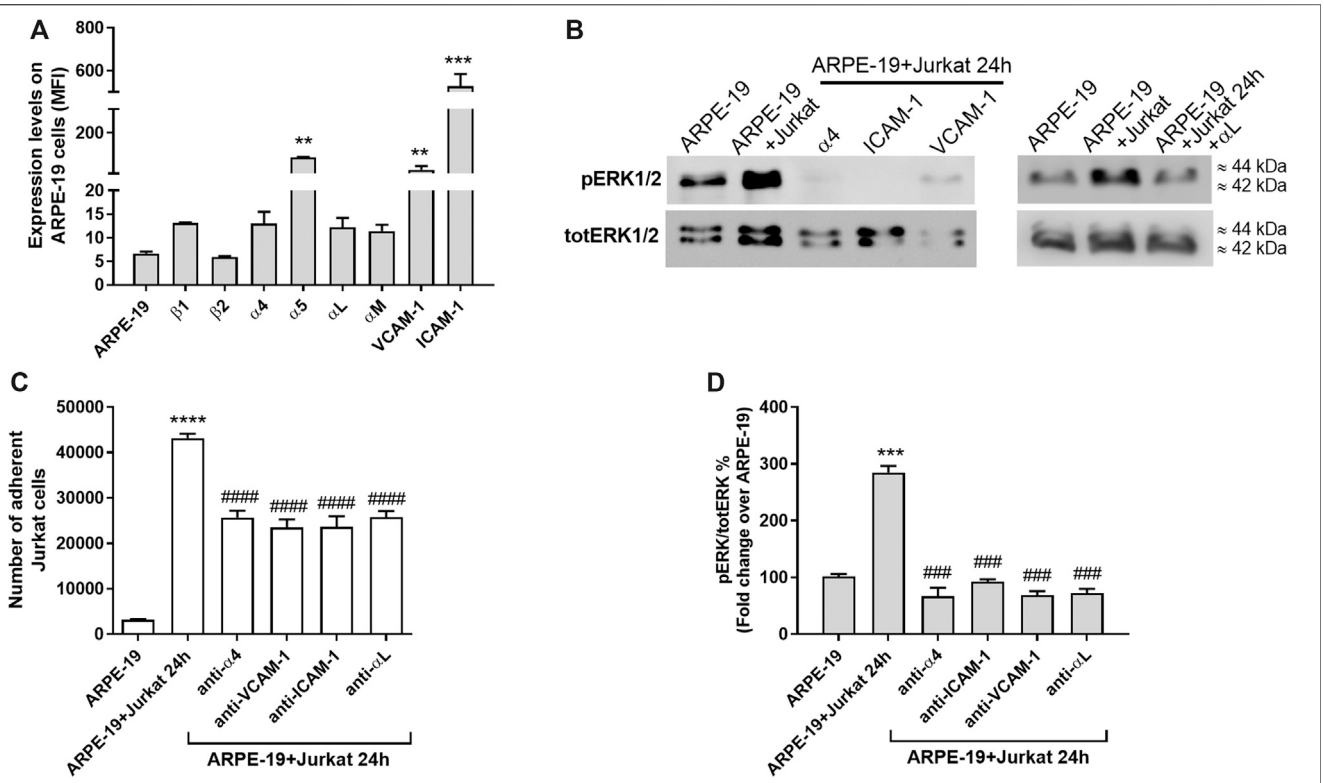

Figure 5 | Integrins and adhesion molecules involvement during co-culture of ARPE-19-Jurkat cells **(A)** Analysis of integrin expression on ARPE-19 cells evaluated by flow cytometry. α_5 integrin, VCAM-1 and ICAM-1 are significantly expressed on ARPE-19 cells; on the contrary ARPE-19 cells express low levels of α_4, α_L, α_M, β_1 and β_2 integrins. Data are expressed as mean fluorescence intensity (MFI) ± SD of four independent experiments carried out in triplicate. MFI values for respective isotype control monoclonal antibody (mAb) were set to 0. Representative histograms are shown in **Supplementary Figure 3**. (B) Blocking VCAM-1 or ICAM-1, expressed on ARPE-19 cells, or α_4 integrin, expressed on Jurkat cells, using specific mAbs, significantly reduced the number of Jurkat cells adhered to ARPE-19 cells. Data are expressed as mean ± SD of four independent experiments carried out in quadruplicate **(C–D)** The blockade of VCAM-1 or ICAM-1, expressed on ARPE-19 cells, or α_4 integrin, expressed on Jurkat cells, using specific mAbs, prevented the activation of integrin-mediated intracellular signaling in ARPE-19 cells after 24 h of co-culture with Jurkat cells. A representative western blot image is shown **(C)** and the semiquantitative densitometric analysis of the bands **(D)** is represented in the graph (mean ± SD of four independent experiments); the amount of pERK1/2 is normalized to that of totERK1/2. $^{**}p < 0.01$; $^{***}p < 0.001$; $^{****}p < 0.0001$ vs ARPE-19; ###$p < 0.001$ vs ARPE-19 + Jurkat 24 h (Newman–Keuls test after ANOVA).

Overall, these data demonstrate the important role played by integrins and adhesion molecules in the interactions between RPE and immune cells.

Integrin Antagonists Could Disrupt ARPE-19-Jurkat Interactions Via the Modulation of Adhesion, Apoptosis/ Necrosis, MAPK Signaling Pathway and IL-1β Expression

In previous studies we developed several ligands targeting different types of integrin (De Marco et al., 2015; Tolomelli et al., 2015; Baiula et al., 2016, Baiula et al., 2020; Dattoli et al., 2018; Martelli et al., 2019). From the screening of a small library of β-lactam derivatives that were specifically designed by a structure-based strategy to target RGD-binding or leukocyte integrin we obtained selective and potent integrin ligands (Baiula et al., 2016). MN27 (compound 15 in (Baiula et al., 2016)), which contains an aniline basic moiety, is a very potent and selective $\alpha_L\beta_2$ integrin antagonist, able to reduce significantly $\alpha_L\beta_2$-mediated cell adhesion and integrin-mediated intracellular signaling pathway. SR714 (compound 4 in (Baiula et al., 2016)), an azetidinone with a short carboxylic acid terminus, selectively binds to $\alpha_4\beta_1$ integrins and acts as an antagonist in cell adhesion assays and intracellular signaling evaluation (**Table 1**). In another study, we identified the compound named DS-70 that possesses a linear sequence completed by o-methylphenylureaphenylacetyl (MPUPA) and a simple glycine (Dattoli et al., 2018). The β-amino acid in its structure contributed to stable conformation of the overall structure and to increased serum stability. Through pharmacological characterization, DS-70 was recognized as an $\alpha_4\beta_1$ antagonist with nanomolar potency: it prevented integrin-mediated cell adhesion and antagonized VCAM-1-induced degranulation of mast cells and eosinophils *in vitro*. Moreover, in a dose-dependent manner, DS-70 significantly reduced the clinical symptoms of allergic conjunctivitis as well as conjunctival levels of chemokines and cytokines in a guinea pig model of allergic conjunctivitis (Dattoli et al., 2018).

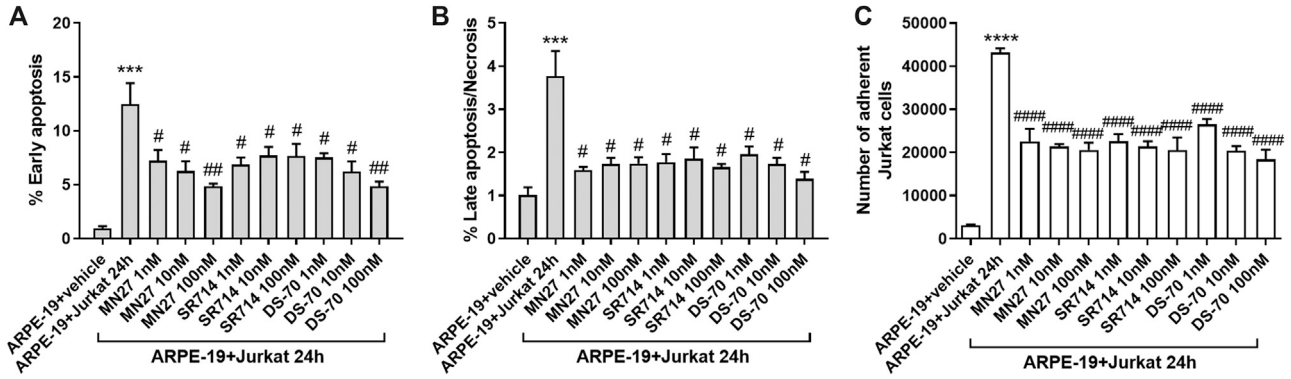

Figure 6 | Integrin antagonists MN27, SR714 and DS-70 (1–100 nM) prevented apoptosis **(A)** and necrosis **(B)** in ARPE-19 cells induced by 24 h of co-culture with Jurkat cells. Cells not co-cultured and treated with the vehicle (DMSO) used to dissolve integrin antagonists were considered as reference (shown as ARPE-19 + vehicle in the figure). Apoptosis and necrosis were measured by flow cytometry and the results are presented as the percentage of early apoptotic cells and late apoptotic/necrotic cells. Values are mean ± SD from four experiments conducted in triplicate using different cell cultures **(C)** Integrin antagonists were also able to significantly reduce Jurkat adhesion to ARPE-19 cells. Data are expressed as mean ± SD of four independent experiments. ***$p < 0.001$ vs ARPE-19; #$p < 0.05$; ##$p < 0.01$; ###$p < 0.001$ vs ARPE-19 + Jurkat 24 h (Newman-Keuls test after ANOVA).

To evaluate the possibility of exploiting integrin antagonists as novel agents to treat dry AMD, MN27, SR714 and DS-70 were employed in ARPE-19-Jurkat cells co-culture. Jurkat cells were pre-treated with different concentrations of MN27, SR714 or DS-70 (1–100 nM) for 30 min to block $\alpha_L\beta_2$ or $\alpha_4\beta_1$ integrin respectively. Thereafter, Jurkat cells were overlaid on ARPE-19 and co-cultured for 24 h; subsequently, ARPE-19 and Jurkat cells were collected separately and analyzed. As shown in **Figure 6**, integrin antagonists were able to significantly reduce apoptosis levels in ARPE-19 cells co-cultured with Jurkat cells for 24 h. Moreover, we found that the effect of DS-70 and MN27 was concentration-dependent (**Figure 6A** and **Supplementary Figure S5**). Integrin antagonists induced also a significant reduction of necrosis levels after disrupting the interactions between ARPE-19 and Jurkat cells. In contrast, we did not observe any change in apoptosis or necrosis levels in Jurkat co-cultured with ARPE-19 cells after the exposure to integrin antagonists (data not shown). Regarding ARPE-19-Jurkat cell adhesion, it was significantly reduced by pre-administering integrin antagonists: blocking integrins expressed on ARPE-19 or Jurkat cells, MN27, SR714 or DS-70 strongly diminished Jurkat cell adhesion to ARPE-19 cells (**Figure 6C**). As control experiments, ARPE-19 cells were exposed to the vehicle employed to dissolve integrin antagonists for 24 h; the vehicle, a volume corresponding to the highest antagonist concentration, did not induce apoptosis and necrosis in ARPE-19 cells, did not influence Jurkat cell adhesion to ARPE-19 cells and did not activate ERK1/2 intracellular signaling pathway in ARPE-19 cells (**Supplementary Figure S6**). The effects of integrin antagonists were also investigated with regard to integrin-mediated intracellular signaling activation. We found that MN27, SR714 and DS-70 fully reverted the increase of ERK1/2 phosphorylation induced during ARPE-19-Jurkat cell co-culture (**Figure 7**). It is intriguing to note that concentration-dependent effect induced by integrin antagonists on intracellular signaling, seen in Jurkat cells in previous studies (Baiula et al., 2016; Dattoli et al., 2018), was not observed in ARPE-19 cells after the interaction with Jurkat cells exposed to different concentrations of DS-70, MN27 or SR714.

In addition, we observed that integrin antagonists prevented the co-culture-induced increase in IL-1β expression both in ARPE-19 and Jurkat cells induced by co-culture incubation (**Figure 8**); this effect is concentration-dependent, especially in ARPE-19 cells, in which the lowest concentration (1 nM) did not exert any effect on IL-1β levels. The noncompetitive blocker of ERK kinase PD 98059 (10 μM), added 30 min before overlaying Jurkat to ARPE-19 cells, significantly reduced the co-culture-induced up-regulation of IL-1β mRNA in both cell types (**Figure 8**). Thus, confirming that ERK1/2 signaling downstream of integrin activation is required for the up-regulation of IL-1β mRNA.

DISCUSSION

In the retina there are two types of BRB: the inner barrier comprises tight junctions of endothelial cells, whereas the outer barrier is formed by tight junctions of RPE cells. Therefore, RPE cells, together with retinal vasculature, limit the entrance of blood component to the retina. Disease conditions, including AMD (Miller et al., 1986), can lead to disruption of BRB allowing inflammatory cells, platelets and macromolecules to encounter RPE cells. In previous studies contacts between RPE and mononuclear phagocyte (Killingsworth et al., 1990; Van Der Schaft et al., 1993; Penfold et al., 2001) or T cells have been described (Liversidge et al., 1990; Devine et al., 1996). Moreover, RPE cells secrete a multitude of cytokines and chemokines (Ablonczy et al., 2011; Juel et al., 2012), contributing to the modulation of retinal inflammation. In the present study we have characterized the crosstalk between lymphocytes and RPE cells. We observed that the interaction between ARPE-19 and Jurkat cells may induce

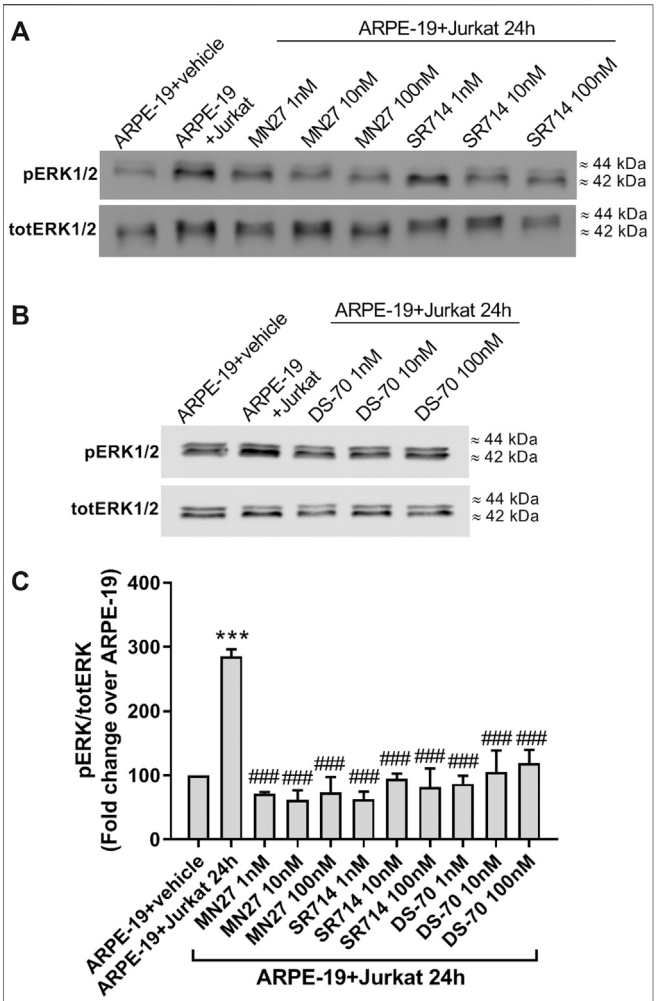

Figure 7 | Integrin antagonists MN27, SR712 and DS-70 (1–100 nM) were able to significantly prevent integrin-mediated activation of intracellular signaling in ARPE-19 after 24 h of co-culture with Jurkat cells. ERK1/2 phosphorylation was induced during ARPE-19-Jurkat cells co-culture; on the contrary, integrin antagonists significantly reduced ERK1/2 activation. Representative western blot images are shown **(A-B)** and the semiquantitative densitometric analysis of the bands **(C)** is represented in the graphs (mean ± SD of four independent experiments); the amount of pERK1/2 is normalized to that of totERK1/2. ***$p < 0.001$ vs ARPE-19; ###$p < 0.001$ vs ARPE-19 + Jurkat 24 h (Newman–Keuls test after ANOVA).

ARPE-19 cells apoptosis and necrosis, suggesting a potential role of inflammatory cells recruited at the BRB in RPE disruption observed in retinal disease conditions. It was previously demonstrated that RPE death can be due to necroptosis (Hanus et al., 2015) and that preventing this phenomenon could be beneficial for patients suffering from AMD. In addition, we found an increased expression of IL-1β in both RPE cells and lymphocytes after 16 and 24 h of co-culture, respectively. These data suggest that the physical interaction between RPE and lymphocytes could trigger and sustain an inflammatory reaction mediated by elevated levels of pro-inflammatory mediators produced by both cell types. IL-1β has important homeostatic functions but is also implicated in pathophysiological changes that occur during inflammatory disease conditions. As a matter of fact, IL-1β can be considered as a marker of inflammation (Lopez-Castejon and Brough, 2011) and is known to be involved in AMD pathogenesis. Accordingly, proinflammatory cytokines, including IL-1 β, maybe partly responsible of RPE death and photoreceptor degeneration (Kauppinen et al., 2012; Wang and Hartnett, 2016). In the eye of patients with AMD, augmented levels of inflammatory cytokines and chemokines have been reported in peripheral blood circulation (Jonas et al., 2010, Jonas et al., 2012). Moreover, previous studies showed that both immune cells (Doyle et al., 2012) and RPE cells (Fukuoka et al., 2003; Kauppinen et al., 2012) are able to produce IL-1β.

Furthermore, to better characterize RPE cell-lymphocyte interaction, we evaluated VCAM-1 and ICAM-1 levels, being these two adhesion molecules involved in immune cells recruitment to inflamed tissues. After ARPE-19-Jurkat co-culture, ICAM-1 expression was significantly reduced in ARPE-19 cells, whereas VCAM-1 levels were unaffected. VCAM-1 and ICAM-1 are endogenous ligands for $\alpha_4\beta_1$ and $\alpha_L\beta_2$ integrin, respectively. Previous studies have shown that the binding between adhesion molecules and integrins may contribute to the interaction between RPE and immune cells (Mesri et al., 1994; Devine et al., 1996; Holtkamp et al., 2001). The data reported in the present study confirm the contribution of integrins in immune cells recruitment to RPE. Accordingly, the adhesion of Jurkat cells to ARPE-19 is mediated by both $\alpha_4\beta_1$ and $\alpha_L\beta_2$ integrins and subsequently we observed integrin-mediated intracellular signaling activation. These results were confirmed by using blocking antibodies directed against $\alpha_4\beta_1$, $\alpha_L\beta_2$ integrins, or adhesion molecules VCAM-1 or ICAM-1. Blocking antibodies were able to reduce Jurkat cell adhesion to ARPE-19 and prevent the activation of integrin-mediated ERK1/2 intracellular pathway. Integrins are heterodimeric transmembrane receptors, that mediate cell-to-cell and cell-to-extracellular matrix adhesion (ECM) and are considered valuable therapeutic target for the development of new drugs. Particularly, drugs targeting leukocyte integrins, mainly $\alpha_4\beta_1$ and $\alpha_4\beta_7$, have proven to be effective for the treatment of inflammatory conditions, including ulcerative colitis, Crohn's disease, multiple sclerosis (Bamias et al., 2013; Lobatõn et al., 2014; Baiula et al., 2019). Regarding ocular diseases involving inflammation, lifitegrast, an $\alpha_L\beta_2$integrin antagonist, has been recently approved and is a safe and effective treatment for dry eye disease (DED) (Haber et al., 2019). Lifitegrast binds competitively to the α_L integrin subunit preventing the adhesion, migration and proliferation of lymphocytes and the subsequently cytokine production, thereby reducing the symptoms of DED (Kelly et al., 2007; Guimaraes De Souza et al., 2018). Moreover, GW559090, a potent α_4 integrin antagonist, has been proposed for the treatment of dry eye disease (Krauss et al., 2015) and for Sjögren's syndrome associated dry eye (Contreras-Ruiz et al., 2016). In addition, the importance of integrins in the pathogenesis of ocular diseases is demonstrated by the possibility to target RGD integrins, such as $\alpha_v\beta_3$, $\alpha_v\beta_5$ and $\alpha_5\beta_1$, expressed on endothelial cells and on RPE. RGD integrins mediate mainly interactions with ECM, and RGD integrin antagonists were shown to prevent the migration of

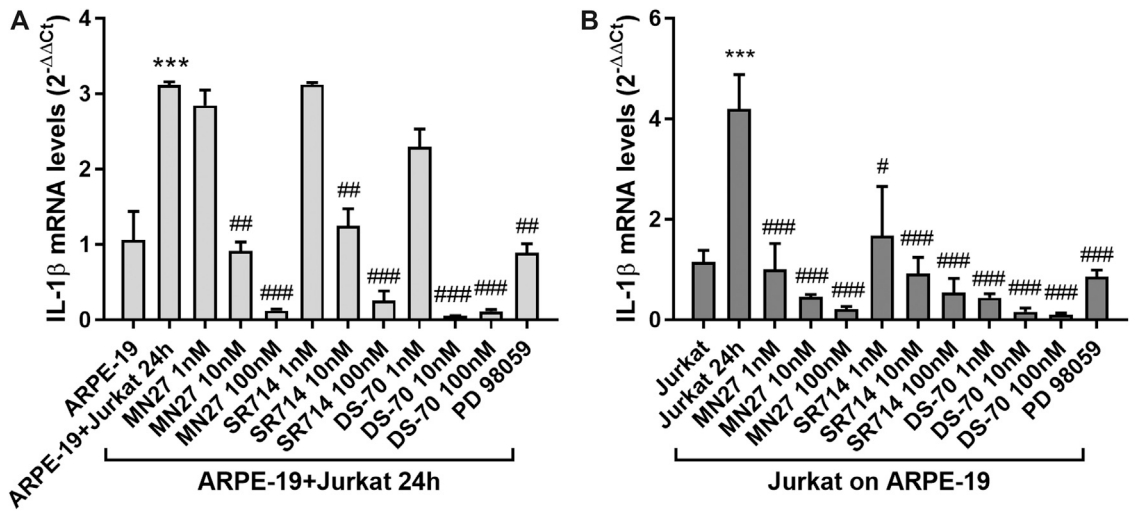

Figure 8 | Effects of integrin antagonists on IL-1β expression in ARPE-19-Jurkat cells after 24 h of co-culture with Jurkat cells. IL-1β expression, significantly increased in both ARPE-19 **(A)** and Jurkat cells **(B)** after 24 h of co-culture, was significantly reduced by integrin antagonists MN27, SR714 and DS-70 in both ARPE-19 and Jurkat cells. PD 98059 (10 μM), an ERK1/2 signaling inhibitor pre-incubated with the cells 30 min before starting the co-culture, prevented IL-1β expression increment both in ARPE-19 and Jurkat cells. Data are expressed as mean ± SD of four independent experiments. ***$p < 0.001$ versus ARPE-19/Jurkat; #$p < 0.05$; ##$p < 0.01$; ###$p < 0.001$ vs ARPE-19 + Jurkat 24 h/Jurkat 24 h (Newman–Keuls test after ANOVA).

endothelial cells and thereby neovascularization (Hu et al., 2019) and to counteract choroidal angiogenesis and vascular leakage (Yasukawa et al., 2004). Therefore, antagonists targeting RGD integrins may be valuable in ocular diseases involving neovascularization, as in wet AMD.

In a previous study we have reported the pharmacological characterization of DS-70, a potent and selective $\alpha_4\beta_1$ integrin antagonist, *in vitro* and *in vivo* in a guinea pig model of allergic conjunctivitis (Dattoli et al., 2018). As a selective antagonist of $\alpha_4\beta_1$, DS-70 prevented integrin-mediated cell adhesion, ERK1/2 phosphorylation and mast cells and eosinophils degranulation *in vitro*. Moreover, DS-70 significantly reduced clinical symptoms of ocular inflammation, $\alpha_4\beta_1$ expressing cell recruitment to the conjunctiva and pro-inflammatory cytokine and chemokine levels in a guinea pig model of allergic conjunctivitis. Within this frame, in the present study we investigated the effects elicited by DS-70 and other leukocyte integrin antagonists (namely MN27 and SR714) on RPE-lymphocyte crosstalk. MN27 and SR714 are β-lactam derivatives that behave as $\alpha_L\beta_2$ and $\alpha_4\beta_1$ antagonists, respectively (Baiula et al., 2016). All three integrin antagonists employed in this study interfere with ARPE-19-Jurkat cells interaction by blocking $\alpha_L\beta_2$ or $\alpha_4\beta_1$, they significantly reduce cell adhesion, activation of integrin-mediated intracellular signaling and expression of pro-inflammatory cytokine IL-1β. Moreover, DS-70, MN27 and SR714 significantly prevent apoptosis and necrosis induced in ARPE-19 cells by interaction with Jurkat cells. The disruption of RPE-lymphocyte crosstalk caused by integrin antagonists could be important for the treatment of dry AMD as it reduces RPE cell death and reduced inflammasome activation. These preliminary results provide further support to the hypothesis that $\alpha_L\beta_2$ or $\alpha_4\beta_1$ integrin can be considered as valuable drug targets in retinal diseases and that the integrin antagonists employed in the present study could be useful to develop new therapeutic agents useful to fight dry AMD.

The *in vitro* model employed in the current study rely on ARPE-19 cells, a spontaneously immortalized RPE cell line widely used to evaluate RPE function. ARPE-19 cell line represents a simplified cell culture model to study RPE cell functions *in vitro* and displays some differences respect to primary RPE, such as little or no pigmentation, variable morphology and weaker tight junctions; due to these properties ARPE-19 cells rather resemble aged eye or pathological conditions-affected RPE cells (Ablonczy et al., 2011). The current investigation is a preliminary research aimed at studying the involvement of integrins in RPE-immune cells interaction in AMD and the potential use of integrin antagonists within this frame. To confirm data obtained in the current study other *in vitro* cell culture models, including polarized human RPE cells (Khristov et al., 2018) and 3D cultured models (Forest et al., 2015; Shokoohmand et al., 2017; Schnichels et al., 2020) should be further employed. Animal models recapitulating several aspects of AMD are needed to further validate results obtained *in vitro* models. Nonetheless, our findings demonstrate for the first time the involvement of $\alpha_4\beta_1$ and $\alpha_L\beta_2$ integrins in the pathophysiology of AMD; thus, pointing at integrin antagonists as promising drug candidates to be further characterized.

In conclusion, integrin antagonists could protect RPE cells from death induced by leukocytes recruited to the retina as they downregulate proinflammatory cytokine expression, reduce ERK1/2 signaling and thereby resulting in the inhibition of the inflammation process. Nevertheless, further studies are needed to better characterize the effects of integrin

antagonists in more complex *in vitro* models and in animal models of AMD.

DATA AVAILABILITY STATEMENT

The datasets generated for this study are available on request to the corresponding author.

AUTHOR CONTRIBUTIONS

MB conceived the study, designed the experiments, carried out most of the work, analyzed the data and contributed to write the manuscript. AC and AB contributed to design and perform the experiments. DG and MC designed, synthesized and analyzed the compounds SR714 and MN17; FS, JZ and LG designed, synthesized, and analyzed the compound DS-70. SS designed the study and contributed to write the manuscript. All the authors revised and approved the final version of the manuscript.

FUNDING

This work was supported by grants from the University of Bologna RFO 2018, RFO 2019, RFO 2020 to MB and SS; and from a research grant from "Fondazione Cassa di Risparmio in Bologna" (2018/0347).

SUPPLEMENTARY MATERIAL

The Supplementary Material for this article can be found online at: https://www.frontiersin.org/articles/10.3389/fphar.2020.617836/full#supplementary-material.

REFERENCES

Ablonczy, Z., Dahrouj, M., Tang, P. H., Liu, Y., Sambamurti, K., Marmorstein, A. D., et al. (2011). Human retinal pigment epithelium cells as functional models for the RPE in vivo. *Investig. Ophthalmol. Vis. Sci.* 52, 8614–8620. doi:10.1167/iovs.11-8021

Akyol, E., and Lotery, A. (2020). Gene, cell and antibody-based therapies for the treatment of age-related macular degeneration. *Biologics.* 14, 83–94. doi:10.2147/btt.s252581

Ambati, J., and Fowler, B. J. (2012). Mechanisms of age-related macular degeneration. *Neuron.* 75, 26–39. doi:10.1016/j.neuron.2012.06.018

Baiula, M., Carbonari, G., Dattoli, S. D., Calienni, M., Bedini, A., and Spampinato, S. (2012). Rest is up-regulated by epidermal growth factor in HeLa cells and inhibits apoptosis by influencing histone H3 acetylation. *Biochim. Biophys. Acta - Mol. Cell Res.* 1823, 1252–1263. doi:10.1016/j.bbamcr.2012.05.026

Baiula, M., Galletti, P., Martelli, G., Soldati, R., Belvisi, L., Civera, M., et al. (2016). New β-lactam derivatives modulate cell adhesion and signaling mediated by RGD-binding and leukocyte integrins. *J. Med. Chem.* 59, 9721–9742. doi:10.1021/acs.jmedchem.6b00576

Baiula, M., Greco, R., Ferrazzano, L., Caligiana, A., Hoxha, K., Bandini, D., et al. (2020). Integrin-mediated adhesive properties of neutrophils are reduced by hyperbaric oxygen therapy in patients with chronic non-healing wound. *PLoS One* 15, e0237746. doi:10.1371/journal.pone.0237746

Baiula, M., Spampinato, S., Gentilucci, L., and Tolomelli, A. (2019). Novel ligands targeting α4β1 integrin: therapeutic applications and perspectives. *Front. Chem.* 7, 489. doi:10.3389/fchem.2019.00489

Bamias, G., Clark, D. J., and Rivera-Nieves, J. (2013). Leukocyte traffic blockade as a therapeutic strategy in inflammatory bowel disease. *Against Curr.* 14, 1490–1500. doi:10.2174/13894501113149990158

Bedini, A., Baiula, M., and Spampinato, S. (2008). Transcriptional activation of human mu-opioid receptor gene by insulin-like growth factor-I in neuronal cells is modulated by the transcription factor rest. *J. Neurochem.* 105, 2166–2178. doi:10.1111/j.1471-4159.2008.05303.x

Bedini, A., Baiula, M., Vincelli, G., Formaggio, F., Lombardi, S., Caprini, M., et al. (2017). Nociceptin/orphanin FQ antagonizes lipopolysaccharide-stimulated proliferation, migration and inflammatory signaling in human glioblastoma U87 cells. *Biochem. Pharmacol.* 140, 89–104. doi:10.1016/j.bcp.2017.05.021

Bian, Z. M., Field, M. G., Elner, S. G., Kahlenberg, J. M., and Elner, V. M. (2018). Distinct CD40L receptors mediate inflammasome activation and secretion of IL-1β and MCP-1 in cultured human retinal pigment epithelial cells. *Exp. Eye Res.* 170, 29–39. doi:10.1016/j.exer.2018.02.014

Contreras-Ruiz, L., Mir, F. A., Turpie, B., Krauss, A. H., and Masli, S. (2016). Sjögren's syndrome associated dry eye in a mouse model is ameliorated by topical application of integrin α4 antagonist GW559090. *Exp. Eye Res.* 143, 1–8. doi:10.1016/j.exer.2015.10.008

Cousins, S. W., Espinosa-Heidmann, D. G., and Csaky, K. G. (2004). Monocyte activation in patients with age-related macular degeneration: a biomarker of risk for choroidal neovascularization?. *Arch. Ophthalmol.* 122, 1013–1018. doi:10.1001/archopht.122.7.1013

Cox, B. D., Natarajan, M., Stettner, M. R., and Gladson, C. L. (2006). New concepts regarding focal adhesion kinase promotion of cell migration and proliferation. *J. Cell. Biochem.* 99, 35–52. doi:10.1002/jcb.20956

Dattoli, S. D., Baiula, M., De Marco, R., Bedini, A., Anselmi, M., Gentilucci, L., et al. (2018). DS-70, a novel and potent α4 integrin antagonist, is an effective treatment for experimental allergic conjunctivitis in Guinea pigs. *Br. J. Pharmacol.* 175, 3891–3910. doi:10.1111/bph.14458

De Marco, R., Mazzotti, G., Dattoli, S. D., Baiula, M., Spampinato, S., Greco, A., et al. (2015). 5-aminomethyloxazolidine-2,4-dione hybrid α/β-dipeptide scaffolds as inductors of constrained conformations: applications to the synthesis of integrin antagonists. *Biopolymers* 104, 636–649. doi:10.1002/bip.22704

Devine, L., Lightman, S. L., and Greenwood, J. (1996). Role of LFA-1, ICAM-1, VLA-4 and VCAM-1 in lymphocyte migration across retinal pigment epithelial monolayers in vitro. *Immunology* 88, 456–462. doi:10.1046/j.1365-2567.1996.d01-666.x

Di Toro, R., Baiula, M., and Spampinato, S. (2005). Expression of the repressor element-1 silencing transcription factor (REST) is influenced by insulin-like growth factor-I in differentiating human neuroblastoma cells. *Eur. J. Neurosci.* 21, 46–58. doi:10.1111/j.1460-9568.2004.03828.x

Doyle, S. L., Campbell, M., Ozaki, E., Salomon, R. G., Mori, A., Kenna, P. F., et al. (2012). NLRP3 has a protective role in age-related macular degeneration through the induction of IL-18 by drusen components. *Nat. Med.* 18, 791–798. doi:10.1038/nm.2717

Elner, S. G., Elner, V. M., Kindzelskii, A. L., Horino, K., Davis, H. R., Todd, R. F., et al. (2003). Human RPE cell lysis of extracellular matrix: functional urokinase plasminogen activator receptor (uPAR), collagenase and elastase. *Exp. Eye Res.* 76, 585–595. doi:10.1016/S0014-4835(03)00028-9

Forest, D. L., Johnson, L. V., and Clegg, D. O. (2015). Cellular models and therapies for age-related macular degeneration. *DMM Dis. Model. Mech.* 8, 421–427. doi:10.1242/dmm.017236

Fukuoka, Y., Strainic, M., and Medof, M. E. (2003). Differential cytokine expression of human retinal pigment epithelial cells in response to stimulation by C5a. *Clin. Exp. Immunol.* 131, 248–253. doi:10.1046/j.1365-2249.2003.02087.x

Ge-Zhi, X., Li, W. W. Y., Tso, M. O. M., and Friedman, A. H. (1996). Apoptosis in human retinal degenerations, *Trans. Am. Ophthalmol. Soc.* 94, 411-430, Available at: /pmc/articles/PMC1312106/?report=abstract (Accessed October 9, 2020).

Gehrs, K. M., Anderson, D. H., Johnson, L. V., and Hageman, G. S. (2006). Age-related macular degeneration - emerging pathogenetic and therapeutic concepts. *Ann. Med.* 38, 450–471. doi:10.1080/07853890600946724

Guimaraes De Souza, R., Yu, Z., Stern, M. E., Pflugfelder, S. C., and De Paiva, C. S. (2018). Suppression of Th1-mediated keratoconjunctivitis sicca by lifitegrast. *J. Ocul. Pharmacol. Therapeut.* 34, 543–549. doi:10.1089/jop.2018.0047

Haber, S. L., Benson, V., Buckway, C. J., Gonzales, J. M., Romanet, D., and Scholes, B. (2019). Lifitegrast: a novel drug for patients with dry eye disease. *Ther. Adv. Ophthalmol.* 11, 2515841419870366. doi:10.1177/2515841419870366

Hanus, J., Anderson, C., and Wang, S. (2015). RPE necroptosis in response to oxidative stress and in AMD. *Ageing Res. Rev.* 24, 286–298. doi:10.1016/j.arr.2015.09.002

Holtkamp, G. M., Kijlstra, A., Peek, R., and De Vos, A. F. (2001). Retinal pigment epithelium-immune system interactions: cytokine production and cytokine-induced changes. *Prog. Retin. Eye Res.* 20, 29–48. doi:10.1016/S1350-9462(00)00017-3

Hu, T. T., Vanhove, M., Porcu, M., Van Hove, I., Van Bergen, T., Jonckx, B., et al. (2019). The potent small molecule integrin antagonist THR-687 is a promising next-generation therapy for retinal vascular disorders. *Exp. Eye Res.* 180, 43–52. doi:10.1016/j.exer.2018.11.022

Hubbard, A. K., and Rothlein, R. (2000). Intercellular adhesion molecule-1 (ICAM-1) expression and cell signaling cascades. *Free Radic. Biol. Med.* 28, 1379–1386. doi:10.1016/S0891-5849(00)00223-9

Jonas, J. B., Tao, Y., Neumaier, M., and Findeisen, P. (2010). Monocyte chemoattractant protein 1, intercellular adhesion molecule 1, and vascular cell adhesion molecule 1 in exudative age-related macular degeneration. *Arch. Ophthalmol.* 128, 1281–1286. doi:10.1001/archophthalmol.2010.227

Jonas, J. B., Tao, Y., Neumaier, M., and Findeisen, P. (2012). Cytokine concentration in aqueous humour of eyes with exudative age-related macular degeneration. *Acta Ophthalmol.* 90, e381–e388. doi:10.1111/j.1755-3768.2012.02414.x

Juel, H. B., Faber, C., Udsen, M. S., Folkersen, L., and Nissen, M. H. (2012). Chemokine expression in retinal pigment epithelial ARPE-19 cells in response to coculture with activated T cells. *Investig. Ophthalmol. Vis. Sci.* 53, 8472–8480. doi:10.1167/iovs.12-9963

Kauppinen, A., Niskanen, H., Suuronen, T., Kinnunen, K., Salminen, A., and Kaarniranta, K. (2012). Oxidative stress activates NLRP3 inflammasomes in ARPE-19 cells-Implications for age-related macular degeneration (AMD). *Immunol. Lett.* 147, 29–33. doi:10.1016/j.imlet.2012.05.005

Kelly, M., Hwang, J. M., and Kubes, P. (2007). Modulating leukocyte recruitment in inflammation. *J. Allergy Clin. Immunol.* 120, 3–10. doi:10.1016/j.jaci.2007.05.017

Khristov, V., Wan, Q., Sharma, R., Lotfi, M., Maminishkis, A., and Bharti, K. (2018). Polarized human retinal pigment epithelium exhibits distinct surface proteome on apical and basal plasma membranes, *Methods Mol.* 1722, 223–247. doi:10.1007/978-1-4939-7553-2_15

Killingsworth, M. C., Sarks, J. P., and Sarks, S. H. (1990). Macrophages related to bruch's membrane in age-related macular degeneration. *Eye* 4, 613–621. doi:10.1038/eye.1990.86

Krauss, A. H., Corrales, R. M., Pelegrino, F. S. A., Tukler-Henriksson, J., Pflugfelder, S. C., and de Paiva, C. S. (2015). Improvement of outcome measures of dry eye by a novel integrin antagonist in the murine desiccating stress model. *Invest. Ophthalmol. Vis. Sci.* 56, 5888–5895. doi:10.1167/iovs.15-17249

Liversidge, J., Sewell, H. F., and Forrester, J. V. (1990). Interactions between lymphocytes and cells of the blood-retina barrier: mechanisms of T lymphocyte adhesion to human retinal capillary endothelial cells and retinal pigment epithelial cells in vitro. *Immunology* 71, 390–396 Available at: http://www.ncbi.nlm.nih.gov/pubmed/1980120 (Accessed October 9, 2020).

Lobatōn, T., Vermeire, S., Van Assche, G., and Rutgeerts, P. (2014). Review article: anti-adhesion therapies for inflammatory bowel disease. *Aliment. Pharmacol. Ther.* 39, 579–594. doi:10.1111/apt.12639

Lopez-Castejon, G., and Brough, D. (2011). Understanding the mechanism of IL-1β secretion. *Cytokine Growth Factor Rev.* 22, 189–195. doi:10.1016/j.cytogfr.2011.10.001

Martelli, G., Baiula, M., Caligiana, A., Galletti, P., Gentilucci, L., Artali, R., et al. (2019). Could dissecting the molecular framework of β-lactam integrin ligands enhance selectivity?. *J. Med. Chem.* 62, 10156–10166. doi:10.1021/acs.jmedchem.9b01000

Meldolesi, J. (2016). Pharmacology of the cell/matrix form of adhesion. *Pharmacol. Res.* 107, 430–436. doi:10.1016/j.phrs.2015.10.019

Mesri, M., Liversidge, J., and Forrester, J. V. (1994). ICAM-1/LFA-1 interactions in T-lymphocyte activation and adhesion to cells of the blood-retina barrier in the rat. *Immunology* 83, 52–57 Available at: http://www.ncbi.nlm.nih.gov/pubmed/7821966 (Accessed October 9, 2020).

Miller, H., Miller, B., and Ryan, S. J. (1986). The role of retinal pigment epithelium in the involution of subretinal neovascularization. *Investig. Ophthalmol. Vis. Sci.* 27, 1644–1652 Available at: https://pubmed.ncbi.nlm.nih.gov/2429937/ (Accessed October 9, 2020).

Penfold, P. L., Madigan, M. C., Gillies, M. C., and Provis, J. M. (2001). Immunological and aetiological aspects of macular degeneration. *Prog. Retin. Eye Res.* 20, 385–414. doi:10.1016/S1350-9462(00)00025-2

Platts, K. E., Benson, M. T., Rennie, I. G., Sharrard, R. M., and Rees, R. C. (1995). Cytokine modulation of adhesion molecule expression on human retinal pigment epithelial cells, *Invest Ophthalmol Vis Sci*, 36, 2262–2269, Available at: https://iovs.arvojournals.org/article.aspx?articleid=2161202

Raab-Westphal, S., Marshall, J. F., and Goodman, S. L. (2017). Integrins as therapeutic targets: successes and cancers. *Cancers* 9, 110. doi:10.3390/cancers9090110

Schnichels, S., Paquet-Durand, F., Löscher, M., Tsai, T., Hurst, J., Joachim, S. C., et al. (2020). Retina in a dish: cell cultures, retinal explants and animal models for common diseases of the retina. *Prog. Retin. Eye Res.* 100880, doi:10.1016/j.preteyeres.2020.100880

Shokoohmand, A., Jeon, J. E., Theodoropoulos, C., Baldwin, J. G., Hutmacher, D. W., and Feigl, B. (2017). A novel 3D cultured model for studying early changes in age-related macular degeneration. *Macromol. Biosci.* 17, 1700221 (1-8) doi:10.1002/mabi.201700221

Strauss, O. (2005). The retinal pigment epithelium in visual function. *Physiol. Rev.* 85, 845–881. doi:10.1152/physrev.00021.2004

Supuran, C. T. (2019). Agents for the prevention and treatment of age-related macular degeneration and macular edema: a literature and patent review. *Expert Opin. Ther. Pat.* 29, 761–767. doi:10.1080/13543776.2019.1671353

Tolomelli, A., Baiula, M., Viola, A., Ferrazzano, L., Gentilucci, L., Dattoli, S. D., et al. (2015). Dehydro-*β*-proline containing α4*β*1 integrin antagonists: stereochemical recognition in ligand-receptor interplay. *ACS Med. Chem. Lett.* 6, 701–706. doi:10.1021/acsmedchemlett.5b00125

Tolomelli, A., Galletti, P., Baiula, M., and Giacomini, D. (2017). Can integrin agonists have cards to play against cancer? A literature survey of small molecules integrin activators. *Cancers* 9, 78. doi:10.3390/cancers9070078

Van Der Schaft, T. L., Mooy, C. M., De Bruijn, W. C., and De Jong, P. T. V. M. (1993). Early stages of age-related macular degeneration: an immunofluorescence and electron microscopy study. *Br. J. Ophthalmol.* 77, 657–661. doi:10.1136/bjo.77.10.657

Van Lookeren Campagne, M., Lecouter, J., Yaspan, B. L., and Ye, W. (2014). Mechanisms of age-related macular degeneration and therapeutic opportunities. *J. Pathol.* 232, 151–164. doi:10.1002/path.4266

Wang, H., and Hartnett, E. M. (2016). Regulation of signaling events involved in the pathophysiology of neovascular AMD. *Mol. Vis.* 22, 189–202 Available at: http://www.molvis.org/molvis/v22/189 (Accessed October 9, 2020).

Winer, J., Jung, C. K. S., Shackel, I., and Williams, P. M. (1999). Development and validation of real-time quantitative reverse transcriptase-polymerase chain reaction for monitoring gene expression in cardiac myocytes in vitro. *Anal. Biochem.* 270, 41–49. doi:10.1006/abio.1999.4085

Yang, D., Elner, S. G., Chen, X., Field, M. G., Petty, H. R., and Elner, V. M. (2011). MCP-1-activated monocytes induce apoptosis in human retinal pigment epithelium. *Investig. Ophthalmol. Vis. Sci.* 52, 6026–6034. doi:10.1167/iovs.10-7023

Yasukawa, T., Hoffmann, S., Eichler, W., Friedrichs, U., Wang, Y. S., and Wiedemann, P. (2004). Inhibition of experimental choroidal neovascularization in rats by an *α*v-integrin antagonist. *Curr. Eye Res.* 28, 359–366. doi:10.1076/ceyr.28.5.359.28678

Zhu, X., Wang, K., Zhang, K., Zhou, F., and Zhu, L. (2016). Induction of oxidative and nitrosative stresses in human retinal pigment epithelial cells by all-trans-retinal. *Exp. Cell Res.* 348, 87–94. doi:10.1016/j.yexcr.2016.09.002

Conflict of Interest: The authors declare that the research was conducted in the absence of any commercial or financial relationships that could be construed as a potential conflict of interest.

frontiers in Pharmacology

ORIGINAL RESEARCH
published: 08 February 2021
doi: 10.3389/fphar.2021.601404

Reduction of Neuroinflammation by δ-Opioids Via STAT3-Dependent Pathway in Chronic Glaucoma Model

Shahid Husain[1]*, *Syed A. H. Zaidi*[1], *Sudha Singh*[1], *Wendy Guzman*[1] and *Shikhar Mehrotra*[2]

[1]Department of Ophthalmology, Storm Eye Institute, Medical University of South Carolina, Charleston, SC, United States, [2]Department of Surgery, Hollings Cancer Center, Medical University of South Carolina, Charleston, SC, United States

The main objective of this study was to determine the inhibition of pro-inflammatory cytokines and their associated signaling molecules by δ-opioid receptor activation by a selective ligand, SNC-121 in chronic rat glaucoma model. Intraocular pressure was raised in rat eyes by injecting 2 M hypertonic saline into the limbal veins. SNC-121 (1 mg/kg; i. p) or Stattic (5 mg/kg; i. p) was administered in Brown Norway rats daily for 7 days. The mRNA expression of IL-1β, TNF-α, Fas, IL-6, leukemia inhibitory factor, and IFN-γ was increased significantly in the retina of ocular hypertensive animals at day 7, post injury. Administration of SNC-121 (1 mg/kg; i. p. injection) for 7 days (once a day) completely inhibited the increase in the mRNA and protein expression of pro-inflammatory cytokines. Mechanistically, we provide data showing a significant increase in the phosphorylation of STAT3 at tyrosine 705 whereas a moderate but significant increase in the total STAT3 protein expression was also seen in the retina of ocular hypertensive animals. Data illustrated that SNC-121 administration completely abrogated ocular hypertension-induced increase in $STAT3^{Y705}$ phosphorylation. Interestingly, acetylation of STAT3 at lysine 685 (AcK685) was reduced in ocular hypertensive animals and subsequently increased significantly by SNC-121 treatment. Stattic, a selective STAT3 inhibitor, administration resulted in a complete attenuation in the production of IL-1β and IL-6 in ocular hypertensive animals. In conclusion, δ-opioid receptor activation suppressed the phosphorylation of STAT3 at tyrosine 705 and increased acetylation at lysine 686 and these posttranslational modifications can regulate the production of some but not all pro-inflammatory cytokines in response to glaucomatous injury.

Keywords: protein acetylation, transcription factors, opioids, glaucoma, neuroinflammantion

OPEN ACCESS

Edited by:
Claudio Bucolo,
University of Catania, Italy

Reviewed by:
Chiara Bianca Maria Platania,
University of Catania, Italy
Monica Baiula,
University of Bologna, Italy

***Correspondence:**
Shahid Husain
husain@musc.edu

Specialty section:
This article was submitted to Inflammation Pharmacology, a section of the journal Frontiers in Pharmacology

Received: *31 August 2020*
Accepted: *05 January 2021*
Published: *08 February 2021*

Citation:
Husain S, Zaidi SAH, Singh S, Guzman W and Mehrotra S (2021) Reduction of Neuroinflammation by δ-Opioids Via STAT3-Dependent Pathway in Chronic Glaucoma Model. Front. Pharmacol. 12:601404. doi: 10.3389/fphar.2021.601404

INTRODUCTION

Glaucoma is the second leading cause of blindness worldwide in which retinal ganglion cells (RGCs) die slowly and progressively over a prolonged period of time. Glaucoma is now considered to be a multi-factorial disease in which biomechanical stress (Boland and Quigley, 2007), epigenetic changes (Crosson et al., 2010; Pelzel et al., 2010; Alsarraf et al., 2014b; Zaidi et al., 2020), mitochondrial dysfunction (Osborne et al., 2016), deprivation of neurotrophic factors (Chitranshi et al., 2018), oxidative stress (Benoist d'Azy et al., 2016), and neuroinflammation (Husain et al., 2012a; Husain et al., 2012b; Abdul et al., 2013; Williams et al., 2017; Adornetto et al., 2019), play critical roles. Studies have shown elevated levels of pro-inflammatory cytokines in human glaucoma patients

(Zenkel et al., 2010; Chua et al., 2012; Ohira et al., 2016) and experimental glaucoma models (Husain et al., 2012a; Abdul et al., 2013; Wilson et al., 2015). Additionally, ocular inflammation which has been a prominent feature of uveitis can also lead to inflammatory or uveitic glaucoma (Bodh et al., 2011; Siddique et al., 2013; Baneke et al., 2016; Ohira et al., 2016). A limited number of glaucoma patients have also shown optic disk hemorrhage (Airaksinen and Heijl, 1983; Drance, 1989; Gordon and Piltz-Seymour, 1997), which indicates a breach of the blood-retina barrier. As a result, circulating immune cells can enter the retina and nerve fiber layer where the hemorrhage has been observed most prominently (Drance, 1989; Choi et al., 2007; Hwang et al., 2014). These observations advocate for a potential role of neuroinflammation in glaucoma, however, it is not clear if neuroinflammation is a primary cause or a compensatory response or it is entirely a secondary event during glaucoma pathology that can slowly and progressively damage RGCs.

Epigenetic modifications appear to be a promising novel approach to modulate cellular function in neurodegenerative diseases (Didonna and Opal, 2015; Neal and Richardson, 2018), however their roles in the regulation of neuroinflammation in glaucoma remains unknown. In general, epigenetic changes control gene expression via histone acetylation, DNA methylation, and non-coding RNAs. Protein acetylation is a dynamic process, which is controlled by two classes of enzymes called histone acetyltransferase (HATs) and histone deacetylates (HDACs). Studies have shown impairment in the acetylation homeostasis in numerous neurodegenerative diseases including glaucoma (Ferrante et al., 2003; Rouaux et al., 2003; Ryu et al., 2005; Saha and Pahan, 2006; Haberland et al., 2009; Crosson et al., 2010; Pelzel et al., 2010; Alsarraf et al., 2014a; Alsarraf et al., 2014b; Schmitt et al., 2014; Lebrun-Julien and Suter, 2015; Alkozi et al., 2017; Berson et al., 2018). Earlier, we have shown that δ-opioid receptor activation by a selective ligand (i.e., SNC-121) provides RGC neuroprotection (Abdul et al., 2013; Husain et al., 2014; Husain et al., 2017; Husain, 2018). We have also shown that activation of δ-opioid receptor reduces oxidative stress and proinflammatory cytokines in acute ischemia/reperfusion, chronic rat glaucoma model, and in the optic nerve head (ONH) astrocytes (Husain et al., 2009; Abdul et al., 2013; Akhter et al., 2013b; Husain et al., 2014). Studies have also shown that Sigma-1 receptor agonist reduced intraocular pressure in normotensive rabbit(Bucolo et al., 1999). Sigma-1 receptor is a ligand-operated chaperone that modulates neurotransmission by interacting with multiple protein partners, including the μ-opioid receptor and sigma-1 antagonists are able to induce opioid analgesia by enhancing the action of endogenous opioid peptides of immune origin during inflammation (Tejada et al., 2018). Additionally, Sigma-1 receptor modulate neuroinflammation in osteoarthritis (Carcole et al., 2019). However, the interaction of sigma-1 and δ-opioid receptors was not determined in the current study. More recently, we have shown that SNC-121 increased histone H2B, H3, and H4 acetylation and reduced the activities and expression of class I and IIb histone deacetylates (HDACs) in ONH astrocytes (Zaidi.et al., 2020). However, it remains in question if protein acetylation of certain transcription factors plays any crucial role in the regulation of pro-inflammatory cytokines in glaucoma.

Based on our data we hypothesize that δ-opioids induced acetylation of transcription factor, such as STAT3, can regulate the production of pro-inflammatory cytokines under glaucomatous conditions. To the best of our knowledge this is the first report in which we have shown that δ-opioid receptor activation regulates phosphorylation of STAT3 at tyrosine 705 which subsequently plays key roles in the regulation of neuroinflammation during glaucoma progression.

MATERIALS AND METHODS

Animals

Equal numbers of adult male and female Brown Norway rats (2–5 months of age; 150–350 g) were used in this study. These animals were obtained from Charles River laboratory (San Diego, CA). Rats were maintained under a cycle of 12-hours light and 12-h dark throughout the studies. All animal handling was performed in accordance with the ARVO Statement for the Use of Animals in Ophthalmic and Vision Research. The study protocol was approved by the Animal Care and Use Committee at the Medical University of South Carolina. Delta (δ)-opioid-receptor agonist, SNC-121 (1 mg/kg body weight; Santa Cruz Biotechnology, Dallas, TX), was dissolved in PBS. Stattic (5 mg/kg body weight) (Tocris, Minneapolis, MN) was dissolved in 75% DMSO. Drugs or vehicle were administered individually in Brown Norway rats intraperitoneally (i.p.) 30 min post hypertonic saline injection. The drug administration (150–200 μL) was continued for 7 days, once daily at the same time (i.e., 9 am–11 am).

Development of Glaucoma Model by Hypertonic Saline Injection

Intraocular pressure (IOP) was raised in Brown Norway rats by injecting 50 μL of 2 M hypertonic saline into the limbal venous system as described earlier (Abdul et al., 2013; Husain et al., 2014; Husain et al., 2017). IOP was recorded at day 0 (prior to injury), day 3 and 7 (post injury). Animals that had elevation in IOP more than 25% were included in the data analysis.

RNA Extraction and Real Time-Polymerase Chain Reaction

RNA from the retina was isolated using TRIzol reagent (Life Technologies, Grand Island, NY) as described previously (Zaidi.et al., 2020). Purity and concentration of the isolated RNA was determined using Nanodrop. Total RNA (1 μg) was used to prepare cDNA using iScript cDNA synthesis Kit (Bio-Rad Laboratories, Inc., Hercules, CA, United States) according to the manufacturer's manual. The changes in mRNA levels for IL-1β, TNF-α, Fas, IL-6, LIF, IFN-γ, STAT1, STAT2, and STAT3 were analyzed by quantitative Real Time (RT) PCR (Bio-Rad iCycler system, Hercules, CA) using specific primers synthesized from Integrated DNA technologies (Coralville, IA). The sequences of specific primer used for each gene are listed in **Table 1**.

TABLE 1 | Primer sequences used for quantitative real time-polymerase chain reaction in the current study.

Primer	Direction	Sequence
IL-1β	Forward	TGAGGCTGACAGACCCCAAAAGAT
IL-1β	Reverse	GCTCCACGGGCAAGACATAGGTAG
IL-6	Forward	TGTATGAACAGCGATGATG
IL-6	Reverse	AGAAGACCAGAGCAGATT
TNF-α	Forward	AAATGGGCTCCCTCTCATCAGTTC
TNF-α	Reverse	TCTGCTTGGTGGTTTGCTACGAC
IFN-γ	Forward	CACGCCGCGTCTTGGT
IFN-γ	Reverse	TCTAGGCTTTCAATGAGTGTGCC
LIF	Forward	ACCAGATCAAGAGTCAACTG
LIF	Reverse	CCTTGAGCTGTGTAATAGGA
FAS	Forward	CTTGGGTGCCGATTACAACC
FAS	Reverse	GCCCTCCCGTACACTCACTC
STAT1	Forward	AGAGCGACCAGAAACAGGAA
STAT1	Reverse	GCTCTCTGCAACAATGGTGA
STAT2	Forward	TGGTTCAACATGCTCAGCTC
STAT2	Reverse	GCTCTCTCGCTTGCTGAAGT
STAT3	Forward	AGTTCTCGTCCACCACCAAG
STAT3	Reverse	CTAGCCAGACCCAGAACGAG
β-actin	Forward	ATGGTCAACCCCACCGTGT
β-actin	Reverse	CGTGTGAAGTCACCACCCT

Conditions for qRT- PCR were: 95°C for 30 s followed by two-step 40 cycles of 95°C for 10 s and 60°C for 30 s. The relative gene expression is calculated based on the comparative threshold cycle (ΔΔCt) method. Expression levels for all genes were normalized to the mean value of housekeeping gene *ß*-actin. We have used 4–9 animals in each group of treatment and a total of 19 animals were used for qRT-PCR.

Immunohistochemistry

Eyes were enucleated on day 7, post hypertonic saline injection and placed in 4% PFA for 12 h at 4°C. The retinas were then transferred to 30% sucrose for 12 h followed by embedding the retinas in OCT on dry ice. Cryosections were cut at −30°C and stored at −20°C until used for immunohistochemistry. Retina sections were rinsed with Tris-buffered saline (TBS) at room temperature followed by permeabilization using 0.5% Triton-X-100 in TBS. The tissues were blocked with 5% BSA for 1 h followed by incubation with primary antibodies (anti-IL-1β, anti-IL-6, or anti-phospho-STAT3) for 16 h at 4°C. After washing, the tissues were incubated with secondary antibody (Alexa Fluor 488 or Rhodamine) for 1 h at room temperature. The details of antibodies dilution and commercial sources are provided in **Table 2**. The sections were observed under a bright-field microscope equipped with epifluorescence, and digitized images were captured by a digital camera (Zeiss) as described earlier (Husain et al., 2012a; Abdul et al., 2013; Husain et al., 2014; Husain et al., 2017). We have used four animals in each group of treatment and a total of 12 animals were used for Immunohistochemistry.

Protein Extraction and Western Blotting

Protein extracts were prepared by homogenizing the retina using handheld micro-grinder in lysis buffer (50 mM Tris-HCl buffer, pH 8.0 containing 10 mM EDTA, 0.5% sodium deoxycholate, 0.5 mM sodium orthovanadate, 1%Triton X-100, and Halt's protease inhibitor cocktail). Protein lysate were then centrifuged at 10,000 rpm for 10 min at 4°C and total proteins in the supernatant were quantified by Bradford Protein Assay (BioRad, Hercules, CA). Total protein (10–20 μg) for each sample were separated by NuPAGE 10% Bis-Tris Gels (Thermo Fisher Scientific, Carlsbad, CA) and proteins were transferred to a nitrocellulose membrane. The membranes were blocked with 5% BSA or non-fat dry milk in a Tris-buffer saline containing 1% Tween-20 for 1 h. Membranes were incubated with primary antibodies (anti-phospho STAT3 Tyr 705, anti-acetyl-STAT3 Lys K685, or anti-STAT3) for 16 h at 4°C. Membranes were probed with horseradish peroxidase-(HRP) linked secondary antibody, and visualized by enhanced chemiluminescence reagent (ECL, Super Signal, Thermo Scientific, Rockford, IL) on Biorad Versadoc imaging system (Biorad, Hercules, CA). All membranes were reprobed with *ß*-actin to ensure equal protein loading. Band intensities of each protein of interest were measured by densitometry as arbitrary units and normalized with *ß*-actin as an internal loading control. The details for the antibody dilution and sources are provided in **Table 2**. We have used 6–9 animals in each group of treatment and a total of 21 animals were used in protein estimations by Western blotting.

TABLE 2 | List of antibodies, vendors, catalog number, and dilutions used in the current study.

Antibody	Company	Catalog No	Application	
			IHC	WB
Anti-acetyl STAT3 lys 685	Cell signaling technology	2,523		1:1,000
Anti-β actin	Sigma aldrich	A5316		1:2000
Anti-IL-6 (10E5)	Invitrogen	ARC0962	1:100	
Anti-IL1β (H-153)	Santa cruz biotechnology	Sc-7884	1:20	
Anti-phospho STAT3 Tyr 705 (D3A7)	Cell signaling technology	9,154	1:100	1:1,000
Anti- STAT3 (124H6)	Cell signaling technology	9,139		1:2000
Anti-rabbit IgG, HRP-linked	Cell signaling technology	7,074		1:5,000
Anti-mouse IgG, HRP-linked	Cell signaling technology	7,076		1:5,000
Alexa fluor 488 anti mouse	Jackson immunoresearch	111–545–044	1:500	
Alexa fluor 488 anti rabbit	Jackson immunoresearch	111–545–144	1:500	
Rhodamine red anti rabbit	Jackson immunoresearch	711–295–152	1:500	
Rhodamine red anti mouse	Jackson immunoresearch	715–025–151	1:500	

Statistical Analysis

Data are presented in this manuscript as ± standard error of mean (SEM) from three or more independent experiments as indicated by n. Where "n" refers to biological replicates. Statistical analysis was performed using one-way ANOVA followed by a post hoc Tukey test for multiple comparisons (GraphPad Software, Inc., San Diego, CA). A p value ≤0.05 was considered significant.

RESULTS

Changes in the Intraocular Pressure in Response to Glaucomatous Injury

Intraocular pressure (IOP) was measured at day 0, 3, and 7, pre- and post-glaucomatous injury. As shown in **Table 3**, a significant increase in the IOP was seen as early as day 3, which was further increased significantly at day 7, post injury. Similar to our previous studies SNC-121 had no effects on IOP (Abdul et al., 2013; Husain et al., 2014). Additionally, we have not seen any effects of Stattic treatment on IOP.

Regulation of Pro-inflammatory Cytokines by δ-Opioid Receptor Activation in Rat Glaucoma Model

We determined the regulatory effects of a selective δ-opioid receptor agonist (SNC-121) on the production of pro-inflammatory cytokines and their associated signaling molecules in the retina of ocular hypertensive animals. We chose to measure changes in the mRNA expression of interleukin-1β (IL-1β), tumor necrosis factor-α (TNF-α), Fas, interleukin-6 (IL-6), leukemia inhibitory factor (LIF), and interferon γ (IFN-γ) based on their potential involvement in neurodegenerative diseases. The mRNA expression of IL-1β was increased by 1.49 ± 0.11 fold (n = 6–9; $p < 0.01$; **Figure 1A**), TNF-α by 1.87 ± 0.26 fold (n = 4–7; $p < 0.05$; **Figure 1B**), Fas by 1.92 ± 0.08 fold (n = 4; $p < 0.001$; **Figure 1C**), IL-6 by 1.84 ± 0.15 fold (n = 4–6; $p < 0.01$; **Figure 1D**), LIF by 1.5 ± 0.1 fold (n = 4; $p < 0.05$; **Figure 1E**), and IFN-γ by 2.64 ± 0.41 fold (n = 4–7; $p < 0.01$; **Figure 1F**), at day 7, post injury. Treatment of SNC-121 (1 mg/kg; i.p. injection) for 7 days (once a day) completely inhibited the increase in the mRNA expression of pro-inflammatory cytokines (**Figures 1A–D**). Earlier, we have shown that elevated TNF-α protein expression was completely blocked by SNC-121 treatment in chronic glaucoma model (Abdul et al., 2013). In the current study, we have also shown that protein expression of IL-1β and IL-6 was remarkably increased in RGC and nerve fiber layers in ocular hypertensive animals (**Figure 2**), which was completely inhibited in SNC-121 treated ocular hypertensive animals.

Effects of δ-Opioid Receptor Agonist (SNC-121) on Transcription Factors STATS in Glaucoma Model

To learn more about the signaling mechanisms that may be involved in the production of pro-inflammatory cytokines in response to glaucomatous injury, we measured the changes in the mRNA transcript of transcription factors, signal transducer and activator of transcription (e.g., STAT1, STAT2, and STAT3) in the retina of normal and ocular hypertensive animals. As shown in **Figure 3**, the mRNA expression of STAT1, STAT2, and STAT3 was increased significantly in the retina of ocular hypertensive animals. The mRNA transcripts of STAT1, STAT2, and STAT3 were increased by 1.56 ± 0.11 fold (n = 4; $p < 0.01$; **Figure 3A**), 1.31 ± 0.07 fold (n = 4; $p < 0.01$; **Figure 3B**), and 1.43 ± 0.11 fold (n = 7–9; $p < 0.01$; **Figure 3C**), respectively. Interestingly, up-regulation of STAT1, STAT2, and STAT3 mRNA was blocked in SNC-121 treated ocular hypertensive animals (**Figures 3A–C**).

Effects of δ-Opioid Receptor Agonist (SNC-121) on STAT3^{Y705} Phosphorylation

In non-ocular systems, studies have shown that phosphorylation of STAT3 at tyrosine 705 (Y705) activates and increases its transcriptional activity. To learn more about STAT3 and its regulatory roles in cytokines production, we measured phosphorylation of STAT3 at tyrosine 705. Our data provides evidence that phosphorylation of STAT3 at tyrosine 705 is significantly ($p < 0.0001$) increased in the retina of ocular hypertensive animals (**Figure 4**). Furthermore, we have seen 144 ± 17% (p = 0.02) increase in the total STAT3 protein expression in ocular hypertensive retina when compared with naïve retina (**Figure 4**). Data illustrated that SNC-121 treatment completely abrogated ocular hypertension-induced increase in STAT3^{Y705} phosphorylation. However, we were not successful to measure any appreciable phosphorylation of STAT1 and STAT2. We encountered technical issues with antibodies picking up numerous non-selective bands while used two antibodies from different sources. Based on our findings, we cannot fully ruled out the involvement of STAT1 and STAT2 in this process. Additional experiments are needed to determine the changes in total and phosphorylated STAT1 and STAT2 in normal and glaucomatous retina, which will be the goal of our future studies. To further identify the retina layers and cell-type in which STAT3 phosphorylation is predominantly increased, we performed immunohistochemistry using retina sections and a selective anti-phospho-STAT3^{Y705} antibodies in the normal, ocular hypertensive, and SNC-121 treated ocular hypertensive animals. As shown in **Figure 5**, phospho-STAT3 immunostaining was remarkably increased in retinal ganglion cell (GCL) and nerve fiber layers, however, a diffuse and punctate immunostaining was also seen in inner nuclear and outer plexiform layers of ocular hypertensive animals. The increase in phosphorylation of STAT3 at tyrosine 705 was drastically inhibited in SNC-121 treated animals specifically in GCL and nerve fiber layers.

Effects of SNC-121 Treatment on STAT3 Acetylation

To establish a link whether transcriptional activity of STAT3 is regulated by phosphorylation, acetylation, or both, we have measured the acetylation of STAT3 using a selective acetyl STAT3 K685 antibody. This antibody recognizes only acetylated STAT3 at lysine 685 (AcK685). As shown in

TABLE 3 | Measurements of IOP in normal, ocular hypertensive, SNC-121, and stattic treated ocular hypertensive animals.

Days	0-Day	3-Days	7-Days
Normal animals	17.3 ± 0.58	17.9 ± 0.40	19.3 ± 0.47
Ocular hypertensive animals	16.8 ± 0.52	22.3 ± 0.92**	25.8 ± 0.59****
Ocular hypertensive animals + SNC 121 (1 mg/kg)	16.9 ± 0.60	20.8 ± 1.0*	25.5 ± 0.6****
Ocular hypertensive animals + Stattic (5 mg/kg)	17.3 ± 0.3	19.2 ± 0.3	22.0 ± 0.6*

Data are expressed as mean ± SE; n = *8–12. Asterisk (*) indicates significant difference from normal animals at each time point.* *p = *0.02,* **p = *0.0025, and* ****p = *0.001.*

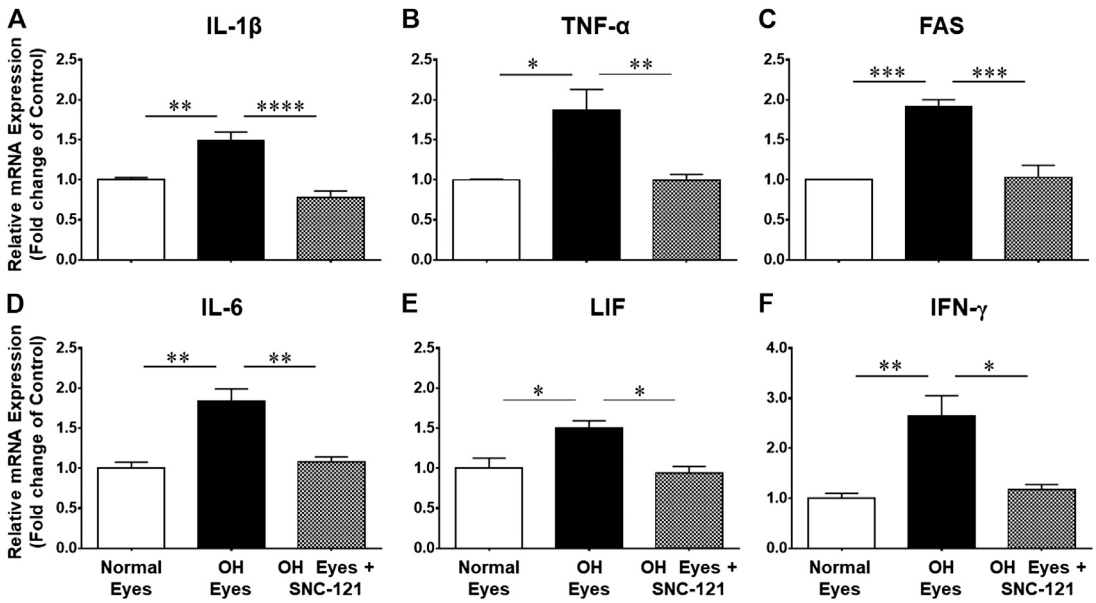

FIGURE 1 | Changes in mRNA expression of pro-inflammatory cytokines in response to ocular hypertension and SNC-121 treatment. Intraocular pressure (IOP) was raised by 2.0 M hypertonic saline injection followed by δ-opioid receptor agonist (1 mg/kg; i. p injections) treatment for 7 days, once a day. The retinas were collected at day 7, post hypertonic saline injection and mRNA was analyzed for IL-1β **(A)**, TNF-α **(B)**, FAS **(C)**, IL-6 **(D)**, LIF **(E)**, and IFN-γ **(F)** using cDNA that was synthesized from 1 μg total RNA. The relative changes in mRNA levels were measured by quantitative RT-PCR (qRT-PCR) using primers specific for each gene as indicated in **Table 1**. The qRT-PCR data was normalized using *β*-actin gene expression as an internal control. The relative expression was calculated based on the comparative threshold cycle ($2^{-\Delta\Delta Ct}$) method. Bar graph represents mean data ±SEM. OH Eyes; ocular hypertensive eyes; OH Eyes + SNC-121, ocular hypertensive eyes with SNC-121 treatment. **p* < 0.05; ***p* < 0.01; ****p* < 0.001; *****p* < 0.0001; *n* = 4–9. In this experiment "n" represent a biological replicate.

Figure 6, the acetylation of STAT3 was reduced as a result of glaucomatous injury. Moreover, we have seen a significant increase in the STAT3 acetylation at lysine 685 (AcK685) by SNC-121 treatment in ocular hypertensive animals. These data provide initial clues that protein acetylation of STAT3 will negatively regulate the transcriptional activity of STAT3, which may have reduced the activities of downstream signaling pathways including the production of pro-inflammatory cytokines.

Inhibition of Pro-inflammatory Cytokines by a STAT3 Inhibitor in Rat Glaucoma Model

Stattic, a STAT3 inhibitor, was used to block the mRNA expression of pro-inflammatory cytokines. As shown in **Figures 7A,B**, Stattic administration (5 mg/kg, intraperitoneal, once a day for 7 days) fully attenuated the production of IL-1β and IL-6 in ocular hypertensive animals.

DISCUSSION

The current therapeutic modalities focus on lowering the elevated intraocular pressure (IOP), which is considered to be a primary risk factor for glaucoma (Boland and Quigley, 2007; Almasieh et al., 2012). However, patients undergoing glaucoma therapy continue to lose vision as a result of retinal ganglion cell (RGC) death suggesting IOP is not the only causative factor for RGC death in glaucoma. Primarily, RGCs die during glaucomatous injury but what causes the initiation of RGC degeneration is unknown. Numerous factors including neuroinflammation, epigenetic changes, biomechanical stress, neurotrophic factor deprivation, oxidative stress, and activation of glial cells (astrocytes and/or microglia) have been shown to be potentially involved in RGC death in glaucoma.

The eye is an "immune privileged" organ because peripheral immune cells are not able to cross blood-retinal barriers. Instead, the glial cells (e.g., microglia and astrocytes) are constituents of a

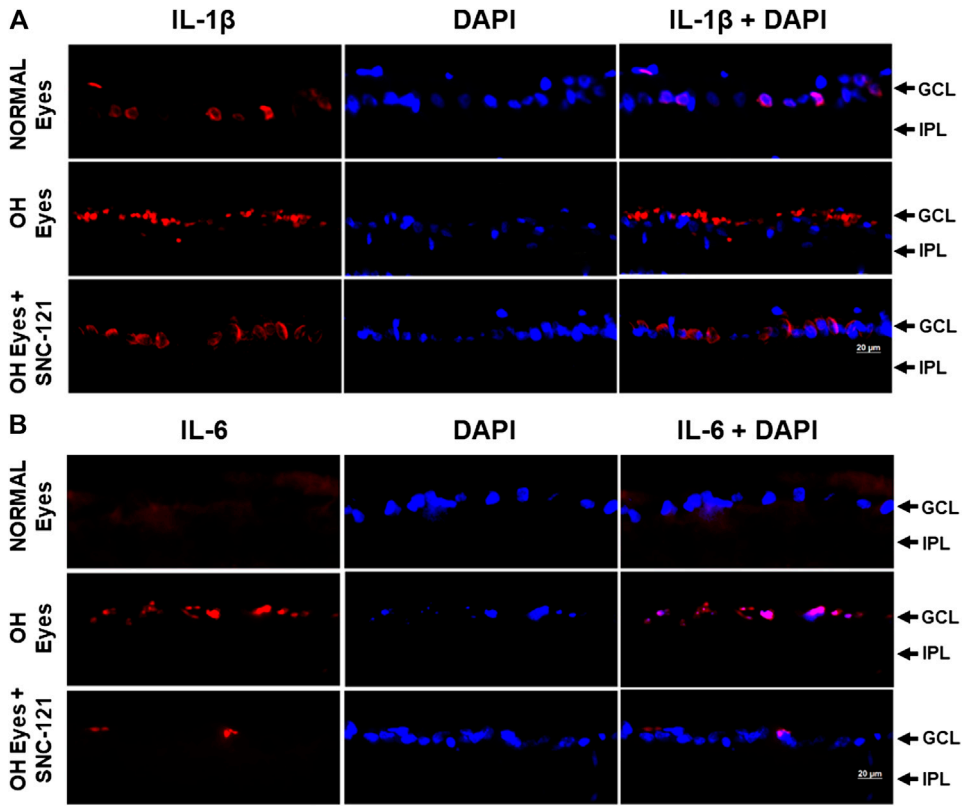

FIGURE 2 | Effects of δ-opioid receptor agonist (SNC-121) treatment on interleukin-1β (IL-1β) **(A)** and interleukin-6 (IL-6) **(B)** production in ocular hypertensive animal. Animals were euthanized and eyes were enucleated at day 7, post hypertonic saline injections. Retina cryosections were immunostained using a selective anti-IL-1β or anti-IL-6 antibody. The nuclei were counterstained with DAPI. Red color indicates staining for IL-1β and IL-6 and blue for the nuclei. There was no positive immunostaining when primary antibodies were omitted (not shown). Data shown here is a representation of at least four independent experiments. We have used four animals in each treatment group. OH Eyes; ocular hypertensive eyes; OH Eyes + SNC-121, ocular hypertensive eyes with SNC-121 treatment, bar size 20 μm.

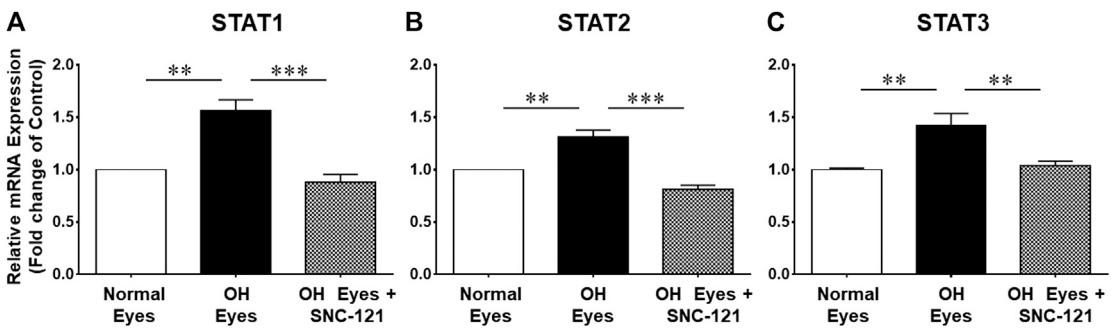

FIGURE 3 | Effects of SNC-121 treatment on mRNA expression of STAT1 **(A)**, STAT2 **(B)**, and STAT3 **(C)**. The retina from normal, ocular hypertensive, and SNC-121 treated ocular hypertensive animals were collected at day 7, post hypertonic saline injection. Complementary DNA was synthesized from 1 μg total RNA extracted from retina. The relative changes in mRNA levels were measured by quantitative RT-PCR (qRT-PCR) using primers specific for each gene as indicated in **Table 1**. The qRT-PCR data was normalized using *β*-actin gene expression as an internal control. The relative expression was calculated based on the comparative threshold cycle ($2^{-\Delta\Delta Ct}$) method. Bar graph represents mean data ±SEM. OH Eyes; ocular hypertensive eyes; OH Eyes + SNC-121, ocular hypertensive eyes with SNC-121 treatment. $^{**}p < 0.01$; $^{***}p < 0.001$; $n = 4–9$. In this experiment "n" represent a biological replicate.

dedicated neuroimmune system and provide immune surveillance. In physiological conditions, the glial cells provide both pro- and anti-inflammatory cytokines and they play crucial roles in normal and disease condition including phagocytosis, free radical reduction, cellular repairs, and maintaining metabolites to provide energy (Grieshaber et al., 2007; da

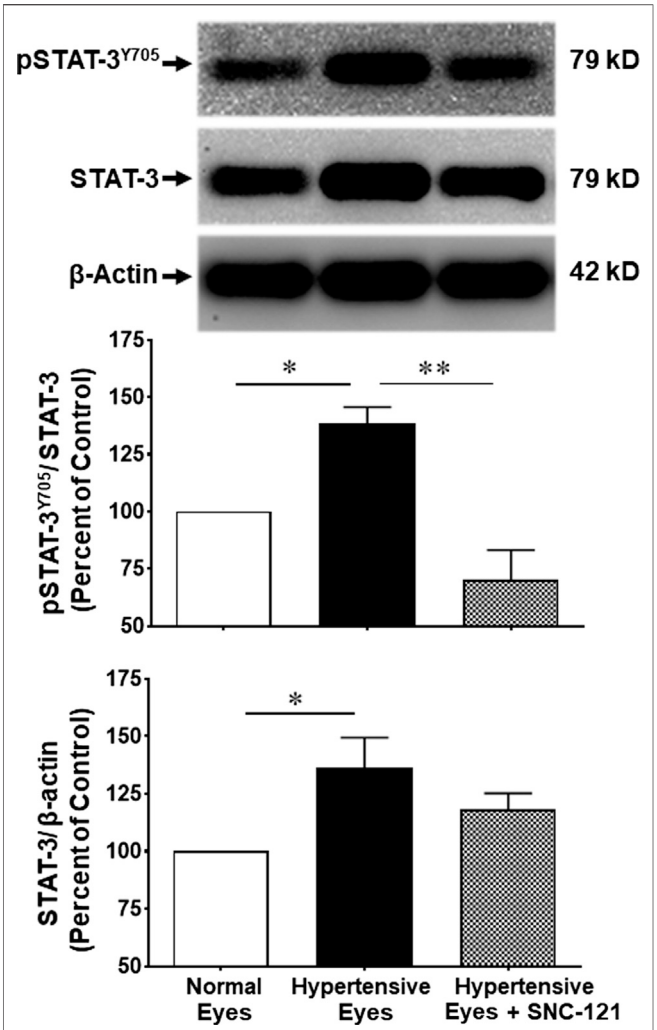

FIGURE 4 | Changes in the phosphorylation of STAT3 (Tyr 705) and total STAT3 by SNC-121 treatment in ocular hypertensive animals. The retina from normal, ocular hypertensive, and SNC-121 treated ocular hypertensive animals were collected at day 7, post hypertonic saline injection. Equivalent amount of retina protein extracts (20 μg) were analyzed by Western blotting using a selective anti-phosphoSTAT3 (Tyr 705), anti-STAT3, and anti-β-actin antibodies. The band intensities were measured using enhanced chemiluminescence reagent and Versadoc imaging system. Bar graph represents mean data ±SEM. OH Eyes; ocular hypertensive eyes; OH Eyes + SNC-121, ocular hypertensive eyes with SNC-121 treatment. *$p < 0.05$; ****$p < 0.0001$; $n = 6–9$. In this experiment "n" represent a biological replicate.

Fonseca et al., 2014; Sanderson et al., 2014). However, under pathological conditions the excessive release of pro-inflammatory cytokines and reactive oxygen species may cause synaptic dysfunction, disruption of axonal transport, and ultimately RGC death. Reactive astrocytes can secret a variety of cytokines and chemokines including CCL2, CXCL1, CXCL10, GM-CSF, and IL-6 that may further activate microglia, infiltrating dendritic cells, monocytes/macrophages and T cells in the inflamed tissues (Liddelow et al., 2017). Studies have also shown that mechanical strain due elevated IOP leads to the activation of NLRP3 inflammasome components *IL-1β*, *NLRP3, ASC*, and *CASP1* in rat and mouse retinas (Albalawi et al., 2017). As a result, an imbalance in pro- and anti-inflammatory cytokines will develop neuroinflammation that will slowly and progressively damage RGCs. In neurodegenerative diseases, neuroinflammation has been shown to be regulated by glial cells (astrogliosis and microglial activation), elements of blood brain barriers, and systemic inflammatory process (immune cells) that may be harmful or beneficial depending upon the severity and the duration of the neuroinflammation. As a result, neuroinflammation has been shown to play crucial roles in numerous neurodegenerative diseases including Alzheimer's disease, Atrophic Lateral Sclerosis, and glaucoma (Husain et al., 2012a; Calsolaro and Edison, 2016; Ransohoff, 2016; Liu and Wang, 2017; Williams et al., 2017).

In this manuscript, we have shown a significant increase in mRNA expression of pro-inflammatory cytokines and their associated signaling molecules including IL-1β, TNF-α, Fas, IL-6, LIF, and IFN-γ in response to glaucomatous injury, which was blocked by SNC-121 treatment. We chose 1 mg/kg body weight of SNC-121 based on our previous studies using a broad range opioid agonist and found 1 mg/kg body weight provide optimal neuroprotection (Husain et al., 2009). Additionally, we evaluated multiple doses of SNC-121 (0.01–10 mg/kg body weight) for RGC neuroprotection and found that 1–10 mg/kg doses of SNC-121 provide similar amount of RGC neuroprotection. Considering the addictive nature of opioids, we chose lower dose (1 mg/kg body weight) in all of our previous and current studies. Additionally, we did not find any additional beneficial effects if animals were treated with SNC-121 for up to 28 days (once a day) so we kept our drug treatment regimen to 7 days (Abdul et al., 2013). As a result of systemic treatment of SNC-121 for 7 days, we did not see any changes in the blood pressure, IOP, and body weight when compared with vehicle treated animal. Furthermore, we have shown that elevated protein expression of TNF-α (Abdul et al., 2013), IL-1β, and IL-6 were attenuated by SNC-121 treatment in ocular hypertensive animals. These data provide initial clues that elevated levels of pro-inflammatory cytokines that have been seen in glaucomatous retina is an early event. It important to emphasize that we have seen reduction of mRNA expression of Fas and LIF while their protein expressions were not measured in this study. We do understand that changes in mRNA expression may not always correspond to the changes in protein levels. Further studies will be required to confirm if SNC-121 treatment also affect the protein levels of Fas and LIF. In chronic glaucoma rat model, we have shown the loss of RGCs and their function (measured by Pattern Electroretinograms) at 14 days, post glaucomatous injury (Abdul et al., 2013), which indicates that production of pro-inflammatory cytokines preceded any RGC loss during glaucoma progression. Additionally, we have shown that SNC-121 treatment for 7 days reduces the production of pro-inflammatory cytokine (TNF-α), improved RGC function (as measured by Pattern ERGs), and reduced the loss of RGC numbers (as measured by retrograde labeling of RGCs) in rat glaucoma model (Abdul et al., 2013). Earlier, we have

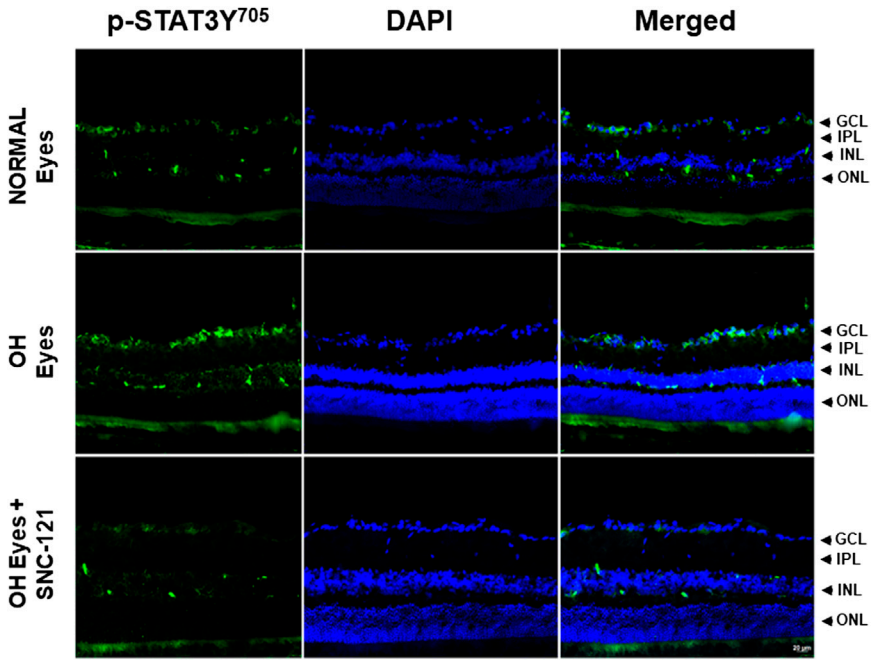

FIGURE 5 | Changes in the signal transducer and activator of transcription 3 (STAT3) phosphorylation in response to ocular hypertension and δ-opioid receptor agonist (SNC-121) treatment. The retina from normal, ocular hypertensive, and SNC-121 treated ocular hypertensive animals were collected at day 7, post hypertonic saline injection. Retina cryosections were immunostained using a selective anti-phosphoSTAT3 (Tyr 705) antibody and the nuclei were counterstained with DAPI. Green color indicates staining for phosphorylation of STAT3 and blue for the nuclei. There was no positive immunostaining when primary antibodies were omitted (not shown). Data shown here is a representation of at least four independent experiments. We have used four animals in each treatment group. OH Eyes; ocular hypertensive eyes; OH Eyes + SNC-121, ocular hypertensive eyes with SNC-121 treatment, bar size 20 μm.

demonstrated that SNC-121 actions were fully blocked by Naltrindole, a selective δ-opioid receptor antagonist (Akhter et al., 2013b; Husain et al., 2014; Zaidi.et al., 2020).

Similar to our data, studies have also shown that dysregulation of cytokine signaling in the RGC projections in DBA/2J mice was seen before IOP induction and axonal loss (Wilson et al., 2015). These findings prompted us to believe that activities of certain transcription factors may have been increased during the early stages of glaucoma. To shed more light on this idea, we measured the changes in the mRNA expression of transcription factors STAT1, STAT2, and STAT3 and found that mRNA levels of all STATs were increased in the retina of ocular hypertensive animals. Moreover, phosphorylation of STAT3 at tyrosine 705 was increased, which is known to be required for its activation and transcriptional activity. Intriguingly, STAT3 mRNA expression and phosphorylation were fully blocked by SNC-121 treatment. Based on these data, we believed that phosphorylation of STAT3 at tyrosine 705 is critical and plays a crucial role in the production of certain pro-inflammatory cytokines. This idea was further supported by the data that mRNA expression of IL-1β and IL-6 were completely inhibited by a selective STAT3 inhibitor, Stattic. Contrary to this, TNF-α and IFN-γ were partially inhibited by Stattic, suggesting that production of interleukins are mediated through STAT3 dependent pathways whereas other transcriptional factors such as p53, NF-κB, and c-fos could be involved in the production of other cytokines. Increases in IL-6 and JAK/STAT have been shown in early pressure-induced optic nerve head injury (Johnson et al., 2011). Conversely, IL-6 released from glial cells has been shown to protect RGCs in response to hydrostatic pressure induced apoptotic RGC death (Sappington et al., 2006). Earlier, we have shown that activation of δ-opioids receptors suppressed "redox-sensitive" transcriptional factor, nuclear factor-kappa B (NF-κB) in optic nerve head astrocytes (Akhter et al., 2013a). Proteomic analysis of glaucomatous retina obtained from human and experimental animal models also showed an up-regulation of receptor-interacting protein kinase (RIPK) that are also involved in the regulation of NF-κB (Tezel, 2013). Furthermore, studies have shown that antioxidant treatment can reduce NF-κB and neuroinflammation and provide neuroprotection in glaucoma model (Yang et al., 2016). Taken together, previous studies have shown that NF-κB plays key roles in glaucoma pathology (Kitaoka et al., 2006; Akhter et al., 2013a). However, we have not evaluated its direct involvement in the regulation of pro-inflammatory cytokines in the current study.

As a result of neuroinflammation, numerous downstream signaling pathways (e.g., cytokines-dependent proteins, caspases, and pro-apoptotic proteins) could also be up-regulated and facilitate the RGC death in glaucoma. We have shown a significant increase in Fas expression in ocular hypertensive animals. Fas is a constitutively expressed 45 kDa membrane bound protein that belongs to the TNF-α receptor superfamily (Watanabe-Fukunaga et al., 1992). FasL is a ligand

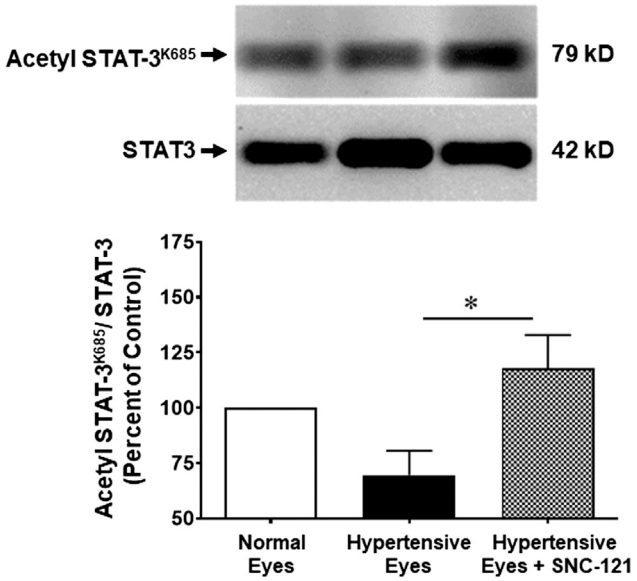

FIGURE 6 | Changes in STAT3 acetylation at lysine 685 (AcK685) in response to ocular hypertension and SNC-121 treatment. The retina from normal, ocular hypertensive, and SNC-121 treated ocular hypertensive animals were collected at day 7, post hypertonic saline injection. Equivalent amount of retina protein extracts (20 μg) were analyzed by Western blotting using a selective anti-Acetyl STAT3 (AcK685) or anti-β-actin antibodies. The band intensities were measured using enhanced chemiluminescence reagent and Versadoc imaging system. Bar graph represents mean data ±SEM. OH Eyes; ocular hypertensive eyes; OH Eyes + SNC-121, ocular hypertensive eyes with SNC-121 treatment. *$p < 0.05$. $n = 6$, In this experiment "n" represent a biological replicate.

for Fas, which is expressed in numerous activated T cells (Suda et al., 1995) and glial cells (Lee et al., 2000; Krishnan et al., 2019). The Fas/FasL system is essential for homeostasis of the immune system and its impairment can lead to neuroinflammation. Studies have also shown that pro-inflammatory cytokines can also increase the expression of Fas (Kondo et al., 2009). Our data shows an increase in Fas expression, which could be as a result of increased production of pro-inflammatory cytokines. Mechanistically, pro-inflammatory cytokines may facilitate Fas-mediated apoptosis of RGCs. Increased levels of both pro-inflammatory cytokines and Fas in the retina of ocular hypertensive animals indicated that these pro-inflammatory cytokines may have facilitated RGC death by caspases activation and apoptosis in Fas-dependent pathways as shown earlier in other systems (Ye et al., 2019). Our data showed that proinflammatory cytokines are inhibited by SNC-121 treatment, suggesting that δ-opioid agonist are potential agents to regulate neuroinflammation and RGC death in glaucoma. Earlier, we have shown that glaucomatous injury increased the protein expression of TNF-α, caspases-3, and 8 and all of them were blocked by a broad-range opioid agonist, Morphine (Husain et al., 2012a).

Data illustrated an increase in the leukemia inhibitory factor (LIF) and IL-6 in ocular hypertensive animals. LIF is a multi-functional cytokine which belongs to the IL-6 superfamily. IL-6 superfamily comprised of oncostatin M (OSM), IL-6, IL-11, ciliary neurotrophic factor (CNTF), and cardiotrophin-1 (CT-1) (Taupin et al., 1998; Turnley and Bartlett, 2000). LIF binds to its specific receptors LIFR, then recruit gp130 to form a high affinity receptor complex to induce the activation of the downstream signaling pathways such as JAK/STAT3, PI3K/Akt, ERK, and mTOR pathways (Burdon et al., 2002; Pera and Tam, 2010). We have shown that both LIF and STAT3 mRNA expression and STAT3 phosphorylation at tyrosine 705 were increased in the ocular hypertensive animals, which were fully blocked by SNC-121 treatment, suggesting that LIF might be required for the STAT3 activation for pro-inflammatory cytokines production. However, we did not measured the association of LIF with gp130 and JAK/STAT3 in the current study and this will be the goal for our future studies.

Recently, we have also shown that a sustained activation of δ-opioid receptors can lead to epigenetic changes via regulating histone acetylation and histone deacetylates (HDACs) in optic nerve head astrocytes and rat glaucoma model (Zaidi et al., 2020) and *unpublished results*). Considering our latest findings, we measured if δ-opioids-mediated epigenetic changes can regulate neuroinflammation in glaucoma. We hypothesized that protein acetylation provides RGC neuroprotection. We provide a mechanistic link that acetylation of STAT3 is reduced in response to glaucomatous injury when it was normalized with total STAT3. Conversely, we have seen a significant increase in the acetylation of STAT3 at lysine 685 (Ac-K685) by SNC-121 treatment in ocular hypertensive animals. Mechanistically, we proposed that δ-opioids will reduce HDACs and NF-κB activities and simultaneously increased acetylation of STAT3. Studies have shown that transcriptional activities of numerous transcription factors including STAT3 are regulated by lysine acetylation, which is regulated by HDACs. More recently, studies have shown that transcriptional factor NF-κB-mediated cytokines production is inhibited by HDAC inhibitors via acetylation-mediated NF-κB transcriptional activity (Kramer et al., 2006; Leus et al., 2016). Recently, we also have shown that reduced acetylation of Foxo1 (transcription factor) in hybrid Th1/17 cells results in its enhanced transcriptional activity (Chatterjee et al., 2018). These unique epigenetic-mediated signaling mechanisms play pivotal roles in non-ocular systems, however, if such transcription dysregulation exist in glaucoma remains largely unknown. We speculate existence of similar molecular mechanisms for δ-opioid-induced acetylation of STAT3 in the retina. In other systems, studies have shown that inhibition of HDACs enhances STAT acetylation, blocks NF-κB, and suppressed the production of pro-inflammatory cytokines (Kumar et al., 2017). In addition, HDAC inhibitor (sodium butyrate) attenuated STAT1-HDAC1/2 complex formation and simultaneously increased STAT1 acetylation. Increased acetylation of STAT1 increased its physical interaction with transcription factors (NF-κB or others), thereby inhibiting downstream signaling and production of pro-inflammatory cytokines (Feng et al., 2016; Li et al., 2016; Kumar et al., 2017). Data presented in the current manuscript

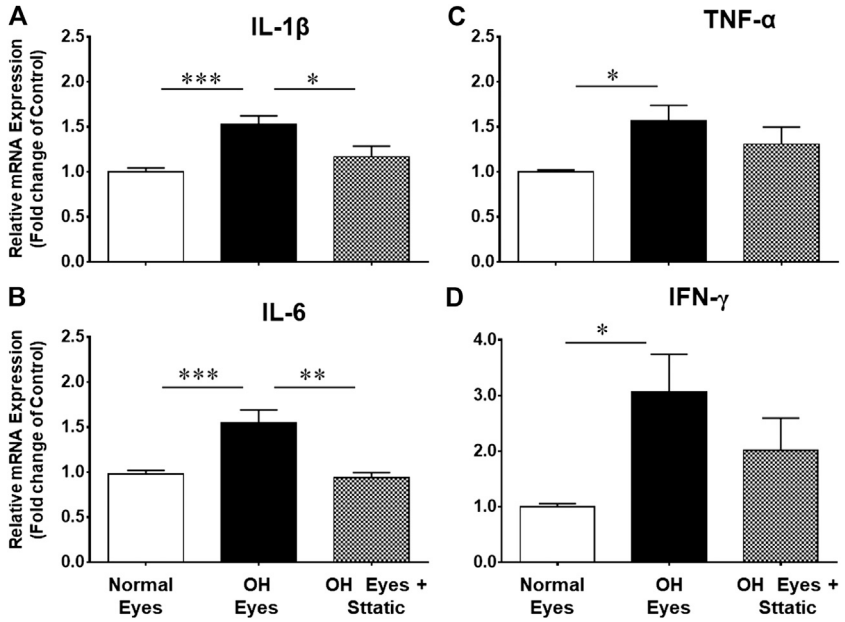

FIGURE 7 | Inhibitory effects of Stattic, a selective STAT3 inhibitor, on the mRNA expression of IL-1β **(A)**, TNF-α **(B)**, IL-6 **(C)**, and IFN-γ **(D)**. The retina from normal, ocular hypertensive, and Stattic treated ocular hypertensive animals were collected at day 7, post hypertonic saline injection. Complementary DNA was synthesized from 1 μg total RNA extracted from retina. The relative changes in mRNA levels were measured by quantitative RT-PCR (qRT-PCR) using primers specific for each gene as indicated in **Table 1**. The qRT-PCR data was normalized using β-actin gene expression as an internal control. The relative expression was calculated based on the comparative threshold cycle ($2^{-\Delta\Delta Ct}$) method. Bar graph represents mean data ±SEM. OH Eyes; ocular hypertensive eyes; OH Eyes + Stattic, ocular hypertensive eyes with Stattic treatment. *$p < 0.05$; **$p < 0.01$; ***$p < 0.001$; n = 6–9. In this experiment "n" represent a biological replicate.

support our hypothesis that protein acetylation regulates the activity of transcription factor STAT3, which will subsequently negatively regulate the production of pro-inflammatory cytokines (IL-1β and IL-6). Data also provide concrete evidence that δ-opioids regulate neuroinflammation via STAT3 dependent pathway in which protein acetylation played a regulatory role in the production of selective pro-inflammatory cytokines (e.g., IL-1β and IL-6), however, other transcription factors such as NF-κB may also be involved directly or indirectly in the regulation of cytokines. We cannot ruled out the anti-inflammatory roles of other non-opioid agents during glaucoma pathology.

Taken together, data presented in this manuscript provide evidence that numerous pro-inflammatory cytokines and their associated signaling molecules are up-regulated in response to glaucomatous injury. These cytokines are up-regulated at early stages of glaucoma and even prior to any RGC loss. Additionally, transcription factor (STAT3) activation and phosphorylation at tyrosine 705 is significantly increased in ocular hypertensive animals. In contrast, STAT3 acetylation at lysine 686 (Ac-K685) was not reduced by glaucomatous injury but significantly increased by δ-opioid receptor activation. Moreover, all pro-inflammatory cytokines and STAT3 phosphorylation were fully blocked by SNC-121. Intriguingly, a selective inhibitor of STAT3, Stattic, fully blocked the production of IL-1β and IL-6 but it had a partial inhibitory effect on TNF-α and IFN-γ, suggesting the involvement of other transcriptional factors.

CONCLUSION

In conclusion, data presented in the current manuscript support the idea that multiple neuroinflammatory genes and pathways are involved in the development of glaucoma. However, more work is needed to determine when and how these genes and pathways are activated. It is also equally important to know which genes and pathways are neuroprotective or pathogenic in glaucoma. The current study provides novel insights that pro-inflammatory cytokines such as IL-1β and IL-6 are regulated by δ-opioids via STAT3-dependent pathways in rat glaucoma model. The understanding of the regulatory mechanisms involved in components of inflammatory responses will be highly desired to develop a better therapy that can target neuroinflammation. This information would then guide future therapeutic strategies, which would include the use of selective inhibitors to target pro-inflammatory cytokines or its upstream regulators to treat glaucoma patients.

Opioid receptor agonists (e.g., morphine and buprenorphine) are widely used in clinics for pain management. However, chronic use of opioids can also results in unwarranted side effects (e.g., addiction and withdrawal). However, δ-opioids have lesser side effects as compared to broad range non-selective opioids. Alternatively, side-effects of opioids can be overcome by local application (e.g., topical or intravitreal) vs. systemic application. Nevertheless, the therapeutic potential of δ-opioid agonists have been shown in preclinical models for other conditions including Parkinson's disease, pain management, and depression. Based on

our data, we strongly believe that δ-opioid agonists represent to have a high potential for glaucoma therapy.

DATA AVAILABILITY STATEMENT

The raw data supporting the conclusions of this article will be made available by the authors, without undue reservation.

ETHICS STATEMENT

The animal study was reviewed and approved by IACUC MUSC.

AUTHOR CONTRIBUTIONS

SH contributed in conception, design of the work, analysis, and interpretation of data. SZ contributed in collection and analyzing of data. SS and WG contributed in collection of data. SM contributed in acquisition of mRNA data. All authors read and approved the final manuscript.

FUNDING

This study was supported by NIH/NEI grant EY-027355 (SH).

REFERENCES

Abdul, Y., Akhter, N., and Husain, S. (2013). Delta-opioid agonist SNC-121 protects retinal ganglion cell function in a chronic ocular hypertensive rat model. *Invest. Ophthalmol. Vis. Sci.* 54 (3), 1816–1828. doi:10.1167/iovs.12-10741

Adornetto, A., Russo, R., and Parisi, V. (2019). Neuroinflammation as a target for glaucoma therapy. *Neural Regen Res.* 14 (3), 391–394. doi:10.4103/1673-5374.245465

Airaksinen, P. J., and Heijl, A. (1983). Visual field and retinal nerve fibre layer in early glaucoma after optic disc haemorrhage. *Acta Ophthalmol.* 61 (2), 186–194. doi:10.1111/j.1755-3768.1983.tb01412.x

Akhter, N., Nix, M., Abdul, Y., Singh, S., and Husain, S. (2013a). Delta-opioid receptors attenuate TNF-alpha-induced MMP-2 secretion from human ONH astrocytes. *Invest. Ophthalmol. Vis. Sci.* 54 (10), 6605–6611. doi:10.1167/iovs.13-12196

Akhter, N., Nix, M., Abdul, Y., Singh, S., and Husain, S. (2013b). Delta-opioid receptors attenuate TNF-α-induced MMP-2 secretion from human ONH astrocytes. *Invest. Ophthalmol. Vis. Sci.* 54 (10), 6605–6611. doi:10.1167/iovs.13-12196

Albalawi, F., Lu, W., Beckel, J. M., Lim, J. C., McCaughey, S. A., and Mitchell, C. H. (2017). The P2X7 receptor primes IL-1beta and the NLRP3 inflammasome in astrocytes exposed to mechanical strain. *Front. Cell. Neurosci.* 11, 227. doi:10.3389/fncel.2017.00227

Alkozi, H. A., Franco, R., and Pintor, J. J. (2017). Epigenetics in the eye: an overview of the most relevant ocular diseases. *Front. Genet.* 8, 144. doi:10.3389/fgene.2017.00144

Almasieh, M., Wilson, A. M., Morquette, B., Cueva Vargas, J. L., and Di Polo, A. (2012). The molecular basis of retinal ganglion cell death in glaucoma. *Prog. Retin. Eye Res.* 31 (2), 152–181. doi:10.1016/j.preteyeres.2011.11.002

Alsarraf, O., Fan, J., Dahrouj, M., Chou, C. J., Menick, D. R., and Crosson, C. E. (2014a). Acetylation: a lysine modification with neuroprotective effects in ischemic retinal degeneration. *Exp. Eye Res.* 127, 124–131. doi:10.1016/j.exer.2014.07.012

Alsarraf, O., Fan, J., Dahrouj, M., Chou, C. J., Yates, P. W., and Crosson, C. E. (2014b). Acetylation preserves retinal ganglion cell structure and function in a chronic model of ocular hypertension. *Invest. Ophthalmol. Vis. Sci* 55 (11), 7486–7493. doi:10.1167/iovs.14-14792

Baneke, A. J., Lim, K. S., and Stanford, M. (2016). The pathogenesis of raised intraocular pressure in uveitis. *Curr. Eye Res* 41 (2), 137–149. doi:10.3109/02713683.2015.1017650

Benoist d'Azy, C., Pereira, B., Chiambaretta, F., and Dutheil, F. (2016). Oxidative and anti-oxidative stress markers in chronic glaucoma: a systematic review and meta-analysis. *PLoS One.* 11 (12), e0166915. doi:10.1371/journal.pone.0166915

Berson, A., Nativio, R., Berger, S. L., and Bonini, N. M. (2018). Epigenetic regulation in neurodegenerative diseases. *Trends Neurosci* 41 (9), 587–598. doi:10.1016/j.tins.2018.05.005

Bodh, S. A., Kumar, V., Raina, U. K., Ghosh, B., and Thakar, M. (2011). Inflammatory glaucoma. *Oman J. Ophthalmol.* 4 (1), 3–9. doi:10.4103/0974-620X.77655

Boland, M. V., and Quigley, H. A. (2007). Risk factors and open-angle glaucoma: classification and application. *J. Glaucoma.* 16 (4), 406–418. doi:10.1097/IJG.0b013e31806540a1

Bucolo, C., Campana, G., Di Toro, R., Cacciaguerra, S., and Spampinato, S. (1999). Sigma1 recognition sites in rabbit iris-ciliary body: topical sigma1-site agonists lower intraocular pressure. *J. Pharmacol. Exp. Ther.* 289 (3), 1362–1369

Burdon, T., Smith, A., and Savatier, P. (2002). Signalling, cell cycle and pluripotent in embryonic stem cells. *Trends Cell Biol.* 12 (9), 432–438. doi:10.1016/s0962-8924(02)02352-8

Calsolaro, V., and Edison, P. (2016). Neuroinflammation in alzheimer's disease: current evidence and future directions. *Alzheimers Dement* 12 (6), 719–732. doi:10.1016/j.jalz.2016.02.010

Carcole, M., Kummer, S., Goncalves, L., Zamanillo, D., Merlos, M., Dickenson, A. H., et al. (2019). Sigma-1 receptor modulates neuroinflammation associated with mechanical hypersensitivity and opioid tolerance in a mouse model of osteoarthritis pain. *Br. J. Pharmacol.* 176 (20), 3939–3955. doi:10.1111/bph.14794

Chatterjee, S., Daenthanasanmak, A., Chakraborty, P., Wyatt, M. W., Dhar, P., Selvam, S. P., et al. (2018). CD38-NAD(+)axis regulates immunotherapeutic anti-tumor T cell response. *Cell Metabol.* 27 (1), 85–100.e8. doi:10.1016/j.cmet.2017.10.006

Chitranshi, N., Dheer, Y., Abbasi, M., You, Y., Graham, S. L., and Gupta, V. (2018). Glaucoma pathogenesis and neurotrophins: focus on the molecular and genetic basis for therapeutic prospects. *Curr. Neuropharmacol.* 16 (7), 1018–1035. doi:10.2174/1570159X16666180419121247

Choi, F., Park, K. H., Kim, D. M., and Kim, T. W. (2007). Retinal nerve fiber layer thickness evaluation using optical coherence tomography in eyes with optic disc hemorrhage. *Ophthalmic Surg. Laser. Imag.* 38 (2), 118–125. doi:10.3928/15428877-20070301-06

Chua, J., Vania, M., Cheung, C. M., Ang, M., Chee, S. P., Yang, H., et al. (2012). Expression profile of inflammatory cytokines in aqueous from glaucomatous eyes. *Mol. Vis.* 18, 431–438

Crosson, C. E., Mani, S. K., Husain, S., Alsarraf, O., and Menick, D. R. (2010). Inhibition of histone deacetylase protects the retina from ischemic injury. *Invest. Ophthalmol. Vis. Sci.* 51 (7), 3639–3645. doi:10.1167/iovs.09-4538

da Fonseca, A. C., Matias, D., Garcia, C., Amaral, R., Geraldo, L. H., Freitas, C., et al. (2014). The impact of microglial activation on blood-brain barrier in brain diseases. *Front. Cell. Neurosci.* 8, 362. doi:10.3389/fncel.2014.00362

Didonna, A., and Opal, P. (2015). The promise and perils of HDAC inhibitors in neurodegeneration. *Ann Clin Transl Neurol.* 2 (1), 79–101. doi:10.1002/acn3.147

Drance, S. M. (1989). Disc hemorrhages in the glaucomas. *Surv. Ophthalmol.* 33 (5), 331–337. doi:10.1016/0039-6257(89)90010-6

Feng, Q., Su, Z., Song, S., Chiu, H., Zhang, B., Yi, L., et al. (2016). Histone deacetylase inhibitors suppress RSV infection and alleviate virus-induced airway inflammation. *Int. J. Mol. Med* 38 (3), 812–822. doi:10.3892/ijmm.2016.2691

Ferrante, R. J., Kubilus, J. K., Lee, J., Ryu, H., Beesen, A., Zucker, B., et al. (2003). Histone deacetylase inhibition by sodium butyrate chemotherapy ameliorates the neurodegenerative phenotype in huntington's disease mice. *J. Neurosci.* 23 (28), 9418–9427. doi:10.1523/jneurosci.23-28-09418.2003

Gordon, J., and Piltz-Seymour, J. R. (1997). The significance of optic disc hemorrhages in glaucoma. *J. Glaucoma*. 6 (1), 62–64

Grieshaber, M. C., Orgul, S., Schoetzau, A., and Flammer, J. (2007). Relationship between retinal glial cell activation in glaucoma and vascular dysregulation. *J. Glaucoma*. 16 (2), 215–219. doi:10.1097/IJG.0b013e31802d045a

Haberland, M., Montgomery, R. L., and Olson, E. N. (2009). The many roles of histone deacetylates in development and physiology: implications for disease and therapy. *Nat. Rev. Genet* 10 (1), 32–42. doi:10.1038/nrg2485

Husain, S., Abdul, Y., and Crosson, C. E. (2012a). Preservation of retina ganglion cell function by morphine in a chronic ocular-hypertensive rat model. *Invest. Ophthalmol. Vis. Sci*. 53 (7), 4289–4298. doi:10.1167/iovs.12-9467

Husain, S., Abdul, Y., and Potter, D. E. (2012b). Non-analgesic effects of opioids: neuroprotection in the retina. *Curr. Pharmaceut. Des*. 18 (37), 6101–6108. doi:10.2174/138161212803582441

Husain, S., Abdul, Y., Singh, S., Ahmad, A., and Husain, M. (2014). Regulation of nitric oxide production by δ-opioid receptors during glaucomatous injury. *PLoS One* 9 (10), e110397. doi:10.1371/journal.pone.0110397

Husain, S., Ahmad, A., Singh, S., Peterseim, C., Abdul, Y., and Nutaitis, M. J. (2017). PI3K/Akt pathway: a role in delta-opioid receptor-mediated RGC neuroprotection. *Invest. Ophthalmol. Vis. Sci*. 58 (14), 6489–6499. doi:10.1167/iovs.16-20673

Husain, S. (2018). Delta opioids: neuroprotective roles in preclinical studies. *J. Ocul. Pharmacol. Ther*. 34 (1-2), 119–128. doi:10.1089/jop.2017.0039

Husain, S., Potter, D. E., and Crosson, C. E. (2009). Opioid receptor-activation: retina protected from ischemic injury. *Invest. Ophthalmol. Vis. Sci*. 50 (8), 3853–3859. doi:10.1167/iovs.08-2907

Hwang, Y. H., Kim, Y. Y., Kim, H. K., and Sohn, Y. H. (2014). Changes in retinal nerve fiber layer thickness after optic disc hemorrhage in glaucomatous eyes. *J. Glaucoma* 23 (8), 547–552. doi:10.1097/IJG.0000000000000083

Johnson, E. C., Doser, T. A., Cepurna, W. O., Dyck, J. A., Jia, L., Guo, Y., et al. (2011). Cell proliferation and interleukin-6-type cytokine signaling are implicated by gene expression responses in early optic nerve head injury in rat glaucoma. *Invest. Ophthalmol. Vis. Sci* 52 (1), 504–518. doi:10.1167/iovs.10-5317

Kitaoka, Y., Kitaoka, Y., Kwong, J. M., Ross-Cisneros, F. N., Wang, J., Tsai, R. K., et al. (2006). TNF-alpha-induced optic nerve degeneration and nuclear factor-kappab p65. *Invest. Ophthalmol. Vis. Sci*. 47 (4), 1448–1457. doi:10.1167/iovs.05-0299

Kondo, M., Murakawa, Y., Harashima, N., Kobayashi, S., Yamaguchi, S., and Harada, M. (2009). Roles of proinflammatory cytokines and the fas/fas ligand interaction in the pathogenesis of inflammatory myopathies. *Immunology* 128 (1 Suppl. l), e589–599. doi:10.1111/j.1365-2567.2008.03039.x

Kramer, O. H., Baus, D., Knauer, S. K., Stein, S., Jager, E., Stauber, R. H., et al. (2006). Acetylation of stat1 modulates NF-kappab activity. *Genes Dev*. 20 (4), 473–485. doi:10.1101/gad.364306

Krishnan, A., Kocab, A. J., Zacks, D. N., Marshak-Rothstein, A., and Gregory-Ksander, M. (2019). A small peptide antagonist of the fas receptor inhibits neuroinflammation and prevents axon degeneration and retinal ganglion cell death in an inducible mouse model of glaucoma. *J. Neuroinflammation* 16 (1), 184. doi:10.1186/s12974-019-1576-3

Kumar, P., Gogulamudi, V. R., Periasamy, R., Raghavaraju, G., Subramanian, U., and Pandey, K. N. (2017). Inhibition of HDAC enhances STAT acetylation, blocks NF-kappab, and suppresses the renal inflammation and fibrosis in Npr1 haplotype male mice. *Am. J. Physiol. Ren. Physiol*. 313 (3), F781–F795. doi:10.1152/ajprenal.00166.2017

Lebrun-Julien, F., and Suter, U. (2015). Combined HDAC1 and HDAC2 depletion promotes retinal ganglion cell survival after injury through reduction of p53 target gene expression. *ASN Neuro*. 7 (3). doi:10.1177/1759091415593066

Lee, S. J., Zhou, T., Choi, C., Wang, Z., and Benveniste, E. N. (2000). Differential regulation and function of fas expression on glial cells. *J. Immunol* 164 (3), 1277–1285. doi:10.4049/jimmunol.164.3.1277

Leus, N. G., Zwinderman, M. R., and Dekker, F. J. (2016). Histone deacetylase 3 (HDAC 3) as emerging drug target in NF-kappaB-mediated inflammation. *Curr. Opin. Chem. Biol*. 33, 160–168. doi:10.1016/j.cbpa.2016.06.019

Li, Z. Y., Li, Q. Z., Chen, L., Chen, B. D., Wang, B., Zhang, X. J., et al. (2016). Histone deacetylase inhibitor RGFP109 overcomes temozolomide resistance by blocking NF-kappaB-dependent transcription in glioblastoma cell lines. *Neurochem. Res* 41 (12), 3192–3205. doi:10.1007/s11064-016-2043-5

Liddelow, S. A., Guttenplan, K. A., Clarke, L. E., Bennett, F. C., Bohlen, C. J., Schirmer, L., et al. (2017). Neurotoxic reactive astrocytes are induced by activated microglia. *Nature* 541 (7638), 481–487. doi:10.1038/nature21029

Liu, J., and Wang, F. (2017). Role of neuroinflammation in amyotrophic lateral sclerosis: cellular mechanisms and therapeutic implications. *Front. Immunol* 8, 1005. doi:10.3389/fimmu.2017.01005

Neal, M., and Richardson, J. R. (2018). Epigenetic regulation of astrocyte function in neuroinflammation and neurodegeneration. *Biochim. Biophys. Acta (BBA) Mol. Basis Dis* 1864 (2), 432–443. doi:10.1016/j.bbadis.2017.11.004

Ohira, S., Inoue, T., Iwao, K., Takahashi, E., and Tanihara, H. (2016). Factors influencing aqueous proinflammatory cytokines and growth factors in uveitic glaucoma. *PLoS One* 11 (1), e0147080. doi:10.1371/journal.pone.0147080

Osborne, N. N., Nunez-Alvarez, C., Joglar, B., and Del Olmo-Aguado, S. (2016). Glaucoma: focus on mitochondria in relation to pathogenesis and neuroprotection. *Eur. J. Pharmacol* 787, 127–133. doi:10.1016/j.ejphar.2016.04.032

Pelzel, H. R., Schlamp, C. L., and Nickells, R. W. (2010). Histone H4 deacetylation plays a critical role in early gene silencing during neuronal apoptosis. *BMC Neurosci* 11, 62. doi:10.1186/1471-2202-11-62

Pera, M. F., and Tam, P. P. (2010). Extrinsic regulation of pluripotent stem cells. *Nature* 465 (7299), 713–720. doi:10.1038/nature09228

Ransohoff, R. M. (2016). How neuroinflammation contributes to neurodegeneration. *Science* 353 (6301), 777–783. doi:10.1126/science.aag2590

Rouaux, C., Jokic, N., Mbebi, C., Boutillier, S., Loeffler, J. P., and Boutillier, A. L. (2003). Critical loss of CBP/p300 histone acetylase activity by caspases-6 during neurodegeneration. *EMBO J* 22 (24), 6537–6549. doi:10.1093/emboj/cdg615

Ryu, H., Smith, K., Camelo, S. I., Carreras, I., Lee, J., Iglesias, A. H., et al. (2005). Sodium phenylbutyrate prolongs survival and regulates expression of anti-apoptotic genes in transgenic amyotrophic lateral sclerosis mice. *J. Neurochem*. 93 (5), 1087–1098. doi:10.1111/j.1471-4159.2005.03077.x

Saha, R. N., and Pahan, K. (2006). HATs and HDACs in neurodegeneration: a tale of disconcerted acetylation homeostasis. *Cell Death Differ* 13 (4), 539–550. doi:10.1038/sj.cdd.4401769

Sanderson, J., Dartt, D. A., Trinkaus-Randall, V., Pintor, J., Civan, M. M., Delamere, N. A., et al. (2014). Purines in the eye: recent evidence for the physiological and pathological role of purines in the RPE, retinal neurons, astrocytes, Muller cells, lens, trabecular meshwork, cornea and lacrimal gland. *Exp. Eye Res*. 127, 270–279. doi:10.1016/j.exer.2014.08.009

Sappington, R. M., Chan, M., and Calkins, D. J. (2006). Interleukin-6 protects retinal ganglion cells from pressure-induced death. *Invest. Ophthalmol. Vis. Sci* 47 (7), 2932–2942. doi:10.1167/iovs.05-1407

Schmitt, H. M., Pelzel, H. R., Schlamp, C. L., and Nickells, R. W. (2014). Histone deacetylase 3 (HDAC3) plays an important role in retinal ganglion cell death after acute optic nerve injury. *Mol. Neurodegener* 9, 39. doi:10.1186/1750-1326-9-39

Siddique, S. S., Suelves, A. M., Baheti, U., and Foster, C. S. (2013). Glaucoma and uveitis. *Surv. Ophthalmol* 58 (1), 1–10. doi:10.1016/j.survophthal.2012.04.006

Suda, T., Okazaki, T., Naito, Y., Yokota, T., Arai, N., Ozaki, S., et al. (1995). Expression of the fas ligand in cells of T cell lineage. *J. Immunol* 154 (8), 3806–3813

Taupin, J. L., Pitard, V., Dechanet, J., Miossec, V., Gualde, N., and Moreau, J. F. (1998). Leukemia inhibitory factor: part of a large ingathering family. *Int. Rev. Immunol* 16 (3-4), 397–426. doi:10.3109/08830189809043003

Tejada, M. A., Montilla-Garcia, A., Gonzalez-Cano, R., Bravo-Caparros, I., Ruiz-Cantero, M. C., Nieto, F. R., et al. (2018). Targeting immune-driven opioid analgesia by sigma-1 receptors: opening the door to novel perspectives for the analgesic use of sigma-1 antagonists. *Pharmacol. Res*. 131, 224–230. doi:10.1016/j.phrs.2018.02.008

Tezel, G. (2013). Immune regulation toward immunomodulation for neuroprotection in glaucoma. *Curr. Opin. Pharmacol*. 13 (1), 23–31. doi:10.1016/j.coph.2012.09.013

Turnley, A. M., and Bartlett, P. F. (2000). Cytokines that signal through the leukemia inhibitory factor receptor-beta complex in the nervous system. *J. Neurochem*. 74 (3), 889–899. doi:10.1046/j.1471-4159.2000.0740889.x

Watanabe-Fukunaga, R., Brannan, C. I., Itoh, N., Yonehara, S., Copeland, N. G., Jenkins, N. A., et al. (1992). The cDNA structure, expression, and chromosomal assignment of the mouse fas antigen. *J. Immunol* 148 (4), 1274–1279

Williams, P. A., Marsh-Armstrong, N., Howell, G. R., Lasker, I. I. o. A., and Glaucomatous Neurodegeneration, P. (2017). neuroinflammation in glaucoma: a new opportunity. *Exp. Eye Res.* 157, 20–27. doi:10.1016/j.exer.2017.02.014

Wilson, G. N., Inman, D. M., Dengler Crish, C. M., Smith, M. A., and Crish, S. D. (2015). Early pro-inflammatory cytokine elevations in the DBA/2J mouse model of glaucoma. *J. Neuroinflammation.* 12, 176. doi:10.1186/s12974-015-0399-0

Yang, X., Hondur, G., and Tezel, G. (2016). Antioxidant treatment limits neuroinflammation in experimental glaucoma. *Invest. Ophthalmol. Vis. Sci.* 57 (4), 2344–2354. doi:10.1167/iovs.16-19153

Ye, Q., Lin, Y. N., Xie, M. S., Yao, Y. H., Tang, S. M., Huang, Y., et al. (2019). Effects of etanercept on the apoptosis of ganglion cells and expression of fas, TNF-alpha, caspases-8 in the retina of diabetic rats. *Int. J. Ophthalmol* 12 (7), 1083–1088. doi:10.18240/ijo.2019.07.05

Zaidi, S., Thakore, N., Singh, S., Mehrotra, S., Gangaraju, V., and Husain, S. (2020). Histone deacetylases regulation by δ-opioids in human optic nerve head astrocytes. *Invest. Ophthalmol. Vis. Sci.* [Epub ahead of print]. 10.1167/iovs.61.11.17

Zenkel, M., Lewczuk, P., Junemann, A., Kruse, F. E., Naumann, G. O., and Schlotzer-Schrehardt, U. (2010). Proinflammatory cytokines are involved in the initiation of the abnormal matrix process in pseudoexfoliation syndrome/glaucoma. *Am. J. Pathol.* 176 (6), 2868–2879. doi:10.2353/ajpath.2010.090914

Conflict of Interest: The authors declare that the research was conducted in the absence of any commercial or financial relationships that could be construed as a potential conflict of interest.

frontiers in Pharmacology

ORIGINAL RESEARCH
published: 26 February 2021
doi: 10.3389/fphar.2021.606232

The Effect of Plasma Rich in Growth Factors on Microglial Migration, Macroglial Gliosis and Proliferation, and Neuronal Survival

Noelia Ruzafa[1,2], *Xandra Pereiro*[1,2], *Alex Fonollosa*[1,3,2], *Javier Araiz*[1,2], *Arantxa Acera*[1,4] *and Elena Vecino*[1,2]*

[1]Experimental Ophthalmo-Biology Group (GOBE, www-ehu.eus/GOBE), Department of Cell Biology and Histology, University of Basque Country UPV/EHU, Leioa, Spain, [2]Begiker-Ophthalmology Research Group, BioCruces Health Research Institute, Cruces Hospital, Bilbao, Spain, [3]Department of Ophthalmology, University of Basque Country UPV/EHU, Leioa, Spain, [4]Biodonostia Health Research Institute, Donostia Hospital, San Sebastian, Spain

Plasma rich in growth factors (PRGF) is a subtype of platelet-rich plasma that has being employed in the clinic due to its capacity to accelerate tissue regeneration. Autologous PRGF has been used in ophthalmology to repair a range of retinal pathologies with some efficiency. In the present study, we have explored the role of PRGF and its effect on microglial motility, as well as its possible pro-inflammatory effects. Organotypic cultures from adult pig retinas were used to test the effect of the PRGF obtained from human as well as pig blood. Microglial migration, as well as gliosis, proliferation and the survival of retinal ganglion cells (RGCs) were analyzed by immunohistochemistry. The cytokines present in these PRGFs were analyzed by multiplex ELISA. In addition, we set out to determine if blocking some of the inflammatory components of PRGF alter its effect on microglial migration. In organotypic cultures, PRGF induces microglial migration to the outer nuclear layers as a sign of inflammation. This phenomenon could be due to the presence of several cytokines in PRGF that were quantified here, such as the major pro-inflammatory cytokines IL-1β, IL-6 and TNFα. Heterologous PRGF (human) and longer periods of cultured (3 days) induced more microglia migration than autologous porcine PRGF. Moreover, the migratory effect of microglia was partially mitigated by: 1) heat inactivation of the PRGF; 2) the presence of dexamethasone; or 3) anti-cytokine factors. Furthermore, PRGF seems not to affect gliosis, proliferation or RGC survival in organotypic cultures of adult porcine retinas. PRGF can trigger an inflammatory response as witnessed by the activation of microglial migration in the retina. This can be prevented by using autologous PRGF or if this is not possible due to autoimmune diseases, by mitigating its inflammatory effect. In addition, PRGF does not increase either the proliferation rate of microglial cells or the survival of neurons. We cannot discard the possible positive effect of microglial cells on retinal function. Further studies should be performed to warrant the use of PRGF on the nervous system.

Keywords: retina, ophthalmology, plasma rich in growth factors, microglia, inflammation, cytokines, neuron, glia

OPEN ACCESS

Edited by:
Julie Sanderson, University of East Anglia, United Kingdom

Reviewed by:
Debasis Nayak, Indian Institute of Technology Indore, India
Stephanie C Joachim, Ruhr University Bochum, Germany

***Correspondence:**
Elena Vecino
elena.vecino@ehu.es

Specialty section:
This article was submitted to Inflammation Pharmacology, a section of the journal Frontiers in Pharmacology

Received: *14 September 2020*
Accepted: *25 January 2021*
Published: *26 February 2021*

Citation:
Ruzafa N, Pereiro X, Fonollosa A, Araiz J, Acera A and Vecino E (2021) The Effect of Plasma Rich in Growth Factors on Microglial Migration, Macroglial Gliosis and Proliferation, and Neuronal Survival. Front. Pharmacol. 12:606232. doi: 10.3389/fphar.2021.606232

INTRODUCTION

Platelet preparations, including platelet-rich plasma (PRP), contain high concentrations of growth factors that promote regeneration, and they are generally considered to be safe to use and typically inexpensive to obtain (Marx et al., 1998; Wang and Avila, 2007; Cole et al., 2010; Dhurat and Sukesh, 2014). Plasma rich in growth factors (PRGF) is a subtype of P-PRP (pure platelet-rich plasma), which are preparations without leukocytes and with a low-density fibrin network that may stimulate tissue regeneration (Dohan Ehrenfest et al., 2014). Autologous PRGF has been approved for clinical use in the European Community and by the U.S. Food and Drug Administration (FDA: Hayashi and Takagi, 2015; Cui et al., 2017; Osborne et al., 2018), and it has commonly been employed in ophthalmology in the form of eye drops (Lopez-Plandolit et al., 2010; Lopez-Plandolit et al., 2011; Merayo-Lloves et al., 2015; Sanchez-Avila et al., 2018). In addition, pilot studies are currently being carried out regarding the use of PRGF in retinal surgery to treat persistent macular holes (Arias et al., 2019) and autologous platelet injections have been used to treat recurrent retinal detachment (Nadal et al., 2012). However, the full range of responses that could be triggered by PRGF are not fully understood.

The PRGF used in the clinic is often autologous, obtained from the patient's own blood, although human PRGF has also been used in studies with mice (Anitua et al., 2013; Anitua et al., 2014b; Anitua et al., 2015a). This fact could be important to establish therapies for patients suffering from autoimmune diseases whose autologous PRGF may contain auto-antibodies (Anitua et al., 2014a), or for patients in whom their own PRGF is not as effective as expected due to variations in specific factors (Vahabi et al., 2015). Thus, we set out here to assess the effect of PRGF of two different origins. The model animal selected for this study was the pig, as the porcine retina is the most similar to the human retina among large mammals (Prince and Ruskell, 1960; Vecino and Sharma, 2011).

In the central nervous system (CNS), PRGF can interact with glial cells, promoting their survival, proliferation and differentiation (O'kusky et al., 2000; Jin et al., 2002; Anitua et al., 2009; Anitua et al., 2014b), as well as influencing inflammatory processes (Anitua et al., 2015a). Microglia are one of the three main types of glial cells in the mammalian retina and they form a population of resident macrophages within the CNS that are not only involved in immune responses but also, that participate in the development and maintenance of neural networks. Thus, microglia represent an important nexus between the neurological and immunological activity in the CNS (Fernandes et al., 2014; Gertig and Hanisch, 2014; Vecino et al., 2016; Davis et al., 2017).

Microglia are quiescent in the normal adult retina, exhibiting a characteristic ramified morphology that allows them to scan their environment and phagocytose cell debris. In these conditions, resident microglia are strictly limited to the inner retinal layers, mainly populating the plexiform layers (Lee et al., 2008; Buschini et al., 2011). However, microglia become activated in response to neuronal injury or immunological stimuli (Streit et al., 1988; Kreutzberg, 1996; Block and Hong, 2005) and in the retina, the activation of resident microglia drives their migration to the outer retinal layers, where they transform into activated, ameboid, full-blown phagocytes that interact with infiltrating blood cells (Karlstetter et al., 2015). All types of neuroinflammation produce chronic microglial activation, including ocular inflammation, which is coupled to the release of inflammatory mediators and phagocytosis (Block and Hong, 2005). Thus, activated microglia fulfill an important role in the initiation and propagation of neurodegenerative processes (Madeira et al., 2015a). Given the location and size of microglia, and the fact that they may migrate to the outer layers of the retina in an inflammatory explant model, these cells resemble the hyperreflective dots that can be seen in the ONL and external limiting membrane in uveitis and ocular inflammation when studied by optical coherence tomography (OCT) *in vivo* (Coscas et al., 2013; Vujosevic et al., 2013; Pakzad-Vaezi et al., 2014). These dots are a sign of disease progression and prognosis, such that the *in vivo* imaging of microglia by OCT may increase its diagnostic value in clinical ophthalmology, and this can be studied in the model of organotypic retinal culture used here. Therefore, we analyzed the inflammatory response to PRGF by assessing microglial cell migration in retinal explants exposed to PRGF and by characterizing the inflammatory cytokines it contains. Moreover, the inflammatory response to PRGF was compromised by heat inactivation, by adding dexamethasone (Dex) as an anti-inflammatory drug, or by adding antibodies against some pro-inflammatory cytokines to the PRGF in order to study whether these manipulations inhibit the inflammatory response of microglia to PRGF.

In relation to the inflammatory processes, macroglia also respond to and undergo reactive gliosis. Retinal macroglia include Müller cells and astrocytes, the former extending across the thickness of the retina to provide structural stability and maintaining close contact with the majority of retinal neurons. Astrocytes are mostly located in the nerve fiber layer and they accompany the blood vessels. Both these cell types provide trophic factors to neurons, which promote cell survival and repair, as well as maintaining retinal homeostasis and that of the blood–retina barrier (Bringmann and Reichenbach, 2001; Bringmann et al., 2006; Reichenbach and Bringmann, 2013; Vecino et al., 2016). Reactive gliosis is a response to a multitude of insults and disorders, altering the thickening and enlargement of Müller cells, and of astrocyte processes. Typical features of macroglial gliosis involve cellular hypertrophy, such as the up-regulation of intermediate filament (IF) expression (e.g., glial fibrillary acidic protein -GFAP) or increased rates of proliferation (Barres, 2008; Vecino et al., 2016). Thus, the rate of glial cell proliferation may be altered in the presence of PRGF as it is known to contain growth factors that accelerate glial cell proliferation (O'kusky et al., 2000; Jin et al., 2002; Anitua et al., 2009; Anitua et al., 2014b), such as platelet-derived growth factor (PDGF), fibroblast growth factor (FGF), epidermal growth factor (EGF) and nerve growth factor (NGF: Orive

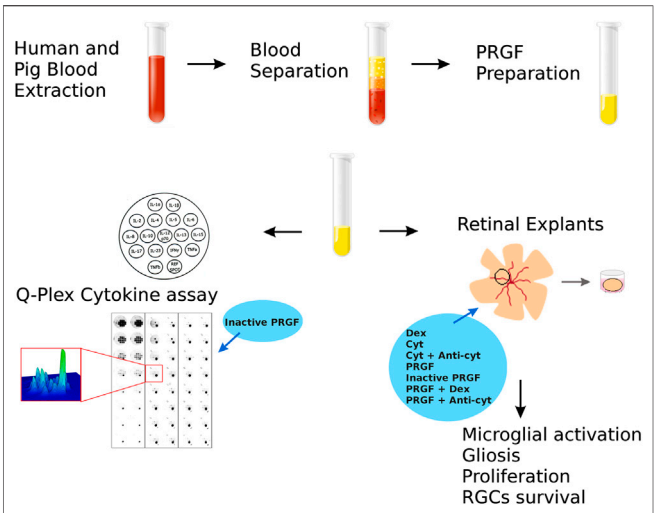

FIGURE 1 | Scheme to analyze the properties of the PRGF in organotypic cultures of adult porcine retinas. First, PRGF was obtained from human and porcine blood by separation and plasma extraction. Subsequently, the effect of the PRGF was evaluated on retinal explants by assessing microglial activation, gliosis and proliferation, and RGC survival. In addition, the cytokines in the human and porcine PRGF was quantified using a Q-plex assay. Finally, given the implication of PRGF in promoting inflammation, the effects of exposing the explants exposed to dexamethasone (Dex), cytokines (Cyt: IL-1β, IL-6 and TNFα) or cytokines plus antibodies raised against these cytokines (anti-cyt: anti-IL-1β, IL-6 and TNFα) were also evaluated. Finally, we examined the effect of heat-inactivated PRGF, as well as PRGF combined with Dex or anti-cyt, analyze their effects on microglial migration.

et al., 2009; Anitua et al., 2010). Therefore, as PRGF may induce an inflammatory response in the retina, we set out to determine whether PRGF stimulates gliosis and the proliferation of glial cells in retinal explants. In cultured Müller cells, we have demonstrated the capacity of PRGF to increase the number of the Müller glia (Ruzafa et al., 2021).

Finally, an intranasal delivery system of PRGF has been designed in order to reverse the neurodegeneration in a transgenic mouse model of Alzheimer's disease (AD: Suga et al., 2014; Osborne et al., 2018), based on PRGF acting as a neurotrophic factor promoting neuronal survival in the presence of amyloid-β (Suga et al., 2014; Pan et al., 2019). The retina, as part of the CNS, has a limited capacity for repair after disease or lesion, and retinal lesions cause the death of retinal ganglion cells (RGCs), the neurons responsible for the communication between the eye and brain. These lesions might result in irreversible blindness (Newman and Reichenbach, 1996; Garcia et al., 2002), as occurs in the case of glaucoma (Glovinsky et al., 1991; Wygnanski et al., 1995), axonal degeneration (Newman and Reichenbach, 1996) or ischemia (Selles-Navarro et al., 1996; Nadal-Nicolas et al., 2012). However, RGCs can recover their regenerative capacities in appropriate environments (Fischer and Reh, 2003; Berry et al., 2008). Thus, and based on the potential neuroprotective properties of PRGF, we finally set out to determine whether PRGF affects the survival of RGCs.

In summary, we examined here the effect of PRGF of two different origins in organotypic retinal cultures, analyzing microglia migration, gliosis, proliferation and RGC survival. The inflammatory cytokines in PRGF were also quantified and the suppression of its inflammatory response was also studied.

MATERIALS AND METHODS

Study Design

To analyze the effect of PRGF in the retina, we used retinal explants to assess the inflammatory effect of PRGF and the migration of microglial cells in these explants (see **Figure 1**). In addition, the effect of PRGF on the proliferation, gliosis and survival of RGCs was also assessed in these organotypic retinal cultures, as were the cytokines present in the PRGF.

Porcine Samples

Adult porcine eyes (n = 20) and blood (n = 5) were obtained from a local slaughterhouse and the eyes were transported to the laboratory on ice in CO_2-independent medium (Life Technologies, Carlsbad, CA, USA) plus 0.1% gentamicin. The retinas were dissected out of the eyes 1–2 h after enucleation. All animal experimentation adhered to the ARVO Statement for the Use of Animals in Ophthalmic and Vision Research.

Human and Pig Plasma Rich in Growth Factors

Qualified personnel carried out this research and approval for the study was obtained in strict accordance with the tenets of the Helsinki Declaration on Biomedical Research Involving Human Subjects. Before blood collection, signed informed consent was obtained from all the subjects once the nature of the study and the possible consequences of the study had been explained. Human blood samples were obtained through antecubital vein puncture and PRGF was obtained as described previously (Suga et al., 2014), with some minor modifications. Briefly, human (n = 3) and porcine (n = 5) blood was collected into 5 ml tubes containing 3.8% (wt/vol) sodium citrate. Samples were centrifuged at 460 g for 8 min at room temperature and the plasma fraction containing platelets but not the buffy coat and erythrocytes were separated. The plasma fraction (1 ml) was reconstituted for 1 h at 34°C with 50 µL calcium chloride (Braun Medical, Melsungen, Germany) in glass tubes, and the supernatant released was collected after centrifugation at 460 g for 15 min. Finally, part of the total volume of the PRGF obtained was heat-inactivated at 56°C for 60 min following a protocol published previously (Anitua et al., 2014a), and both the samples (PRGF and inactive PRGF) were filtered through a filter pore size of 0.2 mm (Fisher Scientific, Madrid, Spain), aliquoted and stored at −80°C.

Organotypic Retinal Cultures

Under aseptic conditions, each pig eyeball was immersed in 70% ethanol, washed in clean CO_2-independent medium and

TABLE 1 | Different experimental conditions in which the explants were exposed to PRGF.

Control (0% PRGF)
Dex
Cytokines
Cytokines + anti-cytokines
10% autologous pig PRGF
10% heterologous pig PRGF
10% human PRGF
10% inactive human PRGF
10% human PRGF + dex
10% human PRGF + anti-cytokines

neuroretinal explants were obtained as described previously (Del Rio et al., 2011). After removing the lens and the vitreous humor, the entire retina was detached by paint brushing and cutting the optic nerve. Using an 8 mm diameter dissecting trephine, five retinal explants were obtained from the middle part of the retina of each eye, at the same distance from the optic nerve and excluding the larger vessels. The explants were transferred to cell culture inserts (0.45 μm pore, 12 mm diameter: Merck Millipore, Darmstadt, Germany) with the photoreceptor layer facing the membrane, and they were cultured in Neurobasal A medium (Life Technologies, Carlsbad, CA, USA) supplemented with 1% L-glutamine (2 mM: Life Technologies, Carlsbad, CA, USA) and 0.1% gentamicin (50 mg/ml: Life Technologies, Carlsbad, CA, USA), and they were maintained at 37°C in a humid atmosphere of 5% CO_2 for 1 and 3 days. The culture medium was maintained in contact with the support membrane beneath the explant and changed with freshly prepared warmed medium every other day. To study the inflammatory role of the PRGF, explants were cultured in the different experimental conditions (**Table 1**) and at least three replicates from different animals were used for each condition. No more than one explant from the same eye was used for each experimental condition.

The explants were cultured in the presence or absence of 10% PRGF from the beginning of the organotypic cultures, using PRGF obtained from the same animal (autologous), from another pig (heterologous) or from a human donor. The human PRGF was added in either an active or inactive form. Dexamethasone (Dex, 1 μM: Sigma Aldrich, St. Louis, MO, USA) was also added to the explants or a mixture of three pro-inflammatory cytokines: IL-1β, IL-6 (10 ng/ml) and TNFα (20 ng/ml, as recommended in Madeira et al., 2015b: Sigma-Aldrich, St. Louis, MO, USA). In another experimental condition these cytokines were inactivated by adding antibodies against the three cytokines (1 μg/ml, as recommended in Madeira et al., 2015b): goat anti-IL-1β and mouse anti-IL-6 (R&D System, Minneapolis, MN, USA); and rabbit anti-TNFα (Peprotech, London, United Kingdom) antibodies). In both cases, the cytokines were also added from the beginning of the culture of the explants with or without their inhibitors. The explants were cultures for 1 day and for 3 days. On the other hand, to study the effect of PRGF on gliosis, proliferation and RGC survival, selected explants were cultured for 3 days in the presence of 10% human PRGF, which induced a stronger effect on microglia.

At the end of each experiment, the retinal explants were fixed overnight in 4% paraformaldehyde (PFA), cryoprotected overnight at 4°C in 30% sucrose in 0.1 M PB (phosphate buffer, pH 7.4), and they were then embedded in Tissue-Tek O.C.T. Compound to obtain cryosections (14 μm) that were stored at −20°C.

Immunochemistry

The cryostat sections of the explants were immunostained to detect microglia, gliosis, proliferative cells and RGCs, as described previously (Vecino et al., 2002). The sections were washed twice for 10 min with PBS (phosphate buffered saline, pH 7.4) containing Triton X-100 (0.25%, TX) and they were incubated overnight with primary antibodies in PBS-TX containing BSA. The primary antibodies used were an: anti-Iba1 rabbit antibody (1:2,000, WAKO, Osaka, Japan), anti-GFAP mouse antibody (1:1,000, Sigma, Steinheim, Germany), anti-Ki67 rabbit antibody (1:100, Abcam, Cambridge, England), and anti-Brn3a goat antibody (1:1,000, Santa Cruz Biotechnology, Santa Cruz, USA). After two washes with PBS, the sections were incubated for 1 h with a secondary antibodies at a dilution of 1:1,000 in PBS-BSA (1%), and with a 1:10,000 dilution of the DAPI nuclear marker (Life Technologies, Carlsbad, AC, USA). The secondary antibodies used were anti-rabbit Alexa Fluor 555 or 488, anti-mouse Alexa Fluor 488 and anti-goat Alexa Fluor 568 (Life Technologies, Carlsbad, AC, USA). The sections were washed twice with PBS for 10 min and mounted with PBS-Glycerol (1:1) before observation under an epifluorescence microscope.

Cells Quantification

Microglia were analyzed in at least three slides containing a minimum of six cryostat sections from each explant. The total extension of the retina analyzed was approximately 10 linear centimetres and this procedure was carried out on at least three replicates for each condition. The total number of microglia cells (Iba1) was manually counted and the number of microglia per linear mm of retina was calculated. In addition, the number of microglia in the outer nuclear layer (ONL) was also counted and the proportion of microglia in this layer of the retina was calculated for each condition. Similarly, RGC density was also analyzed, calculated as the mean number of RGCs ($Brn3a^+$) per linear mm of retina. Cell quantification and images of Müller and astrocyte gliosis (GFAP), or images of proliferative cells (Ki67), were obtained on an epifluorescence microscope (Zeiss, Jena, Germany) coupled to a digital camera (Zeiss Axiocam MRM, Zeiss, Jena, Germany), and using the Zeiss Zen software (Zeiss, Jena, Germany).

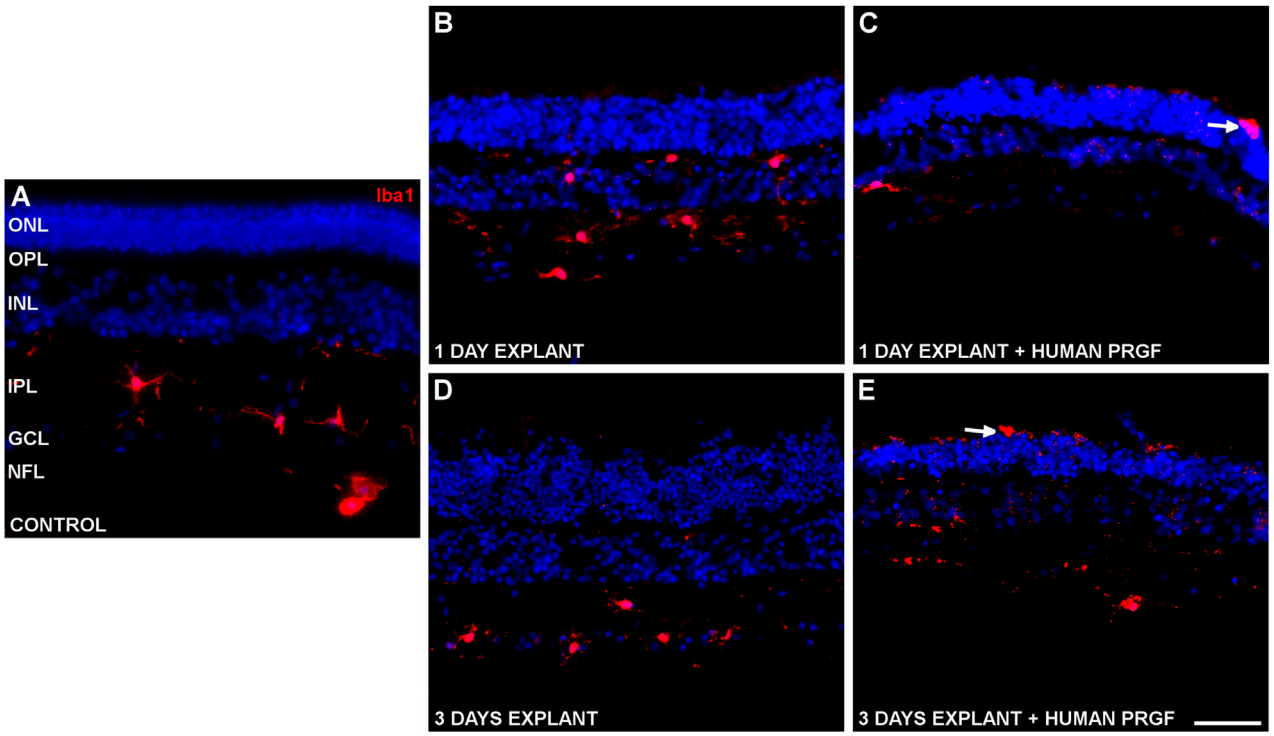

FIGURE 2 | Microglia in a control retina and in organotypic retinal cultures maintained in the presence or absence of human PRGF. Representative images of an adult pig retina from a control eye **(A)**, or of explants of organotypic cultures maintained in the absence **(B,D)** or in the presence **(C,E)** of 10% human PRGF. The explants were cultured for 1 **(B,C)** or 3 **(D,E)** days, labeling the microglial cells with antibodies against Iba1 (red, anti-Iba1 rabbit antibody, 1:2,000, WAKO, Osaka, Japan) and the nuclei with DAPI (blue). The white arrows point to microglial cells in the ONL: ONL, outer nuclear layer; OPL, outer plexiform layer; INL, inner nuclear layer; IPL, inner nuclear layer; GCL, ganglion cell layer; NFL, nerve fiber layer. Scale bar = 100 μm.

Multiplex Cytokine Assays

To detect and quantify the cytokines present in the different PRGF samples, a multiplex enzyme-linked immunosorbent assay (ELISA) was used to measure: IL-1α, IL-1β, IL-2, IL-4, IL-5, IL-6, IL-8, IL-10, IL-12p70, IL-13, IL-15, IL-17, IL-23, IFNγ, TNFα, and TNFβ (Q-Plex™, Human Cytokine Screen, 110996HU, Quansys Bioscience, Logan, UT, USA). The assay was performed according to the manufacturer´s instructions, analyzing 100 μL of the different human and porcine PRGF samples (pig, inactive pig, human, inactive human and human plus Dex) in each well of a 98-well plate Q-Plex™. The standards were measured in duplicate and cytokine concentrations were calculated using a standard curve. Each individual sample was assessed in four experimental replicates and the arithmetic averages were calculated.

Statistical Analyses

Statistical analyses were carried out using the SPSS software v. 21.0 (IBM), and the mean and standard error was calculated for each condition. The data from the different experimental conditions were compared using an analysis of variance (ANOVA), followed by the Games-Howell test as there was no homogeneity of the variances according to a Levene test. For the multiplex cytokine assays, a non-parametric test was used, the Kruskal-Wallis H test. The minimum value for significant differences in all the tests was defined as $p < 0.05$.

RESULTS

Microglial Migration in Retinal Organotypic Cultures in the Presence of Plasma Rich in Growth Factors

Changes in microglial morphology were evident in the retinal explants (**Figure 2**), these cells adopting an ameboid shape distinct to the ramified morphology observed in the control retina. However, there were no changes in the total number of microglial cells, with an average of 12.24 ± 0.25 microglial cells/mm. These microglia were generally located in the inner part of the retina (**Figure 2A**), yet the microglia were able to migrate to the outer plexiform layer (OPL) when maintained in the absence of PRGF during the culture (**Figures 2B,D**). However, these cells migrated to the ONL only when the retinal explants were cultured in the presence of PRGF (**Figures 2C,E**).

Since microglial migration is a sign of activation, the proportion of microglia that migrated to the ONL was

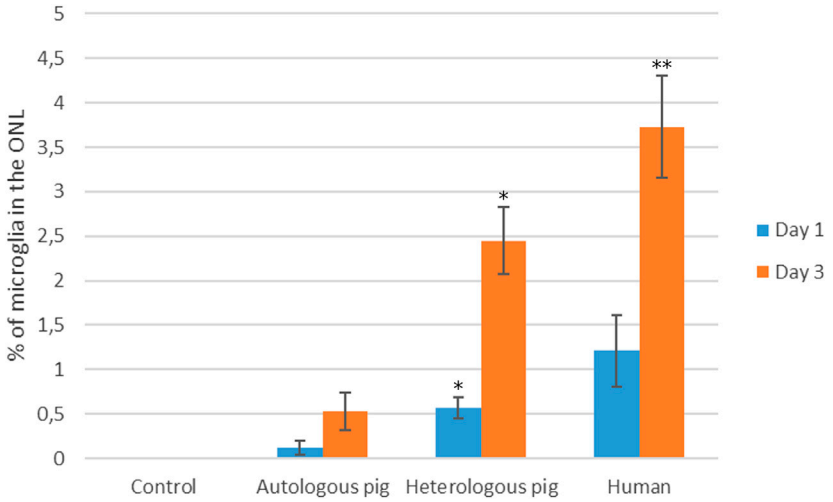

FIGURE 3 | Quantification of microglia migration in the presence of autologous and heterologous porcine PRGF or human PRGF. Microglial migration on day 1 and 3 in retinal explants treated with 10% PRGF from the same pig as the retinal explant (autologous) (n = 5), from another pig (heterologous) (n = 5) or from human blood (n = 5). Microglial migration is represented as the percentage of microglial cells located in the outer nuclear layer (ONL) relative to the total number of microglia: *$p < 0.05$, **$p < 0.01$ relative to the control.

TABLE 2 | Concentration (pg/ml) of the cytokines in porcine and human PRGF

Cytokine	Pig PRGF	Inactive pig PRGF	Human PRGF	Inactive human PRGF
IL-1α	8.15 ± 1.67	10.31 ± 0.87	6.34 ± 2.18	6.55 ± 2.39
IL-1ß	14.65 ± 4.93	20.91 ± 7.06	17.03 ± 4.35	17.01 ± 2.54
IL-2	4.58 ± 1.15	6.93 ± 0.13	4.54 ± 0.54	6.17 ± 1.66
IL-4	0.29 ± 0.28	0.87 ± 0.70	0.39 ± 0.32	0.17 ± 0.17
IL-6	3.61 ± 0.49	5.21 ± 0.18	4.24 ± 1.08	3.99 ± 1.14
IL-8[a]	1.32 ± 0.42	1.24 ± 0.05	29.59 ± 5.73	29.21 ± 3.38
IL-10	4.65 ± 1.47	6.85 ± 2.65	7.21 ± 1.52	4.73 ± 1.61
IL-12	4.96 ± 1.11	5.86 ± 2.11	5.00 ± 3.87	6.71 ± 3.90
IL-13	0.37 ± 0.21	0.29 ± 0.22	0.75 ± 0.75	0.35 ± 0.20
IL-15	2.29 ± 0.49	4.54 ± 1.23	7.09 ± 2.79	6.77 ± 1.92
IL-17	4.59 ± 0.21	2.93 ± 1.02	1.68 ± 0.99	2.88 ± 0.97
IL-23	185.47 ± 43.63	242.71 ± 86.04	283.14 ± 214.27	222.54 ± 158.70
TNFα	4.65 ± 4.25	3.76 ± 3.76	6.61 ± 2.99	1.84 ± 1.84
TNFß	18.40 ± 4.64	14.07 ± 9.76	18.15 ± 14.21	14.88 ± 13.96

[a]*significant differences between pig (n = 5) PRGF and human PRGF (n = 3).*

quantified. Initially, the migration of microglia was analyzed in distinct retinal explants treated with 10% PRGF (**Figure 3**).

On day 1, the proportion of microglia in the ONL of the retinal explants maintained in the presence of 10% PRGF was 0.12 ± 0.07% when autologous PRGF was used, 0.56 ± 0.11% with heterologous pig PRGF and 1.21 ± 0.4% for human PRGF, and on day 3 these values increased to 0.53 ± 0.22%, 2.45 ± 0.38% and 3.73 ± 0.57%, respectively. There were no significant differences between the control explants, in which there was no microglial migration to the ONL, and those maintained in the presence of autologous pig or human PRGF at day 1. However, by day 3 this parameter was significantly different in explants maintained in the presence of heterologous pig PRGF ($p < 0.05$) and human PRGF ($p < 0.01$) relative to the controls (the specific p-values are given in the **Supplementary Material**).

Quantification of the Cytokines in Plasma Rich in Growth Factors

Having shown that PRGF can activate microglial cells and promote their migration, we analyzed the inflammatory cytokines present in the pig and human PRGF, and in the heat-inactivated pig and human PRGF. In the different PRGF samples analyzed, we confirmed the presence of and quantified the following cytokines: IL-1α, IL-1ß, IL-2, IL-4, IL-6, IL-8, IL-10, IL-12, IL13, IL-15, IL-17, IL-23, TNFα, and TNFβ (**Table 2**).

When comparing the cytokine concentrations in pig and human PRGF, IL-8 was the only cytokine detected at a

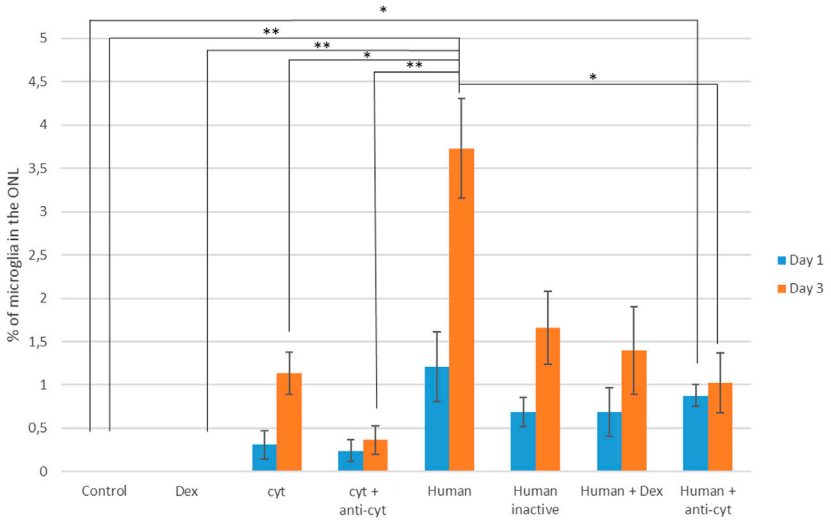

FIGURE 4 | Quantification of microglial migration in the presence of human PRGF, inhibiting its inflammatory effect. Microglial migration is represented as the proportion of microglial cells located in the outer nuclear layer (ONL) relative to the total number of microglia, reflecting the migration in control conditions (n = 5), and in the presence of dexamethasone (Dex: n =), cytokines (cyt, IL-1β, IL-6 and TNFα: n = 4), cytokines plus anti-cytokine antibodies (anti-cyt: n = 3), with 10% human PRGF (Human: n = 5). The inflammatory effect of PRGF (Human) on microglial migration was inhibited by PRGF heat-inactivation (Human inactive: n = 5), or by adding Dex (n = 5) or anti-cytokine antibodies (n = 5). Significant differences relative to the control conditions and the presence of human PRGF are shown: $^{*}p < 0.05$, $^{**}p < 0.01$.

significantly higher concentration in the human than in the pig PRGF ($p < 0.001$). In terms of the heat-inactivated pig and human PRGFs, no differences were found in the cytokine concentrations relative to the PRGF in either species, indicating that this heat-inactivation does not affect the cytokine concentrations (the cytokines activity was not assessed). However, we did appreciate some variability in the quantification of cytokines and thus, we analyzed the different cytokine concentrations between individuals. Significant differences in the cytokine concentrations of human PRGF were found between individuals: IL-8, IL-12, IL-13, IL-15, IL-17, IL-23, and TNFα ($p < 0.05$). Significant differences among the cytokines in pig PRGF were also found between different individuals: IL-1ß, IL-10, IL-15, IL-17, and IL-23 ($p < 0.05$). The remaining cytokines were homogeneously distributed between individuals and no significant differences were found between them (the specific *p*-values are given in the **Supplementary Material**).

Suppression of Microglial Migration in the Presence of Plasma Rich in Growth Factors

The suppression of microglia migration was assessed in retinal explants maintained in the presence of 10% human PRGF, conditions that induced a higher proportion of microglial migration. As such, we analyzed the microglial migration in explants maintained under different culture conditions: adding cytokines or blocking them with antibodies; adding human PRGF, heat-inactivating it or adding antibodies against cytokines; or adding Dex alone or in combination with PRGF (**Figure 4**). To test the role of cytokines, we added a mixture of three major pro-inflammatory cytokines (IL-1β, IL-6 and TNFα) alone or in combination with antibodies raised against these cytokines. The microglia migration in the explants in the presence of cytokines was 0.31 ± 0.16% on day 1 and 1.14 ± 0.25% on day 3, which fell to 0.24 ± 0.12% on day 1 and 0.37 ± 0.16% on day 3 in the presence of antibodies against these cytokines. However, in none of these conditions were significant differences produced relative to the control conditions. Fewer microglia migrated in the presence of PRGF and the anti-cyt mixture, 0.88 ± 0.12% on day 1 and 1.02 ± 0.34% on day 3, and the latter figure in presence of the cytokine antibodies was significantly lower ($p < 0.05$) than in the explants treated with 10% of human PRGF alone on day 3.

The percentage of microglia in the ONL on day 1 was 1.21 ± 0.4% when the explants were exposed to 10% human PRGF and 3.73 ± 0.57% on day 3. When this PRGF was heat-inactivated, microglial migration decreased to 0.68 ± 0.16% on day 1 and 1.65 ± 0.42% on day 3. In the presence of Dex and PRGF, microglial migration also decreased to 0.69 ± 0.28% on day 1 and 1.29 ± 0.5% on day 3. However, this apparent decrease in microglial migration was not significantly different from the migration in the presence of 10% PRGF alone and nor was it significantly different from the values in the control explants. There was a reduction in microglial migration when the PRGF was heat-inactivated, or when it was used in combination with Dex or anti-cyt antibodies, although these conditions never completely suppressed migration. Thus, the pro-migratory effect of PRGF on microglia appears to be multifactorial and not only due to the influence of pro-inflammatory cytokines.

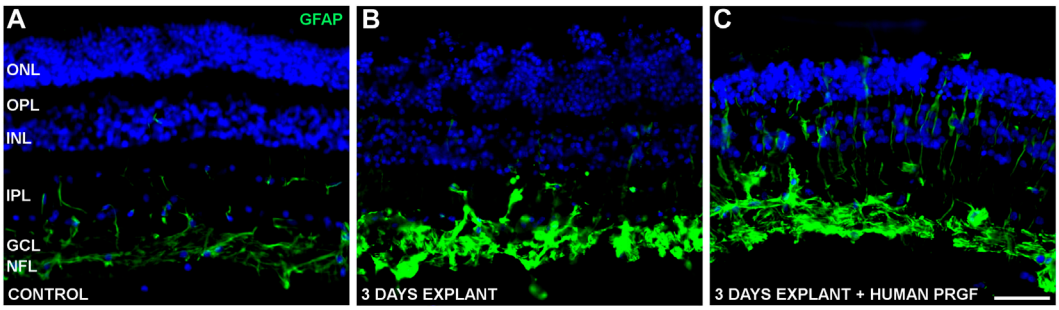

FIGURE 5 | Gliosis in control retinas and in organotypic retinal cultures maintained in the presence or absence of human PRGF. Representative images of adult pig retinas from a control eye (n = 5: **A)**, or from explants of organotypic cultures maintained in the absence (n = 4: **B)** or presence (n = 4: **C)** of 10% human PRGF. The GFAP in astrocytes and Müller cells was immunolabeled (green, anti-GFAP mouse antibody, 1:1,000, Sigma, Steinheim, Germany), and the nuclei were labeled with DAPI (blue): ONL, outer nuclear layer; OPL, outer plexiform layer; INL, inner nuclear layer; IPL, inner nuclear layer; GCL, ganglion cell layer; NFL, nerve fiber layer. Scale bar = 100 μm.

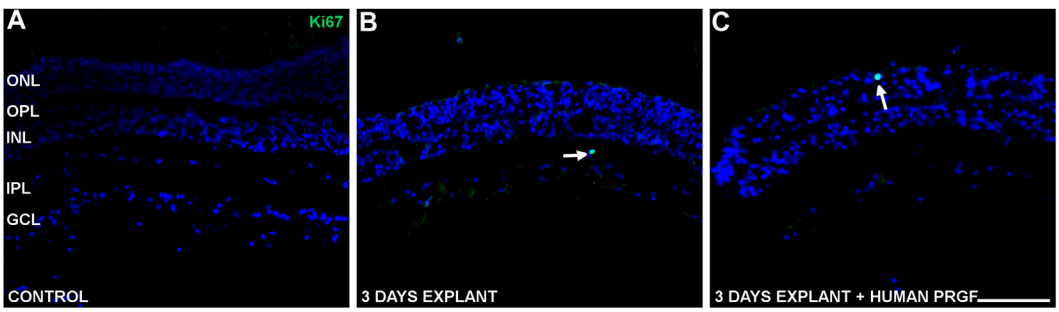

FIGURE 6 | Proliferative cells in control retinas and in organotypic retinal cultures maintained in the presence or absence of human PRGF. Representative images of adult pig retinas from a control eye (n = 5: **A)**, and organotypic cultures maintained in the absence (n = 4: **B)** or presence (n = 4: **C)** of 10% human PRGF. The edge of the explant is also shown **(C)**. The proliferative cells were labeled with antibodies against Ki67 (green, anti-Ki67 rabbit antibody, 1:100, Abcam, Cambridge, England) and the nuclei with DAPI (blue). The white arrows indicate cells in an active phase of the cell cycle. The edge of the explant is shown to demonstrate the absence of proliferation (left in picture C): ONL, outer nuclear layer; OPL, outer plexiform layer; INL, inner nuclear layer; IPL, inner nuclear layer; GCL, ganglion cell layer. Scale bar = 100 μm.

Effect of Plasma Rich in Growth Factors on Gliosis and Proliferation in Organotypic Cultures

To determine if PRGF may modify macroglial (astrocytes and Müller glia) and microglial cells, the distribution of the cytoskeletal protein GFAP was studied in the retinal explants to establish the extent of astrocyte and Müller cell activation. In the control cultures, GFAP labeled astrocytes were detected in the GCL and NFL, and some Müller cells were labeled for GFAP (vertical lines in IPL in **Figure 5A**). The presence of PRGF seemed to induce the gliosis of Müller cells in the retinal explants (**Figure 5C**), although the astrocytes were already activated in explants in the absence of PRGF (**Figure 5B**). Thus, the induction of astrocyte gliosis by PRGF cannot be confirmed.

To study the possible proliferation induced by PRGF we studied Ki67 as a marker of actively dividing cells. In control retinas, a few Ki67 labeled cells were detected in an active phase of the cell cycle (**Figure 6**), whereas in organotypic cultures proliferative cells were labeled with the anti-Ki67 antibody in the presence or absence of human PRGF (**Figures 6B,C**). These proliferative cells were rare, even at the edges of the explants (**Figure 6C**) and consequently, we cannot confirm that PRGF increases the rate of proliferation in organotypic cultures of adult retinas. Considering the position of the proliferative cells and given that only glial cells can divide in the retina, we conclude that these proliferative cells were microglia.

Retinal Ganglion Cells Survival in Organotypic Cultures in the Presence of Plasma Rich in Growth Factors

Finally, we analyzed the survival of retinal neurons, specifically RGCs (**Figure 7**), and relative to the control retinas (20.76 ± 2.3 RGCs/mm), there were significant fewer RGCs in explants maintained in either the presence (5.44 ± 0.95 RGCs/mm) or absence (7.05 ± 1.41 RGCs/mm) of human PRGF. However, we did not find a significant difference in the survival of RGCs in organotypic cultures maintained in the presence of PRGF and thus, PRGF does not appear to offer neuroprotection to RGCs in

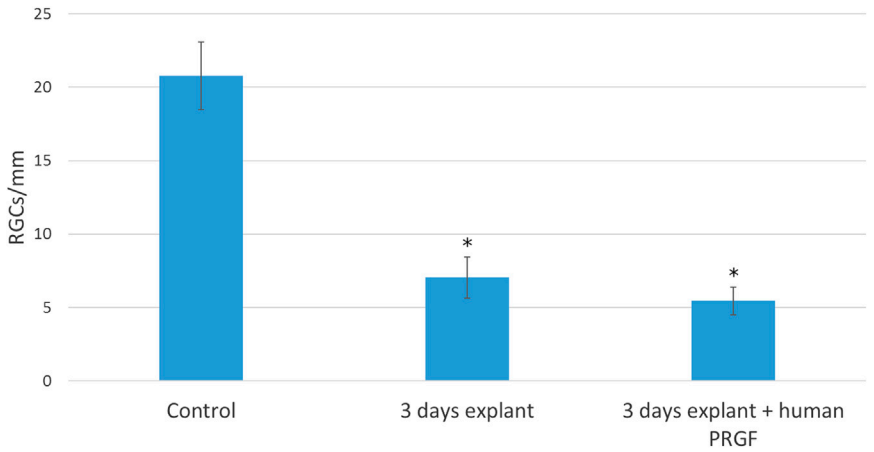

FIGURE 7 | Quantification of RGCs per millimeter of retina in controls retinas and in explants maintained in the presence or absence of human PRGF. The number of RGCs per linear mm of retina are shown in control retinas (n = 5) and in organotypic cultures at day 3, maintained in the presence (n = 4) or absence of 10% human PRGF (n = 4). Significant differences between the controls and explants are indicated: *$p < 0.05$.

explants of adult porcine retinas (the specific p-values are given in the **Supplementary Material**).

DISCUSSION

PRGF is a biological supplement which provides a pool of growth factors that can stimulate and accelerate tissue regeneration, and hence, it may potentially represent a therapeutic agent to treat different diseases, including neurodegenerative diseases (Anitua et al., 2013; Anitua et al., 2014b; Anitua et al., 2015a). In this study, the influence of PRGF on glial cells and CNS neurons was assessed in the retina. In organotypic retinal cultures, PRGF promotes the migration of microglia, a sign of inflammation that could be due to the cytokines it contains. However, PRGF does not induce gliosis among astrocytes and partially in Müller glia, and it does not alter the proliferation of glial cells or modify RGC survival.

One of the critical steps in the inflammatory response is the recruitment and migration of immune and inflammatory cells to inflammatory sites, and in the CNS, microglia are the resident innate immune cells (Lull and Block, 2010; Omri et al., 2011). In a healthy retina, microglia are located in the inner part of retina (Streit et al., 1988; Ling and Wong, 1993; Omri et al., 2011) but when these cells are activated, they migrate into the sub-retinal space, as occurs in several retinopathies associated with ocular inflammation like diabetic retinopathy (Zeng et al., 2008) and age-related macular degeneration (Combadiere et al., 2007). Microglial cells were analyzed in organotypic cultures or explants, a commonly used model of inflammation (Carter and Dick, 2003; Bauer et al., 2016), assessing the effect of PRGF. In addition to the microglial migration observed, we detected a change in their morphology from a ramified to an ameboid shape in the cultured retinas.

It has been suggested that PRGF could fulfill an inherent anti-inflammatory role, mediated by NF-kB (Anitua et al., 2014b; Anitua et al., 2015a). In addition, PRGF could dampen the inflammatory status of a cell culture model of inflammation induced by IL-1β and TNFα, significantly decreasing ICAM-1 and COX-2 levels when compared to autologous serum (Anitua et al., 2016). Thus, to understand how PRGF activates retinal microglia, the presence of inflammatory cytokines in the PRGF was quantified. It has been suggested that pro-inflammatory cytokines are almost absent or limited in PRGF (Anitua et al., 2015b), although some cytokines have been detected in PRGF: IL-6 (Masuki et al., 2016), IL-8 (Anitua et al., 2010), IL-4, and TNFα (Anitua et al., 2012). The concentrations of the cytokines that were observed in PRGF may be lower than that of some interleukins in other PRPs (Pochini et al., 2016). The IL-6 concentration in PRGF was similar to the concentrations seen previously, although IL-1β was not found in PRGF, it was found in other PRPs with values similar to those identified here (Masuki et al., 2016). The presence of these and others inflammatory cytokines in the PRGF was confirmed and corroborated here. Moreover, the activation of microglia by cytokines was demonstrated due to the presence of cytokine receptors on microglia, which express mRNA transcripts for IL-1 receptor I and II, the IL-6, IL-8, IL-10, IL-12, IL-13, IL-15 receptors, and TNF receptors I and II (Lee et al., 2002). In addition, IL-6, IL-12 and TNFα can activate microglia (Luo and Chen, 2012) and thus, the cytokines present in PRGF can themselves trigger an inflammatory response. This activation would be independent of the cytokine secretion by the tissue exposed to the PRGF, as PRGF has been shown to induce the expression of cytokines like IL-1β, IL-6 or IL-10 (Mozzati et al., 2010). In addition, it has been suggested that the anti-inflammatory effect of PRGF is due to a high IL-4 content (Anitua et al., 2012), although the presence of this and other anti-inflammatory cytokines like IL-10 and IL-13 (Cavaillon, 2001) is weak relative to other cytokines that fulfill an opposite effect, such as the pro-inflammatory cytokine IL-1β.

In order to dampen microglial migration in the retinal explants, the PRGF was heat-inactivated prior to exposure to

the explants (Anitua et al., 2014a). We also used Dex to inhibit inflammation (Tsurufuji et al., 1984) and we used antibodies against pro-inflammatory cytokines to block their action. The cytokines selected to mimic a pro-inflammatory environment in the organotypic cultures were the three major pro-inflammatory cytokines: IL-1β, IL-6, and TNFα (Taki et al., 2007; Zhang and An, 2007). It has been demonstrated that reactive microglia increase their expression and the release of these cytokines in retinal organotypic cultures (Madeira et al., 2015b). Moreover, the presence of antibodies against these three cytokines is sufficient to significantly diminish the number of activated microglia. However, the neutralization of the pro-inflammatory cytokines by antibodies did not completely suppress microglial migration, which could be due to the fact that these antibodies are from other species (e.g., goat, mouse and rabbit) and that this might provoke an immune response. Alternatively, Dex and heat-inactivated PRGF can mildly, though not entirely, reduce microglial migration. In addition, the presence of pro-inflammatory cytokines in the cultures does not mimic the effect of PRGF. These results suggest that there are other factors in addition to the cytokines implicated in the activation of microglial migration. It is known that heat-inactivation maintains the biological activity of PRGF, yet it fully reduced complement activity and significantly dampened the presence of IgE (Anitua et al., 2014a). However, in addition to cytokines, IgM and IgG are also present in the heat-inactivated PRGF (Anitua et al., 2014a), and IgG increases microglial activation due to the expression of high affinity IgG receptor (FcαRI: Orr et al., 2005). Thus, complement and immunoglobulins, as well as cytokines, could participate in the activation of the retinal inflammatory response. Moreover, Dex did not totally block the effect of the cytokines in the medium (Pereiro et al., 2018), confirming that microglial activation is triggered by different factors.

By contrast, microglial migration is higher when the PRGF is heterologous (the donor is from a different animal from that which donates the retina) in comparison to the migratory effect when the PRGF is autologous. In addition, human PRGF (when the donor is from a different species) induces stronger microglial activation than the pig PRGF in the porcine retina and this could be due to the presence of the pro-inflammatory cytokine IL-8, which is significantly more abundant in the human PRGF. Moreover, the presence of other receptors in microglial cells, such as toll like receptors (TLR) that respond to self and non-self activators (Shastri et al., 2013), could be implicated in the activation of microglia when the PRGF is not autologous or it is from another species. Therefore, patients suffering from autoimmune diseases, or patients in which their own PRGF is not as effective as expected, should receive PRGF from a donor. Moreover, this heterologous PRGF must be inactivated or combined with an anti-inflammatory treatment in order to mitigate the inflammatory response that might be initiated.

In terms of gliosis, it was suggested that PRGF decreases astrocyte reactivity (Anitua et al., 2013; Anitua et al., 2014b). However, we found that human PRGF initiated an inflammatory response activating porcine microglial migration, inflammation that could activate astrocytes and Müller cells. In gliosis, macroglial cells can divide and become hypertrophic, producing long, thick processes, as well as overexpressing GFAP (Lee et al., 2002; Vecino et al., 2016). Nevertheless, in our model of retinal explants astroglia are activated *per se* and an increase in gliosis was not evident in astrocytes in the presence of PRGF. However, a mild increase in Müller cell gliosis was seen in the presence of PRGF. In summary, some heterogeneity in GFAP expression was found in the organotypic cultures, regardless of PRGF. It is known that biomechanical tension is a vital factor in maintaining retinal tissue integrity in organotypic cultures, and stretched retinal explants displayed no signs of gliosis, as well as increased neuronal survival and preservation of retinal architecture (Taylor et al., 2013). Therefore, some variability in the tensile strength of explants may explain the results obtained.

The proliferative effects of PRGF were first demonstrated in dentistry, oral implantology, orthopedics, sports medicine and the treatment of skin disorders (Anitua et al., 2010). This proliferative effect is due to the growth factors in PRGF, such as IGF-1, PDGF or FGF, powerful stimulators of cell replication/proliferation (Anitua et al., 2009; Vahabi et al., 2015). In ophthalmology, intravitreal injection of PRP induces proliferation of retinal fibroblast-like cells and it was used as a model of proliferative vitreoretinopathy (Pinon et al., 1992). Moreover, different platelet preparations produce similar proliferative effects on immortalized human Müller cells (MIO-M1), in addition to stimulating their migration (Burmeister et al., 2009). However, our results do not demonstrate that PRGF induces the proliferation of glial cells. This could be due to proliferation being inhibited by cell-cell contact, which might occur in many cells (Ribatti, 2017), as the retinal explant used here preserves retinal architecture and the cells are in contact in a physiological manner. However, in cultured Müller cells, the application of PRGF increases the Müller cell number (Ruzafa et al., 2021). It is possible that we could not detect Müller proliferation in our explants due to the preservation of retinal structure, as we have shown *in vitro*. It may be possible that Müller glia proliferation underlies the structural restauration of the retina in patients with macular hole after injecting autologous PRGF. On the other hand, microglia reaction is beneficial by the acquisition of new functions before the alteration of their homeostatic roles (Sierra et al., 2013; Hemonnot et al., 2019). These beneficial properties of microglia could positively affect the restoration of the macular hole in patients.

In the CNS, microglia immediately migrate to sites of tissue damage (Nimmerjahn et al., 2005). By contrast, macroglia do not migrate but they may die in the focal point of severe lesions, or they may become reactive and hypertrophic, in some cases proliferating (Bardehle et al., 2013; Burda and Sofroniew, 2014). PRGF appears to promote microglial migration with only mild signs of gliosis and with no increase in the rate of glial cell proliferation, and interspecific PRGF induces mild signs of inflammation, which could be easily reverted by inactivating the PRGF or combining it with anti-inflammatory drugs or antibodies against cytokines. However, *in vivo* studies will be required to confirm these results as the behavior of the cells could differ.

Previous studies suggested that PRGF induces neuroprotection by activating anti-apoptotic PI3K/Akt signaling and/or diminishing caspase-3 levels (Anitua et al.,

2013). Moreover, it has been suggested that PRGF induces neuroprotection in association with a down-regulation of the activated microglial cell number and a significant decrease of pro-inflammatory mediators (Anitua et al., 2015a). Studies of other neurodegenerative diseases, such as AD (Anitua et al., 2013; Anitua et al., 2014b) and Parkinson's disease (Anitua et al., 2015a), show that cell survival was enhanced by PRGF in primary neuronal cultures, and the number of degenerating neurons was reduced. However, PRGF activated microglia here and we did not find changes in RGC survival. The concentrations of PRGF used here were 10%, as used when studying the effects of human PRGF in mouse models (Anitua et al., 2013; Anitua et al., 2014b). Thus, the concentration and interspecies interactions here are unlikely to affect neuroprotection. By contrast, it was suggested that thrombin-activated PRP releases glutamate, and when it is applied to neuronal cultures it is neurotoxic (Bell et al., 2014). Moreover, some of the morphogens or growth factors present in PRP, like PRGF, could have an adverse effect on neurons, such as TGF-β1 that exerts negative effects on axon growth in rat brain-spinal cord co-culture (Takeuchi et al., 2012). Such results could explain why we did not find a neuroprotective role of PRGF in the retinal explants.

Although PRGF has been successfully used in different medical and surgical specialties, and there is extensive data indicating that PRP induces tissue regeneration, many of these studies are not sufficiently rigorous or controlled, and their data is often limited. Indeed, other studies have produced contrasting results (Kuffler, 2015). Currently, autologous PRP injections have been used as pilot treatments for some retinal lesions (Nadal et al., 2012; Arias et al., 2019). Although structural recovery of the retina may be achieved (for instance closure of a macular hole), a functional recovery might be limited by the potential increase in inflammatory reaction which may have deleterious for the cells and be responsible for several complications like focal macular epithelial pigmentary hypertrophy, development of epiretinal membrane and cataract progression among other (Minihan et al., 1997; Cheung et al., 2005; Nugent and Lee, 2015). Therefore, the impact of PRGF is not fully understood and the applications of PRGF in ophthalmology must be analyzed in more detail. Differences in the levels of the factors present in PRGF and in other blood-derived products may explain the variability in the results obtained in different studies (Vahabi et al., 2015), as evident through the significant differences in the cytokine concentrations between samples observed here. Thus, further animal and clinical studies should be performed to clarify the properties of PRGF.

CONCLUSION

PRGF has been used in ophthalmology to treat persistent macular holes and recurrent retinal detachment, although the mechanisms through which PRGF works in the CNS remain unclear. In retinal organotypic cultures, PRGF induces microglial activation, an inflammatory response that may be due to the presence of inflammatory cytokines. However, we cannot rule out the possible positive effect of microglial cells in repairing the retina, as suggested. Autologous PRGF induces weaker signs of inflammation that heterologous PRGF and that from other species, and this microglia activation may be mitigated. Moreover, PRGF does induce partial gliosis, although it does not appear to induce glial proliferation or RGC neuroprotection. Thus, while PRGF could be a good candidate to stimulate and accelerate tissue regeneration, more studies will be necessary to clarify its effects on the nervous and immune systems.

DATA AVAILABILITY STATEMENT

The raw data supporting the conclusion of this article will be made available by the authors, without undue reservation.

ETHICS STATEMENT

The studies involving human participants were reviewed and approved in strict accordance with the tenets of the Helsinki Declaration on biomedical research involving human subjects. The patients/participants provided their written informed consent to participate in this study.

All animal experimentation adhered to the ARVO Statement for the Use of Animals in Ophthalmic and Vision Research.

AUTHOR CONTRIBUTIONS

Data curation, NR and XP; Formal analysis, NR, Funding acquisition, EV; Methodology, NR and XP; Project administration, EV; Supervision, EV; Writing—original draft, NR; Writing—review & editing, NR, XP, EV, AA, AF, and JA.

FUNDING

We acknowledge the support of MINECO-Retos Fondos Fender (RTC-2016-48231), Gobierno Vasco (PUE_2018_1_0004), ELKARTEK (KK-2019/00086), MINECO-Retos (PID2019-111139RB-I00) and PIBA (2020-1-0026) to EV.

SUPPLEMENTARY MATERIAL

The Supplementary Material for this article can be found online at: https://www.frontiersin.org/articles/10.3389/fphar.2021.606232/full#supplementary-material.

REFERENCES

Anitua, E., Alkhraisat, M. H., and Orive, G. (2012). Perspectives and challenges in regenerative medicine using plasma rich in growth factors. *J. Control. Release* 157, 29–38. doi:10.1016/j.jconrel.2011.07.004

Anitua, E., Muruzabal, F., De La Fuente, M., Merayo-Lloves, J., and Orive, G. (2014a). Effects of heat-treatment on plasma rich in growth factors-derived autologous eye drop. *Exp. Eye Res.* 119, 27–34. doi:10.1016/j.exer.2013.12.005

Anitua, E., Muruzabal, F., De La Fuente, M., Riestra, A., Merayo-Lloves, J., and Orive, G. (2016). PRGF exerts more potent proliferative and anti-inflammatory effects than autologous serum on a cell culture inflammatory model. *Exp. Eye Res.* 151, 115–121. doi:10.1016/j.exer.2016.08.012

Anitua, E., Pascual, C., Antequera, D., Bolos, M., Padilla, S., Orive, G., et al. (2014b). Plasma rich in growth factors (PRGF-Endoret) reduces neuropathologic hallmarks and improves cognitive functions in an Alzheimer's disease mouse model. *Neurobiol. Aging* 35, 1582–1595. doi:10.1016/j.neurobiolaging.2014.01.009

Anitua, E., Pascual, C., Pérez-Gonzalez, R., Antequera, D., Padilla, S., Orive, G., et al. (2013). Intranasal delivery of plasma and platelet growth factors using PRGF-Endoret system enhances neurogenesis in a mouse model of Alzheimer's disease. *PLoS One* 8, e73118. doi:10.1371/journal.pone.0073118

Anitua, E., Pascual, C., Pérez-Gonzalez, R., Orive, G., and Carro, E. (2015a). Intranasal PRGF-Endoret enhances neuronal survival and attenuates NF-κB-dependent inflammation process in a mouse model of Parkinson's disease. *J. Control. Release* 203, 170–180. doi:10.1016/j.jconrel.2015.02.030

Anitua, E., Sánchez, M., and Orive, G. (2010). Potential of endogenous regenerative technology for *in situ* regenerative medicine. *Adv. Drug Deliv. Rev.* 62, 741–752. doi:10.1016/j.addr.2010.01.001

Anitua, E., Sánchez, M., Zalduendo, M. M., De La Fuente, M., Prado, R., Orive, G., et al. (2009). Fibroblastic response to treatment with different preparations rich in growth factors. *Cell Prolif* 42, 162–170. doi:10.1111/j.1365-2184.2009.00583.x

Anitua, E., Zalduendo, M. M., Prado, R., Alkhraisat, M. H., and Orive, G. (2015b). Morphogen and proinflammatory cytokine release kinetics from PRGF-Endoret fibrin scaffolds: evaluation of the effect of leukocyte inclusion. *J. Biomed. Mater. Res. A.* 103, 1011–1020. doi:10.1002/jbm.a.35244

Arias, J. D., Hoyos, A. T., Alcantara, B., Sanchez-Avila, R. M., Arango, F. J., and Galvis, V. (2019). Plasma rich in growth factors for persistent macular hole: a pilot study. *Retin. Cases Brief Rep.*

Bardehle, S., Krüger, M., Buggenthin, F., Schwausch, J., Ninkovic, J., Clevers, H., et al. (2013). Live imaging of astrocyte responses to acute injury reveals selective juxtavascular proliferation. *Nat. Neurosci.* 16, 580–586. doi:10.1038/nn.3371

Barres, B. A. (2008). The mystery and magic of glia: a perspective on their roles in health and disease. *Neuron* 60, 430–440. doi:10.1016/j.neuron.2008.10.013

Bauer, P. M., Zalis, M. C., Abdshill, H., Deierborg, T., Johansson, F., and Englund-Johansson, U. (2016). Inflamed in vitro retina: cytotoxic neuroinflammation and galectin-3 expression. *PLoS One* 11, e0161723. doi:10.1371/journal.pone.0161723

Bell, J. D., Thomas, T. C., Lass, E., Ai, J., Wan, H., Lifshitz, J., et al. (2014). Platelet-mediated changes to neuronal glutamate receptor expression at sites of microthrombosis following experimental subarachnoid hemorrhage. *J. Neurosurg.* 121, 1424–1431. doi:10.3171/2014.3.JNS132130

Berry, M., Ahmed, Z., Lorber, B., Douglas, M., and Logan, A. (2008). Regeneration of axons in the visual system. *Restor Neurol. Neurosci.* 26, 147–174.

Block, M. L., and Hong, J. S. (2005). Microglia and inflammation-mediated neurodegeneration: multiple triggers with a common mechanism. *Prog. Neurobiol.* 76, 77–98. doi:10.1016/j.pneurobio.2005.06.004

Bringmann, A., Pannicke, T., Grosche, J., Francke, M., Wiedemann, P., Skatchkov, S. N., et al. (2006). Müller cells in the healthy and diseased retina. *Prog. Retin. Eye Res.* 25, 397–424. doi:10.1016/j.preteyeres.2006.05.003

Bringmann, A., and Reichenbach, A. (2001). Role of Muller cells in retinal degenerations. *Front. Biosci.* 6, E72–E92. doi:10.2741/bringman

Burda, J. E., and Sofroniew, M. V. (2014). Reactive gliosis and the multicellular response to CNS damage and disease. *Neuron* 81, 229–248. doi:10.1016/j.neuron.2013.12.034

Burmeister, S. L., Hartwig, D., Limb, G. A., Kremling, C., Hoerauf, H., Müller, M., et al. (2009). Effect of various platelet preparations on retinal muller cells. *Invest. Ophthalmol. Vis. Sci.* 50, 4881–4886. doi:10.1167/iovs.08-3057

Buschini, E., Piras, A., Nuzzi, R., and Vercelli, A. (2011). Age related macular degeneration and drusen: neuroinflammation in the retina. *Prog. Neurobiol.* 95, 14–25. doi:10.1016/j.pneurobio.2011.05.011

Carter, D. A., and Dick, A. D. (2003). Lipopolysaccharide/interferon-gamma and not transforming growth factor beta inhibits retinal microglial migration from retinal explant. *Br. J. Ophthalmol.* 87, 481–487. doi:10.1136/bjo.87.4.481

Cavaillon, J. M. (2001). Pro- versus anti-inflammatory cytokines: myth or reality. *Cell Mol. Biol.* 47, 695–702.

Cheung, C. M., Munshi, V., Mughal, S., Mann, J., and Hero, M. (2005). Anatomical success rate of macular hole surgery with autologous platelet without internal-limiting membrane peeling. *Eye* 19, 1191–1193. doi:10.1038/sj.eye.6701733

Cole, B. J., Seroyer, S. T., Filardo, G., Bajaj, S., and Fortier, L. A. (2010). Platelet-rich plasma: where are we now and where are we going?. *Sports Health* 2, 203–210. doi:10.1177/1941738110366385

Combadiere, C., Feumi, C., Raoul, W., Keller, N., Rodéro, M., Pézard, A., et al. (2007). CX3CR1-dependent subretinal microglia cell accumulation is associated with cardinal features of age-related macular degeneration. *J. Clin. Invest.* 117, 2920–2928. doi:10.1172/JCI31692

Coscas, G., De Benedetto, U., Coscas, F., Li Calzi, C. I., Vismara, S., Roudot-Thoraval, F., et al. (2013). Hyperreflective dots: a new spectral-domain optical coherence tomography entity for follow-up and prognosis in exudative age-related macular degeneration. *Ophthalmologica* 229, 32–37. doi:10.1159/000342159

Cui, Y., Xu, N., Xu, W., and Xu, G. (2017). Erratum to: mesenchymal stem cells attenuate hydrogen peroxide-induced oxidative stress and enhance neuroprotective effects in retinal ganglion cells. *In Vitro Cel. Dev. Biol. Anim.* 53, 336–335. doi:10.1007/s11626-017-0139-0

Davis, B. M., Salinas-Navarro, M., Cordeiro, M. F., Moons, L., and De Groef, L. (2017). Characterizing microglia activation: a spatial statistics approach to maximize information extraction. *Sci. Rep.* 7, 1576. doi:10.1038/s41598-017-01747-8

Del Río, P., Irmler, M., Arango-González, B., Favor, J., Bobe, C., Bartsch, U., et al. (2011). GDNF-induced osteopontin from Müller glial cells promotes photoreceptor survival in the Pde6brd1 mouse model of retinal degeneration. *Glia* 59, 821–832. doi:10.1002/glia.21155

Dhurat, R., and Sukesh, M. (2014). Principles and methods of preparation of platelet-rich plasma: a review and author's perspective. *J. Cutan. Aesthet. Surg.* 7, 189–197. doi:10.4103/0974-2077.150734

Dohan Ehrenfest, D. M., Andia, I., Zumstein, M. A., Zhang, C. Q., Pinto, N. R., and Bielecki, T. (2014). Classification of platelet concentrates (Platelet-Rich Plasma-PRP, Platelet-Rich Fibrin-PRF) for topical and infiltrative use in orthopedic and sports medicine: current consensus, clinical implications and perspectives. *Muscles Ligaments Tendons J.* 4, 3–9.

Fernandes, A., Miller-Fleming, L., and Pais, T. F. (2014). Microglia and inflammation: conspiracy, controversy or control?. *Cell Mol. Life Sci.* 71, 3969–3985. doi:10.1007/s00018-014-1670-8

Fischer, A. J., and Reh, T. A. (2003). Potential of Müller glia to become neurogenic retinal progenitor cells. *Glia* 43, 70–76. doi:10.1002/glia.10218

Garcia, M., Forster, V., Hicks, D., and Vecino, E. (2002). Effects of müller glia on cell survival and neuritogenesis in adult porcine retina *in vitro*. *Invest. Ophthalmol. Vis. Sci.* 43, 3735–3743.

Gertig, U., and Hanisch, U. K. (2014). Microglial diversity by responses and responders. *Front Cel Neurosci* 8, 101. doi:10.3389/fncel.2014.00101

Glovinsky, Y., Quigley, H. A., and Dunkelberger, G. R. (1991). Retinal ganglion cell loss is size dependent in experimental glaucoma. *Invest. Ophthalmol. Vis. Sci.* 32, 484–491.

Hayashi, H., and Takagi, N. (2015). Endogenous neuroprotective molecules and their mechanisms in the central nervous system. *Biol. Pharm. Bull.* 38, 1104–1108. doi:10.1248/bpb.b15-00361

Hemonnot, A. L., Hua, J., Ulmann, L., and Hirbec, H. (2019). Microglia in alzheimer disease: well-known targets and new opportunities. *Front. Aging Neurosci.* 11, 233. doi:10.3389/fnagi.2019.00233

Jin, K., Zhu, Y., Sun, Y., Mao, X. O., Xie, L., and Greenberg, D. A. (2002). Vascular endothelial growth factor (VEGF) stimulates neurogenesis *in vitro* and *in vivo*. *Proc. Natl. Acad. Sci. USA* 99, 11946–11950. doi:10.1073/pnas.182296499

Karlstetter, M., Scholz, R., Rutar, M., Wong, W. T., Provis, J. M., and Langmann, T. (2015). Retinal microglia: just bystander or target for therapy?. *Prog. Retin. Eye Res.* 45, 30–57. doi:10.1016/j.preteyeres.2014.11.004

Kreutzberg, G. W. (1996). Microglia: a sensor for pathological events in the CNS. *Trends Neurosci.* 19, 312–318.

Kuffler, D. P. (2015). Platelet-rich plasma promotes axon regeneration, wound healing, and pain reduction: fact or fiction. *Mol. Neurobiol.* 52, 990–1014. doi:10.1007/s12035-015-9251-x

Lee, J. E., Liang, K. J., Fariss, R. N., and Wong, W. T. (2008). *Ex vivo* dynamic imaging of retinal microglia using time-lapse confocal microscopy. *Invest. Ophthalmol. Vis. Sci.* 49, 4169–4176. doi:10.1167/iovs.08-2076

Lee, Y. B., Nagai, A., and Kim, S. U. (2002). Cytokines, chemokines, and cytokine receptors in human microglia. *J. Neurosci. Res.* 69, 94–103. doi:10.1002/jnr.10253

Ling, E. A., and Wong, W. C. (1993). The origin and nature of ramified and amoeboid microglia: a historical review and current concepts. *Glia* 7, 9–18. doi:10.1002/glia.440070105

Lopez-Plandolit, S., Morales, M. C., Freire, V., Etxebarría, J., and Durán, J. A. (2010). Plasma rich in growth factors as a therapeutic agent for persistent corneal epithelial defects. *Cornea* 29, 843–848. doi:10.1097/ICO.0b013e3181a81820

Lopez-Plandolit, S., Morales, M. C., Freire, V., Grau, A. E., and Durán, J. A. (2011). Efficacy of plasma rich in growth factors for the treatment of dry eye. *Cornea* 30, 1312–1317. doi:10.1097/ICO.0b013e31820d86d6

Lull, M. E., and Block, M. L. (2010). Microglial activation and chronic neurodegeneration. *Neurotherapeutics* 7, 354–365. doi:10.1016/j.nurt.2010.05.014

Luo, X. G., and Chen, S. D. (2012). The changing phenotype of microglia from homeostasis to disease. *Transl Neurodegener* 1, 9. doi:10.1186/2047-9158-1-9

Madeira, M. H., Boia, R., Santos, P. F., Ambrósio, A. F., and Santiago, A. R. (2015a). Contribution of microglia-mediated neuroinflammation to retinal degenerative diseases. *Mediators Inflamm.* 2015, 673090. doi:10.1155/2015/673090

Madeira, M. H., Elvas, F., Boia, R., Gonçalves, F. Q., Cunha, R. A., Ambrósio, A. F., et al. (2015b). Adenosine A2AR blockade prevents neuroinflammation-induced death of retinal ganglion cells caused by elevated pressure. *J. Neuroinflammation* 12, 115. doi:10.1186/s12974-015-0333-5

Marx, R. E., Carlson, E. R., Eichstaedt, R. M., Schimmele, S. R., Strauss, J. E., and Georgeff, K. R. (1998). Platelet-rich plasma: growth factor enhancement for bone grafts. *Oral Surg. Oral Med. Oral Pathol. Oral Radiol. Endod.* 85, 638–646. doi:10.1016/s1079-2104(98)90029-4

Masuki, H., Okudera, T., Watanebe, T., Suzuki, M., Nishiyama, K., Okudera, H., et al. (2016). Growth factor and pro-inflammatory cytokine contents in platelet-rich plasma (PRP), plasma rich in growth factors (PRGF), advanced platelet-rich fibrin (A-PRF), and concentrated growth factors (CGF). *Int. J. Implant Dent.* 2, 19. doi:10.1186/s40729-016-0052-4

Merayo-Lloves, J., Sanchez, R. M., Riestra, A. C., Anitua, E., Begoña, L., Orive, G., et al. (2015). Autologous plasma rich in growth factors eyedrops in refractory cases of ocular surface disorders. *Ophthalmic Res.* 55, 53–61. doi:10.1159/000439280

Minihan, M., Goggin, M., and Cleary, P. E. (1997). Surgical management of macular holes: results using gas tamponade alone, or in combination with autologous platelet concentrate, or transforming growth factor beta 2. *Br. J. Ophthalmol.* 81, 1073–1079. doi:10.1136/bjo.81.12.1073

Mozzati, M., Martinasso, G., Pol, R., Polastri, C., Cristiano, A., Muzio, G., et al. (2010). The impact of plasma rich in growth factors on clinical and biological factors involved in healing processes after third molar extraction. *J. Biomed. Mater. Res. A.* 95, 741–746. doi:10.1002/jbm.a.32882

Nadal, J., Lopez-Fortuny, M., Sauvageot, P., and Pérez-Formigó, D. (2012). Treatment of recurrent retinal detachment secondary to optic nerve coloboma with injection of autologous platelet concentrate. *J. AAPOS* 16, 100–101. doi:10.1016/j.jaapos.2011.10.007

Nadal-Nicolas, F. M., Jiménez-López, M., Salinas-Navarro, M., Sobrado-Calvo, P., Alburquerque-Béjar, J. J., Vidal-Sanz, M., et al. (2012). Whole number, distribution and co-expression of brn3 transcription factors in retinal ganglion cells of adult albino and pigmented rats. *PLoS One* 7, e49830. doi:10.1371/journal.pone.0049830

Newman, E., and Reichenbach, A. (1996). The Müller cell: a functional element of the retina. *Trends Neurosci.* 19, 307–312.

Nimmerjahn, A., Kirchhoff, F., and Helmchen, F. (2005). Resting microglial cells are highly dynamic surveillants of brain parenchyma *in vivo*. *Science* 308, 1314–1318. doi:10.1126/science.1110647

Nugent, R. B., and Lee, G. A. (2015). Ophthalmic use of blood-derived products. *Surv. Ophthalmol.* 60, 406–434. doi:10.1016/j.survophthal.2015.03.003

O'kusky, J. R., Ye, P., and D'ercole, A. J. (2000). Insulin-like growth factor-I promotes neurogenesis and synaptogenesis in the hippocampal dentate gyrus during postnatal development. *J. Neurosci.* 20, 8435–8442. doi:10.1523/JNEUROSCI.20-22-08435.2000

Omri, S., Behar-Cohen, F., De Kozak, Y., Sennlaub, F., Verissimo, L. M., Jonet, L., et al. (2011). Microglia/macrophages migrate through retinal epithelium barrier by a transcellular route in diabetic retinopathy: role of PKCζ in the Goto Kakizaki rat model. *Am. J. Pathol.* 179, 942–953. doi:10.1016/j.ajpath.2011.04.018

Orive, G., Anitua, E., Pedraz, J. L., and Emerich, D. F. (2009). Biomaterials for promoting brain protection, repair and regeneration. *Nat. Rev. Neurosci.* 10, 682–692. doi:10.1038/nrn2685

Orr, C. F., Rowe, D. B., Mizuno, Y., Mori, H., and Halliday, G. M. (2005). A possible role for humoral immunity in the pathogenesis of Parkinson's disease. *Brain* 128, 2665–2674. doi:10.1093/brain/awh625

Osborne, A., Sanderson, J., and Martin, K. R. (2018). Neuroprotective effects of human mesenchymal stem cells and platelet-derived growth factor on human retinal ganglion cells. *Stem Cells* 36, 65–78. doi:10.1002/stem.2722

Pakzad-Vaezi, K., Or, C., Yeh, S., and Forooghian, F. (2014). Optical coherence tomography in the diagnosis and management of uveitis. *Can. J. Ophthalmol.* 49, 18–29. doi:10.1016/j.jcjo.2013.10.005

Pan, D., Chang, X., Xu, M., Zhang, M., Zhang, S., Wang, Y., et al. (2019). UMSC-derived exosomes promote retinal ganglion cells survival in a rat model of optic nerve crush. *J. Chem. Neuroanat.* 96, 134–139. doi:10.1016/j.jchemneu.2019.01.006

Pereiro, X., Ruzafa, N., Acera, A., Fonollosa, A., Rodriguez, F. D., and Vecino, E. (2018). Dexamethasone protects retinal ganglion cells but not Müller glia against hyperglycemia *in vitro*. *PLoS One* 13, e0207913. doi:10.1371/journal.pone.0207913

Piñon, R. M., Pastor, J. C., Saornil, M. A., Goldaracena, M. B., Layana, A. G., Gayoso, M. J., et al. (1992). Intravitreal and subretinal proliferation induced by platelet-rich plasma injection in rabbits. *Curr. Eye Res.* 11, 1047–1055. doi:10.3109/02713689209015076

Pochini, A. C., Antonioli, E., Bucci, D. Z., Sardinha, L. R., Andreoli, C. V., Ferretti, M., et al. (2016). Analysis of cytokine profile and growth factors in platelet-rich plasma obtained by open systems and commercial columns. *Einstein (Sao Paulo)* 14, 391–397. doi:10.1590/S1679-45082016AO3548

Prince, J. H., and Ruskell, G. L. (1960). The use of domestic animals for experimental ophthalmology. *Am. J. Ophthalmol.* 49, 1202–1207. doi:10.1016/0002-9394(60)91636-6

Reichenbach, A., and Bringmann, A. (2013). New functions of Müller cells. *Glia* 61, 651–678. doi:10.1002/glia.22477

Ribatti, D. (2017). A revisited concept: contact inhibition of growth. From cell biology to malignancy. *Exp. Cel. Res.* 359, 17–19. doi:10.1016/j.yexcr.2017.06.012

Ruzafa, N., Pereiro, X., Fonollosa, A., Araiz, J., Acera, A., and Vecino, E. (2021). Plasma rich in growth factors (PRGF) increases the number of retinal müller glia in culture but not the survival of retinal neurons. *Front. Pharmacol.*

Sanchez-Avila, R. M., Merayo-Lloves, J., Riestra, A. C., Fernandez-Vega Cueto, L., Anitua, E., Begoña, L., et al. (2018). Treatment of patients with neurotrophic keratitis stages 2 and 3 with plasma rich in growth factors (PRGF-Endoret) eye-drops. *Int. Ophthalmol.* 38, 1193–1204. doi:10.1007/s10792-017-0582-7

Selles-Navarro, I., Villegas-Perez, M. P., Salvador-Silva, M., Ruiz-Gomez, J. M., and Vidal-Sanz, M. (1996). Retinal ganglion cell death after different transient periods of pressure-induced ischemia and survival intervals. A quantitative *in vivo* study. *Invest. Ophthalmol. Vis. Sci.* 37, 2002–2014.

Shastri, A., Bonifati, D. M., and Kishore, U. (2013). Innate immunity and neuroinflammation. *Mediators Inflamm.* 2013, 342931. doi:10.1155/2013/342931

Sierra, A., Abiega, O., Shahraz, A., and Neumann, H. (2013). Janus-faced microglia: beneficial and detrimental consequences of microglial phagocytosis. *Front. Cel Neurosci* 7, 6. doi:10.3389/fncel.2013.00006

Streit, W. J., Graeber, M. B., and Kreutzberg, G. W. (1988). Functional plasticity of microglia: a review. *Glia* 1, 301–307. doi:10.1002/glia.440010502

Suga, A., Sadamoto, K., Fujii, M., Mandai, M., and Takahashi, M. (2014). Proliferation potential of Müller glia after retinal damage varies between mouse strains. *PLoS One* 9, e94556. doi:10.1371/journal.pone.0094556

Takeuchi, M., Kamei, N., Shinomiya, R., Sunagawa, T., Suzuki, O., Kamoda, H., et al. (2012). Human platelet-rich plasma promotes axon growth in brain-spinal cord coculture. *Neuroreport* 23, 712–716. doi:10.1097/WNR.0b013e3283567196

Taki, N., Tatro, J. M., Lowe, R., Goldberg, V. M., and Greenfield, E. M. (2007). Comparison of the roles of IL-1, IL-6, and TNFalpha in cell culture and murine models of aseptic loosening. *Bone* 40, 1276–1283. doi:10.1016/j.bone.2006.12.053

Taylor, L., Moran, D., Arnér, K., Warrant, E., and Ghosh, F. (2013). Stretch to see: lateral tension strongly determines cell survival in long-term cultures of adult porcine retina. *Invest. Ophthalmol. Vis. Sci.* 54, 1845–1856. doi:10.1167/iovs.12-11420

Tsurufuji, S., Kurihara, A., and Ojima, F. (1984). Mechanisms of anti-inflammatory action of dexamethasone: blockade by hydrocortisone mesylate and actinomycin D of the inhibitory effect of dexamethasone on leukocyte infiltration in inflammatory sites. *J. Pharmacol. Exp. Ther.* 229, 237–243.

Vahabi, S., Vaziri, S., Torshabi, M., and Rezaei Esfahrood, Z. (2015). Effects of plasma rich in growth factors and platelet-rich fibrin on proliferation and viability of human gingival fibroblasts. *J. Dent.* 12, 504–512.

Vecino, E., Garcia-Crespo, D., Garcia, M., Martinez-Millán, L., Sharma, S. C., and Carrascal, E. (2002). Rat retinal ganglion cells co-express brain derived neurotrophic factor (BDNF) and its receptor TrkB. *Vis. Res* 42, 151–157. doi:10.1016/s0042-6989(01)00251-6

Vecino, E., Rodriguez, F. D., Ruzafa, N., Pereiro, X., and Sharma, S. C. (2016). Glia-neuron interactions in the mammalian retina. *Prog. Retin. Eye Res.* 51, 1–40. doi:10.1016/j.preteyeres.2015.06.003

Vecino, E., and Sharma, S. C. (2011). "Glaucoma animal models," in *Glaucoma - basic and clinical concepts*. Editor S. Rumelt, London, United Kingdom: IntechOpen. 319–334.

Vujosevic, S., Bini, S., Midena, G., Berton, M., Pilotto, E., and Midena, E. (2013). Hyperreflective intraretinal spots in diabetics without and with nonproliferative diabetic retinopathy: an *in vivo* study using spectral domain OCT. *J. Diabetes Res.* 2013, 491835. doi:10.1155/2013/491835

Wang, H. L., and Avila, G. (2007). Platelet rich plasma: myth or reality?. *Eur. J. Dent.* 1, 192–194.

Wygnanski, T., Desatnik, H., Quigley, H. A., and Glovinsky, Y. (1995). Comparison of ganglion cell loss and cone loss in experimental glaucoma. *Am. J. Ophthalmol.* 120, 184–189. doi:10.1016/s0002-9394(14)72606-6

Zeng, H. Y., Green, W. R., and Tso, M. O. (2008). Microglial activation in human diabetic retinopathy. *Arch. Ophthalmol.* 126, 227–232. doi:10.1001/archophthalmol.2007.65

Zhang, J. M., and An, J. (2007). Cytokines, inflammation, and pain. *Int. Anesthesiol Clin.* 45, 27–37. doi:10.1097/AIA.0b013e318034194e

Conflict of Interest: The authors declare that the research was conducted in the absence of any commercial or financial relationships that could be construed as a potential conflict of interest.

frontiers in Pharmacology

ORIGINAL RESEARCH
published: 09 March 2021
doi: 10.3389/fphar.2021.606275

Plasma Rich in Growth Factors (PRGF) Increases the Number of Retinal Müller Glia in Culture but Not the Survival of Retinal Neurons

Noelia Ruzafa[1,2†], *Xandra Pereiro*[1,2†], *Alex Fonollosa*[1,2,3], *Javier Araiz*[1,3], *Arantxa Acera*[1,4] *and Elena Vecino*[1,2*]

[1]Experimental Ophthalmo-Biology Group, Department of Cell Biology and Histology, University of Basque Country UPV/EHU, Leioa, Spain, [2]Begiker-Ophthalmology Research Group, Cruces Hospital, BioCruces Health Research Institute, Bilbao, Spain, [3]Department of Ophthalmology, University of Basque Country UPV/EHU, Leioa, Spain, [4]Biodonostia Health Research Institute, Donostia Hospital, San Sebastian, Spain

OPEN ACCESS

Edited by:
Julie Sanderson,
University of East Anglia,
United Kingdom

Reviewed by:
Javier Francisco-Morcillo,
University of Extremadura, Spain
Ricardo P. Casaroli-Marano,
University of Barcelona, Spain

***Correspondence:**
Elena Vecino
elena.vecino@ehu.es

[†]These authors contributed equally to this article

Specialty section:
This article was submitted to Inflammation Pharmacology, a section of the journal Frontiers in Pharmacology

Received: 14 September 2020
Accepted: 02 February 2021
Published: 09 March 2021

Citation:
Ruzafa N, Pereiro X, Fonollosa A, Araiz J, Acera A and Vecino E (2021) Plasma Rich in Growth Factors (PRGF) Increases the Number of Retinal Müller Glia in Culture but Not the Survival of Retinal Neurons. Front. Pharmacol. 12:606275. doi: 10.3389/fphar.2021.606275

Plasma rich in growth factors (PRGF) is a subtype of platelet-rich plasma (PRP) that stimulates tissue regeneration and may promote neuronal survival. It has been employed in ophthalmology to achieve tissue repair in some retinal pathologies, although how PRGF acts in the retina is still poorly understood. As a part of the central nervous system, the retina has limited capacity for repair capacity following damage, and retinal insult can provoke the death of retinal ganglion cells (RGCs), potentially producing irreversible blindness. RGCs are in close contact with glial cells, such as Müller cells, that help maintain homeostasis in the retina. In this study, the aim was to determine whether PRGF can protect RGCs and whether it increases the number of Müller cells. Therefore, PRGF were tested on primary cell cultures of porcine RGCs and Müller cells, as well as on co-cultures of these two cell types. Moreover, the inflammatory component of PRGF was analyzed and the cytokines in the different PRGFs were quantified. In addition, we set out to determine if blocking the inflammatory components of PRGF alters its effect on the cells in culture. The presence of PRGF compromises RGC survival in pure cultures and in co-culture with Müller cells, but this effect was reversed by heat-inactivation of the PRGF. The detrimental effect of PRGF on RGCs could be in part due to the presence of cytokines and specifically, to the presence of pro-inflammatory cytokines that compromise their survival. However, other factors are likely to be present in the PRGF that have a deleterious effect on the RGCs since the exposure to antibodies against these cytokines were insufficient to protect RGCs. Moreover, PRGF promotes Müller cell survival. In conclusion, PRGF hinders the survival of RGCs in the presence or absence of Müller cells, yet it promotes Müller cell survival that could be the reason of retina healing observed in the *in vivo* treatments, with some cytokines possibly implicated. Although PRGF could stimulate tissue regeneration, further studies should be performed to evaluate the effect of PRGF on neurons and the implication of its potential inflammatory role in such processes.

Keywords: retina, retinal disease, PRP, PRGF, inflammation, cytokines, neuron, glia

INTRODUCTION

As a part of the central nervous system (CNS), the retina has a limited capacity for repair after disease or lesion. Different diseases affect retinal ganglion cells (RGCs), the neurons responsible for communication between the eye and the brain. RGCs die by apoptosis in glaucoma, a neurodegenerative disease that provokes irreversible blindness (Glovinsky et al., 1991; Garcia-Valenzuela et al., 1995; Quigley et al., 1995; Quigley, 2011). However, they can also die following axon degeneration (Knoferle et al., 2010), ischemia (Selles-Navarro et al., 1996; Joo et al., 1999) or in diabetes (Lieth et al., 2000; Zhang et al., 2000). Nevertheless, it has been seen that RGCs can recover their regenerative capacities in appropriate environments (Garcia et al., 2002; Berry et al., 2008; Ruzafa and Vecino, 2015; Vecino et al., 2015).

Plasma rich in growth factors (PRGF), a subtype of P-PRP (pure platelet-rich plasma), is a supernatant enriched in plasma and platelet-derived morphogens, proteins and growth factors. PRGF represents a complex pool of active mediators that may stimulate and accelerate tissue regeneration, which is generally safe to use and inexpensive to obtain. Indeed, autologous PRGF has been approved for clinical use by the European Community and the U.S. Food and Drug Administration (Anitua et al., 2014b), and it is generally employed in ophthalmology as eye drops to treat the ocular surface (Lopez-Plandolit et al., 2010; Lopez-Plandolit et al., 2011). Furthermore, different PRPs are being used in clinic: autologous platelet injections are being used to treat recurrent retinal detachment (Nadal et al., 2012) and pilot studies are being carried out to use PRGF in retinal surgery to treat persistent macular holes (Arias et al., 2019). Although visual acuity may be improved in patients, these treatments could be associated with complications such as focal macular epithelial pigmentary hypertrophy, retinal folds emanating from the macula, development of epiretinal membrane or cataract progression (Cheung et al., 2005; Nugent and Lee, 2015). Thus, although PRGF has been successfully used, the events that could be triggered by PRGF in the retina are not completely understood.

An intranasal delivery system has been used with human PRGF to reverse neurodegeneration and rescue memory in a transgenic mouse model of Alzheimer's disease (AD). Moreover, PRGF can exert a neurotrophic effect in response to amyloid beta and promote neuronal survival (Anitua et al., 2015a). Since PRGF could offer neuroprotection and it is approved for use in clinical practice, we set out to study if PRGF can protect RGCs and enhance the survival of these cells.

RGCs are in close contact with Müller glia, the main glial cells in the mammalian retina. These cells that serve to maintain retinal homeostasis, and they are involved in retinal metabolism, in the phagocytosis of neuronal debris, in the release of certain transmitters and trophic factors, as well as in K^+ uptake (reviewed in (Vecino et al., 2016)). Müller cells extend across the thickness of the retina, providing structural stability and maintaining close contact with the majority of retinal neurons (Bringmann and Reichenbach, 2001). In addition to their involvement in maintaining homeostasis, these cells also provide trophic factors to neurons that potentially promote their survival and repair (Bringmann et al., 2006; Reichenbach and Bringmann, 2013), and they have been seen to enhance RGC survival (Garcia et al., 2002; Ruzafa et al., 2018). Therefore, in the CNS, PRGF may interact with these glial cells as it contains growth factors known to accelerate cell proliferation, stimulate differentiation and promote cell survival (O'kusky et al., 2000; Jin et al., 2002). Among the growth factors present in PRGF, those implicated in proliferation include platelet-derived growth factor (PDGF), transforming growth factor beta (TGF-β), vascular endothelial growth factor (VEGF), fibroblast growth factor (FGF), epidermal growth factor (EGF), insulin-like growth factor I (IGF-I) and nerve growth factor (NGF: (Orive et al., 2009).

In light of the neuroprotective and pro-survival properties of PRGF, and knowing that PRPs are being used to treat retinal disorders (Nadal et al., 2012; Arias et al., 2019); we aimed to determine whether PRGF stimulates Müller cell survival and if it provides neuroprotection to RGCs. The effect of the PRGF on these two cell types were studied separately and together in a well-established adult culture system (Garcia et al., 2002; Garcia and Vecino, 2003; Ruzafa and Vecino, 2015; Vecino et al., 2015; Pereiro et al., 2020). In addition, since PRGF contains molecules with other activities and some that are implicated in immune responses (Anitua et al., 2015b), we set out to define the cytokines that could be implicated in the effects in PRGF. Finally, in order to relate the presence of cytokines in PRGF with its effect on retinal cells, we set out to suppress the possible pro-inflammatory response of PRGF through heat inactivation, or by adding the anti-inflammatory drug dexamethasone or antibodies against the three major pro-inflammatory cytokines (IL-1β, IL-6, and TNFα), studying how the inhibition of the inflammatory response affects RGCs.

MATERIALS AND METHODS

Study Design

On the present study, the effect of the PRGF was analyzed on different retinal cell cultures and the cytokines in the PRGF were quantified (**Figure 1**).

Porcine Samples

Adult porcine eyes ($n = 20$) and blood ($n = 5$) were obtained at a local slaughterhouse and the eyes were transported to the laboratory on ice in CO_2-independent medium (Life Technologies, Carlsbad, CA, United States) with 0.1% gentamicin. The retinas were obtained from the eyes 1–2 h after enucleation. All animal experimentation adhered to the ARVO Statement for the Use of Animals in Ophthalmic and Vision Research.

Human and Pig PRGF

This study was carried out by qualified personnel in strict accordance with the tenets of the Helsinki Declaration on Biomedical Research Involving Human Subjects. Before blood collection, signed informed consent was obtained from all subjects once the nature of the study and the possible

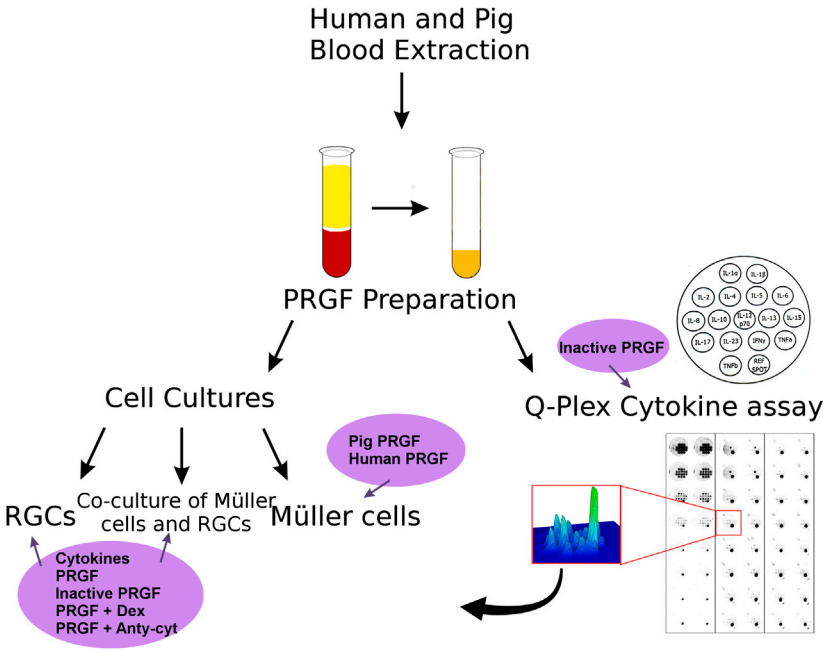

FIGURE 1 | Scheme of the analysis of the properties of the PRGF and its effects on retinal cell cultures performed in this study. First, human and porcine blood was extracted and PRGF was obtained by plasma extraction. The effect of the PRGF was analyzed on three different types of cell cultures: pure RGCs or Müller cell cultures, and co-cultures of both these cell types. In addition, the presence of cytokines in the human and porcine PRGF was quantified through a Q-plex assay. The heat-inactivated form of PRGFs were also analyzed. After confirming the presence of cytokines in the PRGF, we checked the effect of the presence of pro-inflammatory cytokines (IL-1β, IL-6, and TNFα) on the RGCs cultures and co-cultures. We heat-inactivated the PRGF, and we added the inflammatory drug dexamethasone (Dex) or antibodies against cytokines (anti-cyt) to the PRGF in order to analyze its effect on the cell cultures. The survival effect of porcine and human PRGF on pure Müller cells cultures were also assessed.

consequences of the study had been explained to them. Human blood samples were obtained through antecubital vein puncture and PRGF was obtained as described previously (Anitua et al., 2015a), with some minor modifications. Briefly, human (n = 3) and porcine (n = 5) blood was collected in 5 ml tubes containing 3.8% (wt/vol) sodium citrate. Samples were centrifuged at 460 g for 8 min at room temperature and the plasma fraction containing platelets was separated, avoiding the buffy coat and erythrocytes. The plasma fraction (1 ml) was reconstituted for 1 h at 34°C with 50 µl calcium chloride (Braun Medical, Melsungen, Germany) in glass tubes, and the supernatant released was collected after centrifugation at 460 g for 15 min. Finally, part of the total volume of the PRGF obtained was heat-inactivated at 56°C for 60 min, following a previously published protocol (Anitua et al., 2014a), and both the samples (PRGF and inactive PRGF) were filtered through a filter with a 0.2 µm pore size of (Fisher Scientific, Madrid, Spain), aliquoted and stored at −80°C.

Cell Culture

Retinal cell cultures were prepared according to the method reported previously (Garcia et al., 2002; Ruzafa et al., 2018), with the following minor modifications. Three types of cultures were used: 1) RGCs cultured in B27-supplemented Neurobasal-A medium (Life Technologies, Carlsbad, CA, United States); 2) a co-culture of RGCs and Müller cells in B27-supplemented Neurobasal-A medium with 10% fetal bovine serum (FBS: Life Technologies, Carlsbad, CA, United States); and 3) Müller cell cultures in DMEM (Life Technologies, Carlsbad, CA, United States) supplemented with 10% FBS. 1% L-glutamine (2 mM) and 0.1% gentamycin (50 mg/ml) were added to all media.

The retinas were dissected out and 8 mm diameter pieces were obtained with a dissecting trephine (Biomedical Research Instruments, MD, United States), avoiding the most peripheral retina and visible blood vessels. The tissue was disrupted enzymatically with papain at 37°C (Worthington Papain Dissociation kit, Worthington Biochemical Lakewood, NJ, United States) for 90 min in the presence of 10% DNAse I (Worthington Papain Dissociation kit, Worthington Biochemical Lakewood, NJ, United States) to obtain RGCs, or for 30 min to obtain Müller cells and for co-cultures. Papain activity was stopped by adding medium and the tissue was disaggregated by gentle trituration using pipette tips of decreasing diameter. Dissociated retinal cells were collected by a 5 min centrifugation at 300 g and resuspended in medium. The RGC culture was prepared following the protocol of the Worthington Papain Dissociation kit (Worthington Biochemical Lakewood, NJ, United States), plating the resuspended cells in twenty four well plates on 13 mm poly-L-lysine (100 µg/ml: Sigma, P4832) and laminin (10 µg/ml: Sigma, L2020) coated glass coverslips. The cells were maintained in a

TABLE 1 | Different experimental conditions to which the RGC cultures and the co-cultures of RGCs and Müller cells were exposed.

Control (0% PRGF)
Cytokines (IL-1β, IL-6 and TNFα)
10% Human PRGF
10% Inactive Human PRGF
10% Human PRGF + Dex
10% Human PRGF + anti-cytokines

humidified incubator at 37°C in an atmosphere of 5% CO_2. For the Müller cell cultures and the co-cultures, the entire medium was changed on day 1 and to maintain all the cells, half of the medium was replaced every 3 days. The cells were fixed for 10 min with methanol at -20°C after 7 days, before the Müller cells cultures reached confluence. At least three replicates of each culture were studied and the procedures were carried out in triplicate.

PRGF (10%) was added at the beginning of the cell culture and maintained throughout, and for the Müller cell cultures PRGF was added in the absence of FBS. To analyze the effect of PRGF in Müller cells, non-autologous porcine and human PRGF were used. The RGCs and the co-cultures were subjected to different experimental conditions (**Table 1**), using only human PRGF due to the difficulties in obtaining porcine PRGF.

Dexamethasone (Dex, 1 μM: Sigma Aldrich, St. Louis, MO, United States) was added to the cultures, or a mix of the three major pro-inflammatory cytokines at a concentration of 10 ng/ml each (as recommended by (Madeira et al., 2015): IL-1β, IL-6 and TNFα (Sigma-Aldrich, St. Louis, MO, United States). To inactivate these pro-inflammatory cytokines, antibodies against these cytokines were added to the cultures (at 1 μg/ml, the concentration recommended by (Madeira et al., 2015): goat anti-IL-1β and mouse anti-IL-6 (R&D System, Minneapolis, MN, United States), and rabbit anti-TNFα (Peprotech, London, United Kingdom) antibodies). The cytokines, in the presence or absence of their antibodies, were also added from the beginning of the cultures.

Immunochemistry

The cells were fixed in methanol, washed with PBS (phosphate-buffered saline, pH 7.4) and immunostained as described previously (Vecino et al., 2002). After blocking non-specific antigens with blocking buffer (3% BSA and 0.1% Triton X-100 in PBS) the cultures were exposed to the following antibodies: a rabbit polyclonal anti-βIII-tubulin antiserum (diluted 1:2,000: Promega, Madison, WI, United States), an RGC marker; and mouse monoclonal anti-vimentin antibody (diluted 1:10,000: Dako, Glostrup, Denmark) as specific marker for Müller cells. After again washing in PBS, antibody binding was detected with the following secondary antibodies (diluted 1:1,000): anti-rabbit Alexa Fluor 555 and anti-mouse Alexa Fluor 488 (Life Technologies, Carlsbad, CA, United States). The cells were also stained with the DAPI nuclear marker at a dilution of 1: 10,000 (Life Technologies, Carlsbad, CA, United States).

Cell Quantification

The surfaces of the whole 13 mm diameter coverslips were analyzed and at least three replicates of each culture condition were analyzed, performing these experiments in triplicate. The images were taken with an epifluorescence microscope (Zeiss, Jena, Germany) coupled to a digital camera (Zeiss Axiocam MRM, Zeiss, Jena, Germany) and using the Zeiss Zen software (Zeiss, Jena, Germany). A mosaic of the entire coverslip was analyzed using 359, 488, and 555 nm filters with a 10X objective, and once the mosaic was defined, the coverslip surface area was calculated (132.73 mm^2). The Zeiss Zen software (Zeiss, Jena, Germany) was used to count the Müller cell nuclei and for the mosaic definition, and the RGC density was also analysed. The cell density was calculated as the mean number of cells/mm^2, and the data were normalized to the control to simplify its representation.

Multiplex Cytokine Assays

To detect and quantify the cytokines present in the different PRGF samples, a multiplex enzyme-linked immunosorbent assay (ELISA) was used (Q-Plex™, Human Cytokine Screen, 110996HU, Quansys Bioscience, Logan, UT, United States), measuring: IL-1α, IL-1β, IL-2, IL-4, IL-6, IL-8, IL-10, IL-12p70, IL-13, IL-15, IL-17, IL-23, TNFα, and TNFβ. The assay was performed according to the manufacturer´s instruction, analysing 100 μl of the different human and porcine PRGF samples (pig, inactive pig, human, inactive human) in each well of a 98-well plate Q-Plex™. The standards were measured in duplicate and the cytokine concentrations were calculated using a standard curve. All samples were assessed in four replicates and arithmetic averages were calculated.

Statistical Analyses

Statistical analyses were carried out using the SPSS Statistics software v. 21.0 (IBM) and, the mean and the standard error for each condition were calculated. The data from the different experimental conditions were compared using an analysis of variance (ANOVA), followed by the Games-Howell test as the variances were not homogeneous according to a Levene test. For the multiplex cytokine assays, a non-parametric Kruskal-Wallis H test was used. The minimum value accepted for significant differences in all the tests was defined as $p < 0.05$.

RESULTS

The inflammatory cytokines in the pig and human PRGF were assessed, quantifying the following cytokines in these PRGF samples: IL-1α, IL-1ß, IL-2, IL-4, IL-6, IL-8, IL-10, IL-12, IL13, IL-15, IL-17, IL-23, TNFα and TNFß (**Table 2**).

When the cytokine concentrations in pig and human samples were compared, only the IL-8 concentration was significantly higher in the human PRGF than in the pig PRGF ($p < 0.001$). Moreover, heat inactivation did not alter the cytokine concentrations in either the pig or human PRGFs (their activity was not assessed). As some individual variability was detected in the quantification of the cytokines, we analysed the

TABLE 2 | Concentration (pg/ml) of the cytokines in active and inactive porcine and human PRGF

Cytokine	Pig PRGF	Inactive pig PRGF	Human PRGF	Inactive human PRGF
IL-1α	8.15 ± 1.67	10.31 ± 0.87	6.34 ± 2.18	6.55 ± 2.39
IL-1ß	14.65 ± 4.93	20.91 ± 7.06	17.03 ± 4.35	17.01 ± 2.54
IL-2	4.58 ± 1.15	6.93 ± 0.13	4.54 ± 0.54	6.17 ± 1.66
IL-4	0.29 ± 0.28	0.87 ± 0.70	0.39 ± 0.32	0.17 ± 0.17
IL-6	3.61 ± 0.49	5.21 ± 0.18	4.24 ± 1.08	3.99 ± 1.14
IL-8 *	1.32 ± 0.42	1.24 ± 0.05	29.59 ± 5.73	29.21 ± 3.38
IL-10	4.65 ± 1.47	6.85 ± 2.65	7.21 ± 1.52	4.73 ± 1.61
IL-12	4.96 ± 1.11	5.86 ± 2.11	5.00 ± 3.87	6.71 ± 3.90
IL-13	0.37 ± 0.21	0.29 ± 0.22	0.75 ± 0.75	0.35 ± 0.20
IL-15	2.29 ± 0.49	4.54 ± 1.23	7.09 ± 2.79	6.77 ± 1.92
IL-17	4.59 ± 0.21	2.93 ± 1.02	1.68 ± 0.99	2.88 ± 0.97
IL-23	185.47 ± 43.63	242.71 ± 86.04	283.14 ± 214.27	222.54 ± 158.70
TNFα	4.65 ± 4.25	3.76 ± 3.76	6.61 ± 2.99	1.84 ± 1.84
TNFß	18.40 ± 4.64	14.07 ± 9.76	18.15 ± 14.21	14.88 ± 13.96

(significant differences between pig and human PRGF).

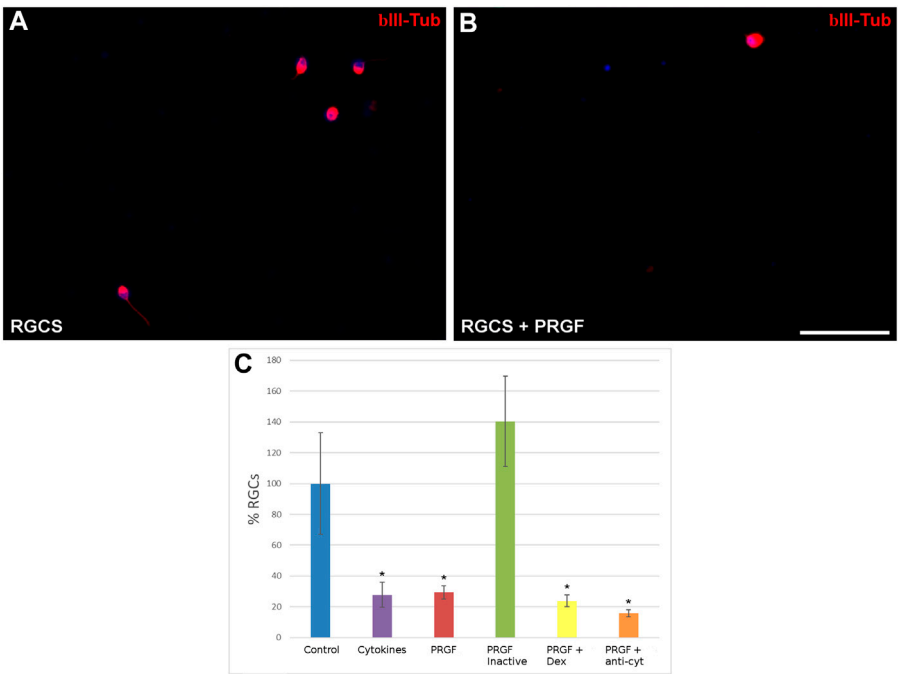

FIGURE 2 | The effect of PRGF on RGC cultures. Images of control adult pig RGC cultures **(A)** or RGCs maintained in the presence of PRGF **(B)**. The RGCs were labeled with antibodies against βIII-Tubulin (red) staining the nuclei with DAPI (blue). The percentage of RGCs **(C)** relative to the controls are represented in the histograms. RGCs were cultured in the presence of cytokines (IL-1β, IL-6, and TNFα), 10% human PRGF (PRGF), PRGF inactivated by heat, PRGF with dexamethasone (Dex) and PRGF with antibodies against cytokines (anti-cyt). Significant differences relative to the controls are shown:*$p < 0.05$. Scale bar = 100 μm.

differences in the cytokine concentrations between individuals. We detected significant differences between individuals for the IL-8, IL-12, IL-13, IL-15, IL-17, IL-23 and TNFα ($p < 0.05$) in the human PRGF, and for the IL-1ß, IL-10, IL-15, IL-17 and IL-23 ($p < 0.05$) in the pig PRGF. The remaining cytokines were relatively homogeneous between individuals, with no significant differences detected.

In light of the cytokines detected in the PRGF, their neuroprotective effects were analyzed by initially quantifying the density of RGCs in the presence or absence of 10% human PRGF (**Figure 2**). The density of RGCs was 0.55 ± 0.11 cells/mm^2 in control cultures, considered as 100%, yet a significant decrease in RGC density was evident in the presence of PRGF (29.29 ± 4.31%, $p < 0.05$), similar to that detected when the cultures were exposed to the pro-inflammatory cytokines IL-1β, IL-6 and TNFα (27.80 ± 8.03%, $p < 0.05$). Heat inactivation of the PRGF did not affect to RGC survival (140.36 ± 29.29%), favoring the survival of these cells to a similar extent as that seen in the control cultures. However, the

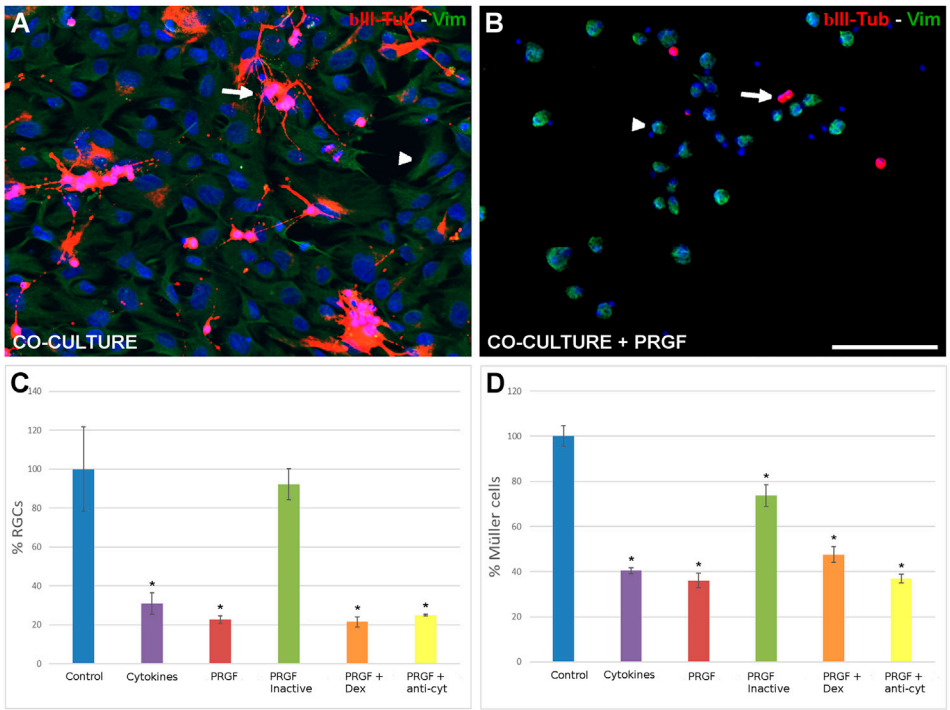

FIGURE 3 | The effect of PRGF on RGCs and Müller cells in co-culture. Control co-cultures of adult pig RGCs and Müller cells **(A)** and those maintained in the presence of PRGF **(B)**. The RGCs (arrows) were labeled with antibodies against βIII-Tubulin (red) and Müller cells (arrowheads) with antibodies against vimentin (green) and the nuclei were labeled with DAPI (blue). The number of RGCs **(C)** and Müller cells **(D)** in the co-cultures relative to the total number of cells in the control condition (100%) are represented in the histograms. RGCs and Müller cells were co-cultured with cytokines (cyt: IL-1β, IL-6 and TNFα), 10% human PRGF (PRGF), heat inactivated PRGF, PRGF with dexamethasone (Dex) and PRGF with antibodies against the cytokines (anti-cyt). Significant differences relative to the control conditions are shown: $^*p < 0.05$. Scale bar = 100 μm.

presence of the inflammatory drug dexamethasone (23.76 ± 3.76%) or of antibodies against the pro-inflammatory cytokines (15.69 ± 2.35%) did not reverse the deleterious effect of PRGF on RGCs, provoking similar survival of RGCs to the PRGF alone ($p < 0.05$, **Figure 2C**). Thus, these cytokines could be at least partially responsible for the detrimental effect on the PRGF as RGC survival diminished in their presence alone. However, others factors in the PRGF must also have a deleterious effect on the RGCs, as in the presence of the antibodies against these cytokines the survival of RGCs was still compromised.

Since Müller cells possess neuroprotective properties and given that PRGF enhances their number, we assessed the effect of PRGF on the RGCs co-cultured in the presence of Müller cells in co-cultures (**Figures 3A,B**). Interestingly, PRGF had a similar effect on RGCs in co-cultures as in the pure RGC cultures. In the presence of Müller cells, the RGC density still decreased in the presence of PRGF (22.67 ± 1.91%) or cytokines (30.89 ± 5.49%) relative to the control conditions (12.97 ± 1.33 RGCs/mm^2, 100%: $p < 0.05$). The heat inactivation of PRGF abrogated its deleterious effects on RGCs (92.22 ± 8.11%), the survival of which was no different to the controls. However, the presence of dexamethasone (21.54 ± 2.65%) or the presence of antibodies against the cytokines (24.99 ± 0.28%) did not revert the deleterious effects of PRGF on RGCs, diminishing their survival relative to the controls ($p < 0.05$, **Figure 3C**).

In terms of Müller cells, the increase in their number in the presence of 10% human PRGF was dampened when they were co-cultured with RGCs (36.09 ± 3.31%) and relative to the control conditions (209.29 ± 28.43 Müller cells/mm^2 as 100%, $p < 0.05$: **Figure 3B**). This decrease in the number of Müller cells was similar to the witnessed in the presence of the cytokines alone (40.43 ± 1.24%). Moreover, heat inactivation (73.56 ± 4.8%), the presence of dexamethasone (47.61 ± 3.46%) or of the antibodies against the cytokines (36.96 ± 1.88%) did not revert the effect of PRGF and the density of Müller cells remained lower than in the control cultures ($p < 0.05$). This difference in the behavior of Müller cells in the presence of PRGF is probably due to the inclusion of FBS in the co-culture medium, which in these co-cultures had to be maintained for the cells to grow correctly.

Finally, to assess the influence of PRGF on the survival of Müller cells, the density of Müller cells in the pure cultures was evaluated in the presence or absence of pig and human PRGF. We compared the density of Müller cell in positive control where 10% FBS was added to the medium (569.69 ± 59.85 cells/mm^2, considered as 100%), as opposed to those in which the medium was supplemented with 10% pig or human PRGF. DMEM medium without either the FBS or PRGF supplement served as the negative control, was not increase Müller cell survival. The density of Müller cells maintained in the presence of PRGF was less than when these cells were

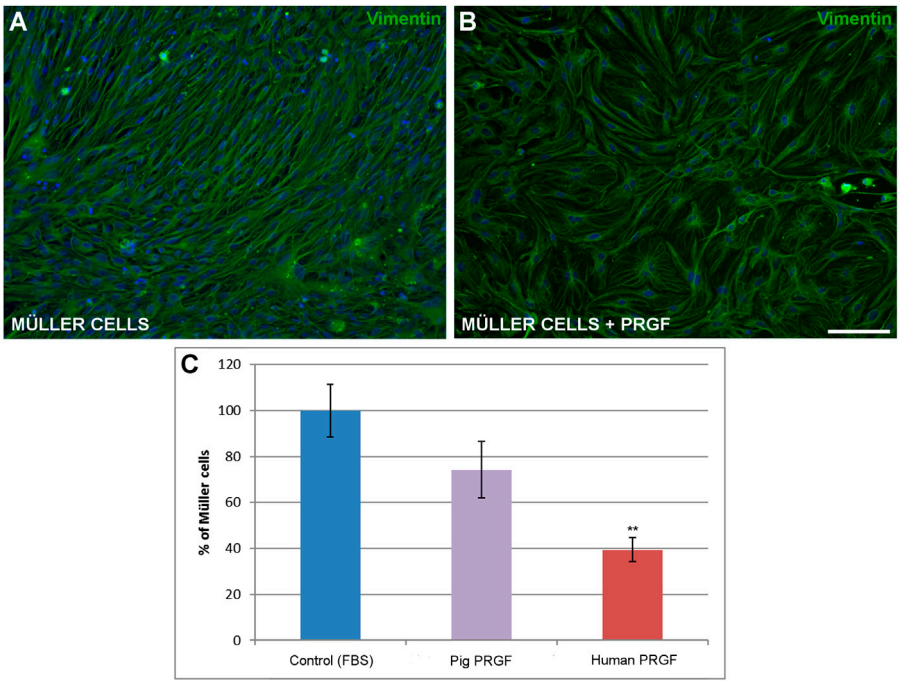

FIGURE 4 | The effect of PRGF on Müller cell density. Images of adult pig Müller cells cultured in the absence **(A)** or in the presence of PRGF **(B)**. The Müller cells were labeled with antibodies against vimentin (green) and the nuclei with DAPI (blue). The number of Müller cells represents the percentage **(C)** relative to the total number of Müller cells in the control conditions (100%). Müller cells were cultured with 10% fetal bovine serum (FBS) in control, 10% pig PRGF or 10% human PRGF. Significant differences of control and human PRGF are shown: $^{**}p < 0.01$. Scale bar = 100 μm.

maintained in the presence of FBS, although in both cases the cultures reached confluence (**Figures 4A,B**). When the 10% FBS was replaced by 10% porcine PRGF there was no significant difference in the density of Müller cells (74.21 ± 12.19%) relative to the controls, whereas the Müller cell density did decrease significantly in the presence of 10% human PRGF (39.44 ± 5.34%, $p < 0.01$) relative to the control conditions (100%, **Figure 4C**). Nevertheless, the substitution of FBS with PRGF induced an increase of Müller cells, and Müller cells failed to proliferate or survive in the absence of either PRGF or FBS.

DISCUSSION

PRGF provides tissues with a pool of growth factors, suggesting that it may stimulate and accelerate tissue regeneration (Anitua et al., 2015b). For this reason, PRGF is considered a potential therapeutic agent suitable to treat neurodegenerative diseases Anitua et al., 2015a). However, in this study on retinal cells, we found that PRGF reduced the number of retinal neurons, such as RGCs, while promoting the increase of Müller glial cells.

The proliferative effects of PRGF were first demonstrated in dentistry and oral implantology, orthopedics, in the treatment of skin disorders and sports medicine (Sánchez et al., 2003). Indeed, several studies have described the potential of PRGF eye drops to produce tissue regeneration in the ophthalmological field, where it has advantages over other PRPs (Lopez-Plandolit et al., 2010; Lopez-Plandolit et al., 2011). Our results demonstrate that PRGF may induce an increase in Müller cells density. Porcine PRGF is capable of substituting serum when Müller cells are cultured alone. This is likely to be due to the growth factors present in the PRGF, such as IGF-1, PDGF or FGF, powerful stimulators of cell replication and proliferation (Vahabi et al., 2015).

The ability to induce cells division of PRGF is not only evident in the pig PRGF but also, to a lesser extent in the human PRGF that partially activated the division of porcine Müller cells, showing that this effect of PRGF could be interspecific, although the pig PRGF increased higher the number of Müller cells than the human PRGF. This behavior is similar in different types of cells, because different PRPs, including PRGF, induce a proliferative response (Vahabi et al., 2015), as seen here in the Müller cells in the absence of serum. Moreover, different platelet preparations produce similar proliferative effects on immortalized human Müller cells (MIO-M1) (Burmeister et al., 2009). In addition, intravitreal injection of PRPs induces pre-retinal proliferation of fibroblast-like cells (Pinon et al., 1992) and these fibroblast-like cells could be Müller cells. Currently, autologous platelet injections are being used in the clinic as a treatment for recurrent retinal detachment (Nadal et al., 2012), and pilot studies are being carried out to use PRGF in retinal surgery to treat persistent macular holes (Arias et al., 2019), showing benefits in patients but possibly also associated with some complication including focal macular epithelial pigmentary hypertrophy, retinal folds emanating from the macula, development of epiretinal membrane, among others (Minihan et al., 1997; Cheung et al., 2005; Nugent and Lee, 2015). The

success in the clinical uses of PRPs, such as PRGF, could be due to their proliferative effects on cells like Müller glia.

It has also been suggested that PRGF induces neuroprotection by activating the anti-apoptotic PI3K/Akt signaling pathway, and/or through reducing caspase-3, promoting proliferation and survival in primary neuronal cultures. In addition, PRGF has been proposed to reduce the number of degenerating neurons in a mouse model of AD, where it dampens astrocyte reactivity, prevents the loss of synaptic proteins and stimulates global improvements in anxiety, learning and memory behaviors (Anitua et al., 2014b). However, our data show PRGF compromises the survival of RGCs, even when they are co-cultured with Müller cells. It is important to note that in these earlier studies, PRGF obtained from human blood was used in mouse models (Anitua et al., 2015a) and thus, interspecific interactions did not appear to affect neuroprotection. However, we have founded that the porcine and human PRGF did not exert the same effect on the cultures as was mentioned previously. Moreover, the concentrations of PRGF used here were 10%, the same as those used in these aforementioned studies of neurodegenerative diseases (Anitua et al., 2014b; Anitua et al., 2015a), although these were *in vivo* studies and the behavior of the retinal cells in cultures may differ in response to the same concentration of PRGF. Although the plasma concentrate is distinct, some results are consistent with our findings, where other PRPs may produce neurotoxic effects, such as thrombin-activated platelet-rich plasma, possibly due to the release of glutamate in neuronal cultures (Bell et al., 2014; Zhou et al., 2017). Moreover, PRGF contains many different factors that are also present in PRP, including morphogens and growth factors (Anitua et al., 2015b), and that exert negative effects on axon growth in rat brain/spinal cord co-cultures, such as TGF-β1 (Takeuchi et al., 2012). These mechanisms could partially explain the results obtained here on RGCs.

In co-cultures, the negative effect of PRGF on RGCs survival was observed as well as when they were maintained in pure cultures. Müller cells provide structural support, maintain retinal homeostasis, promote the survival of neurons, and secrete neurotrophins and growth factors that offer protection to neurons (Garcia et al., 2003; Vecino et al., 2016). Thus, since PRGF increases Müller cell number, we expected that the survival of RGCs would be enhanced in co-culture thanks to their possible neuroprotective action. However, the presence of Müller cells was not sufficient to rescue RGCs from the detrimental effects of the PRGF. In addition, the Müller cells density was weaker in the co-cultures in presence of PRGF, possibly due to the extra effort of these cells to maintain the RGCs alive or to other mechanisms not assessed here. In addition, we observed that the morphology of the cells dramatically change when they are in co-culture in the presence of PRGF. The decrease in the survival of both Müller cells and RGCs suggest that both types of cells are stressed or even dying. In the first steps of the apoptosis, there is a shrinkage of the cells (Saraste and Pulkki, 2000) that correspond to the rounded morphology of Müller cells in this condition.

In order to better understand the effect of PRGF on RGCs and Müller glia, we analyzed the cytokines that it contains. Some cytokines have already been defined in PRGF, like IL-6 (Masuki et al., 2016), IL-8, IL-4 and TNFα (Anitua et al., 2015b), yet here we confirmed the presence of the 16 selected cytokines analyzed in five porcine and three human samples: IL-1α, IL-1β, IL-2, IL-4, IL-5, IL-6, IL-8, IL-10, IL-12p70, IL-13, IL-15, IL-17, IL-23, IFNγ, TNFα and TNFβ. Moreover, there were no significant differences in the cytokine concentrations between porcine and human PRGF, except for the higher abundance of the pro-inflammatory cytokine IL-8 in human PRGF.

Despite the wide range of cytokines identified in the PRGF, the presence of the pro-inflammatory cytokines IL-1α, IL-1β and IL-2 is particularly noteworthy due to their possible contribution to the neurotoxic and proliferative effects of PRGF. The neurotoxic effect of IL-1 is evident through an increase in neuronal apoptosis in the hippocampus and dentate gyrus (Rincon-Lopez et al., 2016), and in the retina (Kido et al., 2001). Moreover, the neurotoxicity of IL-1β could be specifically mediated by glial cells (Thornton et al., 2006), and/or to enhanced endoplasmic reticulum stress as a result of the disturbance of intracellular Ca^{2+} homeostasis provoked via NMDARs (Dong et al., 2017). In addition, IL-2 may also be neurotoxic and produce nervous tissue damage (Hanisch et al., 1997). However, these interleukins have also been implicated in proliferation and IL-1 can stimulate diverse cell types (Rangnekar et al., 1991; Jerde and Bushman, 2009). Indeed, IL-1α can stimulate proliferation of neural progenitor cells (Mcpherson et al., 2011) and IL-1β significantly augments smooth muscle cell proliferation (Zhai et al., 2004). Furthermore, IL-2 can increase the proliferation of T lymphocytes (Pesoa et al., 2000) or other cell types like enterocytes (O'loughlin et al., 2001). However, we do not rule out the possibility that there are other molecules in addition to these that could be implicated in these effects. Moreover, microglial cells may also be implicated in the effect of PRGF in the retina as we have described a migration of these cells as a sing of inflammation in presence of PRGF. (Ruzafa et al., 2021).

The presence of the three major pro-inflammatory cytokines (IL-1β, IL-6 and TNFα (Taki et al., 2007; Zhang and An, 2007) in the cultures could compromise RGC survival due to the neurotoxic effect that they can exert (Downen et al., 1999; Ye et al., 2013). However, the suppression of their effects by adding antibodies against these cytokines to the PRGF previous to be added to the cultures was insufficient to prevent RGC death. Thus, the mechanism implicated in neuronal death triggered by PRGF appears to be multifactorial. On the other hand, RGC death can be reversed by the heat-inactivation of PRGF, which maintains the biological activity of PRGF but completely reduces the complement activity and significantly deceases the presence of IgE (Anitua et al., 2014a). Although the inactivated PRGF apparently contains the same cytokines as the active PRGF, and in similar amounts, heat-inactivated PRGF is a safer format to administrate this therapy, especially for subjects affected by immune disorders, due to the cytokines activity, that was not assessed here, may have been compromised. This response could be due to the reduction in neuronal viability by complement (Peterson et al., 2017), the inhibition of which could be neuroprotective (Yang et al., 2013) and sufficient to protect RGCs from death. In addition, it should be noted that although inflammatory pathways are implicated in neuronal

death, the presence of the anti-inflammatory drug dexamethasone does not enhance the RGCs survival.

Although PRGF has been successfully used in different medical and surgical specialties, and there is extensive data indicating that PRP induces tissue regeneration, many of these studies may not have been sufficiently rigorous or well-controlled, and their data is often limited, whereas other studies have yielded contrasting results (Kuffler, 2015). The impact exerted by PRGF is as yet not fully understood, such as its neurotoxic effect, and as such its application in ophthalmology must be studied in greater depth. Indeed, the deleterious effect of PRGF on RGCs demonstrated in our study should be taken into account when using it to treat retinal disorders like macular holes. Though a structural recovery might be achieved, for instance macular hole closure, probably due to the promotion of increases Müller cell number, the functional recovery might be limited due to its toxic effects on RGCs. The differences in the concentrations of the multitude of factors in PRGF and other PRPs may explain the variability in the results obtained between different studies (Vahabi et al., 2015). Indeed, we found significant differences in cytokine concentrations between individuals and thus, further animal and clinical studies should be performed to clarify the full range of properties of PRGF.

In conclusion, PRGF does not offer neuroprotection to RGCs but rather, it markedly compromises the survival of RGCs, even when these cells are co-cultured with Müller cells. However, this effect could be reverted by heat-inactivating the PRGF. Conversely, PRGF increases Müller cell number, and it may be a good candidate to stimulate and accelerate tissue regeneration due to these properties. These responses could be produced by the presence of several cytokines in PRGF, such as the IL-1α, IL-1β and IL-2 that are present in both human and pig PRGF. Although the factors responsible for promoting glial survival in the PRGF could be the neurotrophins identified previously, other molecules could also participate in this effect. Therefore, further studies will be necessary to clarify the effect of PRGF in the nervous system, as well as the other properties of PRGF, including the implication of the cytokines it contains.

DATA AVAILABILITY STATEMENT

The raw data supporting the conclusions of this article will be made available by the authors, without undue reservation.

ETHICS STATEMENT

The studies involving human participants were reviewed and approved by the Helsinki Declaration on Biomedical Research Involving Human Subjects. The patients/participants provided their written informed consent to participate in this study. The animal study was reviewed and approved by the ARVO Statement for the Use of Animals in Ophthalmic and Vision Research.

AUTHOR CONTRIBUTIONS

Data curation, NR and XP; Formal analysis, NR and XP, Funding acquisition, EV; Methodology, XP; Project administration, EV; Supervision, EV; Writing—original draft, NR; Writing—review & editing, NR, XP, AF, JA, AA, and EV. All authors have read and agreed to the published version of the manuscript

FUNDING

We acknowledge the support of MINECO-Retos Fondos Fender (RTC-2016-48231), Gobierno Vasco (PUE_2018_1_0004), ELKARTEK (KK-2019/00086), PIBA 2020-1-0026 and MINECO-Retos (PID2019-111139RB-I00) to EV.

REFERENCES

Anitua, E., Muruzabal, F., De La Fuente, M., Merayo-Lloves, J., and Orive, G. (2014a). Effects of heat-treatment on plasma rich in growth factors-derived autologous eye drop. *Exp. Eye Res.* 119, 27–34. doi:10.1016/j.exer.2013.12.005

Anitua, E., Pascual, C., Antequera, D., Bolos, M., Padilla, S., Orive, G., et al. (2014b). Plasma rich in growth factors (PRGF-Endoret) reduces neuropathologic hallmarks and improves cognitive functions in an Alzheimer's disease mouse model. *Neurobiol. Aging* 35, 1582–1595. doi:10.1016/j.neurobiolaging.2014.01.009

Anitua, E., Pascual, C., Pérez-Gonzalez, R., Orive, G., and Carro, E. (2015a). Intranasal PRGF-Endoret enhances neuronal survival and attenuates NF-κB-dependent inflammation process in a mouse model of Parkinson's disease. *J. Control Release* 203, 170–180. doi:10.1016/j.jconrel.2015.02.030

Anitua, E., Prado, R., Azkargorta, M., Rodriguez-Suárez, E., Iloro, I., Casado-Vela, J., et al. (2015b). High-throughput proteomic characterization of plasma rich in growth factors (PRGF-Endoret)-derived fibrin clot interactome. *J. Tissue Eng. Regen. Med.* 9, E1–E12. doi:10.1002/term.1721

Arias, J. D., Hoyos, A. T., Alcantara, B., Sanchez-Avila, R. M., Arango, F. J., and Galvis, V. (2019). Plasma rich in growth factors for persistent macular hole: A pilot study. *Retin. Cases Brief Rep.* [Epub ahead of print]. doi:10.1097/ICB.0000000000000957

Bell, J. D., Thomas, T. C., Lass, E., Ai, J., Wan, H., Lifshitz, J., et al. (2014). Platelet-mediated changes to neuronal glutamate receptor expression at sites of microthrombosis following experimental subarachnoid hemorrhage. *J. Neurosurg.* 121, 1424–1431. doi:10.3171/2014.3.JNS132130

Berry, M., Ahmed, Z., Lorber, B., Douglas, M., and Logan, A. (2008). Regeneration of axons in the visual system. *Restor Neurol. Neurosci.* 26, 147–174.

Bringmann, A., Pannicke, T., Grosche, J., Francke, M., Wiedemann, P., Skatchkov, S. N., et al. (2006). Müller cells in the healthy and diseased retina. *Prog. Retin. Eye Res.* 25, 397–424. doi:10.1016/j.preteyeres.2006.05.003

Bringmann, A., and Reichenbach, A. (2001). Role of Muller cells in retinal degenerations. *Front. Biosci.* 6, E72–E92. doi:10.2741/bringman

Burmeister, S. L., Hartwig, D., Limb, G. A., Kremling, C., Hoerauf, H., Müller, M., et al. (2009). Effect of various platelet preparations on retinal Muller cells. *Invest. Ophthalmol. Vis. Sci.* 50, 4881–4886. doi:10.1167/iovs.08-3057

Cheung, C. M., Munshi, V., Mughal, S., Mann, J., and Hero, M. (2005). Anatomical success rate of macular hole surgery with autologous platelet without internal-limiting membrane peeling. *Eye (Lond)* 19, 1191–1193. doi:10.1038/sj.eye.6701733

Dong, Y., Kalueff, A. V., and Song, C. (2017). N-methyl-d-aspartate receptor-mediated calcium overload and endoplasmic reticulum stress are involved in interleukin-1beta-induced neuronal apoptosis in rat hippocampus. *J. Neuroimmunol.* 307, 7–13. doi:10.1016/j.jneuroim.2017.03.005

Downen, M., Amaral, T. D., Hua, L. L., Zhao, M. L., and Lee, S. C. (1999). Neuronal death in cytokine-activated primary human brain cell culture: role of tumor necrosis factor-alpha. *Glia* 28, 114–127.

García, M., Forster, V., Hicks, D., and Vecino, E. (2002). Effects of müller glia on cell survival and neuritogenesis in adult porcine retina *in vitro*. *Invest. Ophthalmol. Vis. Sci.* 43, 3735–3743.

García, M., Forster, V., Hicks, D., and Vecino, E. (2003). *In vivo* expression of neurotrophins and neurotrophin receptors is conserved in adult porcine retina *in vitro*. *Invest. Ophthalmol. Vis. Sci.* 44, 4532–4541. doi:10.1167/iovs.03-0419

García, M., and Vecino, E. (2003). Role of Müller glia in neuroprotection and regeneration in the retina. *Histol. Histopathol.* 18, 1205–1218. doi:10.14670/HH-18.1205

Garcia-Valenzuela, E., Shareef, S., Walsh, J., and Sharma, S. C. (1995). Programmed cell death of retinal ganglion cells during experimental glaucoma. *Exp. Eye Res.* 61, 33–44. doi:10.1016/s0014-4835(95)80056-5

Glovinsky, Y., Quigley, H. A., and Dunkelberger, G. R. (1991). Retinal ganglion cell loss is size dependent in experimental glaucoma. *Invest. Ophthalmol. Vis. Sci.* 32, 484–491.

Hanisch, U. K., Neuhaus, J., Rowe, W., Van Rossum, D., Möller, T., Kettenmann, H., et al. (1997). Neurotoxic consequences of central long-term administration of interleukin-2 in rats. *Neuroscience* 79, 799–818. doi:10.1016/s0306-4522(97)00040-7

Jerde, T. J., and Bushman, W. (2009). IL-1 induces IGF-dependent epithelial proliferation in prostate development and reactive hyperplasia. *Sci. Signal* 2, ra49. doi:10.1126/scisignal.2000338

Jin, K., Zhu, Y., Sun, Y., Mao, X. O., Xie, L., and Greenberg, D. A. (2002). Vascular endothelial growth factor (VEGF) stimulates neurogenesis *in vitro* and *in vivo*. *Proc. Natl. Acad. Sci. USA* 99, 11946–11950. doi:10.1073/pnas.182296499

Joo, C. K., Choi, J. S., Ko, H. W., Park, K. Y., Sohn, S., Chun, M. H., et al. (1999). Necrosis and apoptosis after retinal ischemia: involvement of NMDA-mediated excitotoxicity and p53. *Invest Ophthalmol. Vis. Sci.* 40, 713–720.

Kido, N., Inatani, M., Honjo, M., Yoneda, S., Hara, H., Miyawaki, N., et al. (2001). Dual effects of interleukin-1beta on N-methyl-D-aspartate-induced retinal neuronal death in rat eyes. *Brain Res.* 910, 153–162. doi:10.1016/s0006-8993(01)02706-8

Knöferle, J., Koch, J. C., Ostendorf, T., Michel, U., Planchamp, V., Vutova, P., et al. (2010). Mechanisms of acute axonal degeneration in the optic nerve *in vivo*. *Proc. Natl. Acad. Sci. USA* 107, 6064–6069. doi:10.1073/pnas.0909794107

Kuffler, D. P. (2015). Platelet-rich plasma promotes axon regeneration, wound healing, and pain reduction: Fact or Fiction. *Mol. Neurobiol.* 52, 990–1014. doi:10.1007/s12035-015-9251-x

Lieth, E., Gardner, T. W., Barber, A. J., and Antonetti, D. A.Penn State Retina Research Group (2000). Retinal neurodegeneration: Early pathology in diabetes. *Clin. Exp. Ophthalmol* 28, 3–8. doi:10.1046/j.1442-9071.2000.00222.x

López-Plandolit, S., Morales, M. C., Freire, V., Etxebarría, J., and Durán, J. A. (2010). Plasma rich in growth factors as a therapeutic agent for persistent corneal epithelial defects. *Cornea* 29, 843–848. doi:10.1097/ICO.0b013e3181a81820

López-Plandolit, S., Morales, M. C., Freire, V., Grau, A. E., and Durán, J. A. (2011). Efficacy of plasma rich in growth factors for the treatment of dry eye. *Cornea* 30, 1312–1317. doi:10.1097/ICO.0b013e31820d86d6

Madeira, M. H., Elvas, F., Boia, R., Gonçalves, F. Q., Cunha, R. A., Ambrósio, A. F., et al. (2015). Adenosine A2AR blockade prevents neuroinflammation-induced death of retinal ganglion cells caused by elevated pressure. *J. Neuroinflammation* 12, 115. doi:10.1186/s12974-015-0333-5

Masuki, H., Okudera, T., Watanebe, T., Suzuki, M., Nishiyama, K., Okudera, H., et al. (2016). Growth factor and pro-inflammatory cytokine contents in platelet-rich plasma (PRP), plasma rich in growth factors (PRGF), advanced platelet-rich fibrin (A-PRF), and concentrated growth factors (CGF). *Int. J. Implant Dent* 2, 19. doi:10.1186/s40729-016-0052-4

Mcpherson, C. A., Aoyama, M., and Harry, G. J. (2011). Interleukin (IL)-1 and IL-6 regulation of neural progenitor cell proliferation with hippocampal injury: differential regulatory pathways in the subgranular zone (SGZ) of the adolescent and mature mouse brain. *Brain Behav. Immun.* 25, 850–862. doi:10.1016/j.bbi.2010.09.003

Minihan, M., Goggin, M., and Cleary, P. E. (1997). Surgical management of macular holes: results using gas tamponade alone, or in combination with autologous platelet concentrate, or transforming growth factor beta 2. *Br. J. Ophthalmol.* 81, 1073–1079. doi:10.1136/bjo.81.12.1073

Nadal, J., López-Fortuny, M., Sauvageot, P., and Pérez-Formigó, D. (2012). Treatment of recurrent retinal detachment secondary to optic nerve coloboma with injection of autologous platelet concentrate. *J. AAPOS* 16, 100–101. doi:10.1016/j.jaapos.2011.10.007

Nugent, R. B., and Lee, G. A. (2015). Ophthalmic use of blood-derived products. *Surv. Ophthalmol.* 60, 406–434. doi:10.1016/j.survophthal.2015.03.003

O'kusky, J. R., Ye, P., and D'ercole, A. J. (2000). Insulin-like growth factor-I promotes neurogenesis and synaptogenesis in the hippocampal dentate gyrus during postnatal development. *J. Neurosci.* 20, 8435–8442. doi:10.1523/JNEUROSCI.20-22-08435.2000

O'loughlin, E. V., Pang, G. P., Noltorp, R., Koina, C., Batey, R., and Clancy, R. (2001). Interleukin 2 modulates ion secretion and cell proliferation in cultured human small intestinal enterocytes. *Gut* 49, 636–643. doi:10.1136/gut.49.5.636

Orive, G., Anitua, E., Pedraz, J. L., and Emerich, D. F. (2009). Biomaterials for promoting brain protection, repair and regeneration. *Nat. Rev. Neurosci.* 10, 682–692. doi:10.1038/nrn2685

Pereiro, X., Ruzafa, N., Acera, A., Urcola, A., and Vecino, E. (2020). Optimization of a method to isolate and culture adult porcine, rats and mice müller glia in order to study retinal diseases. *Front Cell Neurosci* 14, 7. doi:10.3389/fncel.2020.00007

Pesoa, S., Martín, A., Mariani, A. L., Vullo, C., and Serra, H. (2000). Interleukin 2 induction of proliferation in resting T lymphocytes requires contact with monocytes. *Medicina (B Aires)* 60, 202–210.

Peterson, S. L., Nguyen, H. X., Mendez, O. A., and Anderson, A. J. (2017). Complement protein C3 suppresses axon growth and promotes neuron loss. *Sci. Rep.* 7, 12904. doi:10.1038/s41598-017-11410-x

Piñon, R. M., Pastor, J. C., Saornil, M. A., Goldaracena, M. B., Layana, A. G., Gayoso, M. J., et al. (1992). Intravitreal and subretinal proliferation induced by platelet-rich plasma injection in rabbits. *Curr. Eye Res.* 11, 1047–1055. doi:10.3109/02713689209015076

Quigley, H. A. (2011). Glaucoma. *Lancet* 377, 1367–1377. doi:10.1016/S0140-6736(10)61423-7

Quigley, H. A., Nickells, R. W., Kerrigan, L. A., Pease, M. E., Thibault, D. J., and Zack, D. J. (1995). Retinal ganglion cell death in experimental glaucoma and after axotomy occurs by apoptosis. *Invest. Ophthalmol. Vis. Sci.* 36, 774–786.

Rangnekar, V. V., Waheed, S., Davies, T. J., Toback, F. G., and Rangnekar, V. M. (1991). Antimitogenic and mitogenic actions of interleukin-1 in diverse cell types are associated with induction of gro gene expression. *J. Biol. Chem.* 266, 2415–2422. doi:10.1016/S0021-9258(18)52260-2

Reichenbach, A., and Bringmann, A. (2013). New functions of Müller cells. *Glia* 61, 651–678. doi:10.1002/glia.22477

Rincon-Lopez, C., Tlapa-Pale, A., Medel-Matus, J. S., Martinez-Quiroz, J., Rodriguez-Landa, J. F., and Lopez-Meraz, M. L. (2016). Interleukin-1beta increases neuronal death in the hippocampal dentate gyrus associated with status epilepticus in the developing rat. *Neurologia* 32, 587–594. doi:10.1016/j.nrl.2016.03.013

Ruzafa, N., Pereiro, X., Lepper, M. F., Hauck, S. M., and Vecino, E. (2018). A proteomics approach to identify candidate proteins secreted by müller glia that protect ganglion cells in the retina. *Proteomics* 18, e1700321. doi:10.1002/pmic.201700321

Ruzafa, N., and Vecino, E. (2015). Effect of Müller cells on the survival and neuritogenesis in retinal ganglion cells. *Arch. Soc. Esp Oftalmol.* 90, 522–526. doi:10.1016/j.oftal.2015.03.009

Ruzafa, N., Pereiro, X., Fonollosa, A., Araiz, J., Acera, A., and Vecino, E. (2021). The effect of plasma rich in growth factors (PRGF) on microglial migration, macroglial gliosis and proliferation, and neuronal survival. *Front. Pharmacol.* 43, 658–670. doi:10.1097/DSS.0000000000001049

Sánchez, M., Azofra, J., Anitua, E., Andía, I., Padilla, S., Santisteban, J., et al. (2003). Plasma rich in growth factors to treat an articular cartilage avulsion: A case report. *Med. Sci. Sports Exerc.* 35 (10), 1648–1652. doi:10.1249/01.MSS.0000089344.44434.50

Saraste, A., and Pulkki, K. (2000). Morphologic and biochemical hallmarks of apoptosis. *Cardiovasc. Res.* 45 (3), 528–537. doi:10.1016/s0008-6363(99)00384-3

Sellés-Navarro, I., Villegas-Pérez, M. P., Salvador-Silva, M., Ruiz-Gómez, J. M., and Vidal-Sanz, M. (1996). Retinal ganglion cell death after different transient

periods of pressure-induced ischemia and survival intervals. A quantitative *in vivo* study. *Invest. Ophthalmol. Vis. Sci.* 37, 2002–2014.

Takeuchi, M., Kamei, N., Shinomiya, R., Sunagawa, T., Suzuki, O., Kamoda, H., et al. (2012). Human platelet-rich plasma promotes axon growth in brain-spinal cord coculture. *Neuroreport* 23, 712–716. doi:10.1097/WNR.0b013e3283567196

Taki, N., Tatro, J. M., Lowe, R., Goldberg, V. M., and Greenfield, E. M. (2007). Comparison of the roles of IL-1, IL-6, and TNFalpha in cell culture and murine models of aseptic loosening. *Bone* 40, 1276–1283. doi:10.1016/j.bone.2006.12.053

Thornton, P., Pinteaux, E., Gibson, R. M., Allan, S. M., and Rothwell, N. J. (2006). Interleukin-1-induced neurotoxicity is mediated by glia and requires caspase activation and free radical release. *J. Neurochem.* 98, 258–266. doi:10.1111/j.1471-4159.2006.03872.x

Vahabi, S., Vaziri, S., Torshabi, M., and Rezaei Esfahrood, Z. (2015). Effects of plasma rich in growth factors and platelet-rich fibrin on proliferation and viability of human gingival fibroblasts. *J. Dent (Tehran)* 12, 504–512.

Vecino, E., García-Crespo, D., García-Grespo, D., García, M., Martinez-Millán, L., Sharma, S. C., et al. (2002). Rat retinal ganglion cells co-express brain derived neurotrophic factor (BDNF) and its receptor TrkB. *Vis. Res* 42, 151–157. doi:10.1016/s0042-6989(01)00251-6

Vecino, E., Heller, J. P., Veiga-Crespo, P., Martin, K. R., and Fawcett, J. W. (2015). Influence of extracellular matrix components on the expression of integrins and regeneration of adult retinal ganglion cells. *PLoS One* 10, e0125250. doi:10.1371/journal.pone.0125250

Vecino, E., Rodriguez, F. D., Ruzafa, N., Pereiro, X., and Sharma, S. C. (2016). Glia-neuron interactions in the mammalian retina. *Prog. Retin. Eye Res.* 51, 1–40. doi:10.1016/j.preteyeres.2015.06.003

Yang, J., Ahn, H. N., Chang, M., Narasimhan, P., Chan, P. H., and Song, Y. S. (2013). Complement component 3 inhibition by an antioxidant is neuroprotective after cerebral ischemia and reperfusion in mice. *J. Neurochem.* 124, 523–535. doi:10.1111/jnc.12111

Ye, L., Huang, Y., Zhao, L., Li, Y., Sun, L., Zhou, Y., et al. (2013). IL-1beta and TNF-alpha induce neurotoxicity through glutamate production: A potential role for neuronal glutaminase. *J. Neurochem.* 125, 897–908. doi:10.1111/jnc.12263

Zhai, W., Eynott, P. R., Oltmanns, U., Leung, S. Y., and Chung, K. F. (2004). Mitogen-activated protein kinase signalling pathways in IL-1 beta-dependent rat airway smooth muscle proliferation. *Br. J. Pharmacol.* 143, 1042–1049. doi:10.1038/sj.bjp.0705971

Zhang, J. M., and An, J. (2007). Cytokines, inflammation, and pain. *Int. Anesthesiol Clin.* 45, 27–37. doi:10.1097/AIA.0b013e318034194e

Zhang, L., Ino-Ue, M., Dong, K., and Yamamoto, M. (2000). Retrograde axonal transport impairment of large- and medium-sized retinal ganglion cells in diabetic rat. *Curr. Eye Res.* 20, 131–136. doi:10.1076/0271-3683(200002)20:2;1-D;FT131

Zhou, T., Che, D., Lan, Y., Fang, Z., Xie, J., Gong, H., et al. (2017). Mesenchymal marker expression is elevated in Müller cells exposed to high glucose and in animal models of diabetic retinopathy. *Oncotarget* 8, 4582–4594. doi:10.18632/oncotarget.13945

Conflict of Interest: The authors declare that the research was conducted in the absence of any commercial or financial relationships that could be construed as a potential conflict of interest.

frontiers in Pharmacology

ORIGINAL RESEARCH
published: 13 January 2021
doi: 10.3389/fphar.2020.593514

Changes in Retinal Structure and Ultrastructure in the Aged Mice Correlate With Differences in the Expression of Selected Retinal miRNAs

Anca Hermenean[1,2], Maria Consiglia Trotta[3], Sami Gharbia[1,2], Andrei Gelu Hermenean[4], Victor Eduard Peteu[5], Cornel Balta[1], Coralia Cotoraci[6]*, Carlo Gesualdo[7], Settimio Rossi[7], Mihaela Gherghiceanu[4,5] and Michele D'Amico[3]*

[1]"Aurel Ardelean" Institute of Life Sciences, Vasile Goldis Western University of Arad, Arad, Romania, [2]Department of Biochemistry and Molecular Biology, University of Bucharest, Bucharest, Romania, [3]Section of Pharmacology, Department of Experimental Medicine, University of Campania "Luigi Vanvitelli", Naples, Italy, [4]Carol Davila University of Medicine and Pharmacy, Bucharest, Romania, [5]Victor Babes National Institute of Pathology, Bucharest, Romania, [6]Faculty of Medicine, Vasile Goldis Western University of Arad, Arad, Romania, [7]Eye Clinic, Multidisciplinary Department of Medical, Surgical and Dental Sciences, University of Campania "Luigi Vanvitelli", Naples, Italy

OPEN ACCESS

Edited by:
Galina Sud'ina,
Lomonosov Moscow State University, Russia

Reviewed by:
Tapas C. Nag,
All India Institute of Medical Sciences, India
Vera Lucia Bonilha,
Cleveland Clinic, United States
Rujuan Dai,
Virginia Tech, United States

***Correspondence:**
Anca Hermenean
anca.hermenean@gmail.com
Coralia Cotoraci
ccotoraci@yahoo.com

Specialty section:
This article was submitted to Inflammation Pharmacology, a section of the journal Frontiers in Pharmacology

Received: 10 August 2020
Accepted: 29 October 2020
Published: 13 January 2021

Citation:
Hermenean A, Trotta MC, Gharbia S, Hermenean AG, Peteu VE, Balta C, Cotoraci C, Gesualdo C, Rossi S, Gherghiceanu M and D'Amico M (2020) Changes in Retinal Structure and Ultrastructure in the Aged Mice Correlate With Differences in the Expression of Selected Retinal miRNAs. Front. Pharmacol. 11:593514. doi: 10.3389/fphar.2020.593514

Age and gender are two important factors that may influence the function and structure of the retina and its susceptibility to retinal diseases. The aim of this study was to delineate the influence that biological sex and age exert on the retinal structural and ultrastructural changes in mice and to identify the age-related miRNA dysregulation profiles in the retina by gender. Experiments were undertaken on male and female Balb/c aged 24 months (approximately 75–85 years in humans) compared to the control (3 months). The retinas were analyzed by histology, transmission electron microscopy, and age-related miRNA expression profile analysis. Retinas of both sexes showed a steady decline in retinal thickness as follows: photoreceptor (PS) and outer layers ($p < 0.01$ for the aged male vs. control; $p < 0.05$ for the aged female vs. control); the inner retinal layers were significantly affected by the aging process in the males ($p < 0.01$) but not in the aged females. Electron microscopy revealed more abnormalities which involve the retinal pigment epithelium (RPE) and Bruch's membrane, outer and inner layers, vascular changes, deposits of amorphous materials, and accumulation of lipids or lipofuscins. Age-related miRNAs, miR-27a-3p ($p < 0.01$), miR-27b-3p ($p < 0.05$), and miR-20a-5p ($p < 0.05$) were significantly up-regulated in aged male mice compared to the controls, whereas miR-20b-5p was significantly down-regulated in aged male ($p < 0.05$) and female mice ($p < 0.05$) compared to the respective controls. miR-27a-3p (5.00 fold; $p < 0.01$) and miR-27b (7.58 fold; $p < 0.01$) were significantly up-regulated in aged male mice vs. aged female mice, whereas miR-20b-5p (–2.10 fold; $p < 0.05$) was significantly down-regulated in aged male mice vs. aged female mice. Interestingly, miR-27a-3p, miR-27b-3p, miR-20a-5p, and miR-20b-5p expressions significantly correlated with the thickness of the retinal PS layer ($p < 0.01$), retinal outer layers ($p < 0.01$), and Bruch's membrane ($p < 0.01$). Our results showed that biological sex

can influence the structure and function of the retina upon aging, suggesting that this difference may be underlined by the dysregulation of age-related mi-RNAs.

Keywords: aging, retina, gender, histology, electron micoscopy, miRNAs

INTRODUCTION

The structural and functional physiological evolution of the retina with age can be influenced by biological sex and susceptibility to retinal diseases (Wagner et al., 2008; Freund et al., 2011). There are anatomical sex differences, visual performances, and divergent molecular profiles (Du et al., 2017) by gender upon aging, which may contribute to different susceptibilities to disease and trace different evolutions for retinal pathologies (Wagner et al., 2008; Ozawa et al., 2015; Schmidl et al., 2015). Numerous eye anatomical changes occur with age, including cell loss (e.g., corneal and trabecular endothelium and retinal pigment epithelium [RPE]) and degenerative processes (e.g., vitreous liquefaction and drusen) (Grossniklaus et al., 2013), that may be influenced by gender differences. Clinical results have reported that women have thinner retinas than men, without any differences in the foveal pit morphology (Wagner-Schuman et al., 2011), whereas the amplitudes of scotopic and photopic electroretinograms (ERGs) of female subjects have been reported to be on average 29% larger than those of males (Brûlé et al., 2007). Morphological studies have shown gender-related structural differences in thickness of the macular retinal layers by spectral-domain optical coherence tomography (SD-OCT) (Adhi et al., 2012; Hashamani et al., 2018). Additionally, the outer nuclear layers and the inner nuclear layer (INL) have been determined to be thicker in men, whereas the nerve fiber layer (NFL) is thicker in women (Ooto et al., 2011).

The anatomical and physiological differences of the retina related to gender are reflected in the associated pathologies (Zetterberg, 2016; Nuzzi et al., 2018). Aging is the first risk factor that leads to glaucoma or age-related macular degeneration (AMD). Some studies have shown a higher incidence and severity of late-stage AMD in women (AREDS Research Group, 2000; Chakravarthy et al., 2010), whereas others have not pointed to a gender difference (Buch et al., 2005; Laitinen et al., 2010). One of the main risk factors for developing AMD is related to macular pigment deficiency, which is more pronounced in women (Beatty et al., 2000; Meyers et al., 2013). Cataracts are more prevalent among women aged 65 and 74 years (24–27%) than men of the same age (14–20%) (Klein et al., 1994; Freeman et al., 2001; Younan et al., 2002). Estrogen exerts a protective effect for women due to its antioxidant properties (Beebe et al., 2010); however, after menopause, the age-related hormonal decline increases the risk of cataracts with age (Lai et al., 2013; van den Beld et al., 2018). In contrast, estrogen levels converted from aromatase to testosterone in men do not appear to be related to age, providing greater protection against cataracts (Zettemberg and Celojevic, 2015). Other results suggested that females may have some protection or resistance to neurodegenerative changes prior to retinopathy in type 2 diabetes (Ozawa et al., 2012). One prediction is that females with type 2 diabetes have better vascular perfusion than man due to estrogen because of the increased production of nitric oxide and nitric oxide synthase (NOS) genes (Mendelsohn and Karas, 2005), attenuating retinal ischemia–reperfusion (Nonaka et al., 2000). However, in an Early Treatment Diabetic Retinopathy Study (ETDRS), the female sex was reported to be a risk factor for severe visual impairment or the need to perform a vitrectomy (Trautner et al., 1997; Davis et al., 1998). Upon aging, gender-related retinal changes may be governed by sexual hormones, such as estrogen. Electroretinogram (ERG) and histology investigations on age-related retinal changes have shown the role of biological sex and age in retinal function (Chaychi et al., 2015).

MicroRNAs (miRNAs), a class of short noncoding RNAs, have been identified that are up- or down-regulated during mammalian aging (Smith-Vikos and Slack, 2012), but no study has particularly referred to retinal aging. A few studies on microRNAs have reported on age-related macular degeneration (AMD), which is the most frequent pathology associated with aging. Recently, four studies analyzed the circulating miRNA expression profiles of AMD patients (Ertekin et al., 2014; Grassmann et al., 2014; Szemraj et al., 2015; Menard et al., 2016), but the results did not completely overlap possibly because of the different inclusion criteria or different applied therapeutic protocols. Recent findings showed miRNA dysregulation in AMD of ocular tissues, which demonstrated some similarities with human AMD findings, including miR-146a, miR-17, miR-125b, and miR-155 (Berber et al., 2017).

Limited results are available regarding the ultrastructural retinal changes upon human aging and in age-related retinal diseases (Nag and Wadhwa, 2012) or in preclinical studies, as in a senescence-accelerated mouse model (Majji et al., 2000), and no results highlighting electron microscopy differences by gender were found. To date, no one has investigated whether the dysregulation of sex-differentiated miRNAs could be correlated with retinal changes during aging. The aim of this study was to delineate the influence that biological sex and age have on the retinal structural and ultrastructural changes in mice and to identify the age-related miRNA dysregulation profiles in the retina by gender.

MATERIALS AND METHODS

Animals and Experimental Design

All experimental procedures were conducted in compliance with the European and national regulations for the care and use of animals for scientific purposes. Ethics approval was obtained from the Ethics Committee for research of the Vasile Goldis Western University of Arad (approval no. 135, January 03, 2019).

Experiments were performed on male and female Balb/c that were 3 months (male/female control groups) and 24 months (male/female aged groups) of age, respectively (n = 10/each group/sex). The life span of laboratory mice ranges from 2 to 2.5 years; thus, 24 months approximate 75–85 years of age for a human (Dutta and Sengupta, 2016). While control females were under physiological and regular estrus cycle, 24-month-old females were under naturally occurring physiological decline for estrus without any manipulation, according to previous evidence showing a progressive decrease in estrogens in Balb-c females after 15 months of age (Nagasawa et al., 1978). Animals were housed in a 22 °C environment in IVC well-ventilated cages with ad libitum access to normal rat chow and water. Lighting (39 ± 7 lux) was regulated on a 12-h light/dark cycle. Particularly, although room light between 130 and 325 lux has been recommended for animals susceptible to phototoxic retinopathy by the National Research Council (US) Committee for the Update of the Guide for the Care and Use of Laboratory Animals (National Research Council, 2011), and a lower illuminance level (39 ± 7 lux) was used in order to minimize the negative effects of standard vivarium lighting on the aged retina (Bell et al., 2015). All the procedures were conducted under ketamine and xylazine anesthesia.

Each mouse was perfused via the left ventricle with 100 ml of 0.1 M ice-cold phosphate-buffered saline (PBS). To increase the efficiency of perfusion, heparin (5000 IU/ml, a final concentration of 0.1% v/v) was added to PBS (Bozycki et al., 2018). This served for the collection of one eye for biochemical assays. In the next step, animals' perfusion was continued with an additional 100 ml of freshly prepared 4% paraformaldehyde (PFA) in PBS for the collection of the remaining eye and investigations as detailed below.

Histology/Light Microscopy

The eye specimens were fixed in 4% paraformaldehyde and were embedded in paraffin and sectioned at 5 µm, and the sections were stained with hematoxylin and eosin (H&E). The light microscopy images were acquired using an Olympus BX43 microscope, with an XC30 CCD and cellSens Dimension Imaging Software (v 1.10, Olympus, Germany).

Electron Microscopy

The eye samples were prefixed in 2.7% glutaraldehyde solution (Sigma-Aldrich, St Louis, Missouri) in 0.1 M phosphate buffer, then washed in 0.15 M phosphate buffer (pH 7.2), and postfixed in 2% osmic acid solution (Sigma-Aldrich, St Louis, Missouri) in 0.15 M phosphate buffer. Dehydration was performed in acetone, followed by embedding in the epoxy resin (Epon 812). Thin sections of 70 nm thickness were cut on a Leica EM UC7 ultramicrotome (Leica Microsystems GmbH, Wetzlar, Germany). The double staining of thin sections on grids was performed with solutions of uranyl acetate and lead citrate. The sections were imaged under a TEM (Morgagni268, FEI, Eindhoven, Netherlands) at 80 kV. Data acquisition was performed with a MegaView III CCD using iTEM SIS software (Olympus Soft Imaging Software, Munster, Germany).

Morphometry

For each mouse, the thickness of the retinal layers (i.e., retinal pigment epithelium [RPE], photoreceptor cells [PS], outer nuclear layer [ONL], outer plexiform layer [OPL], inner nuclear layer [INL], inner plexiform layer [IPL], and retinal ganglion cell layer [RGL]) were measured on ten different histological sections taken from the superior and inferior retinas (central and equatorial) every 300 µm from the optic nerve head (ONH) using CellSens Dimension Imaging Software (v 1.10, Olympus, Germany).

The morphometry on the electron microscopy images was performed for the equatorial retina. The thickness of Bruch's membrane was measured at three different points on the images (n = 50 for each group) acquired at the same magnification (7,100×) using iTEM SIS software (Olympus Soft Imaging Software, Munster, Germany) and exported in Excel format for statistical analysis.

Isolation and Expression Analysis of Retinal microRNAs

After retina dissection following the method described by Rossi et al. (2016), total RNA, including microRNAs, was isolated from aged mouse retina (N = 10 per group) by using the MiRNeasy Mini Kit (Qiagen, Italy), according to the manufacturer's instructions. An appropriate volume of QIAzol Lysis Reagent (Qiagen, Italy) was used for tissue homogenization, and the miRNA isolation efficiency was monitored by adding Syn-cel-miR-39 miScript miRNA Mimic 5 nM (Qiagen, Italy) to each sample before RNA purification. RNA quality and concentration were determined by a NanoDrop 2000c spectrophotometer (Thermo Scientific, Italy). Mature miRNAs were converted into cDNA by reverse transcription performed by using the MiScript II Reverse Transcription Kit (Qiagen, Italy) and a Gene Amp PCR System 9,700 (Applied Biosystems, United States). The levels of eight miRNAs (mmu-miR-20a-5p, mmu-miR-20a-3p, mmu-miR-20b-5p, mmu-miR-106a-5p, mmu-miR-27a-3p, mmu-miR-27b-3p, mmu-miR-206-3p, and mmu-miR-381-3p), which were previously shown to be time-dependently dysregulated in the diabetic retina (Platania et al., 2019), were analyzed by real-time PCR (qPCR) with a CFX96 Real-Time System C1000 Touch Thermal Cycler (BioRad Laboratories, Inc.). The qPCR triplicate measurement was carried out by using miScript primer assays (MS00001309, MS00001869, MS00001316, MS00011039, MS00001315, MS00001385, MS00001869, and MS00032802; Qiagen, Italy), SYBR Green PCR Master Mix (Qiagen, Italy), and Ce_miR-39-5p as an external control (MS00080247, Qiagen, Italy) for normalization of miRNA expression. CFX Manager™ Software (BioRad Laboratories, Inc.) was used to evaluate the cycle threshold (Ct) values to calculate the ΔCt for each miRNA as ΔCt = Ct miRNA–Ct Ce_miR-39-5p and then miRNA expression as $2^{-\Delta Ct}$. For each miRNA profiled, the fold change expression across two experimental groups was calculated as $2^{-\Delta\Delta Ct}$ (equal to $2^{-\Delta Ct}$ of group $2/2^{-\Delta Ct}$ of group 1) and then expressed as the fold regulation. In particular, the fold up-regulation was equal to the fold change value, whereas the fold down-regulation was

calculated as the negative inverse of the fold change value (Platania et al., 2019).

Statistical Analysis

Values are expressed as means ± SD of $n = 5$ mice per group for histological and electron microscopy evaluation, while miRNA results were expressed as means ± SD of $n = 10$ mice per group. Statistical significance was assessed by one-way ANOVA, followed by Tukey's multiple comparisons test. Pearson correlation analysis was used to evaluate the strength of the association between pairs of variables. Statistical analysis was carried out with GraphPad Prism v.6 (GraphPad Software, La Jolla, CA, United States). Differences were considered statistically significant for p values <0.05.

RESULTS

Age-Related Structural Differences in Both Male and Female Mice

The aging-induced changes in the entire retinal structure were analyzed. Representative retinal cross sections obtained from male and female mice are shown in **Figure 1**. As shown in **Figures 1A–G**, all the retinal layers reduced in thickness with age for both sexes. The photoreceptor outer and inner segment layer (PS), outer nuclear layer (ONL), and outer plexiform layer (OPL) thicknesses in the aged retinas were significantly thinner than those in the control ($p < 0.01$ aged male vs. control; $p < 0.05$ aged female vs. control). The thickness of the INL was reduced 1.27-fold for the males and 1.04 times for the females, whereas the IPL decreased 1.25-fold for males and 1.05-fold for females. The retinal pigment epithelium (RPE) and retinal ganglion cell layer (GGL) reduced approximately onefold in older mice compared to young ones and were similar for both sexes.

Male and Female Ultrastructural Differences in the Aged Mouse Retina

The control retinal pigment epithelial cells appeared with a normal aspect, separated from the choroid by Bruch's membrane (BM), showing cytoplasmic melanin granules, mitochondria, and a regular nucleus (**Figures 2**, **3**). The basolateral infoldings of the plasma membrane, the apical villous-like processes, and sheath plaques of the photoreceptor outer segments had a normal aspect. With age, Bruch's membrane showed significantly increased thickness in both of aged male/female retinas compared to the control (**Table 1**), and uploading with lipid drops was observed (**Figures 2**, **3**). In particular, we observed localized areas of increased thickness in Bruch's membrane and abnormal deposits of amorphous material in the sub-RPE space (side of Bruch's membrane), which was similar to the basal laminar deposits of human AMD. In those areas, we noticed fingerlike extensions of the amorphous material that extended from the basal membrane toward the RPE cytoplasm. The basolateral infolding and apical sheaths were reduced or apparently disorganized in the retinal periphery, mainly for the aged male retina. The cells were loaded with lipids or lipofuscin granules and clustered mainly in the apical sheath area. The most damaged epithelial cells with lysis areas and intense macrophage activity, highlighted by accumulation of melanosomes and lipofuscin granules, were observed in both sexes but were more often evident in the aged male retina.

For both controls, the photoreceptor discs were intact and properly aligned and were perpendicular to the photoreceptor axis. In aging states, impairment of the photoreceptor outer segments was observed (**Figure 4**). The rod and cone outer segments were surrounded or intermittently surrounded by the apical sheaths of epithelial cells and were randomly oriented, truncated, or absent. Massive vesiculation and fragmentation of outer segment lamellae were observed in both aged retinas but mainly in male samples upon electron microscopy.

Moreover, in old mice, we found photoreceptor nuclei of variable shapes, sizes, and chromatin densities, and some had pyknotic nuclei and empty spaces, indicating nuclear loss. Swelling of mitochondria was observed mainly in aged male photoreceptor cells (**Figure 4**) compared with similarly processed samples from females.

The inner nuclear layer (INL) of the controls had a normal aspect, was abundant in bipolar cells, and ensheathed by processes of Müller cells. Electron micrographs of both aged retinas showed an extensive network of cytoplasmic processes of Müller cell wrapping around other cells and penetrating the neighboring inner plexiform layer (IPL) (**Figure 5**). Additionally, we registered marked thickening of the endothelial basal membrane of the capillary and lipid accumulation. Microglial hypertrophy was observed in the extended damaged INL areas.

The inner plexiform layer of the controls clearly showed different types of processes (**Figure 6**). The presynaptic endings (PRE) were full of microvesicles and contained one or more large mitochondria (m). Postsynaptic endings (PO) also presented mitochondria (m) but very few or no microvesicles. Müller processes (MP) were clear and contained few filaments (arrows). The aged retinas contained atrophied synaptic endings. The main difference was in the presynaptic endings, which were almost deprived by microvesicles, and most of the mitochondria presented rarefied cristae. The Müller processes (MP) were spread into the INL with proliferate filaments (arrows). The synaptic ribbons in the presynaptic bag (PRE) decreased in number and were in a much smaller size than the control for both sexes.

The ganglion layer was also affected with age (**Figure 6**). The number of ganglion cells decreased, some had apoptotic aspects, and lipofuscin granules were accumulated. Müller cell processes, microglia, and astrocytes surrounded the blood vessels, which possessed a thickened basal membrane.

Aging-Induced Retinal miRNA Dysregulation in Aged Mouse Retina for Both Sexes

Four of the eight miRNAs analyzed (miR-20a-3p, miR-106a-5p, miR-381-3p, and miR-206-3p) were not dysregulated between the control and aged experimental groups (**Figure 7A**).

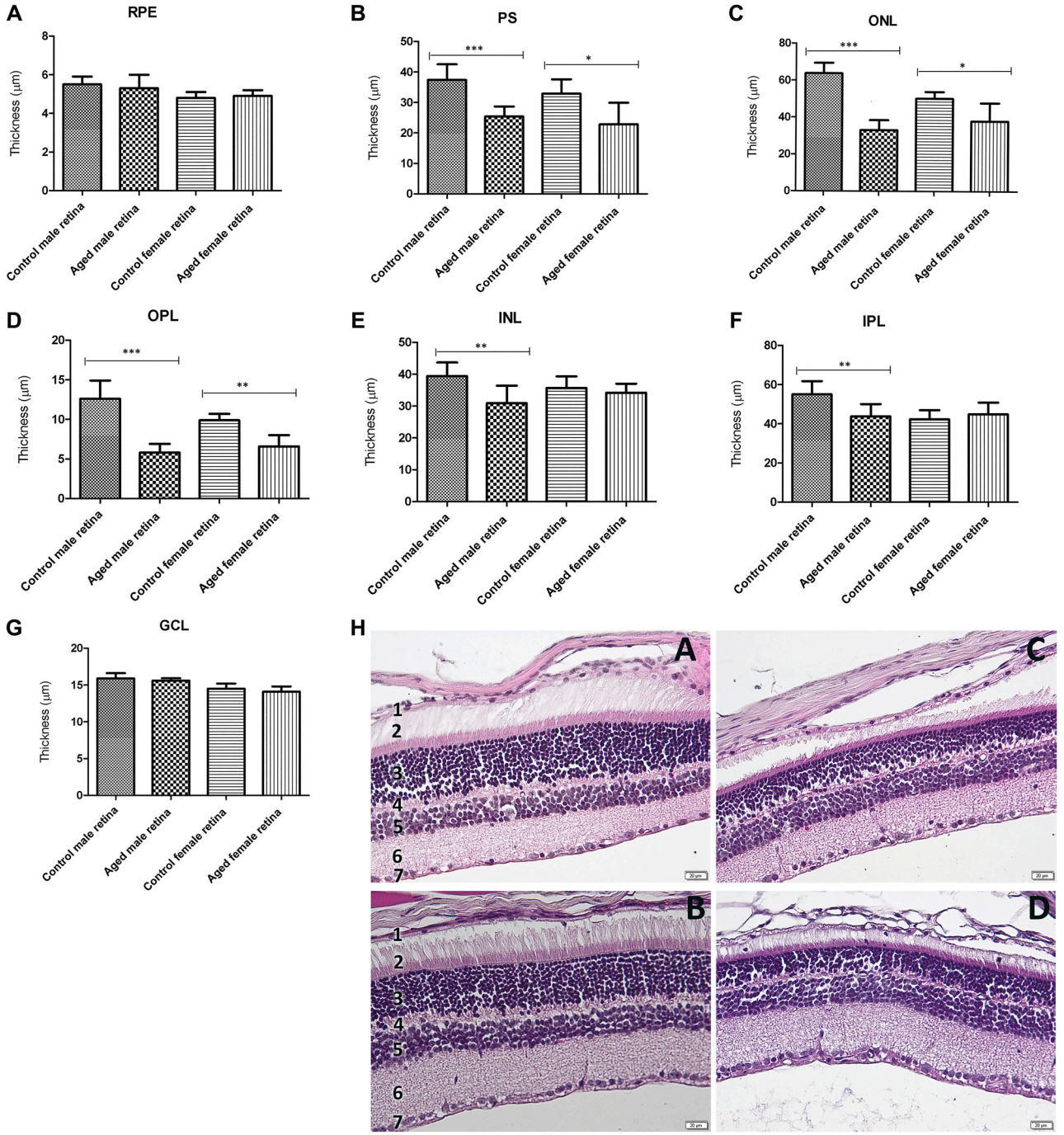

FIGURE 1 | Retinal layer thickness of the aged retinas by gender. **(A)**. The retinal pigment epithelium (RPE) thickness was not significantly modified between aged retinas and controls; **(B)**. photoreceptor outer and inner segment layers (PS) were significantly thinner in both aged males (***$p < 0.001$ vs. controls) and females (*$p < 0.05$ vs. controls) compared to their controls, as well as the outer nuclear layer (ONL) **(C)** (aged males ***$p < 0.001$ vs. controls; aged females *$p < 0.05$ vs. controls), and the outer plexiform layer (OPL) **(D)** (aged males ***$p < 0.001$ vs. controls; aged females **$p < 0.01$ vs. controls). The inner nuclear layer (INL) **(E)** and inner plexiform layer (IPL) **(F)** were both significantly thinner in aged males than the controls (both **$p < 0.01$ vs. controls), while they did not show any significant differences between aged and control female retina; the retinal ganglion cell layer (RGL) thickness **(G)** was not modified between aged retinas and controls; (h.) histological aspect of the retinal layers of the control male **(A)**, control female **(B)**, aged male **(C)**, and aged female **(D)** showing the reduction in thickness with age for both gender; the legend of the retinal layers: 1. RPE, 2. PS, 3. ONL, 4. OPL, 5. INL, 6. IPL, 7. RGL; thickness (μm) of retinal layers was reported as mean ± SD of $n = 10$ histological observations for each individual/group. Statistical significance was assessed by using the one-way ANOVA, followed by Tukey's multiple comparisons test.

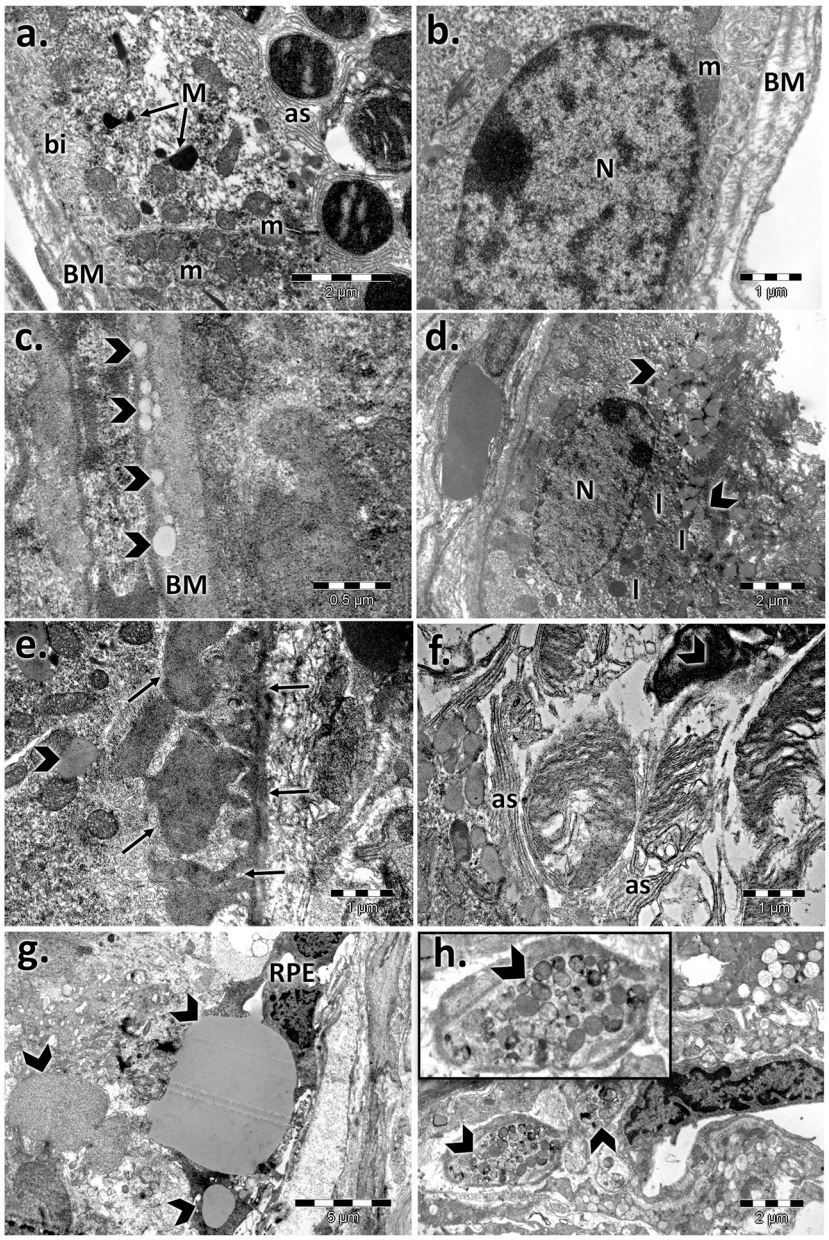

FIGURE 2 | Electron micrographs showing the ultrastructural features of the retinal pigment epithelium (RPE) of the aged male retina. **(A,B)** RPE of the male control, showing the normal aspect of the nucleus (N), mitochondria (m), melanin granules (M), Bruch's membrane (BM), marked basal infolding (bi), and wide apical sheaths (as) surrounding the photoreceptor outer segments; **(C–H)** RPE of the aged male, showing changes in the RPE ultrastructure, highlighted by thickened Bruch's membrane (BM) enriched in lipids (arrowhead) **(C)**; lipid drops accumulated in the cytoplasm and crowded in the apical sheath area (arrowhead), lipofuscin (l) **(D)**; localized thickening of Bruch's membrane on the RPE side and fingerlike extensions of the amorphous material (arrows) **(E)**; atrophic apical sheaths (as) **(F)**; large lipid drops (arrowhead) and atrophied retinal pigment epithelial layer (RPE) **(G)**; clusters of melanosomes and lipofuscin (arrowhead) **(H)**. Figures are representative of $n = 10$ electron micrographs for each individual/group.

Conversely, miR-27a-3p (fold regulation = 8.9; $p < 0.01$), miR-27b-3p (fold regulation = 8.1; $p < 0.05$), and miR-20a-5p (fold regulation = 4.9; $p < 0.05$) were significantly up-regulated in aged male mice compared to control male mice, whereas miR-20b-5p was significantly down-regulated (fold regulation = 3.9; $p < 0.05$) (**Figure 7B**). Moreover, miR-20b-5p was significantly down-regulated in aged female mice compared to control female mice (fold regulation = 2.5; $p < 0.05$) (**Figure 7B**). miR-27a-3p was significantly up-regulated in aged males (fold regulation = 5.00, $p < 0.01$) compared to that in aged females as well as miR-27b-3p (fold regulation = 7.58, $p < 0.01$) and miR-20a-5p (fold regulation = 4.11, $p < 0.01$), whereas miR-20b-5p was significantly down-regulated in aged males (fold regulation = −2,10, $p < 0.05$) compared to that in aged females (**Figure 7B**).

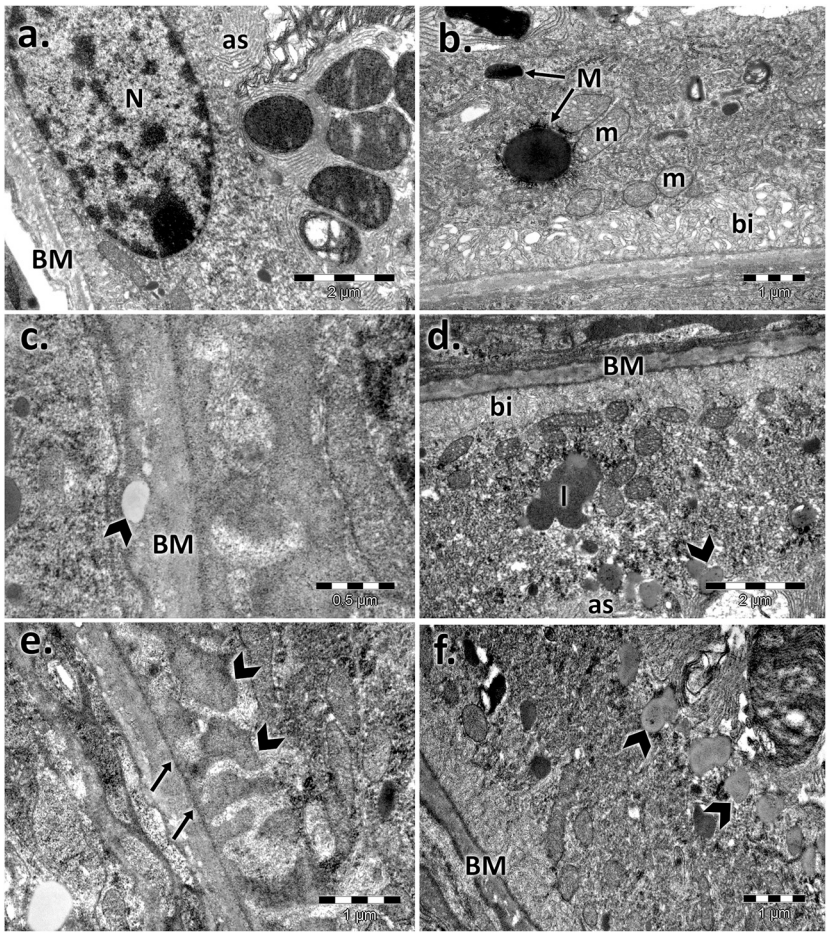

FIGURE 3 | Electron micrographs showing the ultrastructural features of the retinal pigment epithelium (RPE) of the aged female retina. **(A)**–**(B)** RPE of the female control, showing the normal aspect of the nucleus (N), mitochondria (m), melanin granules (M), Bruch's membrane (BM), marked basal infolding (bi), and wide apical sheaths surrounding the photoreceptor outer segments; **(C)**–**(F)** RPE of the aged female, showing ultrastructural changes of the RPE cells highlighted by the thickened basal membrane (BM), lipid drops into the membrane (arrowhead) **(C)**; lipofuscin granules (l), and lipids (arrowheads) clustered in the apical sheath area (as) **(D)**; localized thickening of Bruch's membrane on the RPE side and fingerlike extensions of the amorphous material (arrows) **(E)**; lipids (arrowheads) clustered in the apical sheaths area **(F)**. Figures are representative of n = 10 electron micrographs for each individual/group.

Correlation between Aged miRNAs and Retinal Structure

The thickness of the PS, ONL, and OPL negatively correlated with miR-27a-3p, miR-27b-3p, and miR-20a-5p levels ($p < 0.01$), whereas miR-20b-5p expression was positively correlated with PS, ONL, and OPL thickness ($p < 0.01$) (**Figures 8**, **9**). In contrast, miR-27a-3p, miR-27b-3p, and miR-20a-5p levels were positively correlated with Bruch's membrane thickness ($p < 0.01$), whereas it showed a negative correlation with miR-20b-5p expression ($p < 0.01$) (**Figure 9**).

DISCUSSION

Age and gender are two important factors that may influence the function and structure of the retina. Other results did not show a significant difference between the thickness of the retinal layers and age, by sex in groups of Sprague Dawley rats aged 1, 2, 6, and 10 months (Chaychi et al., 2015), which highlights that major structural changes appear only in the second year of life in rodents (approximately 50 years in humans). In our study, the photoreceptors appeared to be more affected with age. This was particularly evident in males. Our results and a study by DiLoreto et al. (1994) showed that the peripheral retinal thickness reduction documented in female CD mice and female F344

TABLE 1 | Electron microscopy analysis of Bruch's membrane thickness (nm) of the aged retina.

Gender	Control retina	Aged retina
Male	571 ± 117	702 ± 117[a]
Female	409 ± 54	710 ± 83[a]

[a]p < *0.001 aged retina vs. control (young).*

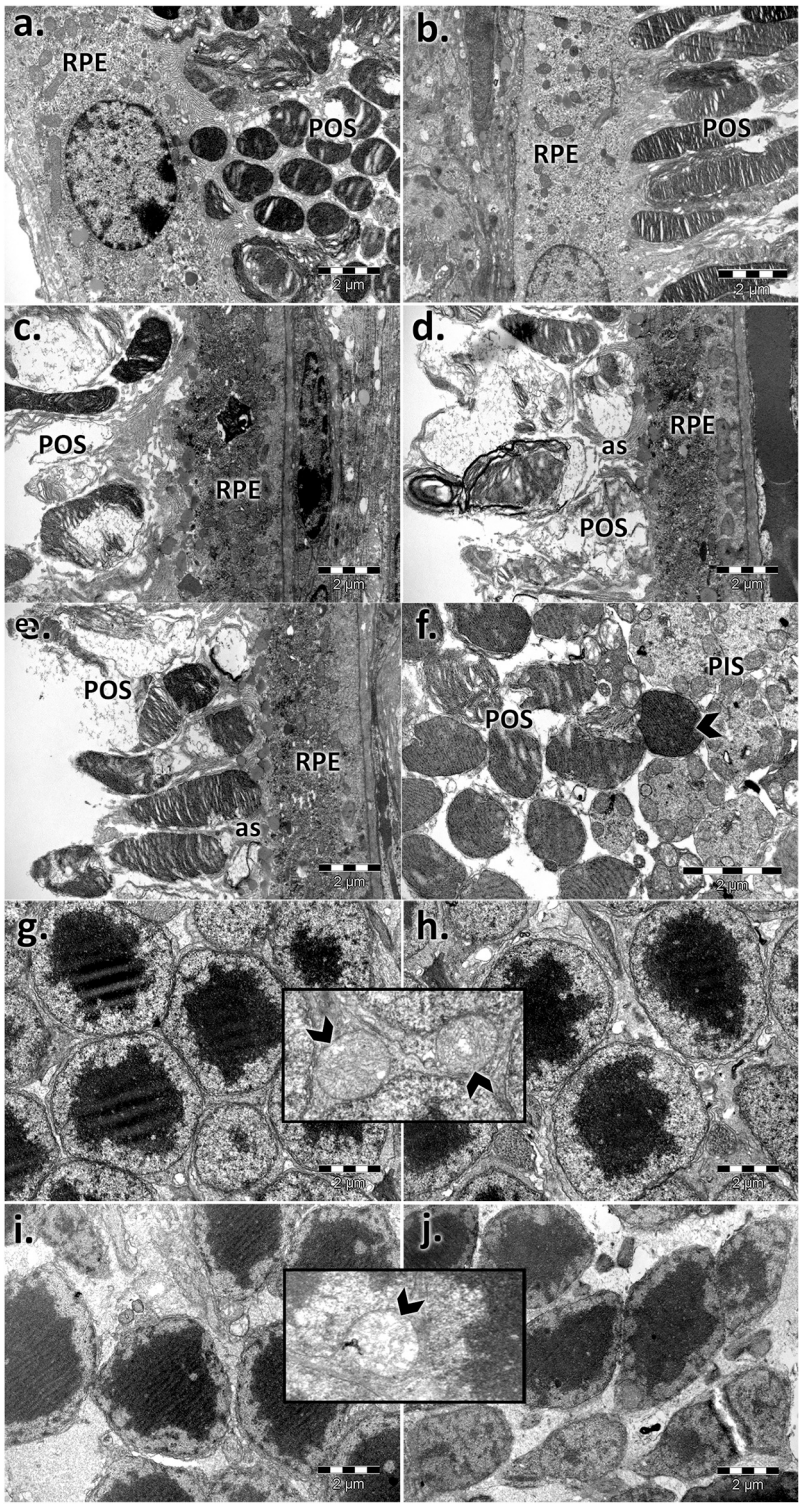

FIGURE 4 | Electron micrographs showing the ultrastructural features of the photoreceptor layer (PS) and outer nuclear layer (ONL) of the young and aged retinas. PS of control male **(A)** and female **(B)** mice; PS of aged male **(C,D)** and female **(E,F)** mice; ONL of control male **(G)** and female **(H)** mice; ONL of aged male **(I)** and female **(J)** mice; photoreceptor outer segments with aligned discs and normal structure **(A,B)**; RPE, retinal pigment epithelial layer; ONL, outer nuclear layer; POS, photoreceptor outer segments; the POS are misoriented, damaged, and inconsistent and accompanied by apical sheaths (as) of the epithelial cells (c, d, and **E)** and condensed **(F)**; photoreceptor outer (POS) and inner segment layer (PIS); normal aspect of the photoreceptor nuclei, aligned and densely packaged **(G and H)** with the normal aspect of the mitochondria (detail—arrowhead); photoreceptor nuclei with different sizes and chromatin density and empty spaces; swelling of mitochondria with a loss of cristae (detail—arrowhead) **(I and J)**. Figures are representative of n = 10 electron micrographs for each individual/group.

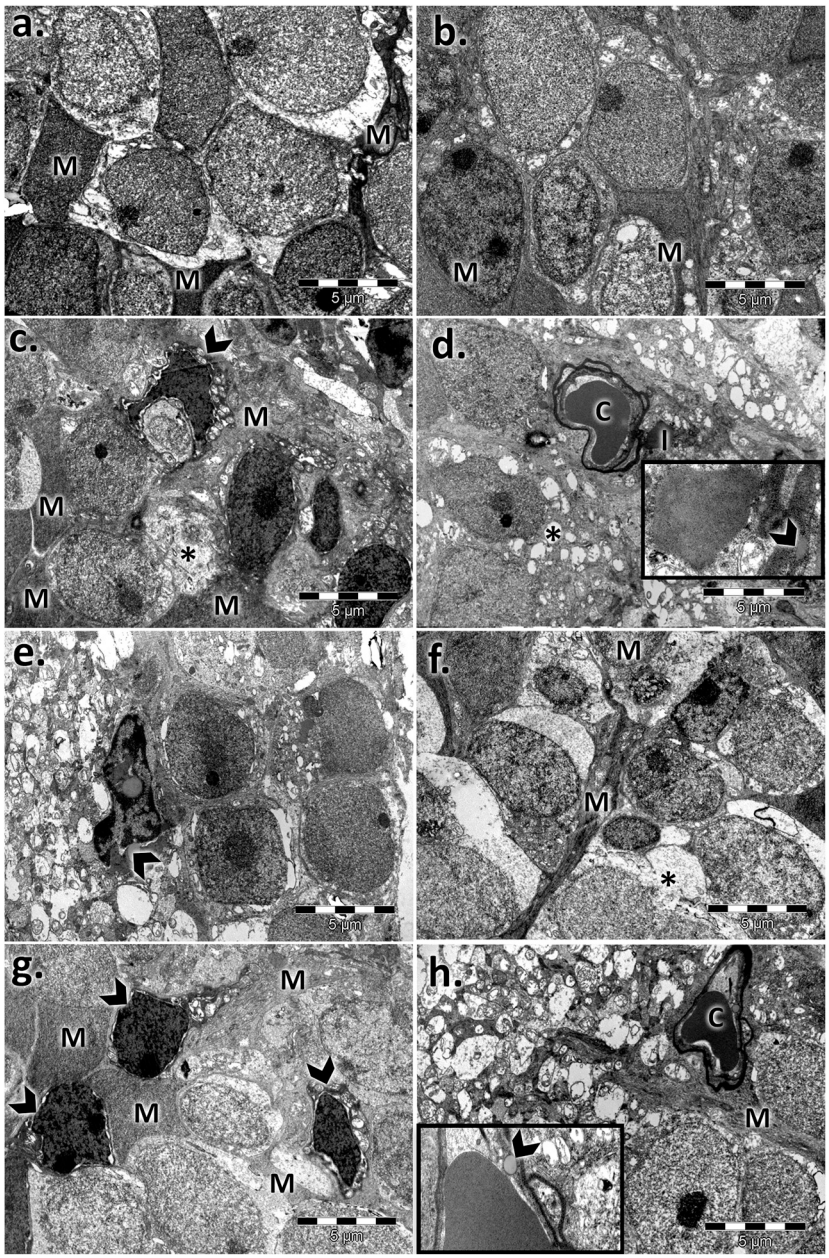

FIGURE 5 | Electron micrographs showing the ultrastructural features of the inner nuclear layer (INL) of the young and aged retinas. **(A)** control male; **(B)** control female; **(C,F)** aged male retina—hypertrophied Müller cells (M), condensed Müller cell nuclei (arrowhead), bipolar cells (B), and capillaries (C) with a thickened basement membrane and lipids (l); empty spaces (*); detail: lipid accumulation beside the capillary and into the basal membrane (arrowhead); damaged INL areas in the aged male retina with microglia (arrowhead) **(G,H)** aged female retina—hypertrophied Müller cells (M); condensed Müller cells nuclei (arrowhead), capillary with thickened basement membrane (C); bipolar cells (B); detail: lipid accumulation beside the capillaries and into the basal membrane (arrowhead). Figures are representative of $n = 10$ electron micrographs for each individual/group.

rats was delayed and less significant compared to that in males. In addition, an attenuation of ERG amplitudes between 1 and 10 months of age was recorded (Chaychi et al., 2015), which may explain the fine changes in the ocular media and the gradual reduction in photopigment contents (Birch and Anderson, 1992) or the reduction in retinal cell number with age (Dorey et al., 1989; Curcio et al., 1990), as our data showed for both sexes.

Age-related macular degeneration (AMD) in humans is associated with progressive degeneration of the retinal pigment epithelium (RPE) cell layer and photoreceptor cells. Because photoreceptors depend for their maintenance on RPE, it was essential to analyze the involvement of RPE in changes related to aging. The senescence-accelerated mouse (SAM) strain was shown to exhibit changes only in Bruch's membrane and RPE

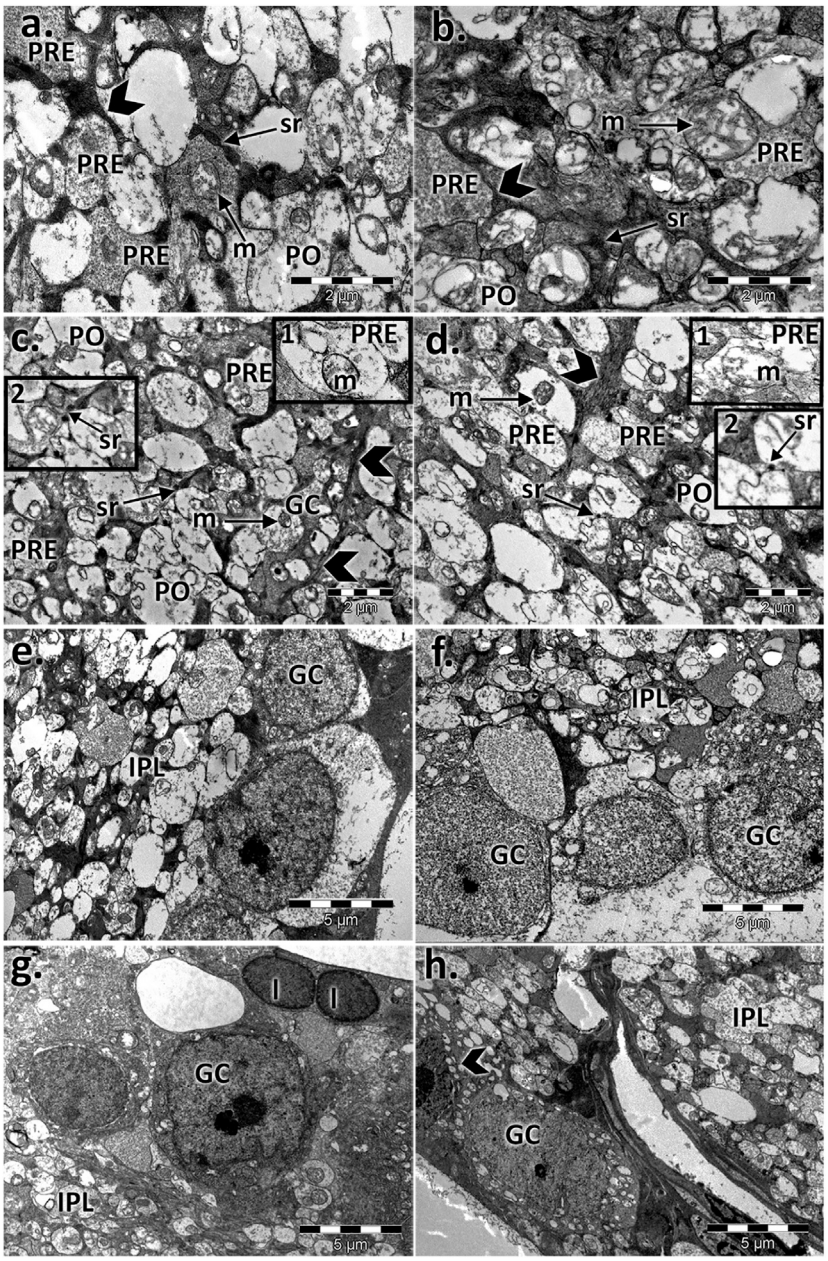

FIGURE 6 | Electron micrographs showing the ultrastructural features of the inner plexiform layer (IPL) and ganglion layer (RGL) of the young and aged retinas. Ultrathin section through the inner plexiform layer (IPL) showing different types of processes in **(A)** the control male, **(B)** control female, **(C)** aged male retina, and **(D)** aged female retina; presynaptic endings (PRE); large mitochondria (m); postsynaptic endings (PO); Müller processes (MP) (arrowhead); detail 1: presynaptic endings (PRE) with rarefied mitochondrial cristae and a few microvesicles—aged males **(C)** and females **(D)**; detail 2: synaptic ribbons (arrows) in a presynaptic bag (PRE)—aged males **(C)** and females **(D)**; electron micrographs of a section through the ganglion cell layer in **(E)** the control male, **(F)** control female **(G)**, aged male retina **(H)**, and aged female retina; ganglion cell (GC), inner plexiform layer (IPL), apoptotic cell (arrowhead), and lipofuscin granules (l). Figures are representative of n = 10 electron micrographs for each individual/group.

(Ogata et al., 1992, Takada et al., 1993; Takada et al., 1994). Electron microscopy measurements of Bruch's membrane of the SAM showed thickening with age, starting with 12 months (Majji et al., 2000), whereas our results in 24-month-old CD1 mice confirmed an increased thickness for both sexes (**Table 1**), and electron micrographs showed deposits with similar characteristics to the basal laminar material seen in AMD (Green and Enger, 1993). The RPE and Bruch's membrane changes observed in our study were also reported by several studies (Ogata et al., 1992; Takada et al., 1993, Takada et al., 1994; Nakamura et al., 1995). They showed disorganization of the basal infolding, extension of the intercellular space, and accumulation

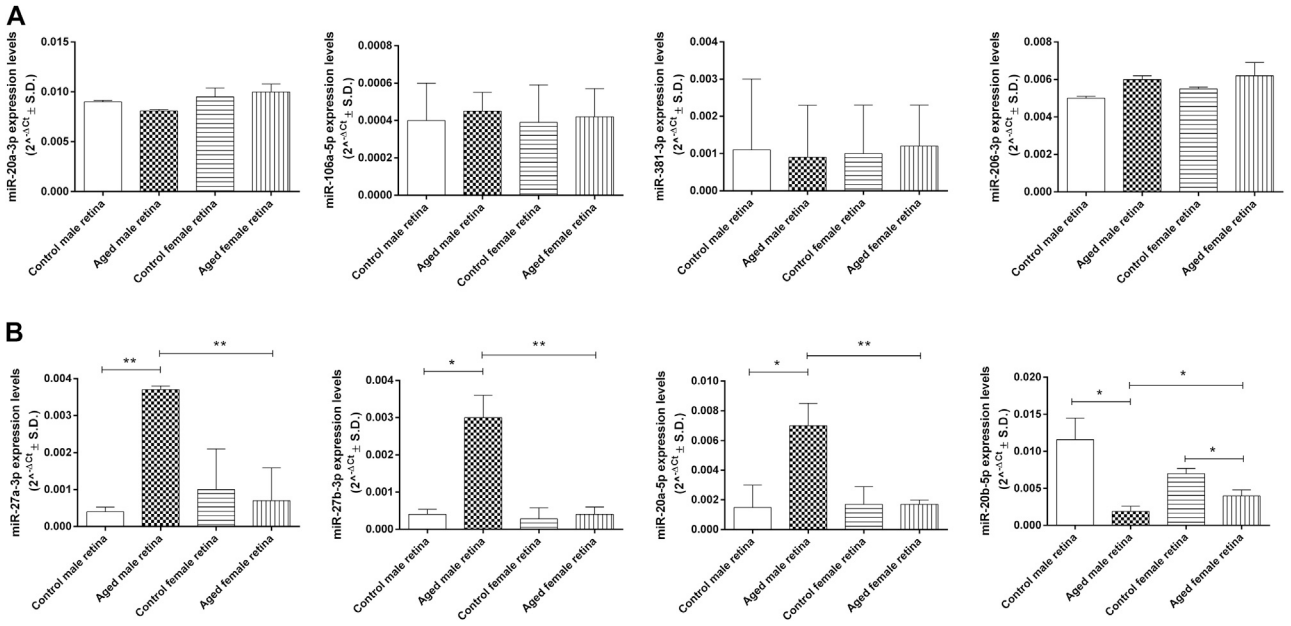

FIGURE 7 | Age-related miRNA expression levels in aged retina. **(A)** Not dysregulated and **(B)** dysregulated retina miRNA expression levels. Data are reported as $2^{-\Delta Ct}$ and shown as mean ± SD of $n = 10$ observations for each experimental group; each run was performed in triplicate. Statistical significance was assessed by using one-way ANOVA, followed by Tukey's multiple comparisons test. *$p < 0.05$ and **$p < 0.01$.

of lipofuscin granules, which are all in agreement with our results. According to a SAM experiment for mice older than 12 months (Majji et al., 2000), we observed at 24 months of age localized rough extensions in Bruch's membrane toward the RPE (related to basal linear deposits found in human AMD) and a general increase in the thickness of Bruch's membrane. Other studies found the presence of drusen between the RPE basal lamina and inner collagenous layer of BM (Farkas et al., 1971; Loffler and Lee, 1986; van der Schaft et al., 1991; van der Schaft et al., 1993; Kliffen et al., 1997; Zarbin, 1998; Curcio and Millican, 1999; Green, 1999; Sarks et al., 1999, 2007; Spraul et al., 1999). Both basal deposits and drusen result from incomplete digestion/removal of RPE cellular constituents (Farkas et al., 1971) and are the main cause of photoreceptor deficiencies, making it difficult to obtain nutrients from the vascular choroid.

Aging is also associated with accumulation of retinal lipids and lipofuscins, subsequently contributing to AMD (Suzuki et al., 2007; Curcio et al., 2009), to best vitelliform macular dystrophy, or to fundus flavimaculatus (Stargardt disease) (Nag and Wadhwa, 2012). In particular, electron micrographs showed RPE lipid accumulation in both aged males and females and infiltrated into Bruch's membrane. The abundant lipids could contribute to the degeneration of the RPE and subsequent to the photoreceptors, whose metabolism depends on normal epithelial function and layer integrity.

The lipid source of photoreceptors is plasma lipids, and their transfer is facilitated by the RPE and Müller cells. Moreover, the receptors for LDL were highlighted on the RPE (Hayes et al., 1989; Gordiyenko et al., 2004) connected with local production of apoE by RPE cells (Trivino et al., 2006), and a disturbed metabolism could cause an imbalance and lead to intracellular lipid accumulation. The metabolism and transport of lipids could be more impaired as a result of a thickened Bruch's membrane with changes in its collagen layers and deposition (Pauleikoff et al., 1990; Curcio et al., 2001; Trivino et al., 2006). Curcio et al. (2001) assumed that the aging process of Bruch's membrane is similar to that of the arterial intima and other connective tissues for which lipoproteins are the source of extracellular cholesterol. The lipid drops observed in Bruch's membrane for both aged males and females may arise from esterified cholesterol-rich apolipoprotein B–containing lipoprotein particles produced by the RPE (Curcio et al., 2010).

The outer segments of the photoreceptors are composed of infolded plasma membrane discs with photopigments that are properly aligned, and establish an anatomical association with the RPE (Johnson et al., 1986; Blanks et al., 1988). Several studies have shown the misalignment of the outer photoreceptor segments in aging and pathology (as AMD) (Green and Enger, 1993; Jackson et al., 2002; Liu et al., 2003; Eckmiller, 2004), and the discs are randomly oriented or disorganized into tubules and membranous whorls (Marshall et al., 1979; Nag and Wadhwa, 2012), as we observed in the 75- to 85-year-old human-equivalent aged mice (24-month-old mice), mainly for aged males. Their occurrence is possibly attributed to the vulnerability of mitochondria via oxidative stress, light, or toxic substances, contributing to energy depletion and cone loss in the human retina with aging (Curcio and Drucker, 1993). Moreover, injured mitochondria have been reported by us in photoreceptor cells and are more widespread for the aged male retina.

A proposed mechanism that could trigger the degenerative process in aging is primarily focused on the outer segments of the photoreceptors, followed by the inner segments, and finally on

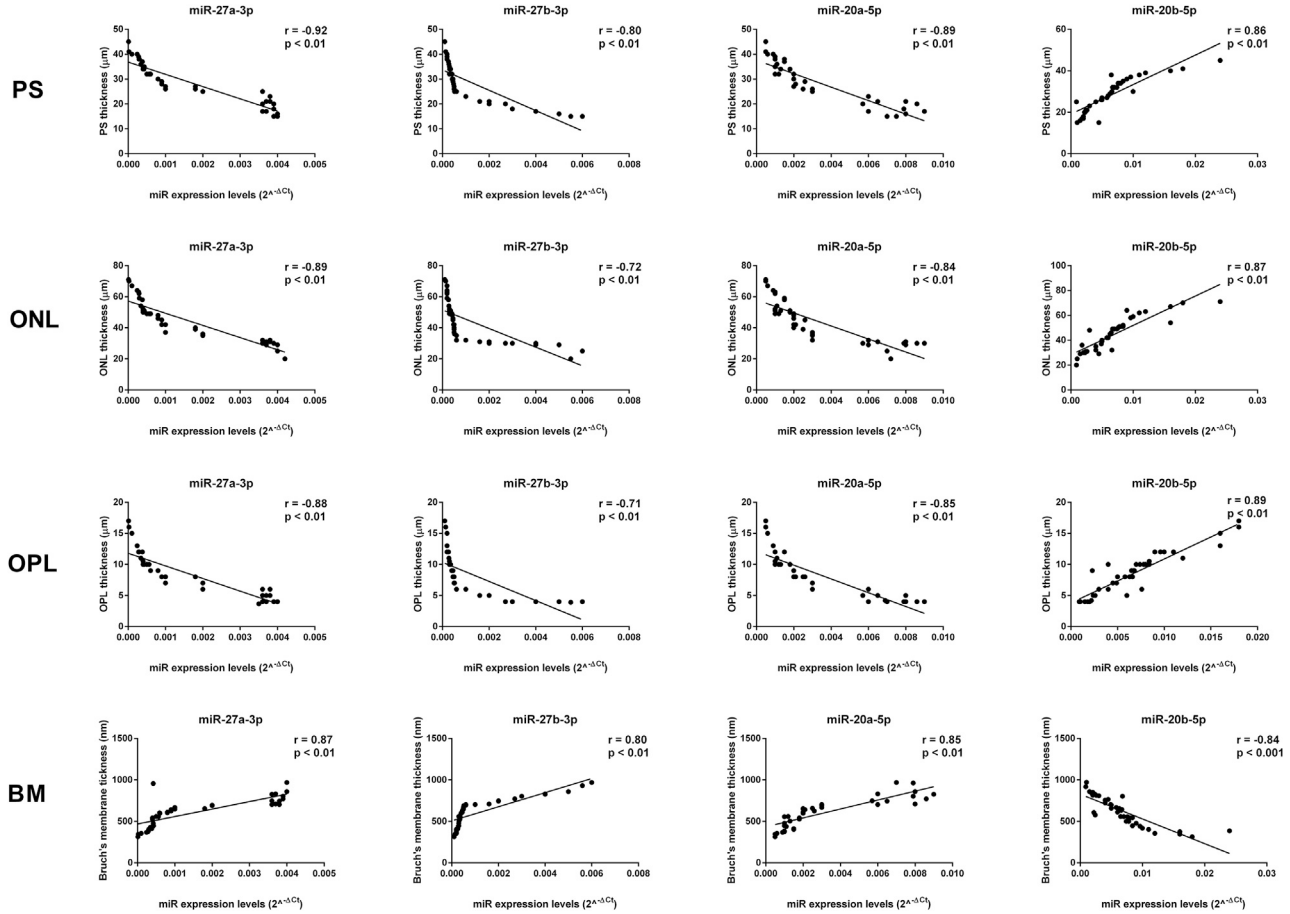

FIGURE 8 | Significant correlation between age-related miRNA expression levels and retinal structure. miR-27a-3p, miR-27b-3p, and miR-20a-5p levels showed a negative correlation with PS, ONL, and OPL thickness, and they showed a positive correlation with Bruch's membrane thickness. miR-20b-5p was positively correlated with PS, ONL, and OPL thickness, and it was negatively correlated with Bruch's membrane thickness. Pearson correlation analysis was used to evaluate the strength of association between pairs of variable, by including all the samples with different age and gender. Differences were considered statistically significant for p values <0.05. PS, retinal photoreceptors layer; ONL, retinal outer nuclear layer; OPL, retinal outer plexiform layer; BM, Bruch's membrane.

the cell body depletion from the ONL (DiLoreto et al., 1994). A deeper investigation of retinal changes with age suggests hormonal involvement in structural and functional preservation, such as estrogen. Chaychi et al. (2015) assumed the role of biological sex and age on the retinal function. They showed better retinal functions in cyclic female rats than in menopausal ones, suggesting a negative effect of the estrus cycle decline related to aging (van den Beld et al., 2018). Other mechanistic involvement in sex difference targets the oxygen supply of the retina. In a recent preclinical experiment, female neurons were reported to be less sensitive than male neurons to hypoxia induced by oxygen–glucose deprivation (Lang and McCullough, 2008). Moreover, estrogen can attenuate retinal ischemia–reperfusion (Nonaka et al., 2000) via nitric oxide and nitric oxide synthase (NOS) activity enhancement genes (Mendelsohn and Karas, 2005).

The INL contain three types of neurons (horizontal, bipolar, and amacrine cells), a macroglia, and a Müller cell, which span the entire thickness of the retina, and they are in anatomical and functional contact with all retinal neurons. The phenotype changes of the Müller glial cells are highlighted by the presence of an extensive network of cytoplasmic processes wrapping around other cells and penetrating the neighboring inner plexiform layer (IPL). The electron microscopy observations may be correlated with data regarding Müller cell resistance in ischemia, anoxia, or hypoglycemia (Silver et al., 1997; Stone et al., 1999) to the detriment of neurons and their passage into the activated or "reactive" state in response to every pathological alteration of the retina (Bringmann et al., 2006). For example, in proliferative vitreoretinopathy (PVR), they undergo hypertrophy (Francke et al., 2001). Moreover, under pathological conditions, they could induce functional changes with microglial activation of the retina (Bringmann et al., 2006), as we pointed out in aging mice. Regarding vascular changes, we showed marked thickening of the endothelial basal membrane of the capillary, which is a change that has been encountered in other pathological conditions, such as AMD (Ramírez et al., 2001) and DR (Ashton, 1974; Garner, 1993; Cai and Boulton, 2002),

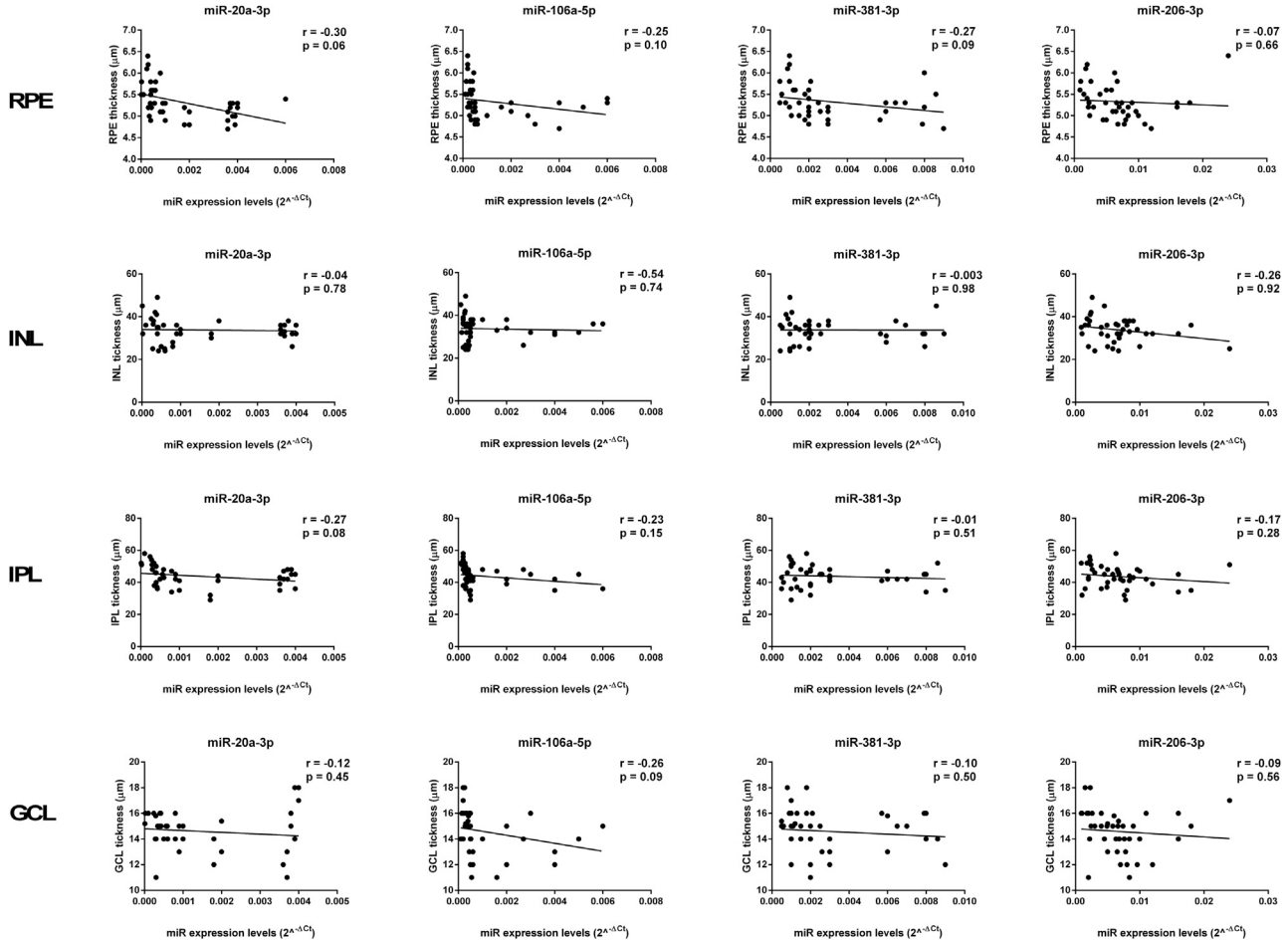

FIGURE 9 | Age-related miRNA expression levels not correlated with retina structure. No significant correlations were observed between RPE, INL, IPL, and GCL thickness and the miR-20a-3p, miR-106a-5p, miR-381-3p, and miR-206-3p expression levels. Pearson correlation analysis was used to evaluate the strength of association between pairs of variables, by including all the samples with different age and gender. Differences were considered statistically significant for p values <0.05. RPE, retinal pigment cells; INL, retinal inner nuclear layer; IPL, retinal inner plexiform layer; GCL, retinal ganglion cell layer.

although the thickening of the endothelial basal membrane of retinal capillaries was recently reported to occur with aging, besides in diseases (Nag et al., 2019).

The ultrastructural aspect of the ganglionar layer was affected with age with a decline in the number of ganglion cells, as was shown by other aging studies (Curcio and Drucker, 1993) or other ocular pathology studies, such as those on glaucoma, optic neuritis, RP, and Alzheimer's disease (Hinton et al., 1986; Stone et al., 1992; Curcio and Drucker, 1993; Trip et al., 2005; Osborne, 2008). In our electron microscopy investigation, we observed lipofuscin granule accumulation, which prominently occurred in ganglion cells in patients with Batten disease (Bensaoula et al., 2000) but were also observed in other aging experiments (Nag et al., 2006).

MicroRNAs (miRNAs) have been established as significant regulators of senescence and cell aging (Smith-Vikos and Slack, 2012) by inducing mRNA degradation or translational repression (Bartel, 2004). miR-27a target genes are important for glutathione metabolism (Smith-Vikos and Slack, 2012) and are involved in suppression of the expression of the enzymes important for polyamine biosynthesis, such as ornithine decarboxylase (Bates et al., 2010). In our study, we found a significant up-regulation of miR-27a-3p in aged retinas compared to young ones, as well as in aged males compared to aged females. This was paralleled by our electron microscopic observations showing ultrastructural changes segregated by sex, which were specific to aged males. In particular, miR-27a was negatively correlated with the thickness of PS, ONL, and OPS, whereas it was positively correlated with Bruch's membrane thickness. Of note, glutathione reduction leads to photoreceptor cell death, a reduction in ONL thickness, and increased Bruch's membrane thickness in accordance with our data (Winkler and Giblin, 1983; Schimel et al., 2011; Fernandez-Robredo et al., 2013). Interestingly, miR-27a-3p and miR-20a-5p up-regulation in aged mice is in line with previous studied that showed an elevation of these miRNAs in the serum and plasma of

patients affected by wet or dry age-related macular degeneration (AMD), an ocular pathology characterized by cellular debris between the choroid and retina (Ertekin et al., 2014; Berber et al., 2017; Romano et al., 2017). miR-27b-3p, an oxidative stress-responsive microRNA, was found to be up-regulated in aged mice and previously showed significant age differences in the male mice thymus (Guo et al., 2017; Xu et al., 2017). Moreover, miR-20b-5p, which was found to be down-regulated by oxidative stress (Tai et al., 2020), was one of the most important causes underlying oxidative damage during aging (Liguori et al., 2018), and it was reported to inhibit the senescence of human umbilical vein endothelial cells induced by oxidative stress by promoting cell viability (Dong et al., 2020).

Further evidence supporting a dysregulation of age-related miRNAs in the retinal structure and function was shown by our correlation analysis, showing a significant association between miRNA expression levels and the thicknesses of PS, ONL, OPL, and Bruch's membrane. Although miR-27a-3p, miR-27b-3p, miR-20a-5p, and miR-20b-5p were shown to be dysregulated in retinal derangement induced by diabetes (Platania et al., 2019), these miRNAs were here strictly correlated with the alterations of the retina induced during aging. Indeed, although gender-related miRNA expression remains largely unexplored, with few studies showing a higher tissue specificity associated with histone modification and circadian rhythm for male-biased miRNAs and a higher disease spectrum associated with metabolism and cell cycle process for female-biased miRNA (Cui et al., 2018), our results showed that biological sex can influence the structure and function of the retina upon aging, suggesting that this difference may be underlined by the dysregulation of age-related mi-RNAs.

Interestingly, gender-related miRNAs have been previously reported to be dysregulated in neurological disorders: miR-27a was up-regulated in epilepsy and autoimmune encephalomyelitis (Wang et al., 2014; Morquette et al., 2019); higher levels of miR-27b exacerbate intracerebral hemorrhage-induced brain injury (Xu et al., 2017) and are related to the development of neurological disorders with HCMV infection (Wang et al., 2017); miR-20a showed an increased expression in traumatic injury (Wang et al., 2014); and miR-20b was found to be down-regulated in multiple sclerosis (Ingwersen et al., 2015). Although there is no evidence regarding the gender-related expression of miR-27a, miR-27b, miR-20a, and miR-20b in these neurological disorders, miR-20b expression was higher in males during aging of the thymus (Guo et al., 2017); miR-20a-5p has recently been found to be associated with male infertility (Cito et al., 2020), whereas miR-27a has been found to be related to endometritis (Di Pietro et al., 2018). The expression of mir-20a and miR-20b was highest in the male lung, whereas miR-27b was more expressed in the female lung (Cui et al., 2018). Therefore, studying the gender-related retinal morphological differences and the dysregulation of some retinal miRNAs upon aging, which are closely related to the functional alterations and the development of subsequent pathologies, may provide insights into the neuroprotective mechanisms. From these age-related damaging mechanisms, the increased susceptibility of Balb-c mice to light damage seems to be excluded because one would expect to observe higher retinal morphological damage in young animals than in aged animals (Kalesnykas et al., 2016).

DATA AVAILABILITY STATEMENT

The raw data supporting the conclusions of this article will be made available by the authors, without undue reservation.

ETHICS STATEMENT

The animal study was reviewed and approved by the Ethics Committee for Research of the Vasile Goldis Western University of Arad. Written informed consent was obtained from the owners for the participation of their animals in this study.

AUTHOR CONTRIBUTIONS

AH, MD'A, and CC contributed to the conception, design, data acquisition, analysis, and interpretation of the results and drafted and critically revised the manuscript. SG, MT, HAG, VP, CG, and SR contributed to the acquisition and analysis of data and drafted the manuscript. AH, MD'A, CC, and MG contributed to interpretation of the results and drafted and critically revised the manuscript. All authors gave final approval and agreed to be accountable for all aspects of the work.

FUNDING

VP and MG were supported by the Ministry of Research and Innovation under grants no. PN 1N/2019_19.29.01.02 and no. 7PFE/2018.

REFERENCES

Adhi, M., Aziz, S., Muhammad, K., and Adhi, M. I. (2012). Macular thickness by age and gender in healthy eyes using spectral domain optical coherence tomography. *PLoS One*. 7, e37638. doi:10.1371/journal.pone.0037638

Age-Related Eye Disease Study Research Group (2000). Risk factors associated with age-related macular degeneration. A case-control study in the age-related eye disease study: age-Related Eye Disease Study Report Number 3. *Ophthalmology*. 107, 2224–2232. doi:10.1016/s0161-6420(00)00409-7

Ashton, N. (1974). Vascular basement membrane changes in diabetic retinopathy. Montgomery lecture, 1973. *Br. J. Ophthalmol.* 58, 344–366. doi:10.1136/bjo.58.4.344

Bartel, D. P. (2004). MicroRNAs: genomics, biogenesis, mechanism, and function. *Cell.* 116, 281–297. doi:10.1016/s0092-8674(04)00045-5

Bates, D. J., Li, N., Liang, R., Sarojini, H., An, J., Masternak, M. M., et al. (2010). MicroRNA regulation in Ames dwarf mouse liver may contribute to delayed aging. *Aging Cell.* 9, 1–18. doi:10.1111/j.1474-9726.2009.00529.x

Beatty, S., Koh, H., Phil, M., Henson, D., and Boulton, M. (2000). The role of oxidative stress in the pathogenesis of age-related macular degeneration. *Surv. Ophthalmol.* 45, 115–134. doi:10.1016/s0039-6257(00)00140-5

Beebe, D. C., Holekamp, N. M., and Shui, Y. B. (2010). Oxidative damage and the prevention of age-related cataracts. *Ophthalmic Res*. 44, 155–165. doi:10.1159/000316481

Bell, B. A., Kaul, C., Bonilha, V. L., Rayborn, M. E., Shadrach, K., and Hollyfield, J. G. (2015). The BALB/c mouse: effect of standard vivarium lighting on retinal pathology during aging. *Exp. Eye Res*. 135, 192–205. doi:10.1016/j.exer.2015.04.009

Bensaoula, T., Shibuya, H., Katz, M. L., Smith, J. E., Johnson, G. S., John, S. K., et al. (2000). Histopathologic and immunocytochemical analysis of the retina and ocular tissues in Batten disease. *Ophthalmology*. 107, 1746–1753. doi:10.1016/s0161-6420(00)00264-5

Berber, P., Grassmann, F., Kiel, C., and Weber, B. H. (2017). An eye on age-related macular degeneration: the role of microRNAs in disease pathology. *Mol. Diagn. Ther*. 21, 31–43. doi:10.1007/s40291-016-0234-z

Birch, D. G., and Anderson, J. L. (1992). Standardized full-field electroretinography. Normal values and their variation with age. *Arch. Ophthalmol*. 110, 1571–1576. doi:10.1001/archopht.1992.01080230071024

Blanks, J. C., Hageman, G. S., Johnson, L. V., and Spee, C. (1988). Ultrastructural visualization of primate cone photoreceptor matrix sheaths. *J. Comp. Neurol*. 270, 288–300. doi:10.1002/cne.902700209

Bozycki, L., Łukasiewicz, K., Matryba, P., and Pikula, S. (2018). Whole-body clearing, staining and screening of calcium deposits in the mdx mouse model of Duchenne muscular dystrophy. *Skelet. Muscle*. 8, 21. doi:10.1186/s13395-018-0168-8

Bringmann, A., Pannicke, T., Grosche, J., Francke, M., Wiedemann, P., Skatchkov, S. N., et al. (2006). Müller cells in the healthy and diseased retina. *Prog. Retin. Eye Res*. 25, 397–424. doi:10.1016/j.preteyeres.2006.05.003

Brûlé, J., Lavoie, M. P., Casanova, C., Lachapelle, P., and Hébert, M. (2007). Evidence of a possible impact of the menstrual cycle on the reproducibility of scotopic ERGs in women. *Doc. Ophthalmol*. 114, 125–134. doi:10.1007/s10633-007-9045-1

Buch, H., Nielsen, N. V., Vinding, T., Jensen, G. B., Prause, J. U., and la Cour, M. (2005). 14-year incidence, progression, and visual morbidity of age-related maculopathy: the Copenhagen City Eye Study. *Ophthalmology*. 112, 787–798. doi:10.1016/j.ophtha.2004.11.040

Cai, J., and Boulton, M. (2002). The pathogenesis of diabetic retinopathy: old concepts and new questions. *Eye*. 16, 242–260. doi:10.1038/sj.eye.6700133

Chakravarthy, U., Wong, T. Y., Fletcher, A., Piault, E., Evans, C., Zlateva, G., et al. (2010). Clinical risk factors for age-related macular degeneration: a systematic review and meta-analysis. *BMC Ophthalmol*. 10, 31. doi:10.1186/1471-2415-10-31

Chaychi, S., Polosa, A., and Lachapelle, P. (2015). Differences in retinal structure and function between aging male and female Sprague-Dawley rats are strongly influenced by the estrus cycle. *PLoS One*. 10, e0136056. doi:10.1371/journal.pone.0136056

Cito, G., Coccia, M. E., Salvianti, F., Fucci, R., Picone, R., Giachini, C., et al. (2020). Blood plasma miR-20a-5p expression as a potential non-invasive diagnostic biomarker of male infertility: a pilot study. *Andrology*. 8, 1256–1264. doi:10.1111/andr.12816

Cui, C., Yang, W., Shi, J., Zhou, Y., Yang, J., Cui, Q., et al. (2018). Identification and analysis of human sex-biased microRNAs. *Dev. Reprod. Biol*. 16, 200–211. doi:10.1016/j.gpb.2018.03.004

Curcio, C. A., and Drucker, D. N. (1993). Retinal ganglion cells in Alzheimer's disease and aging. *Ann. Neurol*. 33, 248–257. doi:10.1002/ana.410330305

Curcio, C. A., Johnson, M., Huang, J. D., and Rudolf, M. (2009). Aging, age-related macular degeneration, and the response-to-retention of apolipoprotein B-containing lipoproteins. *Prog. Retin. Eye Res*. 28, 393–422. doi:10.1016/j.preteyeres.2009.08.001

Curcio, C. A., Johnson, M., Huang, J. D., and Rudolf, M. (2010). Apolipoprotein B-containing lipoproteins in retinal aging and age-related macular degeneration. *J. Lipid Res*. 51, 451–467. doi:10.1194/jlr.R002238

Curcio, C. A., Millican, C. L., Bailey, T., and Kruth, H. S. (2001) Accumulation of cholesterol with age in human Bruch's membrane, *Invest. Ophthalmol. Vis. Sci*. 42, 265–274.

Curcio, C. A., and Millican, C. L. (1999). Basal linear deposit and large drusen are specific for early age-related maculopathy. *Arch. Ophthalmol*. 117, 329–339. doi:10.1001/archopht.117.3.329

Curcio, C., Allen, K., and Kalina, R. (1990). Reorganization of the human photoreceptor mosaic following age-related rod loss. *Invest. Ophthalmol. Vis. Sci*. 31, 38–48.

Davis, M. D., Fisher, M. R., Gangnon, R. E., Barton, F., Aiello, L. M., Chew, E. Y., et al. (1998). Risk factors for high-risk proliferative diabetic retinopathy and severe visual loss: early treatment diabetic retinopathy study report #18. *Invest. Ophthalmol. Vis. Sci*. 39, 233–252.

Di Pietro, C., Caruso, S., Battaglia, R., Iraci Sareri, M., La Ferlita, A., Strino, F., et al. (2018). MiR-27a-3p and miR-124-3p, upregulated in endometrium and serum from women affected by Chronic Endometritis, are new potential molecular markers of endometrial receptivity. *Am. J. Reprod. Immunol*. 80, e12858. doi:10.1111/aji.12858

DiLoreto, D., Jr., Cox, C., Grover, D. A., Lazar, E., Cerro, C. D., and Cerro, M. D. (1994). The influences of age, retinal topography, and gender on retinal degeneration in the Fischer 344 rat. *Brain Res*. 647, 181–191. doi:10.1016/0006-8993(94)91316-1

Dong, F., Dong, S., Liang, Y., Wang, K., Qin, Y., and Zhao, X. (2020). miR-20b inhibits the senescence of human umbilical vein endothelial cells through regulating the Wnt/β-catenin pathway via the TXNIP/NLRP3 axis. *Int. J. Mol. Med*. 45, 847–857. doi:10.3892/ijmm.2020.4457

Dorey, C. K., Wu, G., Ebenstein, D., Garsd, A., and Weiter, J. (1989). Cell loss in the aging retina. Relationship to lipofuscin accumulation and macular degeneration. *Invest. Ophthalmol. Vis. Sci*. 30, 1691–1699.

Du, M., Mangold, C. A., Bixler, G. V., Brucklacher, R. M., Masser, D. R., Stout, M. B., et al. (2017). Retinal gene expression responses to aging are sexually divergent. *Mol. Vis*. 152, 707–717.

Dutta, S., and Sengupta, P. (2016). Men and mice: relating their ages. *Life Sci*. 152, 244–248. doi:10.1016/j.lfs.2015.10.025

Eckmiller, M. S. (2004). Defective cone photoreceptor cytoskeleton, alignment, feedback, and energetics can lead to energy depletion in macular degeneration. *Prog. Retin. Eye Res*. 23, 495–522. doi:10.1016/j.preteyeres.2004.04.005

Ertekin, S., Yıldırım, O., Dinç, E., Ayaz, L., Fidancı, S. B., and Tamer, L., (2014). Evaluation of circulating miRNAs in wet age-related macular degeneration. *Mol. Vis*. 20, 1057.

Farkas, T., Sylvester, V., and Archer, D. (1971). The ultrastructure of drusen. *Am. J. Ophthalmol*. 71, 1196–1205. doi:10.1016/0002-9394(71)90963-9

Fernandez-Robredo, P., Sádaba, L. M., Salinas-Alamán, A., Recalde, S., Rodríguez, J. A., and García-Layana, A. (2013). Effect of lutein and antioxidant supplementation on VEGF expression, MMP-2 activity, and ultrastructural alterations in apolipoprotein E-deficient mouse. *Oxid. Med. Cell Longev*. 2013, 213505. doi:10.1155/2013/213505

Francke, M., Faude, F., Pannicke, T., Bringmann, A., Eckstein, P., Reichelt, W., et al. (2001). Electrophysiology of rabbit Müller (glial) cells in experimental retinal detachment and PVR. *Invest. Ophthalmol. Vis. Sci*. 42, 1072–1079.

Freeman, E. E., Munoz, B., Schein, O. D., and West, S. K. (2001). Hormone replacement therapy and lens opacities: the Salisbury Eye Evaluation project. *Arch. Ophthalmol*. 119, 1687–1692. doi:10.1001/archopht.119.11.1687

Freund, P. R., Watson, J., Gilmour, G. S., Gaillard, F., and Sauvé, Y. (2011). Differential changes in retina function with normal aging in humans. *Doc. Ophthalmol*. 122, 177–190. doi:10.1007/s10633-011-9273-2

Garner, A. (1993). Histopathology of diabetic retinopathy in man. *Eye*. 7 (Pt 2), 250–253. doi:10.1038/eye.1993.58

Gordiyenko, N., Campos, M., Lee, J. W., Fariss, R. N., Sztein, J., and Rodriguez, I. R. (2004). RPE cells internalize low-density lipoprotein (LDL) and oxidized LDL (oxLDL) in large quantities *in vitro* and *in vivo*. *Invest. Ophthalmol. Vis. Sci*. 45, 2822–2829. doi:10.1167/iovs.04-0074

Grassmann, F., Schoenberger, P. G., Brandl, C., Schick, T., Hasler, D., Meister, G., et al. (2014). A circulating MicroRNA profile is associated with late-stage neovascular age-related macular degeneration. *PLoS One*. 9, e107461. doi:10.1371/journal.pone.0107461

GreenWeber, W. R., and Enger, C. (1993). Age-related macular degeneration histopathologic studies. The 1992 Lorenz E. Zimmerman Lecture. *Ophthalmology*. 100, 1519–1535. doi:10.1016/s0161-6420(93)31466-1

Green, W. R. (1999) Histopathology of age-related macular degeneration, *Mol. Vis*. 5, 27, 27.

Grossniklaus, H. E., Nickerson, J. M., Edelhauser, H. F., Bergman, L. A., and Berglin, L. (2013). Anatomic alterations in aging and age-related diseases of the

eye. *Invest. Ophthalmol. Vis. Sci.* 54, ORSF23–ORSF27. doi:10.1167/iovs.13-12711

Guo, D., Ye, Y., Qi, J., Tan, X., Zhang, Y., Ma, Y., et al. (2017). Age and sex differences in microRNAs expression during the process of thymus aging. *Acta Biochim. Biophys. Sin.* 49, 409–419. doi:10.1093/abbs/gmx029

HashamaniLi, N., Hashamani, S., Murad, A., Shah, S. M. M., and Hashamani, M. (2018). Assessing reproducibility and the effects of demographic variables on the normal macular layers using the Spectralis SD-OCT. *Clin. Ophthalmol.* 12, 1433–1440. doi:10.2147/OPTH.S172109

Hayes, K. C., Lindsey, S., Stephan, Z. F., and Brecker, D. (1989). Retinal pigment epithelium possesses both LDL and scavenger receptor activity. *Invest. Ophthalmol. Vis. Sci.* 30, 225–232. doi:10.1006/bbrc.2002.6756

Hinton, D. R., Sadun, A. A., Blanks, J. C., and Miller, C. A. (1986). Optic-nerve degeneration in Alzheimer's disease. *N. Engl. J. Med.* 315, 485–487. doi:10.1056/NEJM198608213150804

Ingwersen, J., Menge, T., Wingerath, B., Kaya, D., Graf, J., Prozorovski, T., et al. (2015). Natalizumab restores aberrant miRNA expression profile in multiple sclerosis and reveals a critical role for miR-20b. *Ann. Clin. Transl. Neurol.* 2, 43–55. doi:10.1002/acn3.152

Jackson, G. R., Owsley, C., and Curcio, C. A. (2002). Photoreceptor degeneration and dysfunction in aging and age-related maculopathy. *Ageing Res. Rev.* 1, 381–396. doi:10.1016/s1568-1637(02)00007-7

Johnson, L. V., Hageman, G. S., and Blanks, J. C. (1986). Interphotoreceptor matrix domains ensheath vertebrate cone photoreceptor cells. *Invest. Ophthalmol. Vis. Sci.* 27, 129–135.

Kalesnykas, G., Ragauskas, S., Kaja, S., Tanila, H., and Leinonen, H. O. (2016). Age-related differences in light sensitivity in BALB/c mice. *Investig. Ophthalmol. Vis. Sci.* 57, 2004.

Klein, B. E., Klein, R., and Ritter, L. L. (1994). Is there evidence of an estrogen effect on age-related lens opacities? The Beaver Dam Eye study. *Arch. Ophthalmol.* 112, 85–91. doi:10.1001/archopht.1994.01090130095025

Kliffen, M., van der Schaft, T. L., Mooy, C. M., and de Jong, P. T. (1997). Morphologic changes in age-related maculopathy. *Microsc. Res. Tech.* 36, 106–122. doi:10.1002/(sici)1097-0029(19970115)36:2<106:aid-jemt4>3.0.co;2-n

Lai, K., Cui, J., Ni, S., Zhang, Y., He, J., and Yao, K. (2013). The effects of postmenopausal hormone use on cataract: a meta-analysis. *PLoS One.* 8, e78647. doi:10.1371/journal.pone.0078647

Laitinen, A., Laatikainen, L., Härkänen, T., Koskinen, S., and Reunanen, A. (2010). Prevalence of major eye diseases and causes of visual impairment in the adult Finnish population: a nationwide population-based survey. *Acta Ophthalmol.* 88, 463–471. doi:10.1111/j.1755-3768.2009.01566.x

Lang, J. T., and McCullough, L. D. (2008). Pathways to ischemic neuronal cell death: are sex differences relevant? *J. Transl. Med.* 6, 33. doi:10.1186/1479-5876-6-33

Liguori, I., Russo, G., Curcio, F., Bulli, G., Aran, L., and Della-Morte, D. (2018). Oxidative stress, aging, and diseases. *Clin. Interv.* 13, 757–72. doi:10.2147/CIA.S158513

Liu, Q., Lyubarsky, A., Skalet, J. H., Pugh, E. N., Jr., and Pierce, E. A. (2003). RP1 is required for the correct stacking of outer segment discs. *Invest. Ophthalmol. Vis. Sci.* 44, 4171–4183. doi:10.1167/iovs.03-0410

Loffler, K. U., and Lee, W. R. (1986). Basal linear deposit in the human macula. *Graefes Arch. Clin. Exp. Ophthalmol.* 224, 493–501. doi:10.1007/BF02154735

Majji, A. B., Cao, J., Chang, K. Y., Hayashi, A., Aggarwal, S., Grebe, R. R., et al. (2000). Age-related retinal pigment epithelium and Bruch's membrane degeneration in senescence-accelerated mouse. *Invest. Ophthalmol. Vis. Sci.* 41, 3936–3942.

Marshall, J., Grindle, J., Ansell, P., and Borwein, B. (1979). Convolution in human rods: an ageing process. *Br. J. Ophthalmol.* 63, 181–187. doi:10.1136/bjo.63.3.181

Menard, C., Rezende, F. A., Miloudi, K., Wilson, A., Tétreault, N., et al. (2016). MicroRNA signatures in vitreous humour and plasma of patients with exudative AMD. *Oncotarget.* 7, 19171–19184. doi:10.18632/oncotarget.8280

Mendelsohn, M. E., and Karas, R. H. (2005). Molecular and cellular basis of cardiovascular gender differences. *Science.* 308, 1583–1587. doi:10.1126/science.1112062

Meyers, K. J., Johnson, E. J., Bernstein, P. S., Iyengar, S. K., Engelman, C. D., Karki, C. K., et al. (2013). Genetic determinants of macular pigments in women of the carotenoids in age-related eye disease study. *Invest. Ophthalmol. Vis. Sci.* 54, 2333–2345. doi:10.1167/iovs.12-10867

Morquette, B., Juźwik, C. A., Drake, S. S., Charabati, M., Zhang, Y., Lécuyer, M. A., et al. (2019). MicroRNA-223 protects neurons from degeneration in experimental autoimmune encephalomyelitis. *Brain.* 142, 2979–2995. doi:10.1093/brain/awz245

Nag, T. C., Maurya, M., and Roy, T. S. (2019). Age-related changes of the human retinal vessels: possible involvement of lipid peroxidation. *Ann. Anat.* 226, 35–47. doi:10.1016/j.aanat.2019.06.007

Nag, T. C., Wadhwa, S., and Chaudhury, S. (2006). The occurrence of cone inclusions in the ageing human retina and their possible effect upon vision: an electron microscope study. *Brain Res. Bull.* 71, 224–232. doi:10.1016/j.brainresbull.2006.09.007

Nag, T. C., and Wadhwa, S. (2012). Ultrastructure of the human retina in aging and various pathological states. *Micron.* 43, 759–781. doi:10.1016/j.micron.2012.01.011

Nagasawa, H., Mori, T., Yanai, R., Bern, H. A., and Mills, K. T. (1978). Long-term effects of neonatal hormonal treatments on plasma prolactin levels in female BALB/cfC3H and BALB/c mice. *Cancer Res.* 38, 942–945.

Nakamura, S., Akiguchi, I., Seriu, N., Ohnishi, K., Takemura, M., Ueno, M., et al. (1995). Monoamine oxidase-B-positive granular structures in the hippocampus of aged senescence-accelerated mouse (SAMP8). *Acta Neuropathol.* 90, 626–632. doi:10.1007/BF00318576

National Research Council (2011). *Committee for the update of the Guide for the care and use of laboratory animals (2011). Guide for the care and use of laboratory animals.* 8th Edn. Washington, DC: National Academies Press. doi:10.17226/12910

Nonaka, A., Kiryu, J., Tsujikawa, A., Yamashiro, K., Miyamoto, K., Nishiwaki, H., et al. (2000). Administration of 17beta-estradiol attenuates retinal ischemia-reperfusion injury in rats. *Invest. Ophthalmol. Vis. Sci.* 41, 2689–2696.

Nuzzi, R., Scalabrin, S., Becco, A., and Panzica, G. (2018). Gonadal hormones and retinal disorders: a review. *Front. Endocrinol.* 9, 66. doi:10.3389/fendo.2018.00066

Ogata, N., Ohkuma, H., Kanai, K., Nango, K., Takada, Y., and Uyama, M. (1992). Histological changes in the retinal pigment epithelium and Bruch's membrane in senescence accelerated mouse. *Nippon. Ganka Gakkai Zasshi.* 96, 180–189.

Ooto, S., Hangai, M., Tomidokoro, A., Saito, H., Araie, M., Otani, T., et al. (2011). Effects of age, sex, and axial length on the three-dimensional profile of normal macular layer structures. *Invest. Ophthalmol. Vis. Sci.* 52, 8769–8779. doi:10.1167/iovs.11-8388

Osborne, N. N. (2008). Pathogenesis of ganglion "cell death" in glaucoma and neuroprotection: focus on ganglion cell axonal mitochondria. *Prog. Brain Res.* 173, 339–352. doi:10.1016/S0079-6123(08)01124-2

Ozawa, G. Y., Bearse, M. A., Jr., and Adams, A. J. (2015). Male-female differences in diabetic retinopathy? *Curr. Eye Res.* 40, 234–246. doi:10.3109/02713683.2014.958500

Ozawa, G. Y., Bearse, M. A., Jr., Bronson-Castain, K. W., Harrison, W. W., Schneck, M. E., Barez, S., et al. (2012). Neurodegenerative differences in the retinas of male and female patients with type 2 diabetes. *Invest. Ophthalmol. Vis. Sci.* 53, 3040–3046. doi:10.1167/iovs.11-8226

Pauleikoff, D., Harper, C. A., Marshall, J., and Bird, A. C. (1990). Aging changes in Bruch's membrane. A histochemical and morphologic study. *Ophthalmology.* 97, 171–178. doi:10.1016/s0161-6420(90)32619-2

Platania, C. B. M., Maisto, R., Trotta, M. C., D'Amico, M., Rossi, S., Gesualdo, C., et al. (2019). Retinal and circulating miRNA expression patterns in diabetic retinopathy: an in silico and *in vivo* approach. *Br. J. Pharmacol.* 176, 2179–2194. doi:10.1111/bph.14665

Ramírez, J. M., Ramírez, A. I., Salazar, J. J., de Hoz, R., and Trivino, A. (2001). Changes of astrocytes in retinal ageing and age-related macular degeneration. *Exp. Eye Res.* 73, 601–615. doi:10.1006/exer.2001.1061

Romano, G. L., Platania, C. B. M., Drago, F., Salomone, S., Ragusa, M., Barbagallo, C., et al. (2017). Retinal and circulating miRNAs in age-related macular degeneration: an *in vivo* animal and human study. *Front. Pharmacol.* 8, 168. doi:10.3389/fphar.2017.00168

Rossi, S., Maisto, R., Gesualdo, C., Trotta, M. C., Ferraraccio, F., Kaneva, M. K., et al. (2016). Activation of melanocortin receptors MC 1 and MC 5 attenuates retinal damage in experimental diabetic retinopathy. *Mediat. Inflamm.* 2016, 7368389. doi:10.1155/2016/7368389

Sarks, S., Cherepanoff, S., Killingsworth, M., and Sarks, J. (2007). Relationship of basal laminar deposit and membranous debris to the clinical presentation of

early age-related macular degeneration. *Invest. Ophthalmol. Vis. Sci.* 48, 968–977. doi:10.1167/iovs.06-0443

Sarks, S. H., Arnold, J. J., Killingsworth, M. C., and Sarks, J. P. (1999). Early drusen formation in the normal and aging eye and their relation to age related maculopathy: a clinicopathological study. *Br. J. Ophthalmol.* 83, 358–368. doi:10.1136/bjo.83.3.358

Schimel, A. M., Abraham, L., Cox, D., Sene, A., Kraus, C., Dace, D. S., et al. (2011). N-acetylcysteine amide (NACA) prevents retinal degeneration by up-regulating reduced glutathione production and reversing lipid peroxidation. *Am. J. Pathol.* 178, 2032–2043. doi:10.1016/j.ajpath.2011.01.036

Schmidl, D., Schmetterer, L., Garhöfer, G., and Popa-Cherecheanu, A. (2015). Gender differences in ocular blood flow. *Curr. Eye Res.* 40, 201–212. doi:10.3109/02713683.2014.906625

Silver, I. A., Deas, J., and Erecińska, M. (1997). Ion homeostasis in brain cells: differences in intracellular ion responses to energy limitation between cultured neurons and glial cells. *Neuroscience.* 78, 589–601. doi:10.1016/s0306-4522(96)00600-8

Smith-Vikos, T., and Slack, F. J. (2012). MicroRNAs and their roles in aging. *J. Cell Sci.* 125, 7–17. doi:10.1242/jcs.099200

Spraul, C. W., Lang, G. E., Grossniklaus, H. E., and Lang, G. K. (1999). Histologic and morphometric analysis of the choroid, Bruch's membrane, and retinal pigment epithelium in postmortem eyes with age-related macular degeneration and histologic examination of surgically excised choroidal neovascular membranes. *Surv. Ophthalmol.* 44 Suppl 1, S10–S32. doi:10.1016/s0039-6257(99)00086-7

Stone, E. M., Newman, N. J., Miller, N. R., Johns, D. R., Lott, M. T., and Wallace, D. C. (1992). Visual recovery in patients with Leber's hereditary optic neuropathy and the 11778 mutation. *J. Clin. Neuro Ophthalmol.* 12, 10–14.

Stone, J., Maslim, J., Valter-Kocsi, K., Mervin, K., Bowers, F., Chu, Y., et al. (1999). Mechanisms of photoreceptor death and survival in mammalian retina. *Prog. Retin. Eye Res.* 18, 689–735. doi:10.1016/s1350-9462(98)00032-9

Suzuki, M., Kamei, M., Itabe, H., Yoneda, K., Bando, H., Kume, N., et al. (2007). Oxidized phospholipids in the macula increase with age and in eyes with age-related macular degeneration. *Mol. Vis.* 13, 772–778.

Szemraj, M., Bielecka-Kowalska, A., Oszajca, K., Krajewska, M., Goś, R., Jurowski, P., et al. (2015). Serum MicroRNAs as potential biomarkers of AMD. *Med. Sci. Monit.* 21, 2734–2742. doi:10.12659/MSM.893697

Tai, L., Huang, C. J., Choo, K. B., Cheong, S. K., and Kamarul, T. (2020). Oxidative stress down-regulates MiR-20b-5p, MiR-106a-5p and E2F1 expression to suppress the G1/S transition of the cell cycle in multipotent stromal cells. *Int. J. Med. Sci.* 17, 457–470. doi:10.7150/ijms.38832

Takada, Y., Ogata, N., Ohkuma, H., and Uyama, M. (1993). Age-related changes in Bruch's membrane of the senescence accelerated mouse. *Nippon. Ganka Gakkai Zasshi.* 97, 595–601.

Takada, Y., Uyama, M., Ohkuma, H., Ogata, N., Matsushima, M., Deguchi, J., et al. (1994). Immunohistological study in Bruch's membrane of senescence accelerated mouse. *Nippon. Ganka Gakkai Zasshi.* 98, 955–961.

Trautner, C., Icks, A., Haastert, B., Plum, F., and Berger, M. (1997). Incidence of blindness in relation to diabetes. A population-based study. *Diabetes Care.* 20, 1147–1153. doi:10.2337/diacare.20.7.1147

Trip, S. A., Schlottmann, P. G., Jones, S. J., Altmann, D. R., Garway-Heath, D. F., Thompson, A. J., et al. (2005). Retinal nerve fiber layer axonal loss and visual dysfunction in optic neuritis. *Ann. Neurol.* 58, 383–391. doi:10.1002/ana.20575

Trivino, A., Ramírez, A. I., Salazar, J. J., de Hoz, R., Rojas, B., Padilla, E., et al. (2006). A cholesterol-enriched diet induces ultrastructural changes in retinal and macroglial rabbit cells. *Exp. Eye Res.* 83, 357–366. doi:10.1016/j.exer.2005.12.020

van den Beld, A. W., Kaufman, J. M., Zillikens, M. C., Lamberts, S. W. J., Egan, J. M., and van der Lely, A. J. (2018). The physiology of endocrine systems with ageing. *Lancet Diabetes Endocrinol.* 6, 647–658. doi:10.1016/S2213-8587(18)30026-3

van der Schaft, T. L., de Bruijn, W. C., Mooy, C. M., and de Jong, P. T. (1993). Basal laminar deposit in the aging peripheral human retina. *Graefes Arch. Clin. Exp. Ophthalmol.* 231, 470–475. doi:10.1007/BF02044234

van der Schaft, T. L., de Bruijn, W. C., Mooy, C. M., Ketelaars, D. A., and de Jong, P. T. (1991). Is basal laminar deposit unique for age-related macular degeneration? *Arch. Ophthalmol.* 109, 420–425. doi:10.1001/archopht.1991.01080030122052

Wagner, H., Fink, B. A., and Zadnik, K. (2008). Sex- and gender-based differences in healthy and diseased eyes. *Optometry.* 79, 636–652. doi:10.1016/j.optm.2008.01.024

Wagner-Schuman, M., Dubis, A. M., Nordgren, R. N., Lei, Y., Odell, D., Chiao, H., et al. (2011). Race- and sex-related differences in retinal thickness and foveal pit morphology. *Invest. Ophthalmol. Vis. Sci.* 52, 625–634. doi:10.1167/iovs.10-5886

Wang, C., Ji, B., Cheng, B., Chen, J., and Bai, B. (2014). Neuroprotection of microRNA in neurological disorders (Review). *Biomed. Rep.* 2, 611–619. doi:10.3892/br.2014.297

Wang, L., Yang, M., Liao, S., Liu, W., Dai, G., Wu, G., et al. (2017). Hsa-miR-27b is up-regulated in cytomegalovirus-infected human glioma cells, targets engrailed-2 and inhibits its expression. *Exp. Biol. Med.* 242, 1535370217699535. doi:10.1177/1535370217699535

Winkler, B. S., and Giblin, F. J. (1983). Glutathione oxidation in retina: effects on biochemical and electrical activities. *Exp. Eye Res.* 36, 287–97. doi:10.1016/0014-4835(83)90013-1

Xu, W., Li, F., Liu, Z., Xu, Z., Sun, B., Cao, J., et al. (2017). MicroRNA-27b inhibition promotes Nrf2/ARE pathway activation and alleviates intracerebral hemorrhage-induced brain injury. *Oncotarget.* 8, 70669–70684. doi:10.18632/oncotarget.19974

Younan, C., Mitchell, P., Cumming, R. G., Panchapakesan, J., Rochtchina, E., and Hales, A. M. (2002). Hormone replacement therapy, reproductive factors, and the incidence of cataract and cataract surgery: the Blue Mountains Eye Study. *Am. J. Epidemiol.* 155, 997–1006. doi:10.1093/aje/155.11.997

Zarbin, M. A. (1998). Age-related macular degeneration: review of pathogenesis. *Eur. J. Ophthalmol.* 8, 199–206. doi:10.1177/112067219800800401

Zettemberg, M., and Celojevic, D. (2015). Gender and cataract—the role of estrogen. *Curr. Eye Res.* 40, 176–90. doi:10.3109/02713683.2014.898774

Zetterberg, M. (2016). Age-related eye disease and gender. *Maturitas.* 83, 19–26. doi:10.1016/j.maturitas.2015.10.005

Conflict of Interest: The authors declare that the research was conducted in the absence of any commercial or financial relationships that could be construed as a potential conflict of interest.

frontiers in Pharmacology

CORRECTION
published: 15 March 2021
doi: 10.3389/fphar.2021.652905

Corrigendum: Changes in Retinal Structure and Ultrastructure in the Aged Mice Correlate with Differences in the Expression of Selected Retinal miRNAs

Anca Hermenean[1,2], Maria Consiglia Trotta[3], Sami Gharbia[1,2], Andrei Gelu Hermenean[4], Victor Eduard Peteu[5], Cornel Balta[1], Coralia Cotoraci[6]*, Carlo Gesualdo[7], Settimio Rossi[7], Mihaela Gherghiceanu[4,5] and Michele D'Amico[3]*

[1]"Aurel Ardelean" Institute of Life Sciences, Vasile Goldis Western University of Arad, Arad, Romania, [2]Department of Biochemistry and Molecular Biology, University of Bucharest, Bucharest, Romania, [3]Section of Pharmacology, Department of Experimental Medicine, University of Campania "Luigi Vanvitelli", Naples, Italy, [4]Carol Davila University of Medicine and Pharmacy, Bucharest, Romania, [5]Victor Babes National Institute of Pathology, Bucharest, Romania, [6]Faculty of Medicine, Vasile Goldis Western University of Arad, Arad, Romania, [7]Eye Clinic, Multidisciplinary Department of Medical, Surgical and Dental Sciences, University of Campania "Luigi Vanvitelli", Naples, Italy

Keywords: aging, retina, gender, histology, electron microscopy, miRNAs

OPEN ACCESS

Edited and reviewed by:
Galina Sud'ina, Lomonosov Moscow State University, Russia

****Correspondence:***
Anca Hermenean
anca.hermenean@gmail.com
Coralia Cotoraci
ccotoraci@yahoo.com

Specialty section:
This article was submitted to Inflammation Pharmacology, a section of the journal Frontiers in Pharmacology

Received: *13 January 2021*
Accepted: *15 January 2021*
Published: *15 March 2021*

Citation:
Hermenean A, Trotta MC, Gharbia S, Hermenean AG, Peteu VE, Balta C, Cotoraci C, Gesualdo C, Rossi S, Gherghiceanu M and D'Amico M (2021) Corrigendum: Changes in Retinal Structure and Ultrastructure in the Aged Mice Correlate with Differences in the Expression of Selected Retinal miRNAs. Front. Pharmacol. 12:652905. doi: 10.3389/fphar.2021.652905

A Corrigendum on

Changes in Retinal Structure and Ultrastructure in the Aged Mice Correlate with Differences in the Expression of Selected Retinal miRNAs

by Hermenean, A., Trotta, M. C., Gharbia, S., Hermenean, A. G., Peteu, V. E., Balta, C., Cotoraci, C., Gesualdo, C., Rossi, S., Gherghiceanu, M., D'Amico, M. Front. Pharmacol. 11:593514. doi: 10.3389/fphar.2020.593514

In the original article, there was a mistake in Figure 7 as published. The incorrect y-axis header was miR-27a-3p, miR-27b-3p, miR-20a-5p and miR-20b-5p in Figure 7A. The correct y-axis header in Figure 7A is miR-20a-3p, miR-106a-5p, miR-381-3p and miR-206-3p. Moreover, the incorrect miR-20b-5p graph in Figure 7B has been substituted with the correct miR-20b-5p graph. The corrected **Figure 7** appears below.

In the original article, there was a mistake in the legend for Figure 9 as published. The incorrect legend caption was "miR-27a-3p, miR-27b-3p, miR-20a-5p, and miR-20b-5p expression levels". The correct legend caption is "miR-20a-3p, miR-106a-5p, miR-381-3p, and miR-206-3p expression levels".

In the original article, there was a mistake in Figure 9 as published. The name of each graph was incorrectly reported as miR-27a-3p, miR-27b-3p, miR-20a-5p, and miR-20b-5p. The correct graph names are miR-20a-3p, miR-106a-5p, miR-381-3p, and miR-206-3p. The corrected **Figure 9** appears below.

The authors apologize for these errors and state that this does not change the scientific conclusions of the article in any way. The original article has been updated.

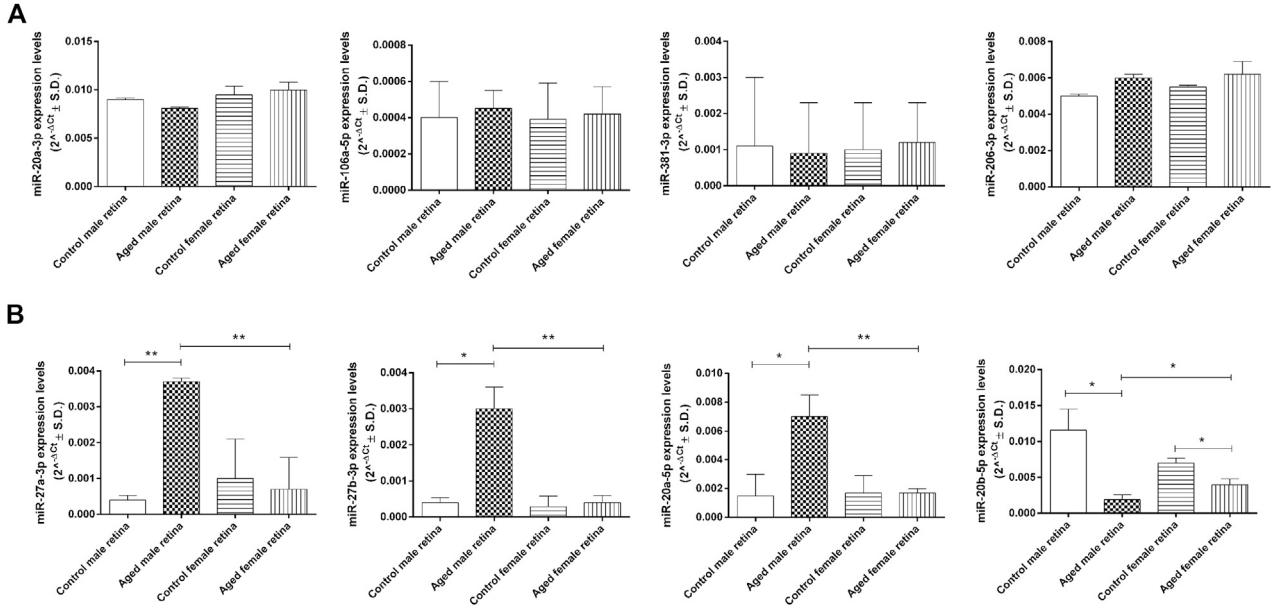

FIGURE 7 | Age-related miRNA expression levels in aged retina. **(A)** Not dysregulated and **(B)** dysregulated retina miRNA expression levels. Data are reported as $2^{-\Delta Ct}$ and shown as mean ± SD of $n = 10$ observations for each experimental group; each run was performed in triplicate. Statistical significance was assessed by using one-way ANOVA, followed by Tukey's multiple comparisons test. *$p < 0.05$ and **$p < 0.01$.

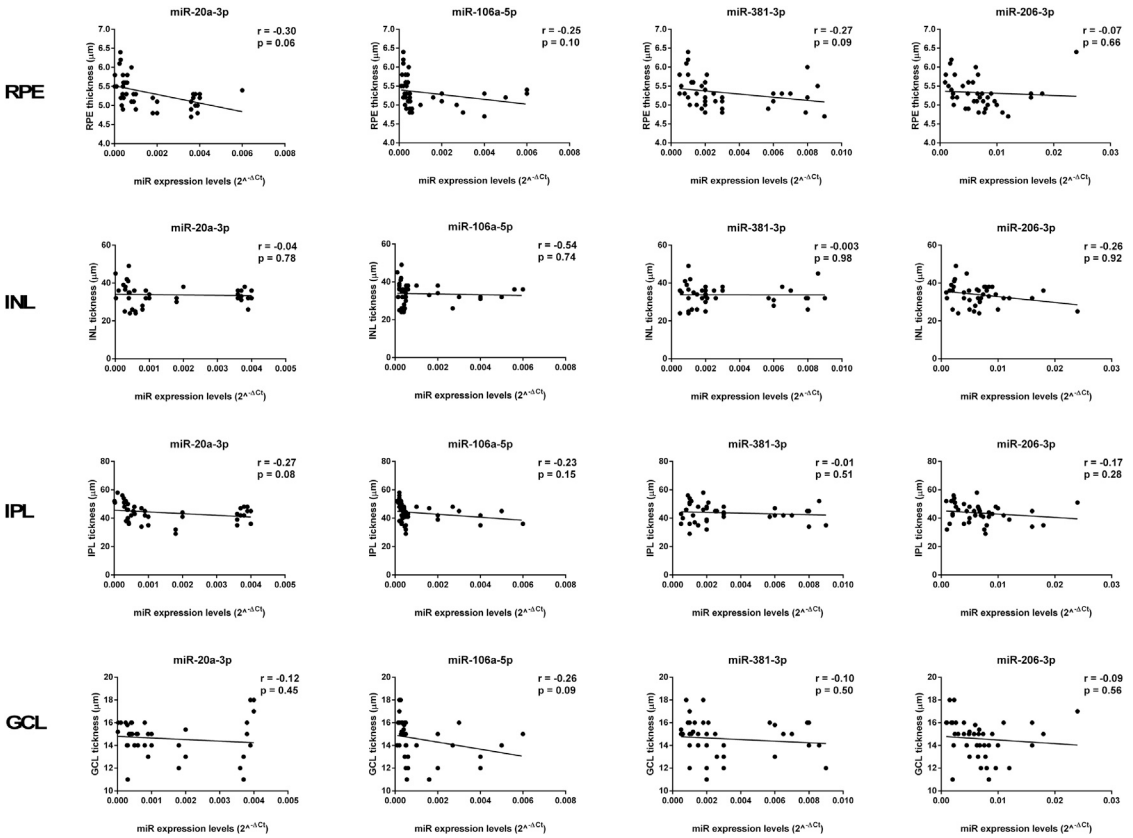

FIGURE 9 | Age-related miRNA expression levels not correlated with retina structure. No significant correlations were observed between RPE, INL, IPL, and GCL thickness and the miR-20a-3p, miR-106a-5p, miR-381-3p, and miR-206-3p expression levels. Pearson correlation analysis was used to evaluate the strength of association between pairs of variables, by including all the samples with different age and gender. Differences were considered statistically significant for p values < 0.05. RPE, retinal pigment cells; INL, retinal inner nuclear layer; IPL, retinal inner plexiform layer; GCL, retinal ganglion cell layer.

Advantages of publishing in Frontiers

OPEN ACCESS
Articles are free to read for greatest visibility and readership

FAST PUBLICATION
Around 90 days from submission to decision

HIGH QUALITY PEER-REVIEW
Rigorous, collaborative, and constructive peer-review

TRANSPARENT PEER-REVIEW
Editors and reviewers acknowledged by name on published articles

Frontiers
Avenue du Tribunal-Fédéral 34
1005 Lausanne | Switzerland

Visit us: www.frontiersin.org
Contact us: frontiersin.org/about/contact

REPRODUCIBILITY OF RESEARCH
Support open data and methods to enhance research reproducibility

DIGITAL PUBLISHING
Articles designed for optimal readership across devices

FOLLOW US
@frontiersin

IMPACT METRICS
Advanced article metrics track visibility across digital media

EXTENSIVE PROMOTION
Marketing and promotion of impactful research

LOOP RESEARCH NETWORK
Our network increases your article's readership